

Justus-Liebig-Universität Gießen

Fachbereich Agrarwissenschaften, Ökotoxikologie und Umweltmanagement

Institut für Insektenbiotechnologie

***Insects as model organisms for
basic and applied research***

Kumulative Habilitationsschrift

Zur Erlangung der Lehrbefähigung für das Fach Insektenphysiologie im
Fachbereich Agrarwissenschaften, Ökotoxikologie und Umweltmanagement der
Justus-Liebig-Universität Gießen

Vorgelegt von Dr. rer. nat. Annely Brandt

Gießen 2019

CONTENTS

1. Foreword	1
2. Summary	2
3. Zusammenfassung	3
4. Introduction	4
5. Part A – Insect models for basic and biomedical research	8
<i>Drosophila melanogaster</i> as a model for cell formation and nuclear shape change	8
<i>Drosophila melanogaster</i> as a model for cellular and organismal aging	9
<i>Tribolium castaneum</i> as a model for drug discovery of neuroprotective substances	11
<i>Locusta migratoria</i> and <i>Schistocerca gregaria</i> as a model for embryonic and larval development	12
6. Part B – Bees as models for pollinator health and risk assessment	14
<i>Apis mellifera</i> as a model organism for acute lethal pesticide effects	17
<i>Apis mellifera</i> as a model organism for chronic lethal pesticide effects	18
<i>Apis mellifera</i> as a model organism for sublethal pesticide effects	19
<i>Apis mellifera</i> colony as a model for sublethal pesticide effects	22
<i>Osmia bicornis</i> as a model for pollinator health and non- <i>Apis</i> pesticide risk assessment	23
Conclusions	25
7. References	26
8. Original Publications	

Appendix Original Publications

Part A - Insect models for basic and preclinical research

1. **Brandt, A.**, Papagiannouli, F., Wagner, N., Wilsch-Bräuninger, M., Braun, M., Furlong, E.E., Loserth, S., Wenzl, C., Pilot, F., Vogt, N., Lecuit, T., Krohne, G., Großhans, J. (2006). Developmental control of nuclear size and shape by Kugelkern and Kurzkern. *Current Biology*. 16(6), 543-52.
2. **Brandt, A.**, Krohne, G., Großhans, J. (2008). The farnesylated nuclear proteins Kugelkern and Lamin B promote aging like phenotypes in *Drosophila* flies. *Aging Cell*. 7(4), 541-51.
3. **Brandt, A.**, Vilcinskas, A. (2013). The Fruit Fly *Drosophila melanogaster* as a Model for Aging Research. *Advances in Biochemical Engineering/Biotechnology*. 135:63-77.
4. **Brandt, A.**, Joop, G., Vilcinskas, A. (2019). *Tribolium castaneum* as a whole-animal-high-throughput-screening system for the targeted identification of neuroprotective substances. *Archives of Insect Biochemistry and Physiology*. e21532
5. Bicker, G., Naujock M., **Haase, A.** (2004). Cellular expression patterns of acetylcholinesterase activity during grasshopper development. *Cell and Tissue Research*. 317(2), 207-20

Part B - Bees as model organisms for pollinator health and risk assessment

6. Schott, M., Bischoff, G., Eichner, G., Vilcinskas, A., Büchler, R., Meixner, M.D., **Brandt, A.** (2017). Temporal dynamics of whole body residues of the neonicotinoid imidacloprid in live or dead honey bees. *Nature Scientific Reports*. 7(1):6288. doi: 10.1038/s41598-017-06259-z.
7. **Brandt, A.**, Gorenflo, A., Siede, R., Meixner, M., Büchler, R. (2016). The neonicotinoids thiacloprid, imidacloprid, and clothianidin affect the immunocompetence of honey bees (*Apis mellifera* L.). *Journal of Insect Physiology*. 2016 Jan 8;86:40-47. doi: 10.1016/j.jinsphys.2016.01.001.
8. **Brandt, A.**, Grikscheit, K., Siede, R., Grosse, R., Meixner, M., Büchler, R. (2017). Immunosuppression in Honeybee Queens by the Neonicotinoids Thiacloprid and Clothianidin. *Nature Scientific Reports*. doi:10.1038/s41598-017-04734-1.
9. Grau, T., **Brandt, A.**, DeLeon, S., Meixner, M. D., Strauß, J. F., Joop, G., & Telschow, A. (2017). A Comparison of *Wolbachia* Infection Frequencies in Varroa with Prevalence of Deformed Wing Virus. *Journal of Insect Science*, 17(3). doi.org/10.1093/jisesa/iex039.
- 10.

11. Schott, M., Sandmann, M., Cresswell, J., Becher, M.A., Eichner, G., Brandt, D.T., Halitschke, R., Krueger, S., Morlock, G., Düring, R.-A., Vilcinskas, A., Meixner M.D., Bächler, R., **Brandt, A.** Honeybee colonies compensate for pesticide-induced brood mortality at the cost of reproductive success. submitted.
12. **Brandt, A.**, Hohnheiser, B., Sgolastra, F., Bosch, J. Meixner, M.D., Bächler, R. Sex-specific Differences in Immunosuppression by the Neonicotinoid Insecticide Thiacloprid in the red mason bee *Osmia bicornis* L. submitted.

Foreword

This habilitation thesis is based on the results obtained through close and appreciated collaborations with several colleagues and postgraduate students in different institutions. Although this synopsis is written in plural form (“we” rather than “I”) to improve readability, I am the only author of this thesis and I take sole responsibility for any errors it may contain.

I would first like to thank Prof Andreas Vilcinskis for his ongoing support and trust and all the great chances he offered to me. I am also deeply indebted to Dr Ralph Böhler, who opened me the doors to the world of bees, which is full of fascinating scientific questions, passionate people and vibrant disputes.

I would like to express my deep gratitude to Prof Gerd Bicker and Prof Klaus Wächter, who shared their scientific enthusiasm with me - a flame they ignited - I still benefit from their thorough training. I would also like to thank Prof Jasprien Noordermeer and Prof Jörg Großhans, who introduced me to *Drosophila* genetics. Many thanks to Prof Dr Dr *h.c.* Konrad Beyreuther for taking me aboard and expanding my horizon.

I would also like to thank my numerous brilliant colleagues, especially Dr Matthias Schott, Dr. Gerrit Joop, and Dr. Marina Meixner. My work could not have been accomplished without our fruitful discussions and their excellent contributions. I would also like to thank my former postgraduate students, especially Dr. Gillian Hertlein, Max Sandmann, Birgitta Hohnheiser, Maïke Achterberg, Jana Stenger and Annika Barme, it was a great experience to see them thriving.

Importantly, I would like to express my very profound gratitude to my husband Dominique for his unwavering love and support. Finally, I thank my daughters, Mathilda and Anna for their patience and encouragement. This accomplishment would not have been possible without them. Thank you.

1. Summary

Model organisms have been extensively used as accessible and convenient systems to study key biological and biomedical questions. A model organism is a simple, tractable system that can be used to study a larger theme of biology or disease. Model organisms must be easy to culture under controlled conditions, have life cycles short enough to allow breeding experiments over many generations, and be small enough to make the production of large numbers of individuals practical and economically feasible. Insects have been popular model organisms for more than 100 years. In contemporary life sciences, obvious ethical and practical handicaps strictly limit the scope for experiments using vertebrates. In contrast, there are many technical and ethical advantages of using insects over vertebrate models. Over decades, many people have worked successfully on these models, which has led to the development of specific tools and resources and the rapid accumulation of extended knowledge, thereby providing the infrastructure for ongoing and future studies.

This cumulative habilitation thesis presents a set of original papers which outline the characteristics of insect species as model organisms in two different areas: (A) *Insect models for basic and biomedical research* and (B) *Bees as model organisms for pollinator health and risk assessment*. The first part describes the role of four insect species in the fields of developmental biology, aging and biomedical research. First, the fruit fly *Drosophila melanogaster* is presented as the most relevant insect model organism for developmental and aging studies. The red flour beetle *Tribolium castaneum* is introduced as a model for biomedical research and the two grasshopper species *Locusta migratoria* and *Schistocerca gregaria* are discussed as models for embryonic development.

In the second part, the economically most relevant pollinator species *Apis mellifera* and a representative of solitary bee species, the red mason bee *Osmia bicornis*, are discussed as model organism for pollinator health. Research articles about lethal and sublethal effects of pesticides demonstrate the usefulness of honey bees and mason bees in pesticide risk assessment schemes, with special focus on effects on the immune system of these important pollinators.

2. Zusammenfassung

Ein Modellorganismus ist ein einfaches, nachvollziehbares Untersuchungssystem, das der Klärung grundlegender biologischer sowie biomedizinischer Fragestellung dient. Modellorganismen sind meist unter kontrollierten (Labor)-Bedingungen leicht zu kultivieren. Sie haben oft kurze Lebenszyklen, um Zuchtversuche über viele Generationen hinweg zu ermöglichen, und sind klein genug, um die Produktion einer großen Anzahl von Individuen praktisch und wirtschaftlich zu ermöglichen. Insekten werden seit mehr als 100 Jahren auf vielfältige Weise als Modellorganismen verwendet. Im Vergleich mit Wirbeltieren, unterliegen Experimente mit Insekten nicht den gleichen, strikten ethischen und praktischen Einschränkungen zu Wirbeltierversuchen. Über Jahrzehnte hinweg haben weltweit zahlreiche Wissenschaftler erfolgreich an Insektenmodellen gearbeitet, was zur Entwicklung spezifischer Werkzeuge, Ressourcen und der Akkumulation von umfangreichen Erkenntnissen führte und somit die Grundlage für laufende und zukünftige Forschung bereitstellt.

Diese kumulative Habilitationsschrift präsentiert eine Reihe von Originalarbeiten, die die Eigenschaften von unterschiedlichen Insektenarten als Modellorganismen in zwei verschiedenen Bereichen skizzieren: (A) *Insektenmodelle für die Grundlagenforschung und biomedizinische Forschung* und (B) *Bienen als Modellorganismen für die Bestäubergesundheit und Risikobewertung*. Der erste Teil beschreibt die Rolle von vier Insektenarten in den Bereichen Entwicklungsbiologie, Alterung und biomedizinischer Forschung. Zunächst wird die Fruchtfliege *Drosophila melanogaster* als der relevanteste Insektenmodellorganismus für Entwicklungs- und Alterungsstudien vorgestellt. Der rote Mehlkäfer *Tribolium castaneum* wird als Modell für die biomedizinische Forschung eingeführt, und die beiden Heuschreckenarten *Locusta migratoria* und *Schistocerca gregaria* werden als Modelle für die Embryonalentwicklung diskutiert.

Im zweiten Teil werden zwei ökonomisch bedeutende Bestäuberarten, *Apis mellifera* und die rote Maurerbiene *Osmia bicornis*, ein Vertreter der solitären Bienenarten, als Modellorganismus für die Bestäubergesundheit diskutiert. Publikationen zu tödlichen sowie zu subletalen Wirkungen von Pflanzenschutzmitteln werden herangezogen, um die Nützlichkeit von Honigbienen und Maurer-Bienen bei Risikobewertung von Pestiziden zu belegen. Der Schwerpunkt liegt dabei auf den sublethalen Auswirkungen von Pflanzenschutzmitteln auf das Immunsystem dieser beiden wichtigen Bestäubermodelle.

3. Introduction

During the 20th century, the transition from a mere description of the variety of biological phenomena to a mechanistic understanding of biological processes was due in large part to the decision to employ model organisms (Davis, 2004). Since then, model organisms have extensively been used in research as accessible and convenient systems to study key biological questions (Russell et al., 2017). Model organisms are defined as non-human species that are extensively studied in order to understand a variety of biological phenomena, with the aim that data and theories generated through use of the model will be applicable to other, more complex organisms (Ankeny and Leonelli, 2011). The study of bacteriophages, bacteria, and yeast uncovered most of the basic molecular biological processes. Whereas *Drosophila melanogaster*, *Caenorhabditis elegans*, *Arabidopsis thaliana* and *Mus musculus* played an equally important role for the study of biological processes in multicellular organisms. These multicellular models were extensively used for the genetic study of cell differentiation, tissue and organ formation, as well as the development of body forms. Model organisms have been chosen partly for their different basic biological properties, and mainly for their small size, short generation time and the ease with which they can be cultivated and propagated under simple controlled conditions (table 1).

In general, the term “model organism” indicates a simplified, tractable system that could be used to study a larger theme of biology (Russell et al., 2017). For the researcher, the understanding of the biological process of a particular organism has often not been the primary goal. Instead, the study of a model organism works is rather as a means to gain a better understanding of general biological principles and processes. For example, scientists have worked with *D. melanogaster* for over a century, not only because they find flies themselves interesting, but because these flies made the genetic analysis of fundamental, developmental processes accessible and fast. Over decades, so many scientists have worked successfully on these models that it has led to the development of specific tools and extensive resources (e.g. stock collections, databases, genetic and molecular tool kits, sequenced genomes) and the rapid accumulation of extended knowledge, thereby providing the infrastructure for ongoing and future studies.

Table 1. Strengths and limitations of model systems

	<i>Mus musculus</i>	<i>Caenorhabditis elegans</i>	<i>Locusta migratoria</i>	<i>Drosophila melanogaster</i>	<i>Tribolium castaneum</i>	<i>Apis mellifera</i>	<i>Osmia bicornis</i>
Simple cultivation	---	+	+	+++	+++	-	+
Simple life cycle	---	+++	+	+++	+++	-	+
Generation time	50 – 60 days	3.5 days	7 – 8 weeks	12 days	55 days (32°C)	1 year	1 year
Year round availability	+++	+++	+++	+++	+++	-	---
Adult Life span	Up to 3 years	90 hours	3 – 6 weeks	2 months (25°C)	4 – 7 months (25°C)	Workers: 20 – 180 days queen: up to 4 -6 years Drones: mating season	Males: 3 weeks Females 3 month
Maintenance costs	high	low	low	low	low	Economically profitable	low
Genetic homogeneity	+++	+++	+	+++	++	---	---
Economic relevance	--	-	++ (pest)	-	+ (pest)	+++	+
Ethical or safety restrictions	+++	-	-	-	-	-	No capturing of wild animals
Simplicity	-	++	+	++	++	-	+
Number of brain neurons	> 14,000,000	302	phase dependent	> 100,000		1,000,000	unknown
Fully annotated genomes	+	+	-	+	+	+	+
Tools and markers (molecular/ genetic/ cellular)	+++	+++	(+)	+++	+	-	---
Large libraries of mutants and transgenics available	+++	+++	-	+++	(+)	-	-
Frozen mutant strains	-	+	-	-	-	-	-
Databases	+++	+++	(+)	+++	+	+	-
Used in study area:							
Development	+++	+++	+	+++	+	(+)	-
Cell biology	+++	++	-	+++	-	(+)	-
Physiology	+++	+++	+	+++	+	+	-
Neurobiology	+++	+++	+	+++	+	++	-
Behaviour	+++	+	+	+++	(+)	+++	-
Social behaviour	+++	-	+	+	-	+++	-
Drug or pesticide tests	+++	+++	+	+++	(+)	+++	+
High throughput drug screening	-	+++	-	+++	-	-	-

It is difficult to trace the precise moment at which the term “model organism” was introduced in scientific literature. Based on a systematic review of the scientific literature using major search engines, it is clear that it became increasingly common in the late 1980s (Ankeny and Leonelli, 2011). In biology, the terms “model” also occur in association with mathematical and mechanistic theories, e.g. in the Lotka-Volterra model of predator-prey dynamics. Theoretical models are based on mathematical or mechanistic constructs that serve as analogies of the target of interest. The modeller develops the theoretical model and then analyses whether the target is sufficiently analogous to it. If successful, this modeller can draw conclusions about the target (Levy and Currie, 2015). In contrast, biological model organisms are often used to obtain empirical information that enables scientists to draw conclusions about other organisms or phenomena. Hence, inferences from work on model organisms are empirical extrapolations, whereby scientists treat the model organism as a representative specimen of a broader class (Levy and Currie, 2015). Many scientists have appreciated the value of model organisms as representatives for all species over time. As a recent genetics textbook puts it:

“The science of genetics discussed in this book is meant to provide an understanding of features of inheritance and development that are characteristic of organisms in general. Some of these features, especially at the molecular level, are true of all known living forms... [S]o we do not have to investigate the basic phenomena of genetics over and over again for every species. In fact, all the phenomena of genetics have been investigated by experiments on a small number of species, model organisms, whose genetic mechanisms are common either to all species or to a large group of related organisms (Griffiths et al., 2008, p. 17).

While the study of a particular model organism can reveal general features of biological phenomena, it's not certain how general such features are unless experiments are carried out on a variety of model organisms (Griffiths et al, 2008).

Insects have been popular model systems in biology for more than 100 years. The fruit fly *D. melanogaster* is an outstanding model system in genetics and developmental biology, but grasshoppers are also relevant models systems in the field of neurobiology, silk moths in pheromone research, or honeybees and crickets in neuroethology (Keil and Steinbrecht, 2010). There are numerous technical advantages of using insect over vertebrate models. In biomedical science, many obvious ethical and practical handicaps strictly limit the scope for experiments using vertebrates. Studies using the most commonly used vertebrate model system, the mouse, face several obstacles. Laboratory experiments using mice are ethically controversial, expensive and time consuming. With up to three years, mice have a considerably longer lifespan than to most insects that have a short life cycle of days or weeks (table 1). Moreover, mice have an intrauterine embryonic development, which makes developmental studies difficult and expensive. In contrast, in *D. melanogaster*, the embryo develops outside the female body and its development can easily be observed through a transparent eggshell.

Insects have become popular model organisms for studying developmental processes and aging, as well as human diseases. This approach has been strengthened with the sequencing of insect genomes and the discovery that 60% of human disease genes have homologues in an insect (Fortini et al., 2000). The organ systems of insects are functionally analogous to those in vertebrates, including humans. Although the gross anatomy and morphology of insects and vertebrates differs considerably, many of the molecular mechanisms that drive cellular and physiological processes are conserved between both groups (Brandt and Vilcinskis, 2013).

In the first part of the synopsis, four original research publications and a review article concerning insect development, aging, and diseases in basic and preclinical research in four model organisms *Locusta migratoria*, *Schistocerca gregaria*, *D. melanogaster* and *Tribolium castaneum*, will be presented. The second part will focus on two insect model organisms for lethal and sublethal pesticide effects and risk assessment analyses, the honey bee *Apis mellifera* and the solitary bee *Osmia bicornis*, presented in two articles in preparation and four published original research articles.

Part A – Insect models for basic and biomedical research

***Drosophila melanogaster* as a model for cell formation and nuclear shape change**

D. melanogaster has been a particularly valuable model organism for the analysis of genetic and molecular mechanisms underlying development - beginning at the early steps of development - the formation of the first cells - to the end of ontogenesis, the aging process.

First, we address the very early steps of embryonic development in the fruit fly - the formation of the first cells of the blastoderm. In *D. melanogaster*, early embryonic development begins with a rapid series of mitotic nuclear divisions, in the absence of cytokinesis, which results in the formation of a uniform monolayer of cortical nuclei forming the syncytial blastoderm. Subsequently, this syncytium undergoes a process of cell formation, called cellularisation, in which the individual nuclei become enclosed into individual cells (Mazumdar and Mazumdar, 2002). The process of cellularisation is rapid and complex and involves highly coordinated mechanisms of nuclear shape changes, rearrangements of the cytoskeleton, cell polarity and cytokinesis. The shape of a nucleus primarily depends on the composition of the nuclear lamina, which is tightly associated with the inner nuclear membrane and the cytoskeleton (Mazumdar and Mazumdar, 2002). However, the molecular mechanisms connecting cellular differentiation to nuclear shape changes are not yet well understood.

We studied this question during *D. melanogaster* cellularisation. We found that during the transition from syncytial to cellular blastoderm, the cortical layer of nuclei synchronously elongate towards the basal plane of the newly forming epithelium. The nuclear shape changes from spherical to oval, accompanied by a 2.5-fold increase in nuclear length (Brandt et al., 2006). During this process of nuclear elongation, the initially homogeneous appearance of the chromatin, which marks the syncytial blastoderm, is lost and distinct chromocenters (densely aggregated sites of pericentric heterochromatin) appear at the apical side of the now elongated nuclei. This chromatin rearrangement coincides with an increase of transcriptional activity in the zygote. In parallel, the nuclear envelope lobulates and forms indentations along the apicobasal axis, thereby doubling the nuclear surface area (Brandt et al., 2006).

Applying both a forward and a reverse genetic screen for zygotic mutants, we identified two genes, *kugelkern* and *kurzkern*, involved in nuclear elongation. In *kugelkern*- or *kurzkern*-depleted embryos, nuclear length was only 50% of the length of the wild-type nuclei at the end of cellularisation. The reduced nuclear size affected chromocenter formation and the expression of zygotic genes (Brandt et al., 2006).

Interestingly, Kugelkern contains a putative coiled-coil domain in the N-terminal half of the protein, a nuclear localization signal (NLS), and a C-terminal CxxM- farnesylation motif, which is assumed to be required for the targeting of Kugelkern to the inner nuclear membrane. Depending on this farnesylation motif, expression of *kugelkern* in *D. melanogaster* embryos or *Xenopus laevis* cells induced an overproliferation of nuclear membrane. Except for lamins, Kugelkern is so far the first nuclear protein known to contain a farnesylation site. This suggests that the association of farnesylated Kugelkern with the inner nuclear membrane induces the expansion of the nuclear surface area during cellularisation (Brandt et al., 2006).

***Drosophila melanogaster* as a model for cellular and organismal aging**

Although many genes and molecular mechanisms are known to coordinate developmental processes, so far none has been found that exclusively cause cell damage or aging. Hence, the aging process could be less evolutionary conserved than developmental and metabolic pathways. However, there is growing evidence that modulators of physiological aging are conserved over large evolutionary distances (Brandt and Vilcinskis, 2013; Partridge and Gems, 2002).

The nuclear lamina is comprised of a meshwork of lamins and lamina-associated proteins, which together provide mechanical stability, control the size and the shape of the nucleus, and enable the attachment of the chromatin to the nuclear envelope (Gruenbaum et al., 2005; Prokocimer et al., 2009). A variety of human diseases can be linked to defects in nuclear envelope proteins and there is growing evidence that nuclear lamina proteins are involved in the process of aging. In humans, abnormal nuclear shapes can be found in aging cells or in children with the progeria syndrome Hutchinson–Gilford Progeria Syndrome (HGPS). Children with HGPS appear normal at birth. During the first few years of their lives, they recapitulate symptoms and pathologies associated with normal physiological aging (e.g. balding, wrinkles, hypertension, arteriosclerosis) and often die of myocardial infarction or cerebrovascular incidents at an average age of 13 years (Goldman et al., 2004; Hennekam, 2006).

In HGPS patients, a dominant point mutation in the Lamin A-gene results in a permanently farnesylated protein called Progerin. It has been unclear, whether these age-related phenotypes are Progerin-specific or whether proteins that affect nuclear shape such as Kugelkern play a causative role in cellular aging. Like Progerin, the *D. melanogaster* protein Kugelkern contains a putative coiled-coil region, a nuclear localization signal, and a C-terminal farnesylation site. Like Progerin, Kugelkern can induce aging-like cellular phenotypes analogous to those described for Progerin (Brandt et al., 2006). Indeed, we were able to show that the size of the nuclei increases with age in adult fruit flies and that the nuclei assume aberrant shapes in wild type flies (Brandt et al., 2008). Moreover, induced expression of the farnesylated lamina protein Kugelkern causes abnormal nuclear shapes and reduces the flies lifespan. Interestingly, the shorter lifespan of the flies correlates with an early decline in age-dependent locomotor behaviour. Supporting these findings, the expression of *kugelkern* in a mammalian cell line induces nuclear lobulation together with DNA damage and histone modifications similar to those described for HGPS cells. We conclude that the insertion of farnesylated lamina-proteins into the nuclear lamina can lead to aging-like phenotypes in cultured mammalian cells and in adult *D. melanogaster* (Brandt et al., 2008; Brandt and Vilcinskis, 2013).

On the basis of these findings, we developed a combined screening system in cell culture and *D. melanogaster* that accelerates the evaluation of potential lifespan-altering interventions (European patent application WO2009133192 "Induction of aging phenotypes", patent holder: ZMBH, Universität Heidelberg, Dr. J. Großhans, Dr. A. Brandt). We could show that the farnesyltransferase inhibitor ABT-100 are able to ameliorate the ageing-like phenotypes induced by the farnesylated nuclear proteins Progerin, Kugelkern, or truncated Lamin B. In survivorship-assays, we successfully demonstrated the practicality of this *D. melanogaster* premature-ageing model system. The treatment of adult fruit flies with ABT-100 reversed the nuclear phenotypes and extended the average lifespan of the *kugelkern*-expressing flies. *Kugelkern*-expression shortens the average lifespan of the fruit flies by approx. 50%. Thus, the time needed to screen for potential pharmacological and genetic interventions is reduced by half (European patent application WO2009133192 "Induction of aging phenotypes").

One of the mayor obstacles on the way to developing anti-aging treatments is that whole-organism screens are time-consuming and therefore very expensive. The fruit fly turns out to be a valuable model organism for the investigation of physiological aging because its

short life span of four to eight weeks allows the experiments to be completed rapidly. In addition, a large number of genetically homogenous individuals can be assessed in parallel, increasing the statistical power of the experiments. Moreover, large numbers of *D. melanogaster* can be cultivated in small bottles, so maintenance is easy and inexpensive.

In conclusion, our results demonstrate that these pharmacological and genetic assays can be used as screening tools for lifespan-extending interventions. Especially the combination of high-throughput cell culture screens with a subsequently performed validation phase in *D. melanogaster* survival assays will allow the number of candidate genes or testing substances that have to be used in vertebrate experiments to be narrowed down (European patent application WO2009133192 “Induction of aging phenotypes”).

***Tribolium castaneum* as model for drug discovery of neuroprotective substances**

For the last 160 years, human life expectancy has increased by three months a year in developed countries (Oeppen and Vaupel, 2002). Life expectancy is steadily increasing and so is the impact of aging and age-related diseases on our societies. Especially the prevalence of age-related neurodegenerative disorders is drastically increasing as people become older. Parkinson’s disease (PD) is one such common neurodegenerative disease. The most relevant pathological feature of PD is the death of dopaminergic neurons in the *Substantia nigra pars compacta*, which leads to the characteristic motor symptoms tremor, postural rigidity, and akinesia. Although the etiology of PD is largely unknown, mitochondrial dysfunction and oxidative stress are thought to actively contribute to the progression of PD (Michel et al., 2006).

The pharmacological inhibition of oxidative stress in dopaminergic neurons is one promising target for the development of new drugs (Santos, 2012). However, large compound libraries need to be screened in order to identify promising candidate substances. This calls for a model organism that on the one hand recapitulate the main characteristics of PD and on the other hand is suitable for large-scale *in vivo* screening (Brandt and Vilcinskas, 2013).

Although the dopaminergic system of *Tribolium castaneum* differs from that of vertebrates, many fundamental cellular and molecular features are conserved (Whitworth et al., 2006). The oxidative stress eliciting herbicide paraquat can be used to induce PD-like symptoms allowing the development of a *T. castaneum* PD model with which to screen for new drugs and potentially neuroprotective substances (Brandt et al., 2019).

In detail, adult *T. castaneum* feign death when attacked, and the duration of this so called tonic immobility behaviour correlates with brain dopamine levels (Miyatake et al., 2004; Nakayama and Miyatake, 2010). We took advantage of the fact that this behaviour is accessible to pharmacological interventions. In our experiments, paraquat was added to the diet of adult beetles in order to induce PD-like symptoms, which were subsequently quantified using the tonic immobility assay and a novel positive geotaxis behavioural assay. To test potentially neuroprotective substances, the adult beetles were reared on a flour diet supplemented with or without candidate neuroprotective substances and with or without paraquat in a fully factorial set-up (Brandt et al., 2019). The paraquat-induced behavioural changes are reduced in beetles fed on diets supplemented with L-DOPA, ascorbic acid, curcumin, hempseed flour or the Chinese herb gou-teng. Thus we demonstrate that proven PD drugs, well characterised antioxidants, and plant extracts can reverse paraquat-induced behavioural deficits in a *T. castaneum* model of PD (Brandt et al., 2019).

T. castaneum is a genetically and pharmacologically tractable insect model system. Like most insects, *T. castaneum* is small, easy and inexpensive to rear in the laboratory, it has a fully sequenced genome, and it has lesser ethical issues to consider than vertebrate models (Grunwald et al., 2013; Grunwald et al., 2014; Knorr et al., 2013). *T. castaneum* is therefore a useful model organism for the discovery and characterization of neuroprotective substances (Brandt et al., 2019), and could be developed as a model for the preclinical testing of therapeutic candidate substances for the treatment of neurodegenerative diseases in high-throughput whole-animal screens.

***Locusta migratoria* and *Schistocerca gregaria* as a model for embryonic and larval development**

Even though research inclines to focus on more genetically-accessible model organisms, the grasshopper is still an outstanding preparation for physiological studies in various research areas such as neurobiology, endocrinology, integrative physiology and biochemistry (Ayali and Yerushalmi, 2010). The grasshopper embryo has been extensively used as a convenient and accessible model system to investigate the development of the nervous system (Seidel and Bicker, 2002). Due to its relatively large size and its basic, segmental pattern, the formation of individual neurons and their neurites within this pattern, can easily be studied (Ayali and Yerushalmi, 2010; Goodman and Bate, 1981).

In our comparative study of embryonic development, we focussed on the expression of acetylcholinesterase (AChE) activity during the formation of the nervous system and epidermal body structures in the two most commonly used grasshopper model species *Locusta migratoria* and *Schistocerca Americana*, and follow the temporal and spatial

appearance of AChE activity during embryonic development. We examined the spatial and temporal expression pattern of AChE in the nervous system as well as in epidermal body structures during embryonic and larval development. Histochemical staining of whole-mount embryos and primary neuronal cell cultures indicates that AChE is synthesized predominantly as a cell surface molecule. In both grasshopper species, the expression of AChE followed a similar spatiotemporal histological staining pattern. At 25 – 30% of embryonic development (0% = egg deposition, 100% = eclosion), mainly epidermal tissue structures are AChE-stained in the various body appendages. Subsequently, AChE-labelling appeared in the outgrowing neurons of the central nervous system and in the nerves innervating the legs and the dorsal body wall (stages 30% – 40%). Later (> 45%), the somata of identified mechanosensory neurons started to express AChE activity, presumably indicating cholinergic differentiation.

Interestingly, AChE expression was also found in glia cells. AChE staining was present in immunohistochemically-stained repo-positive glial cells of the central nervous system, longitudinal glia of connectives, glia of the stomatogastric nervous system and glial cells ensheathing peripheral nerves. Glial cells continued to be AChE-positive during larval to adult development, whereas motoneurons lost their AChE expression. The expression pattern in non-neuronal cells and glutamatergic motoneurons and the developmental appearance of AChE prior to synaptogenesis in the CNS suggest that AChE has non-cholinergic functions during grasshopper embryogenesis. In conclusion, the staining patterns together with the sequence homologies to known cell-adhesion molecules described in the literature suggest a non-cholinergic function of AChE during grasshopper embryogenesis.

Part B- Bees as models for pollinator health and risk assessment

Humans have devised many different ways to use honey bees, either for their products, their pollination service and - more recently - as an object for scientific studies. Bees and humans have a long, interwoven history. For at least 8,000 years, humans have gathered honey, wax, pollen, and proteinaceous larvae by taking combs from wild colonies. The ancient Egyptian civilization was the first to practice organized beekeeping on a large-scale (Kritsky, 2017). To some extent, honey bees also benefited from their association with humans, they provide nesting sites. They protect them from predators and spread have them, along with other farm animals, to all continents except Antarctica.

Research on honeybee physiology, navigation and communication has a long tradition reaching back over 100 years. Ground-breaking discoveries in the field of ethology and neurobiology such as the discovery of colour vision in an invertebrate, detection of ultraviolet light and linearly polarized light, navigation, learning, and a symbolic form of communication based on the work of the Nobel Prize winner Karl von Frisch (von Frisch, 1974, 1994) were first made in honeybees. These observations, together with the relative ease with which honey bees can be trained, and the relative simplicity of their nervous systems compared to vertebrates, have made honeybees an attractive organism in which to investigate general principles of ethology and neurobiology. Technical progress (e.g. intracellular recording and electrical and pharmacological manipulation) allowed researchers to address fundamental biological questions and helped to understand biological processes of memory formation and orientation at a cellular level in the honey bee model (Menzel, 2012). The honey bee combines a relatively small brain of only about 1 million neurons with a complex, flexible and experience-dependent behaviour (Menzel, 2012). Their individual behaviour repertoire can be examined under laboratory conditions and their social behaviour (e.g. communication, task allocation, swarming) has been studied extensively in the colony context. Their relatively complex brains, elaborate behaviour, and eusocial life form clearly distinguishes them from other insects (Menzel, 2012), and makes them an attractive study object for many scientists. However, it can be questioned to what extent insights into their exceptional biology can be generalised to other insects. Moreover, up to date, the honey bee does not offer the same set of molecular genetic tools that are available in other model organisms such as *D. melanogaster* and *C. elegans*, which (currently) restricts their use as a model organism.

The outstanding role of bees in plant pollination, however, makes the health and well-being of bees an important subject for scientific research in themselves. Pollination mediated by insects is one of the essential ecosystem services provided to humankind. Bees (Anthophila) are pollinators of 70 to 90% of wild and cultivated angiosperm plants, and therefore essential for ecosystem function and agricultural production (Fontaine et al., 2005; Bascompte Jordi, 2006; Kennedy et al., 2013; Klein, 2007). Especially crop species used for human food and animal feed benefit from insect pollinators (Klein, 2007), which provide a global service worth \$215 billion in food production (Gallai et al., 2009). The negative impact of pollinator decline on the reproductive success of flowering plants has been documented at the species level (Garibaldi et al., 2013) and at the level of ecosystems (Fontaine et al., 2005), and the abundance and diversity of flowers is decreasing. Serious declines in honeybee abundance and diversity have been reported over the past decades (Potts et al., 2010a; Potts et al., 2010b; Van Engelsdorp, 2010; vanEngelsdorp et al., 2009). Colony losses of 20–30% are regularly registered over the autumn–winter period in most countries in the Northern hemisphere (van der Zee et al., 2015), whereas a survival rate of 95% is considered as normal for honey bee colonies (R. Büchler, pers. communication).

, No single cause can be claimed as responsible for For these losses, but multiple stress factors, such as poor nutrition, habitat degradation, pathogens, parasites, and pesticides, acting alone or in combination, have contributed to these declines. The way that biological, chemical and environmental stressors affect the health and survival of honey bee colonies is poorly understood. The underlying physiological mechanisms remain unclear due to the complex nature of the potential combinations of simultaneously acting stressors and possible interactions between them. It is widely assumed that multiple factors contribute to the health decline and elevated colony losses, since studies focusing only on specific stressors often failed to demonstrate a direct causal link between stressor, bee health decline and colony loss (Goulson et al., 2015a). This generated a general consensus that not a single factor can be causative of colony losses, which are but that most cases are associated with different combinations of stressors.

In particular pesticides have often been considered to be one of the main factors causative for the decline of insect pollinator species (European Food and Safety Authority (EFSA), 2013). More than 150 different chemicals used as herbicides, fungicides and insecticides have been detected in honey bee colonies (Sanchez-Bayo and Goka, 2014). Herbicides minimize weed problems for farmers, but inevitably reduce the availability of flowers for pollinators (Feltham et al., 2015; Goulson et al., 2015b). Fungicides can also directly affect the physiology of honey bees by changing the gut microbiom and increasing disease susceptibility (Motta et al., 2018). Obviously, insecticides are specifically developed to

damage and kill pest insects, but they can unintentionally harm exposed non-target insects like beneficial pollinators. Fungicides of the class of ergosterol biosynthesis inhibitors (EBI) are known to inhibit the detoxification process (Iwasa et al., 2004), thereby drastically increasing the toxicity of insecticides (Iwasa et al., 2004). However, the full relevance of additive interactions between pesticides for the health and survival of colonies is hardly understood.

Among insecticides, neonicotinoids have especially been suspected to be an important factor underlying bee losses. Globally, neonicotinoids are the most widely used class of insecticides. In 2010, they accounted together with fipronil for approximately one third of the world insecticide market in monetary terms (Simon-Delso et al., 2015). Neonicotinoids are neurotoxins that act as agonists of the nicotinic acetylcholine receptor. The disruption of neuronal cholinergic signal transduction leads to abnormal behaviour, immobility and death of target pests (Elbert et al., 2008; Matsuda et al., 2001; Tomizawa and Casida, 2011). However, non-target insects like honeybees frequently come into contact with these systemic insecticides (Pisa et al., 2015), mostly through ingestion of residues in pollen, nectar, or guttation fluids of contaminated plants, or via contaminated water sources (Desneux et al., 2007; Sanchez-Bayo et al., 2016). Foragers take pesticide residues back to their colonies, where they remain stored in beebread or honey until they are fed to larvae, workers, drones, or the queen (Blacquiere et al., 2012; Genersch et al., 2010).

In 2013, the European Commission restricted the use of three of the five approved neonicotinoids in the European Union (EU) in order to protect honeybees (see Regulation (EU) No 485/2013). Based on a risk assessment of the European Food Safety Authority (EFSA, 2012), plant protection products that contain the three nitro-substituted, highly toxic neonicotinoids clothianidin, imidacloprid or thiamethoxam were no longer allowed in outdoor applications in bee-attractive crops (including oilseed rape, maize, and sunflower). At the same time, applicants of the neonicotinoids were obliged to provide further data on the safety of the uses still allowed. Following the assessment of these additional data by EFSA, all outdoor applications were no longer considered to be safe due to the identified risks to bees. Therefore, the European Commission prepared several proposals to completely ban outdoor uses of these three active substances in February 2018. For acetamiprid, the fourth approved neonicotinoid in the EU, the EFSA established a low risk to bees. The fifth neonicotinoid, thiacloprid is classified as a candidate for substitution, based on its endocrine disrupting properties (<https://ec.europa.eu/food/plant/approval>).

***Apis mellifera* as a model organism for acute lethal pesticide effects**

It is likely that bees living in most industrialised farmland areas are exposed to sufficient neonicotinoids to suffer both lethal and sublethal effects (Goulson et al., 2015a). In the event of suspected acute lethal intoxication, a beekeeper can send bee samples to an analytical laboratory (in Germany to the Julius-Kühn Institute), but often no pesticide residues can be detected. In this case, it is not certain whether the bees had no contact to pesticides, or whether the pesticide levels had already decreased below the detection threshold. Pesticide levels could decrease when the intoxicated foragers were lying in front of the hive entrance, exposed to sun-light and changes in temperature and humidity, or in samples during postal shipment without cooling. Numerous controlled laboratory studies have shown that whole-body imidacloprid residues can rapidly decrease (Cresswell et al., 2014; Suchail et al., 2004a; Suchail et al., 2004b). However, hardly any data exist on the dynamics of imidacloprid breakdown under field realistic conditions where bees are acutely poisoned and become immobilised (and are taken for dead), or in bee samples during shipping to analytic facilities. Therefore, we investigated the temporal dynamics of whole-body residues of the neonicotinoid imidacloprid in live or dead honeybees under various environmental conditions, such as exposure to UV light, individual or group feeding, freezing, or transport of individuals through the mail system (Schott et al., 2017). Starved bees were exposed to a single-meal of 41 ng/bee and were immediately paralysed. These immobile, “dead” looking honey bees recovered from paralysis after approx. 48 hours. The decrease of imidacloprid residues in living but paralysed bees was stopped by freezing (= killing) the bees. When exposed to high doses of UV light (equivalent to two weeks sunshine), imidacloprid levels were significantly reduced, but the mode of transport did not affect residue levels. Group feeding increased the variance of residue levels, which is relevant for acute oral toxicity tests (Schott et al., 2017). Our study of the temporal dynamics of imidacloprid residues under field relevant conditions indicate that a short freezing of bee samples stops the decrease of whole-body residues and further shipping time (cooled or non-cooled) does not significantly change the amount of traceable residues. Importantly, even when they are immobile and appear dead, a fast decrease of the ingested pesticides could still occur in the paralysed bees. Therefore, we recommend freezing honeybee samples as fast as possible, before sending them via standard postal routes to the analytical laboratories (Brandt A., 2018).

***Apis mellifera* as a model organism for chronic lethal pesticide effects**

To determine their potential for causing unacceptable harm to non-target organisms (e.g. bees), pesticides are evaluated in a highly regulated risk assessment process. Before the registration of new pesticide chemicals or new uses of existing chemicals, pesticides must be evaluated before they can be marketed, and existing pesticides must be re-evaluated periodically to ensure that they meet the appropriate safety standards. However, concerns have been raised by the public, environmental non-governmental organisations, beekeepers' associations and members of the European Parliament on the appropriateness of the current risk assessment schemes for pesticides (EFSA, 2012; European Food and Safety Authority (EFSA), 2013)

First of all, risk assessments focus on direct acute exposure of bees to agrochemicals (Sanchez-Bayo and Goka, 2014). In acute toxicity tests, the lethal dose (LD50) that kills 50% of individuals after topical or oral exposure in 24 or 48 hours is assessed. Since the standard oral acute LD50 test ignores the possible negative effects derived from repeated or constant exposure (Sanchez-Bayo and Goka, 2014), the OECD recently released the Chronic Oral Toxicity Test (10-Day Feeding) guideline to improve the risk assessment of chronic exposure. In this test, honey bees are exposed to a constant concentration of the active ingredient over a period of 10 days under laboratory conditions (OECD, 2017). Mortality and behavioural abnormalities are observed and recorded daily during the test period. However, worker bees generally live longer than 10 days (summer bees under laboratory conditions up to 35 days, pers. observation), and a study has already shown, that detrimental effects of chronic pesticide exposure can manifest after 10 days (Simon-Delso et al., 2018). Therefore, we adapted the OECD-10 Day Feeding protocol to test for long-term chronic effects. In a ring-test experiment involving eight partner laboratories in six countries, we tested the butenolid flupyradifurone as active ingredient (Tosi et al., in preparation). Like neonicotinoids, flupyradifurone is a systemic insecticide which acts as an agonist at the insect nicotinic acetylcholine receptor. Traded under the name Sivanto® prime, it is a butenolid insecticide, that is widely used in Northern America and Mexico, and on sale in an increasing number of European countries (<https://www.sivanto.bayer.com/sivanto-worldwide.html>).

In our chronic toxicity ring test, five field realistic concentrations (0.4, 4, 12, and 36 ppm) of flupyradifurone were fed *ad libitum*. In contrast to the 10-Day Feeding protocol, the experiment ended, when at least 50% of the bees died. All concentrations of flupyradifurone increased the mortality of the honey bees and induced abnormal behaviour, e.g., rotation, cramps, or shivering in a dose dependent manner. Only the highest concentration of 36 ppm increased mortality in the first 10 days of the experiment. Effects of the lower concentrations manifested only after 10 days. Our results show that only prolonged exposures can reveal

significant negative effects of lower, but field-realistic daily doses and concentrations (Tosi et al., in preparation). These data emphasize the importance of time-to-death experiments rather than fixed-duration studies for evaluating chronic toxicity.

***Apis mellifera* as a model organism for sublethal pesticide effects**

Besides the lethal effects of pesticides, sublethal effects can have a profound impact on pollinator health, especially in conjunction with other chemicals, or biological and environmental stressors. It is assumed that populations of managed and wild pollinators are in decline as a result of multiple interacting factors including parasites, disease, habitat loss, poor nutrition, and pesticides. The mechanisms behind these interactions are not yet fully understood. There is evidence for an interaction between pesticides and pathogens (for review see (Collison et al., 2016)). For instance, Aufauvre et al. (2012) found an interaction between the insecticide fipronil and the microsporidian pathogen *N. ceranae*. Exposure to the neonicotinoid insecticide imidacloprid increases the prevalence of *Nosema spp.* infections in honey bee colonies (Pettis et al., 2012; Wu et al., 2012) and also increases *Nosema*-induced mortality (Alaux et al., 2010). There is growing evidence that exposure to pesticides impairs the immunocompetence of insects, which could explain these interactive effects (Di Prisco et al., 2013; Nazzi et al., 2012; Sanchez-Bayo et al., 2016). A strong immune defence is vital for honey bee health and colony survival. This defence, however, can be impaired by environmental factors such as pesticides that may render honey bees more vulnerable to parasites and pathogens. For example, Di Prisco et al. (2013) showed that exposure to the neonicotinoid clothianidin adversely affects a member of the NF- κ B gene family and promotes the replication of the deformed wing virus in individuals bearing covert infections. However, the role of diminished immunity in these declines is not yet fully understood (Lehmann, 2017).

The individual bee's immune response is comprised of cellular responses such as phagocytosis and encapsulation, and humoral responses via both the prophenoloxidase cascade (leading to melanisation) and antimicrobial effectors (e.g. antimicrobial peptides) (Evans et al., 2006). The cellular immune defence is constituted by hemocytes that are responsible for the phagocytosis of small microbial targets, and the nodulation and encapsulation of larger intruding bacteria and parasites. The melanisation reaction is catalysed by phenoloxidase, whose precursor (prophenoloxidase) is produced by hemocytes and activated by serine proteases (Evans et al., 2006).

Immunocompetence is defined as the ability to mount an immune response (Wilson-Rich et al., 2009). If pesticide exposure leads to reduced immunocompetence, this could increase disease susceptibility, potentially affecting individual and colony fitness and survival. We

could demonstrate that neonicotinoids negatively affect general immune parameters of individual worker honey bees (Brandt, 2016). As measures of the individual immunocompetence, three different aspects of honey bee immunity were used, encapsulation response, hemocyte density and antimicrobial activity of the hemolymph. Our results indicate that all three aspects of the individual immunocompetence of worker bees are affected by sublethal concentrations of neonicotinoids. Imidacloprid (1 µg/l) and thiacloprid (200 µg/l) affected these functional aspects of immune defence even at field realistic concentrations; clothianidin affected the tested immune parameters only at higher than field realistic concentrations (50 – 200 µg/l)(Brandt, 2016).

The study of lethal and sub-lethal effects of neonicotinoids have largely focused on worker bees and, to a much lesser extent, on overall colony function (Blacquiere et al., 2012; Henry et al., 2012; Rundlof et al., 2015; Whitehorn et al., 2012). As highly social insects, honey bees build colonies of several thousand individuals that contain only one fertile female, the queen (Winston, 1987). The queen is responsible for all egg laying and brood production within the colony. Consequently, the health of the queen is crucial for the colony's fitness and survival, and any impairment can result in negative effects on colony performance. The natural lifespan of a honeybee queen is two to four years (Winston, 1987). However, recent reports from the U.S.A. showed increased rates of queen failure, with 50% or more being replaced in colonies within the first six months which coincides with high mortality rates of colonies in the U.S.A., where in some years more than 50% of colonies die (Pettis et al., 2016; vanEngelsdorp et al., 2013).

Despite their outstanding role, there is only little information available about the effects of pesticides on the health and fitness of honeybee queens (Williams et al., 2015). Therefore, we examined the effects of pesticide exposure on young queens. Similar to the experiments with worker bees (Brandt, 2016), we employed a broad array of methods to investigate the immune defence competence of queens: total and differential hemocyte counts, wound healing/melanisation, and antimicrobial activity of the hemolymph after immune stimulation. We could show that all tested aspects of individual immunity are negatively affected by sublethal, environmentally relevant concentrations of thiacloprid and clothianidin in newly emerged honeybee queens (Brandt et al., 2017). As in workers, we found an overall reduction of hemocyte density at all concentrations tested. We also observed changes in the abundance of subclasses in the population of hemocytes in clothianidin exposed queens, which may indicate a severe interference of neonicotinoid treatment with cellular immunity. In detail, there is a significant reduction in the number of granulocyte-like hemocytes in queens exposed to clothianidin. The granulocyte-like cells are widely spread with extensive filopodia and lamellipodia formation and include numerous vesicle-like structures which

may indicate their involvement in phagocytosis (Negri et al., 2014). The reduction of granulocyte-like hemocytes may be of particular importance, since these active, differentiated hemocytes are responsible for the elimination of pathogens and initiate the encapsulation process (Negri et al., 2014).

The ability to encapsulate and melanise intruding pathogens is positively correlated with the resistance to viral and parasitoid infections, as well as blood sucking parasites. Wound closure involves similar mechanisms to encapsulation and is important for the reduction of virus transfer between bees (Evans et al., 2006). The treatment with neonicotinoids significantly reduced the encapsulation and melanisation response (Brandt et al., 2017). Moreover, exposure to neonicotinoids significantly reduced the antimicrobial activity of the hemolymph. The antimicrobial activity depends on the amount of hemolymph antimicrobial peptides, which are produced by hemocytes or cells of the fat body (Strand, 2008). Together with the observed changes in hemocyte composition and decrease in hemocyte density and melanisation response, our findings can be interpreted as immunosuppression of honeybee queens by exposure to neonicotinoids.

The highly toxic neonicotinoids imidacloprid and clothianidin have been banned since 2018 by the European commission. However, thiacloprid, which is classified as “not harmful for bees” (B4) due to its lower acute toxicity, has similar sublethal effects on immune parameters of honey bees and a solitary bee species at a field realistic concentration. Thiacloprid is frequently used in spray application on flowering crops, especially in oil seed rape and was found in more than 50% of bee bread sample, up to maximum concentrations of 200 - 498 µg/kg beebread (Genersch et al., 2010; Rosenkranz et al., 2014).

Our studies on the immunocompetence of honey bee workers and queens complements previous, similar findings on the immunosuppressive effects of neonicotinoids on worker bees (Di Prisco et al., 2013; James and Xu, 2012). Immune suppression by pesticides like neonicotinoids can facilitate the spread and abundance of pathogens and parasites, which are the proximate mortality factors of honeybee colonies (Sanchez-Bayo et al., 2016). Especially the infestation with *Varroa destructor* is the suspected main cause for colony losses and has been shown to be promoted in colonies exposed to neonicotinoid-treated crops (Alburaki et al., 2016). Of all parasites, *V. destructor* is the most important ectoparasite of *A. mellifera*. The varroa mite is an effective vector for several honey bee viruses (Martin, 2001) and assumed to be able to downregulate immune genes of the honey bee (Nazzi et al. 2012)(Yang and Cox-Foster, 2005). High varroa mite infestation rates and, as a consequence, viral infections, strongly correlate with the collapse of colonies (Genersch et al. 2010). In particular, the association between *V. destructor* and Deformed Wing Virus (DWV) is being discussed as one of the main causes for colony losses (de Miranda and Genersch, 2010).

Although the impact of varroa mites on honey bee colonies is evident, we have little understanding of the dynamics and possible interactions between its bacterial endosymbionts and the prevalence of DWV. Although the bacterial endosymbiont *Wolbachia* has been previously detected in *V. destructor*, information about possible interactions of *Wolbachia* with the mite's virome is lacking. For this reason, we investigated the possible role of *Wolbachia* in the prevalence of the deformed wing virus (Grau et al., 2017). More than 180 Varroa mites from 18 colonies were tested for infection with *Wolbachia* and DWV with two sets of primers, for the outer surface-protein coding gene *wsp* or for 16S rDNA. We found a positive correlation between DWV and *Wolbachia* using the *wsp* primer, but no significant association between DWV and *Wolbachia* using the 16S rDNA primer. Our study provides no evidence for an anti-pathogenic effect of *Wolbachia* in varroa mites, but first weak evidence for a pro-pathogenic effect (Grau et al., 2017). These results encourage further studies of interactions between *V. destructor* and its bacterial endosymbiont *Wolbachia*, since an increased vector competence of the varroa mites may impact the virus load in honey bees.

***Apis mellifera* colony as a model for sublethal pesticide effects**

In the last decade, numerous studies have demonstrated that insecticides like neonicotinoids affect physiological or behavioural traits of individual honeybees (Blacquiere et al., 2012; Di Prisco et al., 2013; Fischer et al., 2014; Baines et al., 2015; Brandt et al., 2016, 2017). However, the risk assessment of neonicotinoids on colony size and survival has been divergent, ranging from negative impact (Budge et al., 2015; Tsvetkov et al., 2017; Woodcock et al., 2017; Osterman et al., 2019) to no impact (Cutler, et al. 2014; Rundlof et al., 2015; Rolke et al., 2016; Osterman et al., 2019), sometimes even in the same study (Woodcock et al., 2017). Yet, colony-level performance is of primary interest in managed honeybees since lower performance and higher rates of colony loss directly affect beekeepers and pollination services.

The inability of current risk assessment schemes to substantiate the sublethal effects of pesticides and reliably detect them in field trials (Cutler et al., 2014; Rundlof et al., 2015) may reflect two major problems. First, higher-tier field trials for the risk assessment of pesticides often lack statistical power as a consequence of the relatively low colony number (sampling size). Only well-resourced institutions or companies such as the agrochemical industry have the means to commission large-scale higher-tier field experiments. The outcome of these experiments is in most cases confidential and the data are usually not available for scientific or public evaluation. Second, the capacity of colonies to compensate for detrimental impacts of pesticides adds a layer of complexity to investigations looking for the sublethal effects of pesticides. A honey bee colony is a functionally organized cooperative group in which the tasks and activity levels of each individual are flexible and rapidly adjusted according to the

group's needs (Seeley, 1995). The large number of interacting individuals allows the colony to adaptively reallocate workforce and resources to compensate for potential negative effects on the individual level.

Risk assessment studies are usually conducted with healthy and full-sized colonies. In order to reduce the complexity, we developed a model of a honey bee colony using small nucleus colonies. By using small colonies, we substantially reduced the number of bees but maintained the social coherence of the colony (Bromenshenk et al., 1991). This allowed us to study the sublethal effects of the neonicotinoid clothianidin at the physiological level in individual larvae and nurse bees and also to determine its impact on brood development of an entire colony. We found that the royal jelly producing hypopharyngeal glands of exposed individual workers became smaller and the lipid content and antimicrobial activity of royal jelly they produced was lower. For each colony, we analysed the survival of individual larvae and measured the population of brood cells over 7 weeks. Clothianidin caused a strong dose dependent increase in the mortality of individual larvae, but the population of capped brood remained stable and declined only at the highest pesticide dose. Using a demographic matrix model, we estimated the brood production required to sustain a stable population. Colonies exposed to clothianidin more than doubled their brood initiation rate to compensate for the increased mortality. We extrapolated our findings to full-size colonies using BEEHAVE modelling and found strong effects on survival (100 µg/L) and swarming (1, 10 and 100 µg/L). We conclude colonies are able to compensate for short term detrimental effects of clothianidin on individuals by increasing the brood initiation rate at the cost of colony reproduction. In addition, with a small nucleus colony model approach, it is easy to scale up the number of colonies to achieve sufficient statistical power and to perform field trials at a fraction of the cost of semi-field/field trials with full-sized colonies, thus allowing independent research without industry funding.

This novel, sensitive model system allows the assessment of single or multiple stressors on the compensatory capacity of the colony. It will help to close the knowledge gap between laboratory cage experiments and field trials with full-sized colonies. This will facilitate not only scientific investigations, but also the regulatory testing for new pesticides.

***Osmia bicornis* as a model organism for pollinator health and non-*Apis* pesticide risk assessment**

All bees naturally suffer from a broad range of parasites and pathogens, including mites, viruses, bacteria, protozoans, and fungi. Some bee pathogens, such as *N. ceranae* and DWV can infect both honey bees and bumblebees while others, such as or *Paenibacillus larvae*, seem to be more host-specific (Genersch, 2010). The majority of research has focused on

diseases associated with honey bees or economical relevant bumblebees, with very little known about the parasites and pathogens of solitary bees (Goulson et al., 2015a).

Compromised immunity from exposure to neonicotinoids has been shown for bumblebees (Czerwinski and Sadd, 2017) and honeybees (Brandt, 2016; Brandt et al., 2017; Di Prisco et al., 2013), but information on solitary bees remains scarce. Therefore, we tested the effects of thiacloprid on the immunocompetence of *O. bicornis* females and males. We found that field-realistic concentrations of thiacloprid severely affect the immunocompetence of *O. bicornis* (Brandt et al., in preparation). Males exposed to thiacloprid at a concentration of 200 µg/kg or more show a reduction in hemocyte density. Moreover, the antimicrobial activity of the hemolymph is impaired in males. Interestingly, in females, only a concentration of 555 µg/kg elicited similar immunosuppressive effects. Although males are smaller than females, they consume more food solution. This leads to a higher thiacloprid exposure in males, which may explain the different concentration thresholds observed between the sexes. In contrast to honeybee workers and queens, where thiacloprid reduced the melanisation/wound healing response, thiacloprid does not affect melanisation in *O. bicornis* in the tested, field realistic concentrations.

Investigating the effects of pesticides on the immunocompetence of non-*Apis* bee taxa is relevant. Several studies have demonstrated that different bee species have different sensitivities to pesticides (Sgolastra et al. 2017). Moreover, honey bees and bumblebees are eu-social species. Social bees are assumed to be less vulnerable to pesticides because negative effects at the individual level can be compensated by the rest of the colony (Rundlof et al. 2015, Straub et al. 2015). These differences between species underscore the need to include non-*Apis* species like *O. bicornis* or *O. cornuta* in pesticide risk assessment schemes (Arena and Sgolastra, 2014; Rundlof et al., 2015; Woodcock et al., 2017). The European Food Safety Authority (EFSA, 2012) proposed the red mason bee *O. bicornis* along with *O. cornuta* as a model species in their Guidance Document on the risk assessment of plant protection products on bees (EFSA, 2012). Although males are exposed to pesticides via nectar ingestion, however, in the current guidelines and risk assessment schemes, only females are considered in ecotoxicological studies.

Conclusions

The impairment of the immunocompetence by pesticides like neonicotinoids opens the way to the spread of parasites and pathogens, which ultimately are the proximate mortality factors of bees (Sanchez-Bayo, 2016). Our investigations on the immunocompetence of honey bee worker and queens as well as on *O. bicornis* females and males complement similar findings on the immunosuppressive effects of neonicotinoids on worker bees (Di Prisco et al., 2013). Currently, regulatory requirements for evaluating pesticide risks to bees do not consider sublethal effects on the immune defence (EFSA, 2012). Given the key importance of bee health and survival on ecosystem productivity and food production, the general lack of knowledge concerning sub-lethal effects of pesticides on the immune system is alarming. Our findings highlight the vulnerability of bees to common neonicotinoid pesticides, and demonstrate the need for future studies to identify relevant measures of bee health and disease susceptibility. The improvement of our understanding of the immunocompetence of individual bees as well as the health and fitness of bee colonies could provide new insights into the stress factors and their interactions that threaten honeybee survival, and help us to design strategies to protect them (Brandt et al., 2017; Sanchez-Bayo, 2016).

4. References

- Alaux, C., Brunet, J.L., Dussaubat, C., Mondet, F., Tchamitchan, S., Cousin, M., Brillard, J., Baldy, A., Belzunces, L.P., and Le Conte, Y. (2010). Interactions between *Nosema* microspores and a neonicotinoid weaken honeybees (*Apis mellifera*). *Environmental microbiology* 12, 774-782.
- Alburaki, M., Cheaib, B., Quesnel, L., Mercier, P.L., Chagnon, M., and Derome, N. (2016). Performance of honeybee colonies located in neonicotinoid-treated and untreated cornfields in Quebec. *Journal of Applied Entomology*.
- Ankeny, R.A., and Leonelli, S. (2011). What's so special about model organisms? *Studies in History and Philosophy of Science Part A* 42, 313-323.
- Arena, M., and Sgolastra, F. (2014). A meta-analysis comparing the sensitivity of bees to pesticides. *Ecotoxicology* 23, 324-334.
- Ayali, A., and Yerushalmi, Y. (2010). Locust research in the age of model organisms: Introduction to the Special issue in honor of M.P. Pener's 80th birthday. *Journal of Insect Physiology* 56, 831-833.
- Bascompte Jordi, P.J., Jens M. Olesen (2006). Asymmetric Coevolutionary Networks Facilitate Biodiversity Maintenance. *Science* 312, 431-443.
- Blacquiere, T., Smagghe, G., van Gestel, C.A., and Mommaerts, V. (2012). Neonicotinoids in bees: a review on concentrations, side-effects and risk assessment. *Ecotoxicology* 21, 973-992.
- Brandt, A., Gorenflo, A., Siede, R., Meixner, M., Büchler, R. (2016). The Neonicotinoids Thiacloprid, Imidacloprid and Clothianidin affect the immunocompetence of Honey Bees (*Apis mellifera* L.) *Journal of insect physiology* 86, 40-47.
- Brandt, A., Grikscheit, K., Siede, R., Grosse, R., Meixner, M.D., and Buchler, R. (2017). Immunosuppression in Honeybee Queens by the Neonicotinoids Thiacloprid and Clothianidin. *Scientific reports* 7, 4673.
- Brandt, A., Joop, G., and Vilcinskas, A. (2019). *Tribolium castaneum* as a whole-animal screening system for the detection and characterization of neuroprotective substances. *Archives of insect biochemistry and physiology*, e21532.
- Brandt, A., Krohne, G., and Grosshans, J. (2008). The farnesylated nuclear proteins KUGELKERN and LAMIN B promote aging-like phenotypes in *Drosophila* flies. *Aging Cell* 7, 541-551.
- Brandt, A., Papagiannouli, F., Wagner, N., Wilsch-Brauninger, M., Braun, M., Furlong, E.E., Loserth, S., Wenzl, C., Pilot, F., Vogt, N., *et al.* (2006). Developmental control of nuclear size and shape by Kugelkern and Kurzkern. *Curr Biol* 16, 543-552.
- Brandt, A., and Vilcinskas, A. (2013). The Fruit Fly *Drosophila melanogaster* as a Model for Aging Research. *Advances in biochemical engineering/biotechnology* 135, 63-77.
- Brandt A., S., M., Bischoff, G., Büchler R. (2018). Imidacloprid-Abbau in lebenden und toten Bienen. . *Bienen & Natur/Die Biene/ADIZ/Imkerfreund* 2, 22-24.
- Bromenshenk, J., Gudatis, J., Carlson, S., Thomas, J., and Simmons, M. (1991). Population dynamics of honey bee nucleus colonies exposed to industrial pollutants. *Apidologie*, 2, 359 - 369.

- Collison, E., Hird, H., Cresswell, J., and Tyler, C. (2016). Interactive effects of pesticide exposure and pathogen infection on bee health - a critical analysis. *Biological reviews of the Cambridge Philosophical Society* *91*, 1006-1019.
- Cresswell, J.E., Robert, F.X., Florance, H., and Smirnov, N. (2014). Clearance of ingested neonicotinoid pesticide (imidacloprid) in honey bees (*Apis mellifera*) and bumblebees (*Bombus terrestris*). *Pest management science* *70*, 332-337.
- Cutler, G.C., Scott-Dupree, C.D., Sultan, M., McFarlane, A.D., and Brewer, L. (2014). A large-scale field study examining effects of exposure to clothianidin seed-treated canola on honey bee colony health, development, and overwintering success. *PeerJ* *2*, e652.
- Czerwinski, M.A., and Sadd, B.M. (2017). Detrimental interactions of neonicotinoid pesticide exposure and bumblebee immunity. *Journal of Experimental Zoology Part A: Ecological and Integrative Physiology* *327*, 273-283.
- Davis, R.H. (2004). The age of model organisms. *Nature Reviews Genetics* *5*, 69.
- de Miranda, J.R., and Genersch, E. (2010). Deformed wing virus. *Journal of invertebrate pathology* *103 Suppl 1*, S48-61.
- Desneux, N., Decourtye, A., and Delpuech, J.M. (2007). The sublethal effects of pesticides on beneficial arthropods. *Annual review of entomology* *52*, 81-106.
- Di Prisco, G., Cavaliere, V., Annoscia, D., Varricchio, P., Caprio, E., Nazzi, F., Gargiulo, G., and Pennacchio, F. (2013). Neonicotinoid clothianidin adversely affects insect immunity and promotes replication of a viral pathogen in honey bees. *Proceedings of the National Academy of Sciences of the United States of America* *110*, 18466-18471.
- EFSA (2012). Scientific opinion on the science behind the development of a risk assessment of plant protection products on bees (*Apis mellifera*, *Drosophila* spp. and solitary bees). *EFSA : J10*, 2668.
- Elbert, A., Haas, M., Springer, B., Thielert, W., and Nauen, R. (2008). Applied aspects of neonicotinoid uses in crop protection. *Pest management science* *64*, 1099-1105.
- European Food and Safety Authority (EFSA) (2013). Guidance on the risk assessment of plant protection products on bees (*Apis mellifera*, *Bombus* spp. and solitary bees). *EFSA Journal* *11*, 3295.
- Evans, J.D., Aronstein, K., Chen, Y.P., Hetru, C., Imler, J.L., Jiang, H., Kanost, M., Thompson, G.J., Zou, Z., and Hultmark, D. (2006). Immune pathways and defence mechanisms in honey bees *Apis mellifera*. *Insect molecular biology* *15*, 645-656.
- Feltham, H., Park, K., Minderman, J., and Goulson, D. (2015). Experimental evidence that wildflower strips increase pollinator visits to crops. *Ecology and evolution* *5*, 3523-3530.
- Fortini, M.E., Skupski, M.P., Boguski, M.S., and Hariharan, I.K. (2000). A survey of human disease gene counterparts in the *Drosophila* genome. *The Journal of cell biology* *150*, F23-30.
- Gallai, N., Salles, J.-M., Settele, J., and Vaissière, B.E. (2009). Economic valuation of the vulnerability of world agriculture confronted with pollinator decline. *Ecological Economics* *68*, 810-821.

- Garibaldi, L.A., Steffan-Dewenter, I., Winfree, R., Aizen, M.A., Bommarco, R., Cunningham, S.A., Kremen, C., Carvalheiro, L.G., Harder, L.D., Afik, O., *et al.* (2013). Wild pollinators enhance fruit set of crops regardless of honey bee abundance. *Science* *339*, 1608-1611.
- Genersch, E. (2010). Honey bee pathology: current threats to honey bees and beekeeping. *Applied microbiology and biotechnology* *87*, 87-97.
- Genersch, E., von der Ohe, W., Kaatz, H., Schroeder, A., Otten, C., Büchler, R., Berg, S., Ritter, W., Mühlen, W., Gisder, S., *et al.* (2010). The German bee monitoring project: a long term study to understand periodically high winter losses of honey bee colonies*. *Apidologie* *41*, 332-352.
- Goldman, R.D., Shumaker, D.K., Erdos, M.R., Eriksson, M., Goldman, A.E., Gordon, L.B., Gruenbaum, Y., Khuon, S., Mendez, M., Varga, R., *et al.* (2004). Accumulation of mutant lamin A causes progressive changes in nuclear architecture in Hutchinson-Gilford progeria syndrome. *Proc Natl Acad Sci U S A* *101*, 8963-8968.
- Goodman, C.S., and Bate, M. (1981). Neuronal development in the grasshopper. *Trends in Neurosciences* *4*, 163-169.
- Goulson, D., Nicholls, E., Botias, C., and Rotheray, E.L. (2015a). Bee declines driven by combined stress from parasites, pesticides, and lack of flowers. *Science* *347*, 1255957.
- Goulson, D., Nicholls, E., Rotheray, E., and Botias, C. (2015b). Qualifying pollinator decline evidence-response. *Science* *348*, 982.
- Grau, T., Brandt, A., DeLeon, S., Meixner, M.D., Strauss, J.F., Joop, G., and Telschow, A. (2017). A Comparison of *Wolbachia* Infection Frequencies in Varroa With Prevalence of Deformed Wing Virus. *Journal of insect science (Online)* *17*.
- Gruenbaum, Y., Margalit, A., Goldman, R.D., Shumaker, D.K., and Wilson, K.L. (2005). The nuclear lamina comes of age. *Nat Rev Mol Cell Biol* *6*, 21-31.
- Grunwald, S., Adam, I.V., Gurmai, A.M., Bauer, L., Boll, M., and Wenzel, U. (2013). The Red Flour Beetle *Tribolium castaneum* as a Model to Monitor Food Safety and Functionality. *Advances in biochemical engineering/biotechnology* *135*, 111-122.
- Grunwald, S., Gurmai, A.M., Schuierer, K., Boll, M., and Wenzel, U. (2014). The red flour beetle *Tribolium castaneum* allows for the convenient determination of fitness and survival as a measure of toxic effects of the food contaminant acrylamide. *Food Addit Contam Part A Chem Anal Control Expo Risk Assess* *31*, 1826-1833.
- Hennekam, R.C. (2006). Hutchinson-Gilford progeria syndrome: review of the phenotype. *Am J Med Genet A* *140*, 2603-2624.
- Henry, M., Beguin, M., Requier, F., Rollin, O., Odoux, J.F., Aupinel, P., Aptel, J., Tchamitchian, S., and Decourtye, A. (2012). A common pesticide decreases foraging success and survival in honey bees. *Science* *336*, 348-350.
- Iwasa, T., Motoyama, N., Ambrose, J.T., and Roe, R.M. (2004). Mechanism for the differential toxicity of neonicotinoid insecticides in the honey bee, *Apis mellifera*. *Crop Protection* *23*, 371-378.
- James, R.R., and Xu, J. (2012). Mechanisms by which pesticides affect insect immunity. *Journal of invertebrate pathology* *109*, 175-182.

- Keil, T.A., and Steinbrecht, R.A. (2010). Insects as model systems in cell biology. *Methods in cell biology* 96, 363-394.
- Kennedy, C.M., Lonsdorf, E., Neel, M.C., Williams, N.M., Ricketts, T.H., Winfree, R., Bommarco, R., Brittain, C., Burley, A.L., Cariveau, D., *et al.* (2013). A global quantitative synthesis of local and landscape effects on wild bee pollinators in agroecosystems. *Ecology letters* 16, 584-599.
- Klein, A.-M., Vaissière, B. E., Cane, J. H., Steffan-Dewenter, I., Cunningham, S. A., Kremen, C. (2007). Importance of pollinators in changing landscapes for world crops. In *Proceedings of the Royal Society of London B: Biological Sciences* pp. 303–313.
- Knorr, E., Bingsohn, L., Kanost, M.R., and Vilcinskas, A. (2013). *Tribolium castaneum* as a model for high-throughput RNAi screening. *Advances in biochemical engineering/biotechnology* 136, 163-178.
- Kritsky, G. (2017). Beekeeping from Antiquity Through the Middle Ages. *Annual review of entomology* 62, 249-264.
- Levy, A., and Currie, A. (2015). Model Organisms Are Not Models. *British Journal for the Philosophy of Science* 66, 327 - 348.
- Martin, S.J. (2001). The role of Varroa and viral pathogens in the collapse of honey bee colonies: a modelling approach. *J Appl Ecol* 38.
- Matsuda, K., Buckingham, S.D., Kleier, D., Rauh, J.J., Grauso, M., and Sattelle, D.B. (2001). Neonicotinoids: insecticides acting on insect nicotinic acetylcholine receptors. *Trends in pharmacological sciences* 22, 573-580.
- Mazumdar, A., and Mazumdar, M. (2002). How one becomes many: blastoderm cellularization in *Drosophila melanogaster*. *Bioessays* 24, 1012-1022.
- Menzel, R. (2012). The honeybee as a model for understanding the basis of cognition. *Nature Reviews Neuroscience* 13, 758.
- Michel, P.P., Ruberg, M., and Hirsch, E. (2006). Dopaminergic Neurons Reduced to Silence by Oxidative Stress: An Early Step in the Death Cascade in Parkinson's Disease? *Science's STKE* 2006, pe19-pe19.
- Motta, E.V.S., Raymann, K., and Moran, N.A. (2018). Glyphosate perturbs the gut microbiota of honey bees. *Proceedings of the National Academy of Sciences of the United States of America* 115, 10305-10310.
- Nazzi, F., Brown, S.P., Annoscia, D., Del Piccolo, F., Di Prisco, G., Varricchio, P., Della Vedova, G., Cattonaro, F., Caprio, E., and Pennacchio, F. (2012). Synergistic parasite-pathogen interactions mediated by host immunity can drive the collapse of honeybee colonies. *PLoS pathogens* 8, e1002735.
- Negri, P., Maggi, M., Szawarski, N., Lamattina, L., and Eguaras, M. (2014). *Apis mellifera* haemocytes in-vitro, What type of cells are they? Functional analysis before and after pupal metamorphosis. *Journal of Apicultural Research* 53, 576-589.
- OECD (2017). Test No. 245: Honey Bee (*Apis mellifera* L.), Chronic Oral Toxicity Test (10-Day Feeding).

- Oeppen, J., and Vaupel, J.W. (2002). Demography. Broken limits to life expectancy. *Science* 296, 1029-1031.
- Partridge, L., and Gems, D. (2002). The evolution of longevity. *Curr Biol* 12, R544-546.
- Pettis, J.S., Rice, N., Joselow, K., vanEngelsdorp, D., and Chaimanee, V. (2016). Colony Failure Linked to Low Sperm Viability in Honey Bee (*Apis mellifera*) Queens and an Exploration of Potential Causative Factors. *PLoS one* 11, e0147220.
- Pettis, J.S., vanEngelsdorp, D., Johnson, J., and Dively, G. (2012). Pesticide exposure in honey bees results in increased levels of the gut pathogen *Nosema*. *Die Naturwissenschaften* 99, 153-158.
- Pisa, L.W., Amaral-Rogers, V., Belzunces, L.P., Bonmatin, J.M., Downs, C.A., Goulson, D., Kreutzweiser, D.P., Krupke, C., Liess, M., McField, M., *et al.* (2015). Effects of neonicotinoids and fipronil on non-target invertebrates. *Environmental science and pollution research international* 22, 68-102.
- Potts, S.G., Biesmeijer, J.C., Kremen, C., Neumann, P., Schweiger, O., and Kunin, W.E. (2010a). Global pollinator declines: trends, impacts and drivers. *Trends in ecology & evolution* 25, 345-353.
- Potts, S.G., Roberts, S.P.M., Dean, R., Marris, G., Brown, M.A., Jones, R., Neumann, P., and Settele, J. (2010b). Declines of managed honey bees and beekeepers in Europe. *Journal of Apicultural Research* 49, 15-22.
- Prokocimer, M., Davidovich, M., Nissim-Rafinia, M., Wiesel-Motiuk, N., Bar, D.Z., Barkan, R., Meshorer, E., and Gruenbaum, Y. (2009). Nuclear lamins: key regulators of nuclear structure and activities. *Journal of cellular and molecular medicine* 13, 1059-1085.
- Rosenkranz, P., von der Ohe, W., Moritz, R.F.A., Genersch, E., Buechler, R., Berg, S., and Otten, C. (2014). Schlussbericht: Deutsches Bienenmonitoring – “DeBiMo” 2011–2013.
- Rundlof, M., Andersson, G.K.S., Bommarco, R., Fries, I., Hederstrom, V., Herbertsson, L., Jonsson, O., Klatt, B.K., Pedersen, T.R., Yourstone, J., *et al.* (2015). Seed coating with a neonicotinoid insecticide negatively affects wild bees. *Nature* 521, 77-80.
- Russell, J.J., Theriot, J.A., Sood, P., Marshall, W.F., Landweber, L.F., Fritz-Laylin, L., Polka, J.K., Olfiferenko, S., Gerbich, T., Gladfelter, A., *et al.* (2017). Non-model model organisms. *BMC Biology* 15, 55.
- Sanchez-Bayo, F., and Goka, K. (2014). Pesticide Residues and Bees – A Risk Assessment. *PLoS one* 9, e94482.
- Sanchez-Bayo, F., Goulson, D., Pennacchio, F., Nazzi, F., Goka, K., and Desneux, N. (2016). Are bee diseases linked to pesticides? - A brief review. *Environment international* 89-90, 7-11.
- Santos, C.M. (2012). New agents promote neuroprotection in Parkinson's disease models. *CNS & neurological disorders drug targets* 11, 410-418.
- Schott, M., Bischoff, G., Eichner, G., Vilcinskas, A., Buechler, R., Meixner, M.D., and Brandt, A. (2017). Temporal dynamics of whole body residues of the neonicotinoid insecticide imidacloprid in live or dead honeybees. *Scientific reports* 7, 6288.
- Seeley, T. (1995). *The wisdom of the hive* (London, England: Harvard University Press).

- Seidel, C., and Bicker, G. (2002). Developmental expression of nitric oxide/cyclic GMP signaling pathways in the brain of the embryonic grasshopper. *Brain research Developmental brain research* 138, 71-79.
- Simon-Delso, N., Amaral-Rogers, V., Belzunces, L.P., Bonmatin, J.M., Chagnon, M., Downs, C., Furlan, L., Gibbons, D.W., Giorio, C., Girolami, V., *et al.* (2015). Systemic insecticides (neonicotinoids and fipronil): trends, uses, mode of action and metabolites. *Environmental science and pollution research international* 22, 5-34.
- Simon-Delso, N., San Martin, G., Bruneau, E., and Hautier, L. (2018). Time-to-death approach to reveal chronic and cumulative toxicity of a fungicide for honeybees not revealed with the standard ten-day test. *Scientific reports* 8, 7241.
- Strand, M.R. (2008). The insect cellular immune response. *Insect Science* 15, 1-14.
- Suchail, S., De Sousa, G., Rahmani, R., and Belzunces, L.P. (2004a). In vivo distribution and metabolism of ¹⁴C-imidacloprid in different compartments of *Apis mellifera* L. *Pest management science* 60, 1056-1062.
- Suchail, S., Debrauwer, L., and Belzunces, L.P. (2004b). Metabolism of imidacloprid in *Apis mellifera*. *Pest management science* 60, 291-296.
- Tomizawa, M., and Casida, J.E. (2011). Unique neonicotinoid binding conformations conferring selective receptor interactions. *Journal of agricultural and food chemistry* 59, 2825-2828.
- van der Zee, R., Gray, A., Pisa, L., and de Rijk, T. (2015). An Observational Study of Honey Bee Colony Winter Losses and Their Association with *Varroa destructor*, Neonicotinoids and Other Risk Factors. *PloS one* 10, e0131611.
- Van Engelsdorp, D., Meixner, M. (2010). A historical review of managed honey bee populations in Europe and the United States and the factors that may affect them. *Journal of Invertebrate Pathology*, 15.
- vanEngelsdorp, D., Hayes, J., Jr., Underwood, R.M., and Pettis, J. (2009). A Survey of Honey Bee Colony Losses in the U.S., Fall 2007 to Spring 2008. *PloS one* 3, e4071.
- vanEngelsdorp, D., Tarpy, D.R., Lengerich, E.J., and Pettis, J.S. (2013). Idiopathic brood disease syndrome and queen events as precursors of colony mortality in migratory beekeeping operations in the eastern United States. *Preventive veterinary medicine* 108, 225-233.
- von Frisch, K. (1974). Decoding the language of the bee. *Science* 185, 663-668.
- von Frisch, K. (1994). [The "language" of bees and its utilization in agriculture. 1946]. *Experientia* 50, 406-413.
- Whitehorn, P.R., O'Connor, S., Wackers, F.L., and Goulson, D. (2012). Neonicotinoid pesticide reduces bumble bee colony growth and queen production. *Science* 336, 351-352.
- Whitworth, A.J., Wes, P.D., and Pallanck, L.J. (2006). *Drosophila* models pioneer a new approach to drug discovery for Parkinson's disease. *Drug discovery today* 11, 119-126.
- Williams, G.R., Troxler, A., Retschnig, G., Roth, K., Yanez, O., Shutler, D., Neumann, P., and Gauthier, L. (2015). Neonicotinoid pesticides severely affect honey bee queens. *Scientific reports* 5, 14621.

- Winston, M.L. (1987). *The Biology of the Honey Bee* (Harvard University Press).
- Woodcock, B.A., Bullock, J.M., Shore, R.F., Heard, M.S., Pereira, M.G., Redhead, J., Ridding, L., Dean, H., Sleep, D., Henrys, P., *et al.* (2017). Country-specific effects of neonicotinoid pesticides on honey bees and wild bees. *Science* 356, 1393-1395.
- Wu, J.Y., Smart, M.D., Anelli, C.M., and Sheppard, W.S. (2012). Honey bees (*Apis mellifera*) reared in brood combs containing high levels of pesticide residues exhibit increased susceptibility to *Nosema* (Microsporidia) infection. *Journal of invertebrate pathology* 109, 326-329.
- Yang, X., and Cox-Foster, D. (2005). Impact of an ectoparasite on the immunity and pathology of an invertebrate: evidence for host immunosuppression and viral amplification. *Proc Natl Acad Sci USA* 102.

Current Biology

The background of the cover is a dense field of microscopic cells. Each cell has a bright blue outline and a red nucleus, set against a black background. The cells are scattered across the entire page, creating a textured, patterned effect.

Volume 16 Number 6

March 21, 2006

**Control of Nuclear
Size and Shape**

Developmental Control of Nuclear Size and Shape by *kugelkern* and *kurzkern*

Anneli Brandt,^{1,*} Fani Papagiannouli,¹
Nicole Wagner,² Michaela Wilsch-Bräuninger,³
Martina Braun,⁴ Eileen E. Furlong,⁴ Silke Loserth,²
Christian Wenzl,¹ Fanny Pilot,⁵ Nina Vogt,⁶
Thomas Lecuit,⁵ Georg Krohne,² and Jörg Großhans¹

¹Zentrum für Molekulare Biologie der Universität
Heidelberg (ZMBH)

Im Neuenheimer Feld 282
69120 Heidelberg
Germany

²Biozentrum
Universität Würzburg
Am Hubland
97074 Würzburg
Germany

³Max-Planck-Institut für Molekulare Zellbiologie
und Genetik
Pfotenhauerstr. 108
01307 Dresden
Germany

⁴European Molecular Biology Laboratory
Meyerhofstrasse 1
69117 Heidelberg
Germany

⁵Institut de Biologie du Développement
de Marseille (IBDM)
Laboratoire de Génétique et de Physiologie
du Développement (LGPD)
Centre National de la Recherche Scientifique
Unité Mixte de Recherche 6545
Université de la Méditerranée
Campus de Luminy, case 907
13288 Marseille Cedex 09
France

⁶Max-Planck-Institut für Entwicklungsbiologie
Spemannstr. 35,
72076 Tübingen
Germany

Summary

Background: The shape of a nucleus depends on the nuclear lamina, which is tightly associated with the inner nuclear membrane and on the interaction with the cytoskeleton. However, the mechanism connecting the differentiation state of a cell to the shape changes of its nucleus are not well understood. We investigated this question in early *Drosophila* embryos, where the nuclear shape changes from spherical to ellipsoidal together with a 2.5-fold increase in nuclear length during cellularization.

Results: We identified two genes, *kugelkern* and *kurzkern*, required for nuclear elongation. In *kugelkern*- and *kurzkern*-depleted embryos, the nuclei reach only half

the length of the wild-type nuclei at the end of cellularization. The reduced nuclear size affects chromocenter formation as marked by Heterochromatin protein 1 and expression of a specific set of genes, including early zygotic genes. *kugelkern* contains a putative coiled-coil domain in the N-terminal half of the protein, a nuclear localization signal (NLS), and a C-terminal CxxM-motif. The carboxyterminal CxxM motif is required for the targeting of *kugelkern* to the inner nuclear membrane, where it colocalizes with lamins. Depending on the farnesylation motif, expression of *kugelkern* in *Drosophila* embryos or *Xenopus* cells induces overproliferation of nuclear membrane.

Conclusions: *kugelkern* is so far the first nuclear protein, except for lamins, that contains a farnesylation site. Our findings suggest that *kugelkern* is a rate-determining factor for nuclear size increase. We propose that association of farnesylated *kugelkern* with the inner nuclear membrane induces expansion of nuclear surface area, allowing nuclear growth.

Introduction

The morphology of nuclei varies among different developmental stages, tissues, and cell-cycle states. Age-related alterations of nuclear shape, accompanied by loss of peripheral heterochromatin, have been found in *C. elegans* [1] as well as in human cell lines [2]. Abnormalities in nuclear size and shape are frequently observed in malignant tissues [3] or in patients with nuclear envelopathies or certain progeria syndromes [2]. In addition, there is growing evidence that the nuclear lamina has not only structural but also functional impact on the cell by regulating chromatin configuration and influencing gene expression (for review, see [4]). The mechanisms that link the morphology of the nucleus to the developmental program of a cell have not been much analyzed (for review, see [4, 5]).

The shape of a nucleus depends on the nuclear lamina, which is thought to provide mechanical support for the nuclear membrane (NM) and to mediate attachment of interphase chromatin to the nuclear envelope [6, 7]. The lamina consists of a meshwork of nuclear-specific intermediate filaments, the lamin proteins, plus numerous lamin-associated proteins (for review, see [4, 7]). Targeting and association of lamins with the inner membrane is mediated by an evolutionary conserved farnesylation of the CxxM motif at their C termini (for review, see [8, 9]).

In *Drosophila* development, there is a definite event of nuclear shape change, accompanied by massive nuclear growth during the process of cellularization [10]. During cellularization, all cortical nuclei are simultaneously enclosed into membranes, and there is a marked change in the shape of the nuclei from spherical to ellipsoid together with a 2.5-fold increase in nuclear length [11, 12]. The mechanisms and components involved have remained elusive.

*Correspondence: a.haase@zmbh.uni-heidelberg.de

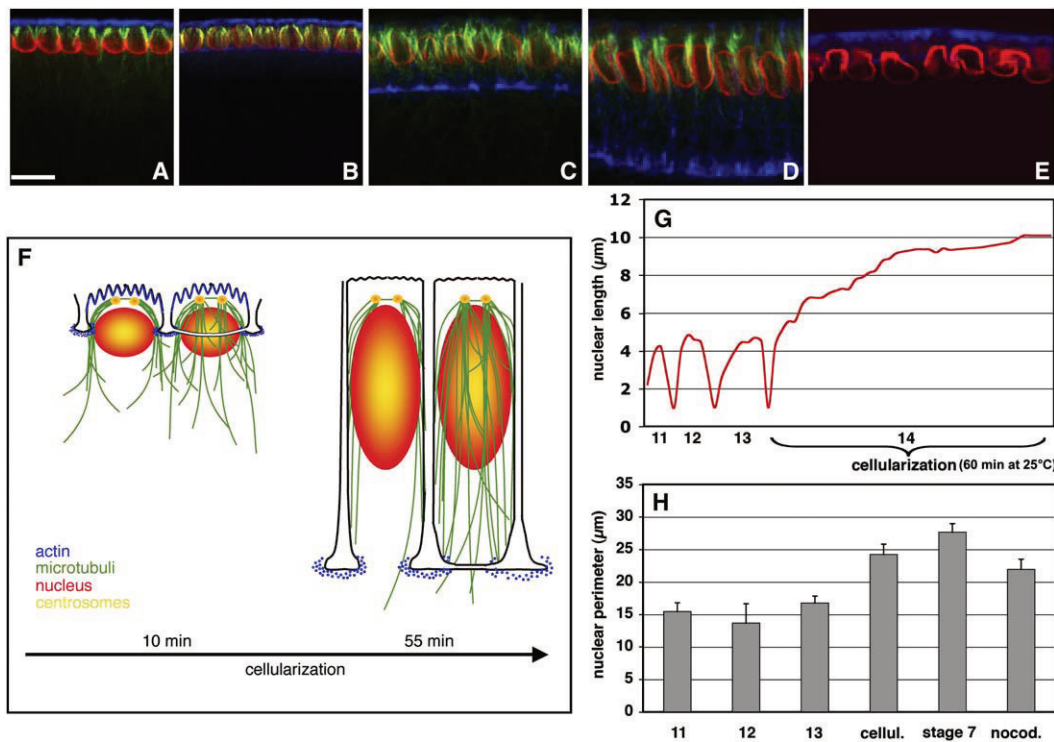


Figure 1. Nuclear Shape Change during Cellularization

(A–E) Wild-type embryos during cellularization stained for Kuk (red), F-actin (blue), and microtubules (green). The scale bar represents 10 μm . (E) Nocodazole-treated embryo; note the absence of microtubuli (green). (F) Schematic overview of cellularization. (G) Kinetics of nuclear length (apical-basal axis) during cell cycles 11 to 14. (H) Perimeter of interphase nuclei in different cell cycles, in gastrulation (stage 7) or in nocodazole-treated embryos. $n = 30$ for each group, error bars = standard deviation. For untreated (cellul.) versus nocodazole-treated (nocod.) embryos: $n = 30$, nondirectional Mann-Whitney test, $p > 0.05$, $U_A = 580$, $z = -1.91$. For cycle-13 embryos versus nocodazole-treated embryos: $n = 30$, nondirectional Mann-Whitney test, $p < 0.01$, $U_A = 867$, $z = -6.16$.

The early syncytial blastoderm is characterized by rapid nuclear division cycles, transcriptional silencing, and a homogeneous appearance of the chromatin. At the transition from syncytial to cellular blastoderm, the cell cycle is paused, the transcription rate increases, and chromatin loses its uniform appearance. This change in chromatin organization is highlighted by the appearance of a conspicuous chromocenter [13]. Strikingly, this reorganization of the chromatin takes place during cycle 14 and coincides with the strong increase of zygotic transcription and nuclear elongation.

Results

Nuclear Elongation during Cellularization

During cellularization, the shape of the nuclei changes from spherical to ellipsoidal together with a 2.5-fold increase in nuclear length from approximately 4 μm up to 10 μm (Figures 1A–1D, 1F, and 1G). A rearrangement of the microtubuli-based cytoskeleton accompanies membrane invagination and nuclear shape change [11]. As the nucleus assumes an elongated appearance, microtubules extend in close association with the nucleus, mirroring nuclear growth in both direction and rate [11]. To determine whether the nuclear growth depends on microtubules, we treated staged embryos with the

microtubule (MT) polymerization inhibitor nocodazole. After incubation in nocodazole, the nuclei maintained a rounded, irregular shape although their nuclear surface area increased significantly in size (Figures 1E and 1H). Confirming data from [14], we found that MT function is essential for the shape change of the nuclei from spherical to ellipsoidal but not for the nuclear growth.

kugelkern and *kurzkern* Are Required for Nuclear Elongation

We identified two genes required for the process of nuclear elongation in independent screens for genes involved in blastoderm formation. *kugelkern* (*kuk*) was identified by its early zygotic expression (see Experimental Procedures). In embryos injected with *kuk* dsRNA (designated *kuk* embryos) or from *kuk*-deficient females (Figures S1A and S1B in the Supplemental Data available online), the cortical nuclei are spherical by the end of cellularization (Figure 2A). The nuclei reached only the same length as in previous interphases (4 μm) as compared to wild-type nuclei that finally reached 10 μm in length (Figure 2B). Nevertheless, the cellularization front invaginated with the same velocity as in wild-type embryos. Microtubules and the actin cytoskeleton seemed to be unaffected (Figure 2A, compare to Figure 1D). We could not find any obvious

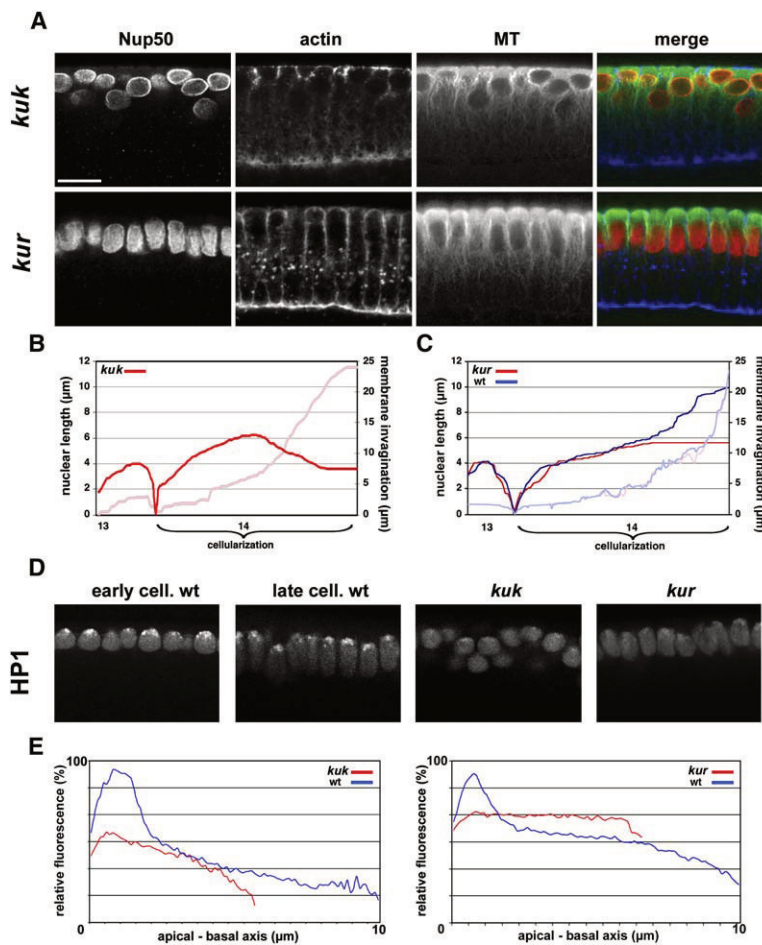


Figure 2. Phenotype of *kuk* and *kur*

(A) *kuk*-RNAi-treated embryo and *kur* embryos at the end of cellularization stained with anti-Nup50 (red), anti- α -Tubulin (green) antibodies, and phalloidin (blue); the scale bar represents 10 μ m.

(B and C) Kinetics of nuclear length increase and membrane invagination during interphases of cell cycles 13 and 14. Blue line shows nuclear length of wild-type embryos; red line shows *kuk*-deficient embryos (B) or *kur* embryos (C). Length of invaginated membrane is depicted in light blue (wt) and light red (*kuk/kur*).

(D) HP1 staining in wild-type at early and late cellularization or in *kuk* and *kur* embryos late during cellularization.

(E) Relative fluorescence of HP1 staining along the apical-basal axis of the nuclei in wild-type *kuk* (RNAi-treated) and *kur* embryos.

morphological differences between *kuk* and wild-type embryos with regard to the positioning of the nuclei by the end of cellularization (data not shown). *kuk* is not an essential gene, because *kuk*-deficient flies are viable and fertile.

In embryos from *kurzkern* (*kur*) germline clones (*kur* embryos), nuclear elongation was significantly reduced. There was no visible defect prior to cellularization in *kur* embryos when compared to wild-type embryos (Figure 2C). The nuclei of *kur* mutants started to elongate normally in the first half of cellularization. When the invaginating membrane front reached the basal outline of the nuclei, the first retardation compared to the wild-type situation was observed (Figure 2C). Finally, the nuclei accomplished only approximately 60% of the length of wild-type nuclei at the end of cellularization (Figures 2A and 2C). However, in contrast to the wild-type situation, *kur* nuclei did not move basally at the end of cellularization. During gastrulation, *kur* embryos fail to form the cephalic furrow and do not accomplish germband extension; this is comparable to the germband-extension phenotype of *eve* described by [15]. Because this gastrulation phenotype was different from that found in *kuk* embryos, it may represent a second function of *kur* independent of the earlier nuclear-elongation function. In conclusion, we identified two genes, *kuk* and *kur*, that are required for nuclear elongation during cellularization.

kuk and *kur* Affect Chromocenter Formation and Correct Gene Expression

During cellularization, a chromocenter is formed by centromeric heterochromatin, which remains condensed even in interphases [13]. At early stages of development, the chromatin is homogenous in appearance and the heterochromatin marker Heterochromatin protein 1 (HP1) is present throughout the nucleoplasm (Figure 2D). During cellularization, HP1 accumulates at the apical-located chromocenter, whereas reduced amounts of the protein are present basally in the nucleus (Figure 2D, [13]).

In *kuk* or *kur* embryos, the formation of a distinct chromocenter was impaired. In many nuclei, the strong apical HP1 staining was absent (Figure 2D). In only few nuclei, a very weakly stained chromocenter was detectable when compared to the wild-type situation at the same stage of development. Conspicuously, HP1 staining was still relatively homogeneously distributed throughout the nucleoplasm (Figure 2E).

For determining whether *kuk* and *kur* have an effect on gene expression, the genome-wide expression profiles in *kuk* and *kur* mutant embryos were compared to those of stage-matched wild-type embryos. We only selected genes with greater than 2-fold change in both genetic conditions. This revealed 96 genes with significant changes in gene expression (Tables S1 and S2). Interestingly, the set of downregulated genes ($n = 88$) is strongly enriched for early zygotic genes ($n = 23$), which

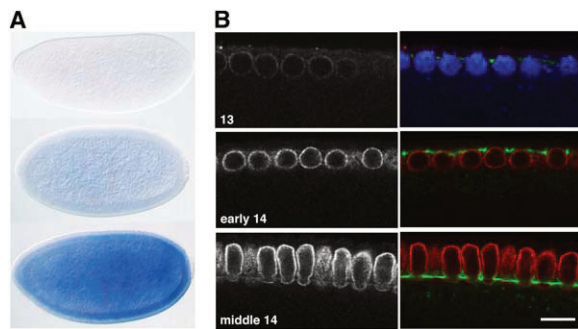


Figure 3. Expression Pattern of *kuk*
(A) In situ hybridization for *kuk* RNA. Embryos prior to pole-cell formation, in cycle 13, and in early cycle 14 (from top).
(B) Wild-type embryos in stages as indicated and stained with Kuk antibody (white, red). The tip of the invaginating membrane is marked by Slam staining (green), and DNA is stained by Dapi (blue, only shown in the upper-right panel). The scale bar represents 10 μ m.

are induced during cellularization, e.g., *nullo*, *serendipity α* , *slam*, *bottleneck*, or *frühstart*. In conclusion, in both *kuk* and *kur* embryos, the heterochromatin organization was affected and gene expression was altered. In the following, we will concentrate on the function of *kuk*, because we have not yet revealed the molecular nature of *kur*.

***kuk* Encodes a Coiled-Coil Protein with Nuclear Localization Signal and CxxM Motif**

kuk encodes a protein of 570 amino acid (aa) residues. It contains a putative coiled-coil domain in the N-terminal half of the protein, a nuclear localization signal (NLS), and a C-terminal CxxM-motif, a putative site for farnesylation (Figure S2A). Kuk is so far the first described nuclear protein (see below), except for lamins, that contains a CxxM motif. Comparison with Kuk from other *Drosophila* species revealed an aa identity of 43% between Kuk from *D. melanogaster* and *D. virilis*. By Blast search, we found in the genomes of *Aedes aegyptii* and *Anopheles gambiae* two homologous, not-yet-annotated sequences (Figure S2B), which contained a conserved NLS together with a C-terminal CxxM motif but no obvious coiled-coil region. We did not find any homologous sequences in nonarthropod species.

In wild-type embryos, there is only weak expression of *kuk* during the first 13 division cycles (Figure 3A). In early interphase of cycle 14, *kuk* expression increased significantly. However, in pole cells, *kuk* expression remained constantly low during cellularization. Thus, increase of *kuk* transcription coincides with nuclear elongation.

Localization of Kuk Protein in Embryos

On a cellular level, Kuk appears to be exclusively localized to the nuclear envelope (Figure 3B). The electron-microscope analysis confirmed the nuclear-envelope localization and clearly showed that Kuk exclusively localizes to the nucleoplasmic side (Figures 4A–4C). As observed by confocal microscopy, Kuk staining only partially overlapped with nuclear pores visualized by antibodies against the nuclear-pore marker Nup50 (Figure 4D). The electron-microscope analysis,

however, revealed that Kuk staining is not present at nuclear pores (Figures 4A and 4C).

The antibody staining is specific because RNAi-injected embryos, embryos from *kuk* females (data not shown), and cultured *Drosophila* cells treated with *kuk* dsRNA (see below) lose the nuclear envelope staining for Kuk. Furthermore, the antibody detects recombinant Kuk protein expressed in reticulocyte lysate and *E. coli* as well as endogenous Kuk in extracts from wild-type embryos but not *kuk*-deficient embryos in western blots (Figure S1C).

The immunohistological localization of Kuk was confirmed by biochemical fractionation of embryos. Kuk and Dm0, the *Drosophila* lamin B, were both highly enriched in the nuclear fraction together other nuclear proteins (Figure 5A). Kuk and Dm0 were both not extracted with high-salt but with high-pH buffer (carbonate), consistent with a membrane anchorage by a farnesyl residue. However, Dm0 required higher salt concentration than Kuk for extraction in the presence of 1% triton, suggesting that Kuk in this respect behaves differently than Dm0 and is not part of salt-stable complexes.

The increase of Kuk protein levels during cellularization is comparable to the increase of the mRNA expression levels. In early division cycles 10–13, Kuk staining was very weak (Figure 3E). It strongly increased in early interphase of cycle 14, when cellularization started (Figure 3E). Throughout cellularization, all somatic nuclei showed prominent Kuk staining. The pole cells showed a staining pattern distinct from that of somatic cells. During cycles 10–14, Kuk labeling was absent from the majority of the pole cells (Figure S3A). During mitosis, *kuk* localizes differently than Dm0 or the nuclear-pore marker antibody A141 (Figure S3B). The presence of Kuk in growing late-telophase or interphase nuclei may suggest a function in nuclear-membrane growth.

The localization of some [16] but not all [17] lamina proteins depends on Dm0. In *Dm0*-RNAi-treated cells, the localization of Kuk in the nuclear envelope was indistinguishable from that in control cells (Figures 5B and 5C). However, the localization of Otefin, a Dm0 interacting protein of the INM [18], was changed after *Dm0*-RNAi treatment, confirming the depletion of Dm0. No alterations in the Dm0 localization were observed in *kuk*-RNAi-treated cells. We conclude that Kuk targeting to the nucleoplasmic side of the nuclear envelope and its retention in this subcompartment is independent of Dm0.

***Kuk* Overexpression in Embryos Results in Highly Lobulated Nuclei**

To study the activity of *kuk* in embryos, we injected *kuk* mRNA and fixed the embryos in blastoderm stage. The nuclei became strongly lobulated and wrinkled already early in cellularization (Figure 6B), whereas uninjected embryos possessed smooth, unruffled nuclear envelopes (Figure 6A). Similarly, embryos from transgenic flies with six copies of the *kuk* gene showed very ruffled and abnormally shaped nuclei (Figure 6F). Thus, overexpression of *kuk* resulted in a changed morphology that may be a consequence of extensive growth of the nuclear envelope. In later stages, during gastrulation, moderately wrinkled and lobulated nuclear shapes are typical for interphase nuclei (Figure 6D). In contrast, nuclei

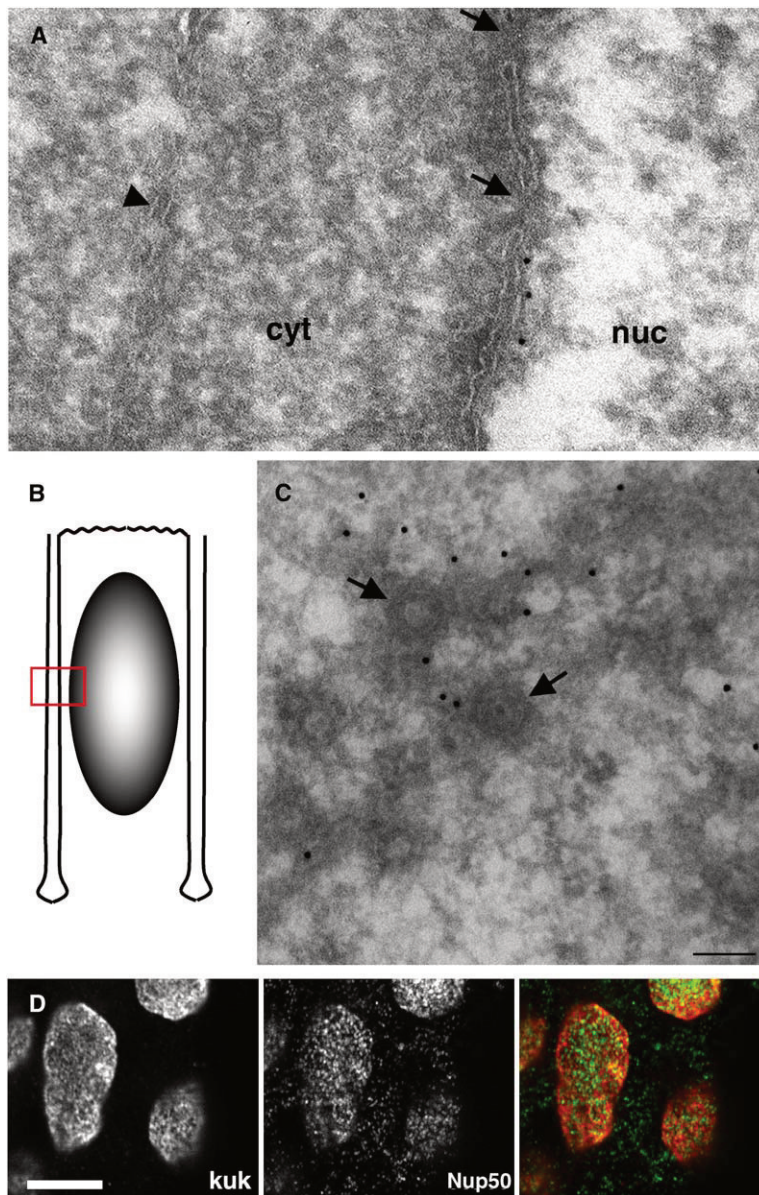


Figure 4. Localization of Kuk

(A) Immunoelectron microscopic analysis of embryonic nuclei reveals localization of Kuk at the inner nuclear membrane (black dots, 10 nm gold particles); arrows indicate nuclear pores, and arrowheads indicate cytoplasmic membranes; cyt denotes cytoplasm, and nuc denotes nucleoplasm.

(B) Schematic drawing of nucleus and invaginating membrane. Red rectangle indicates position of section shown in (A).

(C) Immunolabeling with Kuk antibodies in a tangential section of a nucleus (10 nm gold particles). Several nuclear pores (arrows) are visible (scale bar represents 100 nm). Kuk does not localize to nuclear pores.

(D) Amnioserosa nuclei from late embryos double-labeled with Kuk (red) and Nup50 (green) antibodies. The scale bar represents 5 μ m.

in *kuk*-RNAi-treated embryos or embryos from *kuk* females were round and unruffled (Figure 6E). In conclusion, we observed a correlation of the expression of *kuk* and ruffled nuclear morphology.

To test whether *kur* functions independently of *kuk*, we injected *kuk* dsRNA into *kur* embryos. However, there was no visible alteration from the *kuk* phenotype in those RNAi-treated embryos. When we overexpressed *kuk* mRNA in *kur* embryos, a comparable phenotype to overexpression in wild-type embryos was observed (Figure 6C). This indicates that *kur* may function either upstream or independently of *kuk*.

kuk Affects Nuclear Morphology in *Xenopus* Cells

Kuk localizes exclusively to the nuclear envelope when expressed in *Xenopus* A6 cells (Figures 6G–6J). The transfected nuclei became significantly larger (nuclear perimeter is almost doubled, $p < 0.001$, Figure 7G), and the nuclear envelope was more folded, containing

deep indentations, compared to nuclei of untransfected control cells (Figures 6G–6J). Costaining for Kuk and XLam B2 revealed strict colocalization of Kuk with lamin B2 over the entire nuclear envelope, including additional intranuclear structures (Figures 6G and 6H). The costaining with Concanavalin A indicates that these intranuclear structures contain membranes and may represent deep indentations of the nuclear envelope (Figures 6I and 6J; [19–21]).

A drastic nuclear-surface enlargement accompanied by the presence of membranous structures inside the nucleus (Figure 6K) was observed by transmission electron microscopy. These additional structures within the nucleus (Figure 6L, asterisks) consisted of double membranes that enclose membrane profiles and ribosomes, structures typical for the cytoplasmic compartment. There were no obvious nuclear pores visible in these intranuclear membranes. Conclusively, the ectopic expression of *kuk* in A6 cells caused primarily nuclear

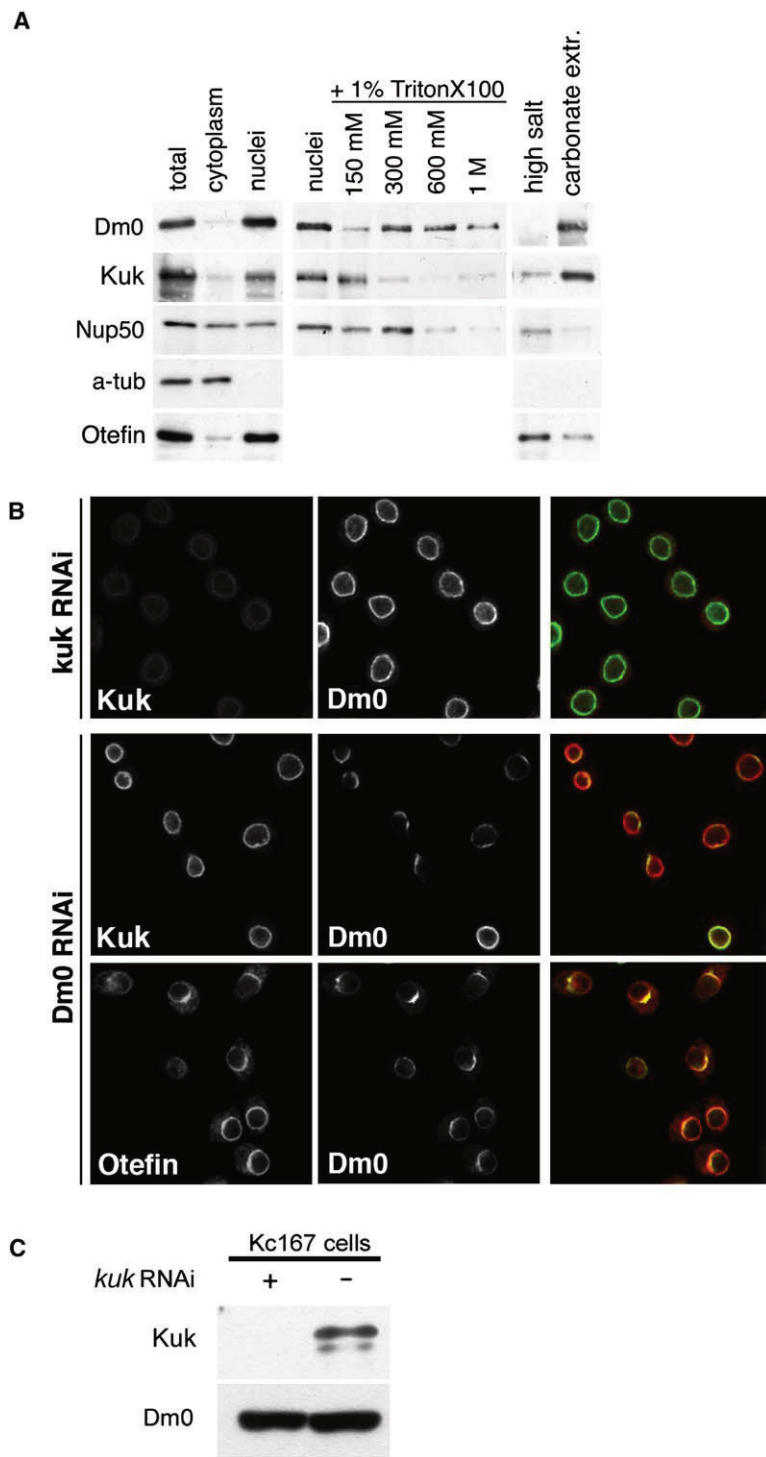


Figure 5. Kugelkern and LaminDm0 Have Independent Functions

(A) Subcellular fractionation and sequential extraction with increasing concentrations of NaCl (α -tub, α - tubulin).

(B) Downregulation of *kuk* and *Dm0*. *Drosophila* Kc167 cells treated with *kuk* or *Dm0* dsRNA were stained for Kuk (white, red), Dm0 (white, green), and Otefin (white, red) as indicated.

(C) Extracts of Kc167 cells treated with *kuk* dsRNA analyzed by western blot with indicated antibodies.

growth that manifests in an extended nuclear surface together with an altered morphology of the nucleus. The activity of *kuk* in *Xenopus* cells suggests that *kuk* employs a conserved mechanism to control nuclear morphology.

All Three Motifs Are Required for Kuk Activity

To characterize the function of the three different structural components of Kuk in detail, we expressed a series of truncated proteins and a nonfarnesylatable mutant

version of Kuk (KukSxxM, Figure 7F). Kuk-SxxM and the deletion protein C489 were distributed evenly throughout the nucleoplasm and did not affect nuclear size and shape (Figure 7A). Deletion proteins missing the NLS were homogeneously localized in the cell (Figure 7C, mutant C328). Deletion proteins lacking N-terminal aa residues (N136, N275) were located at the nuclear envelope. However, alterations in nuclear morphology were only present in cells expressing a mutant that contained the coiled-coil region (N136, Figures 7D and 7G).

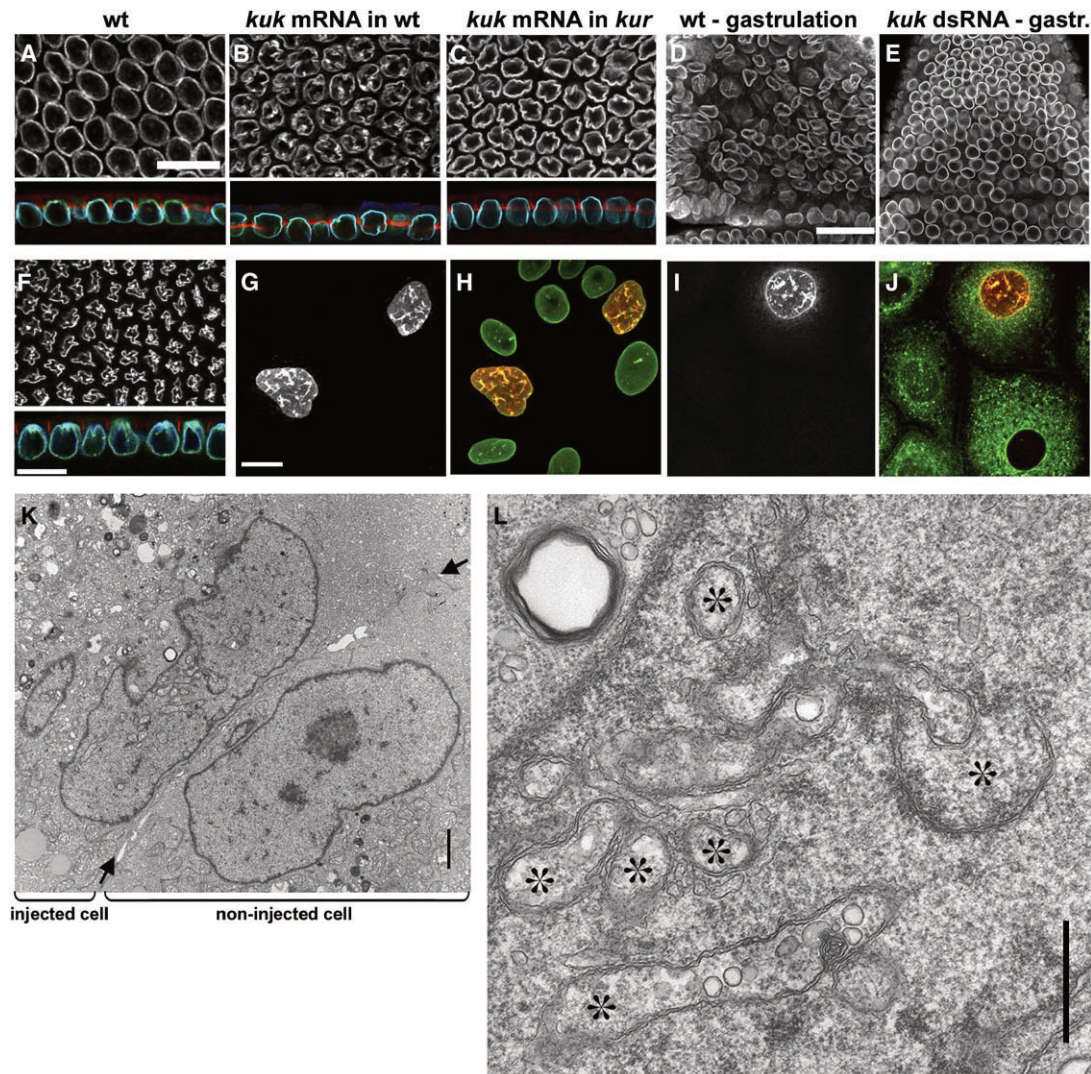


Figure 6. *kugelkern* Induces Nuclear-Membrane Growth

(A–C) Tangential (upper panels) and longitudinal (lower panels) section of embryos ([A], wild-type; [B], wild-type injected with *kuk* mRNA; [C], *kur* embryos injected with *kuk* mRNA) early in cellularization, stained for Kuk (white, green), Dm0 (blue), and f-actin (red). (D and E) Anterior region of a wild-type and *kuk*-RNAi-treated embryo during gastrulation, stained with Dm0. The scale bar (D and E) represents 25 μ m. (F) Embryo with six copies of *kuk* early in cellularization, stained for Kuk (white, green), Dm0 (blue), and Dlg (red). (G–J) Kuk expression in *Xenopus* A6 cells. Cells transfected with full-length *kuk* construct were stained for Kuk (white, red), XLam B2 ([G], green), and membranes (ConcanavalinA, [J], green). The scale bar represents 10 μ m. (K and L) Intranuclear structures analyzed by transmission electron microscopy. (K) Ultrathin section of a *kuk*-injected and an uninjected control cell. The cell borders are indicated by arrows. The scale bar represents 1 μ m. (L) Higher magnification of the *kuk*-expressing nucleus in (G). The lumina of the tubular structures (asterisk) contain vesicles and ribosomes. The scale bar represents 0.5 μ m.

Other C-terminal (C153) or N-terminal (N437) deletion mutants lacking most of the molecule were localized in the nucleoplasm as well as the cytoplasm and did not influence the nuclear morphology (Figure 7F). Thus, all three motifs together are required for the morphogenetic activity of Kuk.

Discussion

The morphology of the nuclei changes dramatically during cellularization. We confirmed [14] that nuclear size indeed increases independently of MT. Thus, nuclear shape change and nuclear growth may be two separate

processes, regulated independently. We favor the model that nuclear size increase is a nuclear-autonomous process and the growing nuclei are directed passively by the MT basket into an ellipsoidal shape.

What may be the function of Kuk during cellularization? Although the nuclear size increase is impaired in *kuk*- and *kur*-depleted embryos, no other defects, e.g., concerning plasma-membrane invagination or the actin cytoskeleton, are observed. Consistent with the hypothesis that in *kuk* embryos a nuclear-intrinsic process is affected, we find that Kuk exclusively localizes to the INM. Because *kuk* and *kur* embryos show divergent phenotypes during gastrulation, we deduce that *kur* has during

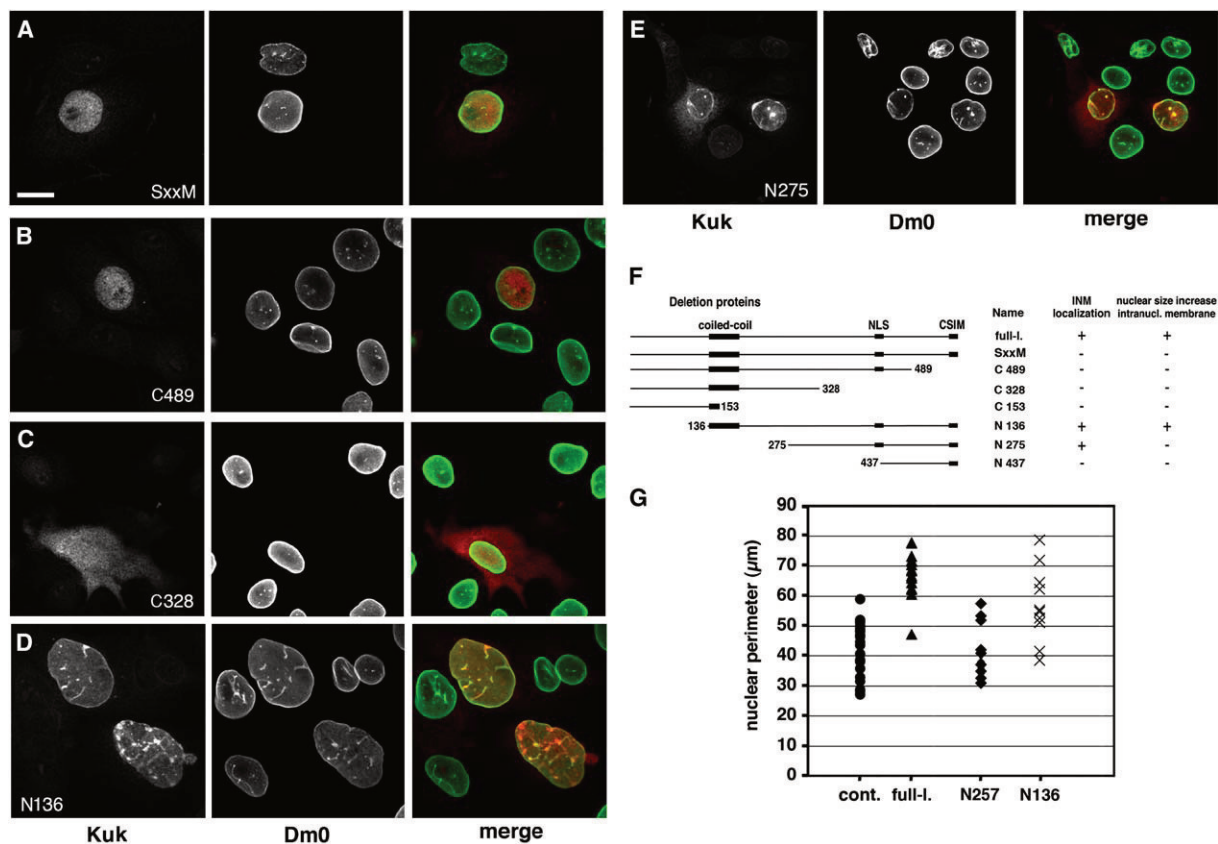


Figure 7. Deletion Mutants of *kuk* Expressed in *Xenopus* A6 Cells

(A–E) *Xenopus* A6 cells transfected with indicated *kuk* constructs and stained for Kuk (white, red) and XLam B2 (white, green).

(F) Schematic overview of the deletion constructs and summary of their activity. NLS denotes nuclear localization signal, and CSIM denotes farnesylation motif. (+) indicates localization of the expressed *kuk* construct to the nuclear envelope (INM) or whether larger nuclei with intranuclear structures were induced.

(G) Quantification of nuclear size by measuring the nuclear perimeter. Bidirectional Mann-Whitney test was applied to *kuk* full-length versus control cells (*kuk*: n = 16, control: n = 30; p < 0.001, $U_A = 14$, z = 5.2), N136 versus control cells (n = 10, p = 0.0005, $U_A = 212$, z = -3.46), and N275 versus control cells (n = 16, p = 0.992, $U_A = 191$, z = 0.01).

development a second, unknown function unrelated to the nuclear-elongation phenotype during cellularization. Insight into the function of *kuk* has to await its molecular characterization.

Kuk shares some structural features, such as the nuclear localization signal (NLS), a coiled-coil domain, and the C-terminal CxxM-motif, with B type lamins. Interestingly, up to now, lamins were the only known nuclear proteins possessing a farnesyl moiety [22]. In addition to these similarities, *Kuk* exhibits properties distinct from that of lamins.

The overexpression of *Kuk* in embryos results in a nuclear morphology comparable to that found in gastrulating wild-type embryos. In contrast, *kuk*-depleted gastrulating embryos have smooth and unwrinkled nuclei typical for earlier stages. Thus, the overexpression phenotype of *kuk* may reflect precocious growth of the nuclear envelope. In *Xenopus* cells, *Kuk* induces additional membrane growth, the nuclei become larger, and the nuclear envelope is highly lobulated. By analyzing deletion constructs and a nonfarnesylated mutant of *Kuk*, we demonstrated that all three motifs, the coiled-coil region, the NLS, and the CxxM motif together are required for the morphogenetic activity of *Kuk*. These findings are

consistent with data from lamin-overexpression experiments in cultured mammalian, amphibian, or fish cells. In these studies, all lamin variants that contain an NLS together with the farnesylation motif show conspicuous overproliferation of NM [19, 22].

It seems unlikely that *kuk* takes part in the general phospholipid synthesis or membrane transport machinery, because in *kuk* embryos we see normal plasma-membrane invagination during cellularization. Most likely, *kuk* is part of a mechanism specific for nuclei. In principle, two different mechanisms are conceivable: (1), a catalytic function, where *Kuk* might induce membrane growth indirectly by activating effector components; and (2), a structural function, where *Kuk* might have a direct effect on the structure of the phospholipid bilayer. Insertion of farnesylated *Kuk* or Lamin B, acting like a wedge, would lead to a modification of the inner phospholipid layer by increasing the lateral packing stress of the membrane. This deformation in turn could induce incorporation of new phospholipids and thus allow expansion of the nuclear-membrane surface area. Consistent with this second model is our estimation of the number of *Kuk* molecules per nucleus ($>10^4$ /nucleus, compared to $>10^5$ /nucleus of Dm0). A structural model

is supported by studies of the activity of amphiphathic proteins on nuclear morphology. Incorporation of amphiphysin [23], CTP:phosphocholine cytidyl-transferase- α (CCT α , [20]), or Nup53 [24] into the nuclear envelope induces intranuclear, tubular membranes. Moreover, CCT α and amphiphysin have been shown to affect membrane curvature in vitro [20, 23]. How increased positive membrane curvature of the INM leads to the growth of the entire nuclear envelope remains to be elucidated.

Coincidental with nuclear elongation is the onset of zygotic transcription together with the rearrangement of the chromatin architecture. Strikingly, in both *kuk* and *kur* embryos, the reorganization of the chromatin is affected. Because this difference in chromatin organization is found independently in *kuk* as well as in *kur* embryos, we conclude that this phenotype might be related to the reduced nuclear size or nuclear surface area in both mutants. HP1 is known to be associated with heterochromatin and to influence gene expression [13, 25]. It can also interact with the inner nuclear-membrane protein LBR (Lamin B receptor, [26]) and thus may represent an adaptor between nuclear lamina and chromatin [27]. Indeed, we found that gene expression is altered in *kuk* and *kur* embryos. Convincingly, a specific set of genes are downregulated in both *kuk* and *kur* embryos in parallel, which suggests a connection between reduced nuclear surface area and transcriptional regulation. It is clear, however, that the nuclear elongation is not essential but only contributes to full onset of gene expression during cellularization.

Mutations in proteins of the lamina cause a wide range of human diseases, collectively called laminopathies [5], e.g., Hutchinson-Gilford progeria syndrome (HGPS), where a dominant point mutation in the *LMNA* gene causes a premature-accelerated-aging-like disorder [28, 29]. In the HGPS cells, the *LMNA* precursor is not properly endoproteolytically processed, resulting in a mutated lamin A form that still contains a farnesylated C terminus. Cultured fibroblasts from HGPS patients show pronounced lobular nuclear shapes that correlate with defects in DNA replication and alteration in heterochromatin organization [5, 27]. Moreover, lymphocytes directly isolated from HGPS patients possess strikingly enlarged nuclei [28]. Cells depleted for the endoprotease FACE1/Zmpste24, the enzyme that cleaves the farnesylated C terminus of the premature lamin A, show similar dramatic changes in the nuclear morphology with extensively lobulated nuclei [9]. These similarities between the phenotypes of HGPS cells and cells overexpressing nuclear proteins, such as Kuk, B type lamins, or uncleaved lamin A, with a farnesylation motif might have implications for our understanding of the Hutchinson-Gilford progeria syndrome.

Conclusions

The nuclear lamina controls the shape of the nucleus but also interacts with chromatin to regulate gene expression. Analyzing the control of nuclear shape in a simple genetic system will allow better investigation of the function of the lamina and its connection to the control of gene expression. One can speculate that overexpression of Kuk or Dm0 in adult flies may cause aging-like symptoms or even influences life span. The finding

that the structural motifs coiled-coil, NLS, and CxxM are characteristic for lamins as well as for nonlamins like Kuk can help to screen for more, functionally important nuclear envelope proteins.

Experimental Procedures

General Procedures

A comprehensive and detailed description of the methods and materials can be found in the Supplemental Data.

kuk (CG5175) was identified in a project that was initiated to reveal the function of early zygotic genes and was performed in a collaboration of the laboratories of T.L and J.G. [30]. *fs(1)kur* maps to 2B17;3C6 and was isolated in a screen for blastoderm mutants (A.B., F.P. and J. G., unpublished data) from a collection of germline clone mutations (N.V., unpublished data) similar to the collection described by S. Luschnig [31]. Embryological procedures were applied according to standard protocols [32]. The microarray data were deposited to EBI MIAMExpress; see Accession Numbers.

Histology

Embryos and *Xenopus* A6 and *Drosophila* Kc167 cells were fixed and stained according to standard procedures (Supplemental Data, [19, 33]). In some cases, 0.5% Triton X-100 was added to the blocking solution to improve permeabilization.

Drug Treatment

For nocodazole treatment, dechorionated embryos were incubated for 2.5 min in n-heptane to permeabilize the vitelline membrane, briefly rinsed in PBS + 0.1% Tween, incubated for 50 min at room temperature in PBS containing 50 μ g/ml nocodazole, and subsequently fixed with FA.

Transfection and Microinjection of Cells

Cells were fixed and stained 24–48 hr after transfection. Microinjection together with a GFP construct and EM processing was performed according to [19, 33].

Microscopy

Control embryos were always mounted on the same slide and processed in parallel. For comparing the relative fluorescence levels of HP1 staining along the apical-basal axis of the nuclei, 10 nuclei in each 5 *kur*- and *kuk*-RNAi-treated embryos were evaluated.

Supplemental Data

Supplemental Data include Supplemental Experimental Procedures, three figures, and two tables and are available with this article online at: <http://www.current-biology.com/cgi/content/full/16/6/543/DC1/>.

Acknowledgments

We thank D. Görlich, K. Kapp, F. Schnorrer, M. Sedorf, and the lab members for discussions, advice, and suggestions on the manuscript. We thank Y. Kussler-Schneider for technical assistance; K. Schild for microinjection and processing for EM; S. Panier, S. Lawo, and P. Gawlinski for antibody purification and characterization and initial fractionation experiments; S. Lawo for western in Figure S3B; and D.T. and A.M. Brandt for support. We are grateful for materials, reagents, and fly stocks from D. Görlich, M. Hild, Drosophila Stock Center (Bloomington, Indiana), and Hybridoma bank (Iowa). N.V. was supported by the Boehringer Ingelheim Fonds, A.B. by a Forschungsstipendium of the Deutsche Forschungsgemeinschaft, and J.G. by the Emmy-Noether Programm of the Deutsche Forschungsgemeinschaft.

Received: December 20, 2005

Revised: January 21, 2006

Accepted: January 24, 2006

Published online: February 2, 2006

References

- Haithcock, E., Dayani, Y., Neufeld, E., Zahand, A.J., Feinstein, N., Mattout, A., Gruenbaum, Y., and Liu, J. (2005). Age-related changes of nuclear architecture in *Caenorhabditis elegans*. *Proc. Natl. Acad. Sci. USA* *102*, 16690–16695.
- Goldman, R.D., Shumaker, D.K., Erdos, M.R., Eriksson, M., Goldman, A.E., Gordon, L.B., Gruenbaum, Y., Khuon, S., Mendez, M., Varga, R., et al. (2004). Accumulation of mutant lamin A causes progressive changes in nuclear architecture in Hutchinson-Gilford progeria syndrome. *Proc. Natl. Acad. Sci. USA* *101*, 8963–8968.
- Gisselsson, D., Bjork, J., Hoglund, M., Mertens, F., Dal Cin, P., Akerman, M., and Mandahl, N. (2001). Abnormal nuclear shape in solid tumors reflects mitotic instability. *Am. J. Pathol.* *158*, 199–206.
- Gruenbaum, Y., Goldman, R.D., Meyuhos, R., Mills, E., Margalit, A., Fridkin, A., Dayani, Y., Prokocimer, M., and Enosh, A. (2003). The nuclear lamina and its functions in the nucleus. *Int. Rev. Cytol.* *226*, 1–62.
- Gruenbaum, Y., Margalit, A., Goldman, R.D., Shumaker, D.K., and Wilson, K.L. (2005). The nuclear lamina comes of age. *Nat. Rev. Mol. Cell Biol.* *6*, 21–31.
- Lenz-Böhme, B., Wismar, J., Fuchs, S., Reifegerste, R., Buchner, E., Betz, H., and Schmitt, B. (1997). Insertional mutation of the *Drosophila* nuclear lamin Dm0 gene results in defective nuclear envelopes, clustering of nuclear pore complexes, and accumulation of annulate lamellae. *J. Cell Biol.* *137*, 1001–1016.
- Cohen, M., Lee, K.K., Wilson, K.L., and Gruenbaum, Y. (2001). Transcriptional repression, apoptosis, human disease and the functional evolution of the nuclear lamina. *Trends Biochem. Sci.* *26*, 41–47.
- Krohne, G. (1998). Lamin assembly in vivo. *Subcell. Biochem.* *1*, 563–586.
- Varela, I., Cadinanos, J., Pendas, A.M., Gutierrez-Fernandez, A., Folgueras, A.R., Sanchez, L.M., Zhou, Z., Rodriguez, F.J., Stewart, C.L., Vega, J.A., et al. (2005). Accelerated ageing in mice deficient in Zmpste24 protease is linked to p53 signalling activation. *Nature* *437*, 564–568.
- Foe, V.E., Odell, G., and Edgar, B. (1993). Mitosis and morphogenesis in the *Drosophila* embryo: point and counterpoint. In *The Development of Drosophila melanogaster*, M. Bate and A. Martinez Arias, eds. (New York: Cold Spring Harbor Laboratory Press), pp. 149–300.
- Schejter, E.D., and Wieschaus, E. (1993). Functional elements of the cytoskeleton in the early *Drosophila* embryo. *Annu. Rev. Cell Biol.* *9*, 67–99.
- Sonnenblick, B.P. (1950). The early embryology of *Drosophila melanogaster*. In *Biology of Drosophila*. M. Demerec, ed. (New York: Wiley and Son), pp. 62–167.
- Kellum, R., Raff, J.W., and Alberts, B.M. (1995). Heterochromatin protein 1 distribution during development and during the cell cycle in *Drosophila* embryos. *J. Cell Sci.* *108*, 1407–1418.
- Edgar, B.A., Odell, G.M., and Schubiger, G. (1987). Cytoarchitecture and the patterning of fushi tarazu expression in the *Drosophila* blastoderm. *Genes Dev.* *1*, 1226–1237.
- Irvine, K.D., and Wieschaus, E. (1994). Cell intercalation during *Drosophila* germband extension and its regulation by pair-rule segmentation genes. *Development* *120*, 827–841.
- Wagner, N., Schmitt, J., and Krohne, G. (2004a). Two novel LEM-domain proteins are splice products of the annotated *Drosophila melanogaster* gene CG9424 (Bocksbeutel). *Eur. J. Cell Biol.* *82*, 605–616.
- Wagner, N., Weber, D., Seitz, S., and Krohne, G. (2004b). The lamin B receptor of *Drosophila melanogaster*. *J. Cell Sci.* *117*, 2015–2028.
- Goldberg, M., Lu, H., Stuurman, N., Ashery-Padan, R., Weiss, A.M., Yu, J., Bhattacharyya, D., Fisher, P.A., Gruenbaum, Y., and Wolfner, M.F. (1998). Interactions among *Drosophila* nuclear envelope proteins lamin, otefin, and YA. *Mol. Cell. Biol.* *18*, 4315–4323.
- Prüfert, K., Vogel, A., and Krohne, G. (2004). The lamin CxxM motif promotes nuclear membrane growth. *J. Cell Sci.* *117*, 6105–6116.
- Lagace, T.A., and Ridgway, N.D. (2005). The rate-limiting enzyme in phosphatidylcholine synthesis regulates proliferation of the nucleoplasmic reticulum. *Mol. Biol. Cell* *16*, 1120–1130.
- Fricke, M., Hollinshead, M., White, N., and Vaux, D. (1997). Interphase nuclei of many mammalian cell types contain deep, dynamic, tubular membrane-bound invaginations of the nuclear envelope. *J. Cell Biol.* *136*, 531–544.
- Ralle, T., Grund, C., Franke, W.W., and Stick, R. (2004). Intracellular membrane structure formations by CaaX-containing nuclear proteins. *J. Cell Sci.* *117*, 6095–6104.
- Peter, B.J., Kent, H.M., Mills, I.G., Vallis, Y., Butler, P.J., Evans, P.R., and McMahon, H.T. (2004). BAR domains as sensors of membrane curvature: the amphiphysin BAR structure. *Science* *303*, 495–499.
- Marelli, M., Lusk, C.P., Chan, H., Aitchison, J.D., and Wozniak, R.W. (2001). A link between the synthesis of nucleoporins and the biogenesis of the nuclear envelope. *J. Cell Biol.* *153*, 709–724.
- Piacentini, L., Fanti, L., Berloco, M., Perrini, B., and Pimpinelli, S.J. (2003). Heterochromatin protein 1 (HP1) is associated with induced gene expression in *Drosophila* euchromatin. *J. Cell Biol.* *161*, 671–672.
- Ye, Q., Callebaut, I., Pezhman, A., Courvalin, J.C., and Worman, H.J. (1997). Domain-specific interactions of human HP1-type chromodomain proteins and inner nuclear membrane protein LBR. *J. Biol. Chem.* *272*, 14983–14989.
- Scaffidi, P., and Misteli, T. (2005). Reversal of the cellular phenotype in the premature aging disease Hutchinson-Gilford progeria syndrome. *Nat. Med.* *11*, 440–445.
- De Sandre-Giovannoli, A., Bernard, R., Cau, P., Navarro, C., Amiel, J., Boccaccio, I., Lyonnet, S., Stewart, C.L., Munnich, A., Le Merrer, M., et al. (2003). Lamin A truncation in Hutchinson-Gilford progeria. *Science* *300*, 2055.
- Eriksson, M., Brown, W.T., Gordon, L.B., Glynn, M.W., Singer, J., Scott, L., Erdos, M.R., Robbins, C.M., Moses, T.Y., Berglund, P., et al. (2003). Recurrent de novo point mutations in lamin A cause Hutchinson-Gilford progeria syndrome. *Nature* *423*, 293–298.
- Pilot, F., Philippe, J.M., Lemmers, C., Chauvin, J.P., and Lecuit, T. (2006). Developmental control of nuclear morphogenesis and anchoring by charleston, identified in a functional genomic screen of *Drosophila* cellularisation. *Development* *133*, 711–723.
- Luschnig, S., Moussian, B., Krauss, J., Desjeux, I., Perkovic, J., and Nusslein-Volhard, C. (2004). An F1 genetic screen for maternal-effect mutations affecting embryonic pattern formation in *Drosophila melanogaster*. *Genetics* *167*, 325–342.
- Roberts, D.B. (1998). *Drosophila*, A Practical Approach. (Oxford, UK: Oxford University Press).
- Prüfert, K., Alsheimer, M., Benavente, R., and Krohne, G. (2005). The myristoylation site of meiotic lamin C2 promotes local nuclear membrane growth and the formation of intranuclear membranes in somatic cultured cells. *Eur. J. Cell Biol.* *84*, 637–646.

Accession Numbers

The microarray data were deposited to EBI MIAMExpress with the accession numbers E-TABM-75 (data) and A-MEXP-314 (array design).

The farnesylated nuclear proteins KUGELKERN and LAMIN B promote aging-like phenotypes in *Drosophila* flies

Annelly Brandt,¹ Georg Krohne² and Jörg Großhans¹

¹Zentrum für Molekulare Biologie der Universität Heidelberg (ZMBH), DKFZ-ZMBH Allianz, Im Neuenheimer Feld 282, D-69120 Heidelberg, Germany

²Div. of Electron Microscopy, Biocentre of the University, Universität Würzburg, Am Hubland, 97074 Würzburg, Germany

Summary

The nuclear lamina consists of a meshwork of lamins and lamina-associated proteins, which provide mechanical support, control size and shape of the nucleus, and mediate the attachment of chromatin to the nuclear envelope. Abnormal nuclear shapes are observed in aging cells of humans and nematode worms. The expression of *laminΔ50*, a constitutively active *lamin A* splicing variant in Hutchinson–Gilford progeria syndrome patients, leads to the lobulation of the nuclear envelope accompanied by DNA damage, and loss of heterochromatin. So far, it has been unclear whether these age-related changes are *laminΔ50* specific or whether proteins that affect nuclear shape such as KUGELKERN or LAMIN B in general play a causative role in senescence. Here we show that in adult *Drosophila* flies, the size of the nuclei increases with age and the nuclei assume an aberrant shape. Moreover, induced expression of the farnesylated lamina proteins Lamin B and Kugelkern cause aberrant nuclear shapes and reduce the lifespan of adult flies. The shorter lifespan correlates with an early decline in age-dependent locomotor behaviour. Expression of *kugelkern* or *lamin B* in mammalian cells induces a nuclear lobulation phenotype in conjunction with DNA damage, and changes in histone modification similar to that found in cells expressing *laminΔ50* or in cells from aged individuals. We conclude that lobulation of the nuclear membrane induced by the insertion of farnesylated lamina-proteins can lead to aging-like phenotypes.

Key words: aging; *Drosophila*; farnesylation; Hutchinson–Gilford Progeria Syndrome (HGPS); lifespan; nuclear lamina.

Introduction

In aging human cells as well as in old worms, progressive changes in nuclear shape take place which result in highly lobulated, folded nuclear envelopes (Haithcock *et al.*, 2005; Scaffidi & Misteli, 2006). Beside these morphological changes, age-related nuclear defects can be observed that include accumulation of DNA damage and reduced levels of heterochromatin accompanied by differences in histone modification pattern in cultured cells from old human individuals (Scaffidi & Misteli, 2006). Similar nuclear defects are known from patients with the premature aging syndrome Hutchinson–Gilford progeria (HGPS), which is caused by a dominant mutation in the lamin A gene (*LMNA*; De Sandre-Giovannoli *et al.*, 2003; Eriksson *et al.*, 2003; Scaffidi & Misteli, 2005, 2006; Capell *et al.*, 2007).

Lamins are structural proteins of the nuclear lamina, which maintain the mechanical stability and shape of the nucleus, and are thought to organize chromatin structure and provide molecular docking sites for heterochromatin (Gruenbaum *et al.*, 2003, 2005; Shumaker *et al.*, 2006; Capell *et al.*, 2007). Lamin A is also present in the nucleoplasm, where it is essential for DNA replication (Goldman *et al.*, 2004). Mutations in the human lamin A gene cause at least 11 different human diseases called laminopathies. These mutations map throughout the entire *LMNA* gene (Wiesel *et al.*, 2008). In seven of these laminopathies, the N-terminal globular domain, or the rod domain, are affected. If known, these mutations are missense mutations that result in protein misfolding or in a failure of protein assembly leading to partial or complete loss of function. For example, in Emery–Dreifuss muscular dystrophy type 2, or dilated cardiomyopathy, LAMIN A assembly is disrupted which compromises the mechanical integrity of the nucleus. Other mutations are located in the C-terminal globular domain, e.g. in Dunningan-type familial partial lipodystrophy, or in mandibulosacral dysplasia and may affect the interaction of LAMIN A with other proteins. Only in HGPS or in restrictive dermopathy is the C-terminal farnesylation site affected, which results in the presence of permanently farnesylated PRELAMIN A (or LAMINΔ50). Restrictive dermopathy can also be caused by a mutation of ZMPSTE24, the endoprotease which cleaves off the farnesylated C-terminus of prelamin A. Restrictive dermopathy is characterized by severe intrauterine growth retardation and early lethality. Premature aging, however, is only described for HGPS, or atypical Werner syndrome (AWS) patients. Mutations that lead to AWS map to the rod domain of *lamin A*. In both diseases, nuclear morphology is altered and DNA damage is impaired. The molecular mechanism of AWS is still unknown (Capell & Collins, 2006).

The *lamin A* mutation that causes HGPS changes the splicing of the primary transcript: a normally rare splicing variant of

Correspondence

Annelly Brandt, Zentrum für Molekulare Biologie der Universität Heidelberg, DKFZ-ZMBH Allianz, Im Neuenheimer Feld 282, 69120 Heidelberg, Germany. Tel.: +49 (0)6221 546867; fax: +49 (0)6221 545892; e-mail: a.brandt@zmbh.uni-heidelberg.de

Accepted for publication 17 April 2008

lamin A encoding *laminΔ50* is constitutively produced. In contrast to the normal splicing variant which loses its farnesyl residue and partly relocates from the nuclear lamina to the nucleoplasm, LAMINΔ50 is permanently inserted into the inner nuclear membrane via its farnesyl residue. Even in healthy individuals, the cryptic splicing site is sporadically active and LAMINΔ50 protein is present in aged human cells. Inhibition of the *laminΔ50*-splicing variant can reverse the nuclear defects seen in cells from aged individuals (De Sandre-Giovannoli *et al.*, 2003; Eriksson *et al.*, 2003; Scaffidi & Misteli, 2005, 2006; Capell *et al.*, 2007). Although, the levels of LAMINΔ50 do not increase during the lifetime in normal cells, it is thought that *lamin A* participates in the physiological aging process (Scaffidi & Misteli, 2006).

Aberrant nuclear shapes with nuclear envelope foldings, lobulations and extra membrane growth can be induced by *laminΔ50* but also by other permanently farnesylated nuclear proteins like B-type lamins or Kugelkern (*kuk*) (Prüfert *et al.*, 2004; Ralle *et al.*, 2004; Brandt *et al.*, 2006). Kugelkern shares some structural features of lamins, such as the C-terminal farnesylation site and a nuclear localization signal. However, it is insect specific and a homolog in vertebrates is not known. To date, it is unclear whether only *laminΔ50* is able to induce aging-like phenotypes or whether permanently farnesylated nuclear lamina proteins in general like Lamin B or Kugelkern can contribute to the aging process.

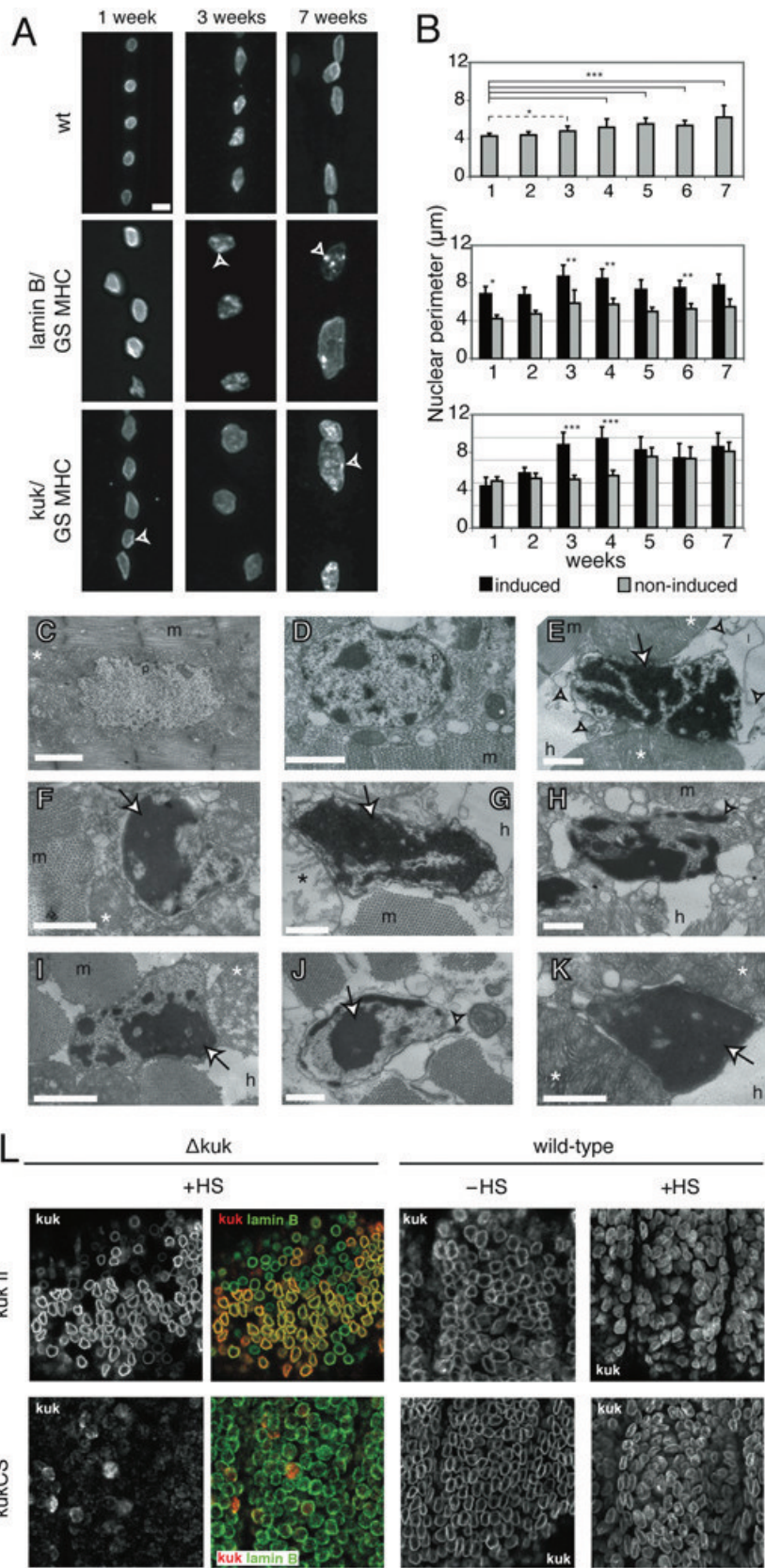
It is a matter of discussion how changes in nuclear morphology relate to cellular or organismal aging. It may be that irregular-shaped nuclei are simply a consequence of aging in cells. Alternatively, it may be that an abnormal nuclear architecture is able to promote the aging process itself. For example, in cultured HGPS cells it has been shown that loss of the H3K27me₃, a mark for facultative heterochromatin, takes place before the morphological changes of the nucleus becomes visible (Shumaker *et al.*, 2006), arguing that nuclear shape changes are a consequence of aging. To distinguish between these alternative models, we induced nuclear shape changes in a *laminΔ50*-independent way and tested their effect on age-related phenotypes on a cellular and organismal level, and on lifespan in *Drosophila* flies. Indeed, farnesylated lamina proteins like lamin B, or Kugelkern cause aberrant nuclear shapes and shorten the lifespan of flies. We provide functional evidence that *kuk* contributes to the regulation of heterochromatin formation in the fly. Moreover, even a truncated lamin B variant that only consists of the nuclear localization signal and the C-terminal farnesylation site as well as the *Drosophila*-specific *kuk* are able to induce age-related cellular defects. These new findings support a model that the nuclear lamina plays a general role for the aging process.

Results

Changes in nuclear architecture are reported for *Caenorhabditis elegans*, where in most non-neuronal cell types, massive nuclear shape changes and a loss of peripheral heterochromatin take

place as the animal ages (Haithcock *et al.*, 2005). Here, we show that the nuclear architecture in adult *Drosophila* longitudinal muscle cells undergo progressive and stochastic alteration as the fly ages (Fig. 1A–K). Most muscle nuclei in young animals were round with a smooth surface. Over time, the nuclei increased significantly in size and assumed an uneven wrinkled shape (Fig. 1A,B). When we overexpressed *lamin B* or *kuk* in adult muscle cells, we observed a significant increase in nuclear perimeter, wrinkled, lobulated nuclei, and accumulations of Kuk (Fig. 1A), or LAMIN B staining (Fig. 3A) at the nuclear envelope. Accumulations of lamina proteins in aged nuclei are also reported for *C. elegans* (Haithcock *et al.*, 2005). Muscle nuclei analysed by transmission electron microscopy (Fig. 1C–K) showed an age-dependent loss of peripheral heterochromatin and a strong increase in dark inclusions, which may contain highly condensed chromatin consistent with the data reported for *C. elegans* (Haithcock *et al.*, 2005). Moreover, there was a separation of the inner and outer nuclear membrane (Fig. 1E). In old nuclei, we found a high number of ring-like structures of less than 50 nm in diameter in the nucleoplasm (Fig. 1E), which are too small to present a complete nuclear pore. The ring-like structures were not marked by the nuclear pore-marker AB414, Lamin B, or with Kuk antibodies in immuno-electron microscopy (data not shown). No trilaminar unit-membrane structure was visible in the rings, which argues against vesicles. Although the actin/myosin array of the muscle fibres seemed to be intact in old flies (Fig. 1D,E), the number of degenerated mitochondria increased and we found organelle-free zones (Supplementary Fig. S1). In flies expressing six genomic copies of *kuk* (Fig. 1F–H) or flies conditionally expressing *lamin B* or *kuk* in the muscle tissue, loss of peripheral heterochromatin, separation of inner and outer nuclear membrane, accumulation of ring-like structures and a strong increase of dark material in the nucleoplasm were observed even in 1-week-old flies (Fig. 1F,I,J). In tissues that were not overexpressing *lamin B* or *kuk*, we found no alteration of nuclear size or shape (Supplementary Fig. S2). In conclusion, we describe age-dependent morphological changes of the nucleus in *Drosophila* flies. Moreover, these morphological alterations can be induced ahead of time by overexpression of *lamin B* or *kuk*.

In cultured *Xenopus* A6 cells, it has been shown that the farnesylation of Lamin B or Kuk is required for localization at the nuclear lamina and the induction of nuclear shape changes (Prüfert *et al.*, 2004; Brandt *et al.*, 2006). To test whether the farnesylation motif is also relevant for *kuk* activity in the fly, we first expressed the *kukCS* mutant allele which lacks its farnesylation site in *kuk* deficient embryos by heat shock and characterized its localization and action towards nuclear morphology. Consistent with the finding in cultured *Xenopus* cells, we found a predominantly nucleoplasmatic localization of KukCS protein, with only a few small dots localized to the nuclear envelope (Fig. 1L). Interestingly, when we expressed the nonfarnesylated KukCS protein in wild-type flies, we found a clear localization to the nuclear envelope. Moreover, in the wild-type background, the mutated protein was able to induce lobulation of



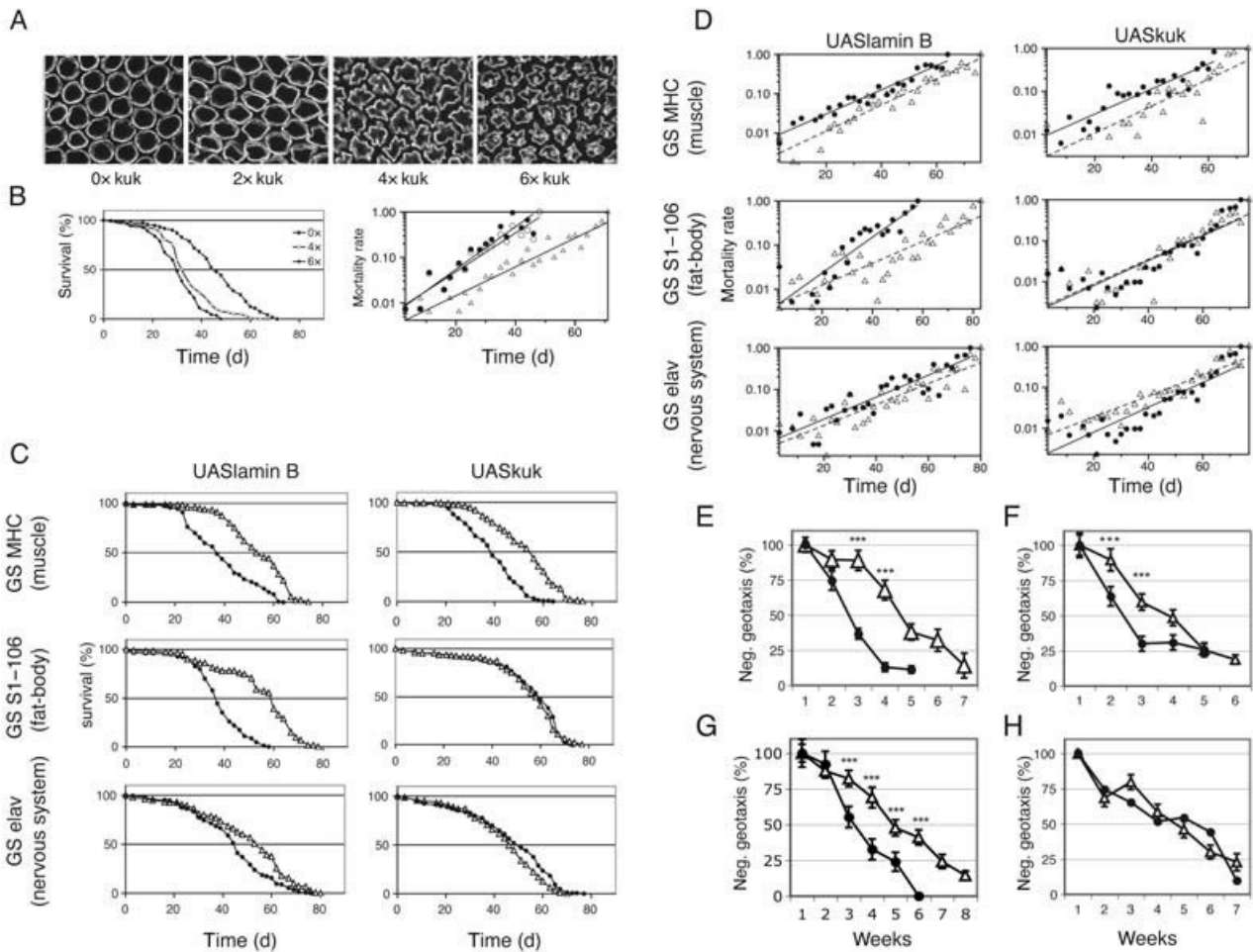


Fig. 2 Overexpression of lamina-proteins Lamin B or Kugelkern shortens *Drosophila* lifespan. (A) 0, 4 or 6 genomic copies of *kuk* in cellularizing embryos. Nuclei are stained with lamin B antibodies, apical side of nuclei in early cycle 14 are shown. In the absence of *kuk*, the nuclei are round and smooth, with increasing amounts of *kuk*, the nuclei show deep infoldings of the nuclear envelope. (B) The mean lifespan of flies is reduced when they contain 4 or 6 genomic copies of *kuk*. (C) Survival experiments of flies overexpressing lamin or *kuk* in specific tissues via the GeneSwitch system (GS) where expression is induced by RU 486 added to the food of the adult flies (solid lines and circles). Control flies have the same genotype but are not fed with RU 486 (dashed lines, open triangles). Log-rank tests compare induced and control flies. UASlamin/GS-MHC males: +RU 486, $n = 120$, 4 experiments; -RU 486, $n = 214$, 3 experiments; log-rank test: $p < 0.001$. UASlamin/GS-S1106: +RU 486, $n = 454$, 3 experiments; -RU 486, $n = 353$, 3 experiments; log-rank test: $p < 0.001$. UASlamin/GS-elav: +RU 486, $n = 441$, 3 experiments; -RU 486, $n = 421$, 3 experiments; log-rank test: $p < 0.001$. UASKuk/GS-MHC: +RU 486, $n = 558$, 5 experiments; -RU 486, $n = 811$, 7 experiments; log-rank test: $p < 0.001$. UASKuk/GS-S1106: +RU 486, $n = 454$, 3 experiments; -RU 486, $n = 353$, 3 experiments; log-rank test: $p = 0.0181$. UASKuk/GS-elav: +RU 486, $n = 441$, 3 experiments; -RU 486, $n = 421$, 3 experiments; log-rank test: $p < 0.001$. (D) Age-specific mortality rates of induced and control flies plotted on a log scale vs. time, fit by Gompertz model [$\ln(m_x) = \ln(m_0) + (ax)$], where m_x = mortality rate at age x , m_0 = baseline mortality [intercept as $\ln(m_0)$] and a = change of mortality with age (slope of the trajectory). The slope of the mortality trajectory only differed significantly between induced and control in UASlamin B/GS-S1106 flies ($p = 0.005$). Significantly different Y-intercepts between induced and control groups are found in UASlamin/GS-MHC ($p = 0.0002$), UASlamin/GS-elav ($p = 0.01$), or UASKuk/GS-MHC flies ($p = 0.04$). For detailed statistical analysis, see Supplementary Table S2. (E–H) Negative geotaxis of RU 486-induced UASlamin B/GS-MHC, UASKuk/GS-MHC, or UASKuk/GS-elav expressing flies (closed circle) as compared to un-induced control flies (open triangle). The mean distance climbed by the control flies in the first week is set as 100% negative geotaxis. (E) UASKuk/GS-MHC (3 replicate experiments). (F) UASlamin B/GS-MHC (three replicate experiments). (G) UASlamin B/GS-S1106 (3 replicate experiments). (H) UASKuk/GS-elav (1 experiment). One-way analysis of variance was followed by Bonferroni multiple comparison test ($***p < 0.001$). Statistical test are two-tailed, mean values are shown, error bars \pm SEM. Primary data of lifespan experiments are shown in Supplementary table 2.

nuclear membrane, albeit weaker than that induced by normally farnesylated Kuk (Fig. 1L). Kuk probably forms homodimers (Brandt et al., 2006). Thus, dimerization could explain the effect of *kukCS* expression in wild-type embryos where the mutant protein probably forms dimers with endogenous Kuk molecules. The finding that KukCS cannot localize to the nuclear envelope in the *kuk* deficient background and is not able to induce

nuclear lobulation argues that the farnesyl residue is indeed required for Kuk localization and function.

Having shown specific age-dependent histological changes, we now tested whether induced expression of farnesylated proteins which affect lamina structure (Prüfert et al., 2004; Ralle et al., 2004; Brandt et al., 2006) (Fig. 2A) would also provoke aging-like phenotypes. First, we tested flies containing 0, 4, or

6 genomic copies of *kuk* for their longevity. An increase in the dosage of *kuk* shortened the lifespan of the adult flies (Fig. 2B). To minimize the problem of genetic background as well as defects which may arise during development, we used tissue-specific drivers inducible with RU 486, where the difference between the experimental and control condition is the presence or absence of the inducing agent in the food of the adult flies (gene-switch system, GS) (Osterwalder *et al.*, 2001; Roman *et al.*, 2001). We found that conditional expression of *lamin B* or *kuk* in the adult muscle cells via the muscle-specific gene switch driver GS-MHC (Supplementary Fig. S3) decreased the lifespan compared to un-induced control flies of the same genotype (UAS*kuk*/GS-MHC 60%, UAS*lamin B*/GS-MHC 54% reduction of mean lifespan; Fig. 2C). Conditional expression of *lamin B* in the abdominal fat body, the fly equivalent of the liver and white adipose tissue via the GS-S1-106 driver (Hwangbo *et al.*, 2004), reduced the mean lifespan to 46% of un-induced control flies (Fig. 2C). Expression in the nervous system (UAS*lamin B*/GS-elav; Osterwalder *et al.*, 2001) from the onset of adulthood decreased the mean lifespan not significantly (90%) (Fig. 2C). The expression of *kuk* in the fat body or in the nervous system did not influence the lifespan of the adult flies significantly (Fig. 2C). The increase of mortality rates of RU 486 induced *kuk*/GS-MHC, *lamin B*/GS-MHC, and *lamin B*/GS-elav flies were similar to non-induced flies, but their onset differed (Fig. 2D, Supplementary Table S2). An increase in the initial mortality may argue for a deleterious effect of *lamin B* or *kuk* overexpression. Only in *lamin B*/GS-S1106 induced flies, we observed a change in the demographic rate of aging (Fig. 2D), which is consistent with a potential role for the aging process (Pletcher *et al.*, 2000).

The variations found between UAS*kuk* and UAS*lamin B* in the tissue-specific driver lines may be due to different expression levels or may reflect tissue-specific functions. To test whether the lifespan data correlate with the morphology of the nuclei in the *lamin B* or *kuk* expressing tissues, we examined the nuclear size in fat body cells or in the optic lamina of 3-week-old RU 486 induced flies vs. control flies (Supplementary Fig. S4). Although we did not quantify nuclear size, after visual inspection we observed an increase of nuclear size in *lamin B* expressing fat body nuclei compared to control nuclei, but no changes in nuclear size in *kuk* expressing cells (Supplementary Fig. S4A). In *lamin B* expressing neuronal tissue, we observed a general increase in nuclear size. In *kuk* expressing brains only few neurons showed changes in nuclear size (Supplementary Fig. S4C). However, we refrained from a formal quantification, since this would require a cell type-specific evaluation and an elaborate analysis of the morphology of the adult brain, which would exceed the focus of this paper. Thus, the nuclear morphology of *lamin B* or *kuk* expressing cells seems to correlate with the tissue-specific effects observed in lifespan experiments. To better analyse our system, we tested the levels of *lamin B* or *kuk* expression in induced flies and found a moderate induction of *lamin B* or *kuk* expression in the different tissues (Supplementary Fig. S5). Between the different driver lines, the GS-MHC driver showed the strongest increase in UAS*kuk* or UAS*lamin*

B expression compared to the lower induction by GS-S1106 (Supplementary Fig. S5), or the GS-elav line (data not shown). The more prominent induction of *kuk* or *lamin B* expression via the GS-MHC driver correlates with a strong effect on lifespan in these lines. Induction driven by the GS-S1106 or the GS-elav driver seems to be less pronounced and correlates with a more differential effect on lifespan. These flies appear to be more sensitive to *lamin B* than to *kuk* overexpression. In conclusion, our data argue more for a correlation of induction levels with phenotypic strength than for a tissue-specific effect of *lamin B* or *kuk* expression.

Negative geotaxis, an innate escape response during which flies climb the wall of a cylinder after being tapped to its bottom, is a well-characterized behavior that senesces in *Drosophila* (Gargano *et al.*, 2005). We found an early decline in the climbing ability in those flies that conditionally express *lamin B* in the muscle tissue, in fat body cells, or flies which express *kuk* in muscle tissue (Fig. 2E–H) but not in flies expressing *kuk* in the fat body (Supplementary Fig. S4B). Thus, the early onset of behavioral decline corresponds to the abnormal nuclear morphology, and the reduced lifespan found in these flies.

In UAS*kuk*/GS-S1106 flies we found no difference between RU486 treated or untreated control flies of the same genotype with regard to lifespan (Fig. 2C), mortality rate (Fig. 2D), negative geotaxis (Supplementary Fig. S4B), or nuclear morphology (Supplementary Fig. S4A). These findings show that RU486 by itself has no effect in the assays we used.

To investigate whether there is an increase in DNA damage in aging flies, we stained 1-week- and 5-week-old muscle tissue with the H2A.X antibody which marks foci of double-stranded DNA damage (Scaffidi & Misteli, 2005). In young flies, only occasionally H2A.X foci were present, whereas the number of muscle nuclei with numerous H2A.X foci increased when the animal became older, indicating more DNA damage (Fig. 3A). The accumulation of H2A.X foci in aging flies is consistent with similar recent observations in aged human cells, cells from patients with HGPS, or baboons and mice (Scaffidi & Misteli, 2005, 2006). To find out whether *kuk* is indeed capable of influencing gene silencing or heterochromatic spreading, we tested whether *kuk* has an effect on position effect variation (PEV) using the *w^{m4}* allele where the white gene is translocated close to the heterochromatic region of the centromere (Ebert *et al.*, 2004). We found that in heterozygous *kuk* mutants the silencing of *w^{m4}* expression was suppressed and there were patches of red-pigmented ommatidia in the fly eyes (Fig. 3B). In homozygous *kuk* mutants the suppression of PEV was pronounced and a high number of ommatidia showed the red eye pigment (Fig. 3B). These results provide functional evidence that *kuk* may contribute to the regulation of heterochromatin formation.

In cultured fibroblasts from aged individuals, in HGPS cells and in cells overexpressing *laminΔ50* aberrant shaped-nuclei, a reduction of HP1 and Tri-Me-H3K9 staining levels, and an increase in DNA damage marked by H2A.X antibodies are found (Scaffidi & Misteli, 2005, 2006). To test if the induction of these changes is a lamin A-specific function or whether other proteins

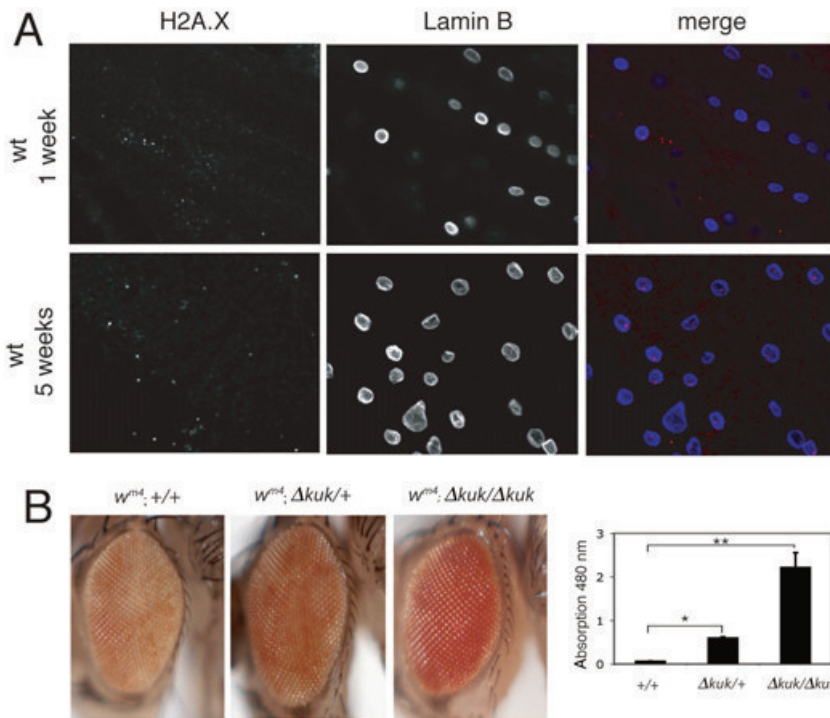


Fig. 3 DNA damage and gene silencing in adult flies. (A) H2A.X staining (red) in 1-week- or 5-week-old wild-type (wt) longitudinal muscle nuclei (lamin B, blue). Z-stacks of confocal images were fused to show several nuclei. (B) Position effect variegation of the w^{md} allele. In heterozygous kuk mutants ($w^{md}; \Delta kuc/+$) the silencing of w^{md} expression is suppressed. In homozygous kuk mutants ($w^{md}; \Delta kuc/\Delta kuc$) the suppression of PEV is even more pronounced compared to control flies ($w^{md}; +/+$). (C) Photometric measurement of the eye pigments of flies from the genotypes described in (B). $n = 50$ males per genotype, error bars show \pm SEM.

that affect nuclear lamina structure are also able to induce age-related phenotypes, we expressed *kuk* or *laminB Δ N*, a truncated *lamin B* variant which only consists of a nuclear localization signal and the C-terminal farnesylation site (Prüfert *et al.*, 2004) in mouse fibroblasts (Fig. 4A–C). Indeed, the number of H2A.X foci containing nuclei was significantly higher in the group of transfected cells compared to the control group (Fig. 4B–D). Moreover, we found a significant reduction in HP1 and Tri-Me-H3K9 staining levels in cells transfected with *kuk* or *laminB Δ N* compared to non-transfected cells (Fig. 4B–D). We conclude that *kuk* as well as *laminB Δ N* are able to induce similar cellular phenotypes as previously characterized in cultured fibroblasts from old individuals or in cells from HGPS patients (Goldman *et al.*, 2004; Liu *et al.*, 2005; Scaffidi & Misteli, 2005, 2006; Shumaker *et al.*, 2006). Strikingly, we found a strong increase in A414 staining, a marker for nucleoporins, in *laminB Δ N* or in *kuk* transfected cells, whereas the control cells showed a normal punctuated nuclear pore staining (Fig. 4B,C). Similar to the nucleoporin staining of late passage-HGPS cells reported by Goldman *et al.* (2004), we found nuclear pores aggregating to large bright masses, which were associated with the infoldings of the nuclear envelope of the highly lobulated nuclei (Fig. 4B,C). In conclusion, we show that a truncated *lamin B* construct reduced to its nuclear localization and farnesylation signal, and even the *Drosophila*-specific *kuk* are able to induce age-related nuclear changes in mammalian cells.

Discussion

Our study demonstrates, taking together the reduced lifespan, the early onset of behavioural decline, the reduced heterochro-

matin levels, and the increase in DNA damage, that expression of *kuk* or *lamin B* induces a pathology which is similar to that observed in aging flies.

So far, *Drosophila* lamins have been characterized mainly in loss-of-function situations. In *Drosophila*, a presumably null mutant of the *Drosophila lamin C* is lethal (Schulze *et al.*, 2005). *Lamin B* deletions are pupal lethal and show defects during cell proliferation, and aberrant tissue differentiation but no obvious defects in nuclear shape has been observed (Osouda *et al.*, 2005). Muñoz-Alarcón *et al.* (2007) found a negative effect of different *lamin B* or *C* loss-of-function mutations concerning the viability and physical fitness in *Drosophila*. Larvae move less and show subtle muscle phenotypes and the few surviving adults are flightless and walk slowly. Overexpression of mutant *lamin C* forms where the rod domain or the N-terminus of the protein were deleted lead to aggregation of the protein in larval salivary gland tissue. The authors found an interaction of *lamin C* with endogenous *lamin B* (Muñoz-Alarcón *et al.*, 2007). These findings may help to analyse the mechanisms of laminopathies other than HGPS where loss-of-function mutations cause the disease (e.g. Emery–Dreifuss muscular dystrophy). However, it is questionable whether these mutants can be used to study aging processes, since it is difficult to distinguish defects caused throughout development and defects directly related to aging. Muñoz-Alarcón *et al.* (2007) overexpressed *Drosophila lamin B*, or *C*, human LMNA, or *lamin Δ 50* in *Drosophila*, using the UAS/GAL system. In all of these cases viability was severely affected, resulting in low eclosing rates and early mortality. To approximate the situation in HGPS where *lamin Δ 50* acts dominantly, overexpression of the gene variants should be in a time and tissue-specific manner. The GeneSwitch system

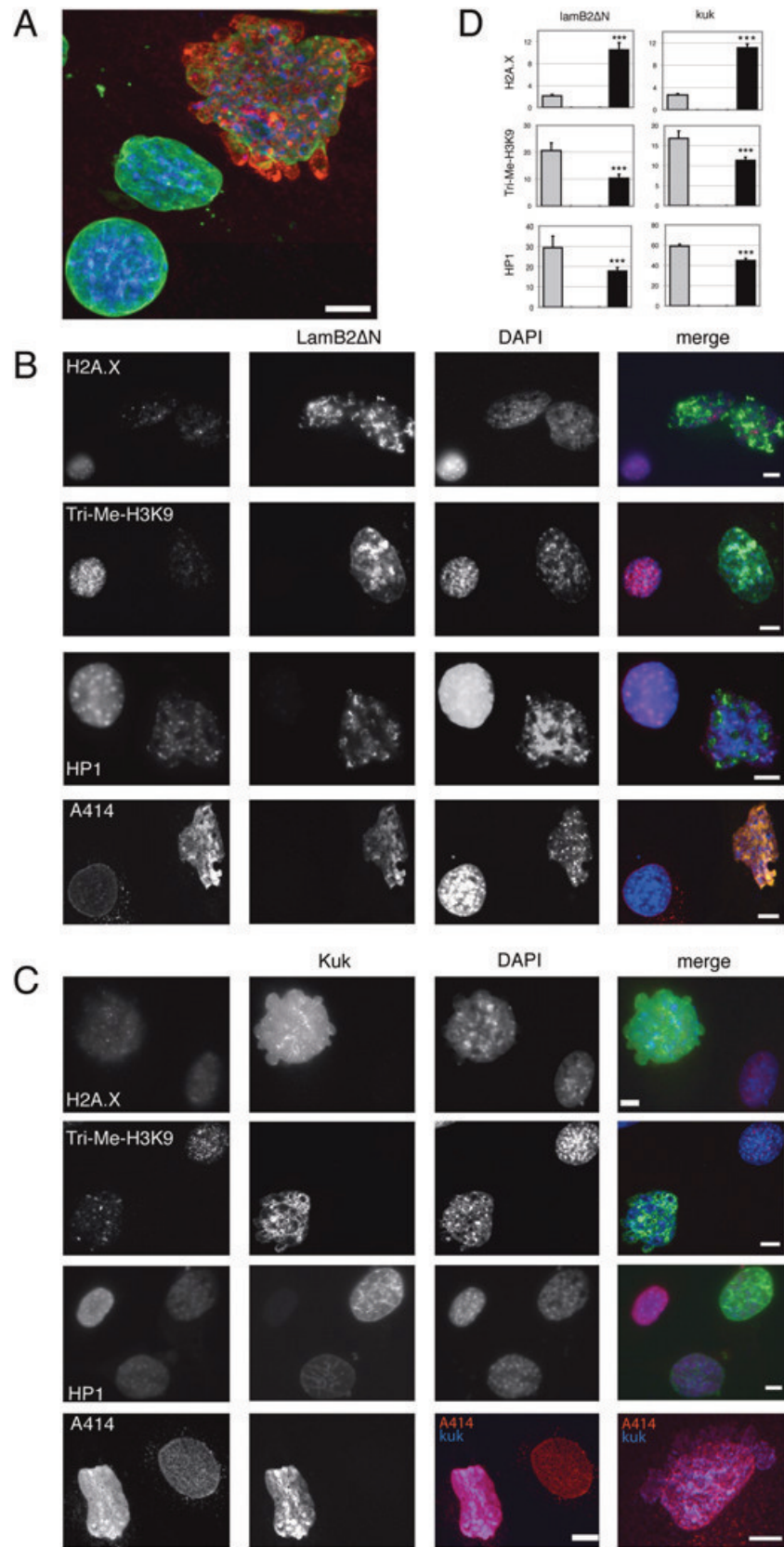


Fig. 4 Overexpression of *laminB2ΔN* or *kugelkern* induces DNA damage and changes the levels of nuclear proteins in cultured mouse fibroblast cells. (A–C) Immunofluorescence microscopy of NIH3T3 mouse fibroblasts transfected with HAkuk (*kuk*, A and C) or laminB2ΔN-GFP (*laminB2ΔN*, B). Cells were stained with DAPI (blue) and antibodies against the indicated proteins (green: laminB2ΔN-GFP, laminA/C, or HA Kuk; red: H2A.X, Tri-Me-H3K9, HP1, A414). Scale bar, 5 μm. (D) Comparison of the total number of H2A.X foci in one focus plane (H2A.X) or of the relative fluorescent intensities (%) between *laminB2ΔN* or *kuk* transfected cells and untransfected control cells (Tri-Me-H3K9, HP1). Mann-Whitney *U*-test for *kuk* transfected cells stained with H2A.X: $U_A = 781.5$; $z = -4.98$; $p < 0.0001$; $N_{\text{control}} = 60$ cells, $N_{\text{kuk}} = 14$ cells. *kuk* transfected cells stained with HP1: Mann-Whitney *U*-test, $U_A = 9855.5$; $z = -25.13$; $p < 0.0001$; $N_{\text{control}} = 90$ cells, $N_{\text{kuk}} = 65$ cells. *kuk* transfected cells stained with Tri-Me-H3K9: Mann-Whitney *U*-test, $U_A = 6683.5$; $z = -26.83$; $p < 0.0001$; $N_{\text{control}} = 82$ cells, $N_{\text{kuk}} = 41$ cells. *laminB2ΔN* transfected cells stained with H2A.X: Mann-Whitney *U*-test, $U_A = 3786.5$; $z = -8.34$; $p < 0.0001$; $N_{\text{control}} = 74$ cells, $N_{\text{kuk}} = 55$ cells. *laminB2ΔN* transfected cells stained with HP1: Mann-Whitney *U*-test, $U_A = 14268$; $z = -34.27$; $p < 0.0001$; $N_{\text{control}} = 123$ cells, $N_{\text{kuk}} = 55$ cells. *laminB2ΔN* transfected cells stained with Tri-Me-H3K9: Mann-Whitney *U*-test, $U_A = 12243$; $z = -12.27$; $p < 0.0001$; $N_{\text{control}} = 148$ cells, $N_{\text{kuk}} = 84$ cells. All test are two-tailed, mean values of three replicates per experiments are shown, error bars \pm SEM.

allowed us to minimize the problem of genetic background as well as to circumvent defects that may arise during development (Osterwalder *et al.*, 2001; Roman & Davis, 2002) and we were able to analyse the effect of the conditional *lamin B* or *kuk* expression in adult flies.

Age-associated accumulation of DNA damage and changes in chromatin organization may act independently of the nuclear envelope configuration (Oberdoerffer & Sinclair, 2007). Since both *LAMIN B* and *KUK* are obligatory localized at the nuclear lamina and can induce phenotypes similar to those observed in aging flies, our data support a model where a dysmorphic nuclear lamina itself can provoke changes in the chromatin organization, thereby affecting DNA repair mechanisms (Lans & Hoeijmakers, 2006). Thus, our work helps to distinguish these models. Since not only *LAMINΔ50* but also other permanently farnesylated lamin variants can induce aging-like symptoms, these findings can extend the focus from *laminΔ50/HGPS* to other lamina proteins and the nuclear lamina as such, which may as well contribute to the physiological aging process.

Several mechanisms by which abnormal nuclear morphology can act on the aging process are discussed. The aberrant nuclear morphology may interfere with mitosis, thereby reducing the regenerative capacity of the organism (Cao *et al.*, 2007). This mechanism cannot play a major role in mostly post-mitotic organisms as *Drosophila* or *C. elegans*. Structurally, the stability of the nucleus may be impaired which would make them more vulnerable to mechanical stress (Lammerding *et al.*, 2004). In HGPS cells, *LAMIN A* and *C* become trapped at the nuclear periphery, which significantly reduces the ability of the nuclear lamina to rearrange under mechanical stress, which might lead to misregulation of mechanosensitive gene expression (Dahl *et al.*, 2006). It would be interesting to see whether similar mechanisms work in cells from aged healthy individuals and to see whether other nuclear lamina proteins are involved. The dramatic changes in nuclear pore complex formation and distribution observed in HGPS cells, also recapitulated in *kuk* or *lamin B* expressing cells, may be linked to the aging process in that the nucleocytoplasmic transport or the interaction of the nuclear pores with chromatin is altered (Akhtar & Gasser, 2007). The normal function of the nonfarnesylated *LAMIN A* in the nucleoplasm may be disrupted, since lamin A and its binding partners are depleted in the nucleoplasm by membrane-bound *LaminΔ50* (Haithcock *et al.*, 2005). We could show that a very truncated *lamin B* variant, *laminBΔN*, which lacks the coiled-coil domain, is able to induce age-related phenotypes. Moreover, even Kugelkern, a *Drosophila*-specific protein, which has no known homolog in vertebrates can induce similar changes as described for human cells expressing *LaminΔ50*. It therefore seems unlikely that a *LAMIN A*-specific effect alone accounts for the phenotypes observed.

The focus on the nuclear lamina will have an influence on our integral understanding of the aging process and possible strategies of how to defy it. Future experiments involving genetically tractable organisms like *Drosophila* may help to resolve the molecular and genetic basis of the link between nuclear morphology, and chromatin structure and stability.

Experimental procedures

Cell culture

NIH3T3 cells were cultured in DMEM (Invitrogen/Gibco, Karlsruhe, Germany) supplemented with 10% fetal bovine serum and 2 mM L-glutamine at 37 °C. We plated NIH3T3 cells in 6-wells containing cover slips and transiently transfected them with Effectene (Qiagen, Hilden, Germany) when they reached a confluence of 25–30% with pCS2*HAKuk* (referred to here as *kuk*; Brandt *et al.*, 2006) or pCS2*XlaminB2ΔNGFP* (referred to here as *laminB2ΔN*; Prüfert *et al.*, 2004) (2 µg construct/6-well). They were cultivated for 48 h (HP1 and Tri-Me-H3K9 staining) or for 72 h (H2A.X staining). After washing in phosphate-buffered saline (PBS), cells were fixed with 2% formaldehyde in PBS containing 0.2% Tween and 0.5% NP-40 for 20 min at room temperature (RT). After washing in PBS, cells were permeabilized in PBS with 0.5% Triton X-100 plus 0.5% Saponin (Sigma, Munich, Germany) for 10 min.

Immunohistochemistry

Adult males were anaesthetised; the head, abdomen, legs, and wings were cut off. The thorax was transferred to ice cold Schneider cell medium where it was split into half and subsequently fixed with 8% formaldehyde in PBS containing 0.2% Tween and 0.5% NP-40 for 40 min at RT. After washing in PBS the thoraces were permeabilized in PBS with 0.5% Triton X-100 plus 0.5% Saponin (Sigma) for 1–5 days at 4 °C. Before staining, the fixed thoraces were manipulated that only one end of the muscles stuck to the cuticle and the other end was free floating and better accessible to the staining reagents. Consecutively the muscles were blocked in PBS plus Tween (Sigma) with 5% BSA and stained in PBT containing primary antibodies, fluorescent secondary antibodies (4 µg mL⁻¹, Alexa, Molecular Probes, Invitrogen, Karlsruhe, Germany) or DAPI and mounted in Aquapolymount (Polyscience, Heidelberg, Germany). Antibodies used were A414 (Sigma, 1 µg mL⁻¹), *Drosophila* HP1 (DSHB, Iowa, USA, C1A9, H2A.X (Chemicon, Hampshire, UK, 1 : 5000), mouse HP1 (Chemicon, 1 : 2500), *Kuk* (0.2 µg mL⁻¹), Tri-Me-H3K9 (upstate, 0.2 µg mL⁻¹, 0.1 µg mL⁻¹), *Drosophila* Lamin B (*LaminDmO*, Saumweber, Berlin, Germany, 0.1 µg mL⁻¹), human laminA/C (0.2 µg mL⁻¹; Santa Cruz Biotechnology, Santa Cruz, CA, USA), and HA (Babco, Richmond, CA, USA, 1 : 2000).

Microscopy

Digital fluorescent images were either taken with a confocal microscope (Leica, Solms, Germany) or with a fluorescent microscope connected to a Progress (Jenoptik, Jena, Germany) camera and processed with Adobe Photoshop. Measurements were performed with ImageJ with the perimeter tool (nuclear perimeter), the mean grey value tool (relative fluorescent intensity) and the maximum intensity tool. For measuring relative fluorescent intensity of HP1 and Tri-Me-H3K9 stainings, three

independent experiments were analysed at the fluorescent microscope. To avoid overexposure, we did not use the entire 8-bit scale of grey values; thus, for each experiment the maximum intensity was set as 100%. The number of H2AX foci per nucleus might be underestimated since we only counted those foci that were in the focus plane of the picture (Mann–Whitney *U*-test, <http://faculty.vassar.edu/lowry/VassarStats.html>). For measurement of the muscle perimeters we acquired confocal image Z-stacks of the longitudinal muscles with a slice distance of approximately 1 μm and assembled them in ImageJ with the z-stack/SUM function. For each time point three individual flies were analysed. Statistical analysis was performed with Prism GraphPad software (one- or two-way analysis of variance followed by Bonferroni post tests).

To induce conditional expression of the full-length *kuk* or the nonfarnesylated SaaX-mutant *kuk* (*kukCS*) in wild-type or in *kuk*-deficient embryos (Δk), transgenic embryos containing the respective heat-shock constructs were heat shocked for 45 min. After 45-min recovery the embryos were fixed and stained with Kuk or Lamin B antibodies. The pictures were taken with identical microscope settings.

Electron microscopy

Thoraces were fixed and processed for electron microscopy as described (Fyrberg *et al.*, 1990). In contrast to Fyrberg *et al.* (1990), we omitted the tannic acid from the 3% glutaraldehyde solution. Ultrathin sections were inspected with a Zeiss EM900 and a Zeiss EM10 electron microscope (Oberkochen, Germany). Negatives were digitalized by scanning and processed with Adobe Photoshop.

Flies and Genetics

GeneSwitch-Gal4 (GS) flies were provided by J. H. Bauer, S. L. Helfand, and H. Keshishian. UASlamin B flies are described in (Guillemin *et al.*, 2001). The w^{m4h} flies were provided by G. Reuter, Halle. For pUASKuk the cDNA from LD09231 was cloned as *NotI*-*ApaI*/blunt fragment into the *NotI*-*XbaI*/blunt sites of pUASp. To obtain heat-shock inducible constructs of full-length *kuk* (*kuk*) or mutant *kuk* (*kukCS*), we first cloned the *kuk* coding sequence with parts of its 3 untranslated region as *NcoI*-*SmaI* fragments from *CS-kuk* or *CS-kukCS* plasmids into the *QEH₁₀ZZ* plasmid. The final constructs HS-*kuk* and HS-*kukCS* were cloned as *ES* fragments with *Eco*-*Stu* sites into the plasmid *casperHS*. Transgenic flies were made by P-element-mediated transformation. The genomic rescue constructs (Brandt *et al.*, 2006) 4 \times and 6 \times *kuk* are located on the second and third chromosome. 0 \times *kuk* consists of a deletion of *kuk* and CG5169 together with a rescue construct of CG5169 over Df(3R)Ex6176 (Brandt *et al.*, 2006).

Lifespan assays

All flies were raised and kept in a humidified, temperature-controlled incubator with 12-h light : dark cycle at 25 °C in vials containing standard cornmeal medium (2.5% yeast, 2.18%

treacle, 1% soya meal, 8% cornmeal, 8% malt, 1.25% propionic acid). In the case of UASlamin B/GS-MHC, flies were raised at 18 °C. Flies were collected under short anaesthesia. Each demography cage was initiated with at least 150 newly eclosed males. The number of deceased flies was recorded every 2–3 days, when flies were transferred to fresh food plates. For induction with the GeneSwitch system, RU 486 (Sigma) was added directly to the food to a final concentration of 200 μM . The data across 3–5 replicate demography cages per treatment and genotype were combined. Both Statview 5.0 and Prism GraphPad software were used for survival data (log-rank test) and mortality curves analysis (linear regression).

Negative geotaxis assays

Negative geotaxis was assessed as previously described (Gargano *et al.*, 2005). Negative geotaxis behaviour was recorded as the net distance (cm) climbed by individual males in a vertical plastic tube during a 10-s test period that began immediately after being tapped to the bottom of the tube. For each genotype and treatment 25 males were tested per week. The mean distance climbed by the control flies in the first week was set as 100% negative geotaxis. One to three replicative experiments were performed and the data were analysed using Prism 3.0 (GraphPad Software, San Diego, CA, USA).

Eye pigment measurement

Ten newly eclosed males were aged for 5 days at 25 °C, decapitated with tweezers and immediately shock-frozen in liquid nitrogen. For extraction of the eye pigments, fly heads were homogenized in 0.1 M glycine/HCl (pH 2) containing 30% ethanol and kept in the dark for 24 h at room temperature. After clarification by several brief centrifugations, the absorption of the pigments was measured at 480 nm. Five independent extractions were performed for each genotype. VassarStat statistical software was used (Mann–Whitney *U*-test; <http://faculty.vassar.edu/lowry/VassarStats.html>).

Biochemistry

Proteins were analysed by sodium dodecyl sulfate–polyacrylamide gel electrophoresis (SDS-PAGE) according to standard protocols. For Western blotting, proteins separated by SDS-PAGE were transferred by semidry blotting to a nitrocellulose membrane (Protran, Schleicher and Schuell) and stained by Ponceau Red. The blots were developed with IgG coupled with peroxidase and chemiluminescence (ECLplus, Amersham, Munich, Germany). The following antibody concentrations were used: lamin B (polyclonal, 1 : 1000), Kuk (rabbit, 0.1 $\mu\text{g mL}^{-1}$).

Acknowledgments

We thank H. Ehret, and D. T. Brandt for technical assistance, and K. Schild for EM processing. We thank all laboratory

members for discussions and H. Reuter, A. Grebe, and S. Vernaldi for fly maintenance. We are grateful for materials, reagents, and fly stocks from J. H. Bauer, S. L. Helfand, H. Keshishian, M. A. Krasnow, G. Reuter, D. Görlich, *Drosophila* Stock Center (Bloomington, Indiana, USA), and Hybridoma bank (Iowa). The work was founded by the Deutsche Forschungsgemeinschaft, and Landesstiftung Baden-Württemberg.

References

- Akhtar A, Gasser SM (2007) The nuclear envelope and transcriptional control. *Nat. Rev. Genet.* **8**, 507–517.
- Brandt A, Papagiannouli F, Wagner N, Wilsch-Brauninger M, Braun M, Furlong EE, Loserth S, Wenzl C, Pilot F, Vogt N, Lecuit T, Krohne G, Grosshans J (2006) Developmental control of nuclear size and shape by Kugelkern and Kurzkern. *Curr. Biol.* **16**, 543–552.
- Cao K, Capell BC, Erdos MR, Djabali K, Collins FS (2007) A lamin A protein isoform overexpressed in Hutchinson-Gilford progeria syndrome interferes with mitosis in progeria and normal cells. *Proc. Natl Acad. Sci. USA* **104**, 4949–4954.
- Capell BC, Collins FS (2006) Human laminopathies: nuclei gone genetically awry. *Nat. Rev. Genet.* **7**, 940–952.
- Capell BC, Collins FS, Nabel EG (2007) Mechanisms of cardiovascular disease in accelerated aging syndromes. *Circ. Res.* **101**, 13–26.
- Dahl KN, Scaffidi P, Islam MF, Yodh AG, Wilson KL, Misteli T (2006) Distinct structural and mechanical properties of the nuclear lamina in Hutchinson-Gilford progeria syndrome. *Proc. Natl Acad. Sci. USA* **103**, 10271–10276.
- De Sandre-Giovannoli A, Bernard R, Cau P, Navarro C, Amiel J, Boccaccio I, Lyonnet S, Stewart CL, Munnich A, Le Merrer M, Levy N (2003) Lamin A truncation in Hutchinson-Gilford progeria. *Science* **300**, 2055.
- Ebert A, Schotta G, Lein S, Kubicek S, Krauss V, Jenuwein T, Reuter G (2004) Su (var) genes regulate the balance between euchromatin and heterochromatin in *Drosophila*. *Genes Dev.* **18**, 2973–2983.
- Eriksson M, Brown WT, Gordon LB, Glynn MW, Singer J, Scott L, Erdos MR, Robbins CM, Moses TY, Berglund P, Dutra A, Pak E, Durkin S, Csoka AB, Boehnke M, Glover TW, Collins FS (2003) Recurrent de novo point mutations in lamin A cause Hutchinson-Gilford progeria syndrome. *Nature* **423**, 293–298.
- Fyrberg E, Kelly M, Ball E, Fyrberg C, Reedy MC (1990) Molecular genetics of *Drosophila* alpha-actinin: mutant alleles disrupt Z disc integrity and muscle insertions. *J. Cell Biol.* **110**, 1999–2011.
- Gargano JW, Martin I, Bhandari P, Grotewiel MS (2005) Rapid iterative negative geotaxis (RING): a new method for assessing age-related locomotor decline in *Drosophila*. *Exp. Gerontol.* **40**, 386–395.
- Goldman RD, Shumaker DK, Erdos MR, Eriksson M, Goldman AE, Gordon LB, Gruenbaum Y, Khuon S, Mendez M, Varga R, Collins FS (2004) Accumulation of mutant lamin A causes progressive changes in nuclear architecture in Hutchinson-Gilford progeria syndrome. *Proc. Natl Acad. Sci. USA* **101**, 8963–8968.
- Gruenbaum Y, Goldman RD, Meyuhos R, Mills E, Margalit A, Fridkin A, Dayani Y, Prokocimer M, Enosh A (2003) The nuclear lamina and its functions in the nucleus. *Int. Rev. Cytol.* **226**, 1–62.
- Gruenbaum Y, Margalit A, Goldman RD, Shumaker DK, Wilson KL (2005) The nuclear lamina comes of age. *Nat. Rev. Mol. Cell Biol.* **6**, 21–31.
- Guillemin K, Williams T, Krasnow MA (2001) A nuclear lamin is required for cytoplasmic organization and egg polarity in *Drosophila*. *Nat. Cell Biol.* **3**, 848–851.
- Haithcock E, Dayani Y, Neufeld E, Zahand AJ, Feinstein N, Mattout A, Gruenbaum Y, Liu J (2005) Age-related changes of nuclear architecture in *Caenorhabditis elegans*. *Proc. Natl Acad. Sci. USA* **102**, 16690–16695.
- Hwangbo DS, Gershman B, Tu MP, Palmer M, Tatar M (2004) *Drosophila* dFOXO controls lifespan and regulates insulin signalling in brain and fat body. *Nature* **429**, 562–566.
- Lammerding J, Schulze PC, Takahashi T, Kozlov S, Sullivan T, Kamm RD, Stewart CL, Lee RT (2004) Lamin A/C deficiency causes defective nuclear mechanics and mechanotransduction. *J. Clin. Invest.* **113**, 370–378.
- Lans H, Hoeijmakers JH (2006) Cell biology: ageing nucleus gets out of shape. *Nature* **440**, 32–34.
- Liu B, Wang J, Chan KM, Tjia WM, Deng W, Guan X, Huang JD, Li KM, Chau PY, Chen DJ, Pei D, Pendas AM, Cadinanos J, Lopez-Otin C, Tse HF, Hutchison C, Chen J, Cao Y, Cheah KS, Tryggvason K, Zhou Z (2005) Genomic instability in laminopathy-based premature aging. *Nat. Med.* **11**, 780–785.
- Muñoz-Alarcón A, Pavlovic M, Wismar J, Schmitt B, Eriksson M, Kylsten P, Dushay MS (2007) Characterization of lamin mutation phenotypes in *Drosophila* and comparison to human laminopathies. *PLoS ONE* **2**, e532.
- Oberdoerffer P, Sinclair DA (2007) The role of nuclear architecture in genomic instability and ageing. *Nat. Rev. Mol. Cell Biol.* **8**, 692–702.
- Osouda SNY, de Saint Phalle B, McConnell M, Horigome T, Sugiyama S, Fisher PA, Furukawa K (2005) Null mutants of *Drosophila* B-type lamin Dm(0) show aberrant tissue differentiation rather than obvious nuclear shape distortion or specific defects during cell proliferation. *Dev. Biol.* **284**, 219–232.
- Osterwalder T, Yoon KS, White BH, Keshishian H (2001) A conditional tissue-specific transgene expression system using inducible GAL4. *Proc. Natl Acad. Sci. USA* **98**, 12596–12601.
- Pletcher SD, Khazaeli AA, Curtsinger JW (2000) Why do life spans differ? Partitioning mean longevity differences in terms of age-specific mortality parameters. *J. Gerontol. A Biol. Sci. Med. Sci.* **55**, B381–B389.
- Prüfert K, Vogel A, Krohne G (2004) The lamin CxxM motif promotes nuclear membrane growth. *J. Cell Sci.* **117**, 6105–6116.
- Ralle T, Grund C, Franke WW, Stick R (2004) Intranuclear membrane structure formations by CaaX-containing nuclear proteins. *J. Cell Sci.* **117**, 6095–6104.
- Roman G, Endo K, Zong L, Davis RL (2001) P[Switch], a system for spacial and temporal control of gene expression in *Drosophila melanogaster*. *Proc. Natl Acad. Sci. USA* **98**, 12602–12607.
- Scaffidi P, Misteli T (2005) Reversal of the cellular phenotype in the premature aging disease Hutchinson-Gilford progeria syndrome. *Nat. Med.* **11**, 440–445.
- Scaffidi P, Misteli T (2006) Lamin A-dependent nuclear defects in human aging. *Science* **312**, 1059–1063.
- Schulze SR, Curio-Penny B, Li Y, Imani RA, Rydberg L, Geyer PK, Wallrath LL (2005) Molecular genetic analysis of the nested *Drosophila melanogaster* lamin C gene. *Genetics* **171**, 185–196.
- Shumaker DK, Dechat T, Kohlmaier A, Adam SA, Bozovsky MR, Erdos MR, Eriksson M, Goldman AE, Khuon S, Collins FS, Jenuwein T, Goldman RD (2006) Mutant nuclear lamin A leads to progressive alterations of epigenetic control in premature aging. *Proc. Natl Acad. Sci. USA* **103**, 8703–8708.
- Wiesel N, Mattout A, Melcer S, Melamed-Book N, Herrmann H, Medalia O, Aebi U, Gruenbaum Y (2008) Laminopathic mutations interfere with the assembly, localization, and dynamics of nuclear lamins. *Proc. Natl Acad. Sci. USA* **105**, 180–185.

Supplementary material

The following supplementary material is available for this article:

Fig. S1 Transmission electron microscopy of muscle cells. Wild-type, 3 days old; wild-type, 35 days old; wild-type, 60 days old;

6 genomic copies of *kuk* ($6\times$ *kuk*), 3 days old; $6\times$ *kuk*, 30 days old; $6\times$ *kuk*, 36 days old; UAS*kuk*/GS-MHC induced with RU 486, 3 days old; UASlamin B/GS-MHC induced with RU 486, 1 week old; UAS*kuk*/GS-MHC induced with RU 486, 31 days old. Magnification is indicated on each panel.

Fig. S2 Transmission-electron microscopy of 1-week-old RU 486 induced UAS*kuk*/GS-MHC (A–C), UASlamin B/GS MHC (D), or of 37-day-old $4\times$ *kuk* flies (E). (A) Shows an enlarged muscle nucleus embedded in intact muscle organelles. (B) Epithelial cell with inconspicuous nucleus located close to the cuticle (cu). (C) Nucleus of a fat body cell surrounded by lipid droplets (lip). (D) Intestinal cell with microvilli (mv). The nucleus appears normal in size and shape. (E) Nucleus in neuronal tissue shows normal morphology. Arrowheads point to nuclear membrane, scale bar: 0.2 μm .

Fig. S3 GeneSwitch-MHC (GS-MHC) drives the expression of UASGFP*kuk* (green, or white; DAPI, blue) in muscle cells. Unfixed tissue was mounted in 50% glycerol containing DAPI staining solution and immediately photographed. (A) Muscle cells of the cibarial pump show pronounced GFP*kuk* expression in the nuclei (arrowhead). Muscle cell nuclei in the leg (B, E) or in the lateral tergosternal muscles of the abdominal body wall (C) show intense GFP*kuk* expression. The direct (D, D') or indirect (F, F') flight muscles show strong GFP*kuk* expression in the nuclei. The un-induced control flies had weak GFP*kuk* expression in the indirect flight muscles (arrowhead); GFP*kuk* was not detected in other tissues. Scale bar 10 μm .

Fig. S4 Conditional expression of *lamin B* or *kuk* in fat body or neuronal cells. Unfixed tissue was mounted in 50% glycerol containing DAPI staining solution and immediately photographed. (A–D) Adult flies of the genotypes UASlamin B, UASactinGFP/GS-S1106 or UAS*kuk*, UASactinGFP/GS-S1106 were fed for 3 weeks with RU 486 to induce expression in fat body cells. In lamin B-expressing cells (B), nuclear size is increased compared to un-induced control cells (A). In *kuk*-expressing cells (D), no increase in nuclear size is observed in induced flies compared to control flies of the same age (C). In *lamin B*-expressing neurons (I–K), nuclear size is increased compared to control cells (E–H). In *kuk*-expressing neurons (O–R), only few cells show an

increase in nuclear size compared to control cells (M, N). (E–R) pictures of the left column show DIC overviews of the corresponding picture of the right column. In red, the red eye pigments of the ommatidia are shown. The right column shows DAPI staining (blue or white) and GFP expression (green). (E, F) shows an overview of an un-induced UASlamin B, UASactinGFP/GS-elav brain. (G, H) show a magnification of the optic lamina of the same brain. (I, J) show an overview of an induced *lamin B*-expressing brain (K, J) in the magnification of the optic lamina most nuclei are enlarged (arrowhead). In (O, P) expression of *kuk* is induced, only few nuclei show an increase in size (arrowhead) compared to un-induced control cells (M, N). Blue, DAPI; green: GFP; scale bar 0.5 μm . (Q) Negative geotaxis assay of UAS*kuk*/GS-S1106 flies.

Fig. S5 Quantification of the tissue-specific induction of *lamin B* (A) or *kuk* (B) expression in 10-day-old males. (+) RU 486 induced expression (–) un-induced flies. The strongest induction of *Kuk* is observed with the GS-MHC driver.

Table S1 Lifetime survival data of adult *Drosophila* flies over-expressing *lamin B* or *kugelkern*. Number of flies entering the age-interval (Nx); number of dead flies within the age interval (dx); number of flies censored within the age interval (cx). Total number of flies (N).

Table S2 Statistical analysis of mortality data. Description of the slope or the Y-intercept of the best-fit regression line, correlation coefficient (r^2). Linear regression analysis of slope or Y-intercepts between induced and control flies.

This material is available as part of the online article from:

<http://www.blackwell-synergy.com/doi/abs/10.1111/j.1474-9726.2008.00406.x>

(This link will take you to the article abstract).

Please note: Blackwell Publishing are not responsible for the content or functionality of any supplementary materials supplied by the authors. Any queries (other than missing material) should be directed to the corresponding author for the article.

The Fruit Fly *Drosophila melanogaster* as a Model for Aging Research

Annely Brandt and Andreas Vilcinskis

Abstract Average human life expectancy is increasing and so is the impact on society of aging and age-related diseases. Here we highlight recent advances in the diverse and multidisciplinary field of aging research, focusing on the fruit fly *Drosophila melanogaster*, an excellent model system in which to dissect the genetic and molecular basis of the aging processes. The conservation of human disease genes in *D. melanogaster* allows the functional analysis of orthologues implicated in human aging and age-related diseases. *D. melanogaster* models have been developed for a variety of age-related processes and disorders, including stem cell decline, Alzheimer's disease, and cardiovascular deterioration. Understanding the detailed molecular events involved in normal aging and age-related diseases could facilitate the development of strategies and treatments that reduce their impact, thus improving human health and increasing longevity.

Keywords Adult stem cells · Age-related diseases · Aging · Dietary restriction · *Drosophila melanogaster* · Drug discovery · Hutchinson–Gilford progeria syndrome

Abbreviations

APH-1	Anterior pharynx-defective 1
aPKC	Atypical protein kinase C
APP	Amyloid precursor protein
A β	Amyloid- β
BACE	β -site APP cleaving enzyme 1
bp	Base pairs
GFP	Green fluorescent protein

A. Brandt
Department of Bioresources, Fraunhofer Institute of Molecular Biology
and Applied Ecology, Winchester Str. 2, 35395 Giessen, Germany

A. Vilcinskis (✉)
Institute of Phytopathology and Applied Zoology, Justus-Liebig-University of Giessen,
Heinrich-Buff-Ring 26-32, 39592 Giessen, Germany
e-mail: andreas.vilcinskis@agrار.uni-giessen.de

HGPS	Hutchinson–Gilford progeria syndrome
KCNQ	Potassium channel, KQT-like subfamily
LMNA	Lamin A gene
MHC	Myosin heavy chain
PDGF	Platelet-derived growth factor
PEN-2	Presenilin enhancer 2
PVF2	PDGF/VEGF-like factor 2
RNAi	RNA interference
UAS	Upstream activating sequence
VEGF	Vascular endothelial growth factor
ZMPSTE24	Zinc metalloproteinase homologous to yeast Ste24

Contents

1	Aging Research	64
2	<i>Drosophila melanogaster</i> in Aging Research	65
2.1	Transgenic Systems for Longevity Analysis	66
2.2	Multipotent Adult Stem Cells in <i>D. melanogaster</i>	67
2.3	Dietary Restriction	68
3	Using <i>D. melanogaster</i> to Model Human Diseases	68
3.1	Alzheimer’s Disease	69
3.2	<i>D. melanogaster</i> Age-Related Cardiovascular Disease Model	70
4	<i>D. melanogaster</i> Premature-Aging Models	70
5	The Role of <i>D. melanogaster</i> in Drug Discovery	72
	References	74

1 Aging Research

The good news is that human life expectancy is steadily increasing in the developed world, as improved health care and hygiene mean that people stay healthier and thus live longer [1]. However, this also means that more people live long enough to experience the drawbacks of aging, for example, physical and mental decline and higher risks of cardiovascular deterioration, cancer, and neurodegenerative disorders [2]. Although many genes are known to coordinate cell growth and differentiation during development, none are known that exclusively cause damage and aging. Therefore aging mechanisms could be less conserved than developmental and metabolic pathways. However, there is growing evidence that modulators of the rate of aging are conserved over large evolutionary distances [3].

Table 1 Comparison of model organisms used in aging research

		<i>C. elegans</i>	<i>D. melanogaster</i>	<i>M. musculus</i>
Practical issues	Generation time	3–5 days	10–14 days	3–4 weeks
	Adult size	1 mm	3 mm	10 cm
	Lifespan	2–3 weeks	4–6 weeks	Years
	Maintenance costs	Low	Low	High
Similarity to humans	Number of genes (approx.)	19,000	13,000	25,000
	Conservation with human genome	>50 %	>60 %	>90 %
	Anatomical similarity to humans	Low	Medium	High
Molecular tools	Targeted gene knockout/time	No	Yes	Yes/month
	Reverse genetics tools	Yes	Yes	Targeted knockout
	Generation of transgenic line	Weeks	Weeks	Months

(modified after 37)

The fruit fly *Drosophila melanogaster* is an excellent model system in which the genetic and cellular basis of important biological processes such as aging can be dissected, allowing the parallel mechanisms in vertebrates to be deciphered [4]. Understanding the details of the molecular events involved in the aging process will eventually help to reduce the impact of age-related diseases, thus improving human health and increasing longevity.

2 *Drosophila melanogaster* in Aging Research

Drosophila melanogaster was introduced as a model species in genetics, developmental biology, signal transduction, and cell biology in the early 1900s [5, 6]. The *D. melanogaster* genome is only 5 % of the size of a typical mammalian genome, but most gene families and pathways are shared with mammals, as well as many tissues and organ systems (Table 1) [7, 8]. Aging research in *D. melanogaster* benefits from a comprehensive range of methods to perturb gene function, such as mutagenesis screens, RNA interference (RNAi), and transgenesis [9, 10]. There are abundant publicly available resources, including thousands of *D. melanogaster* strains provided by the Bloomington Stock Center, as well as many cell lines, clone libraries, antibodies, and microarrays. There is also an exhaustive database containing information relevant to *D. melanogaster* genetics, development, and molecular biology (for review see Refs. [7] and [11]).

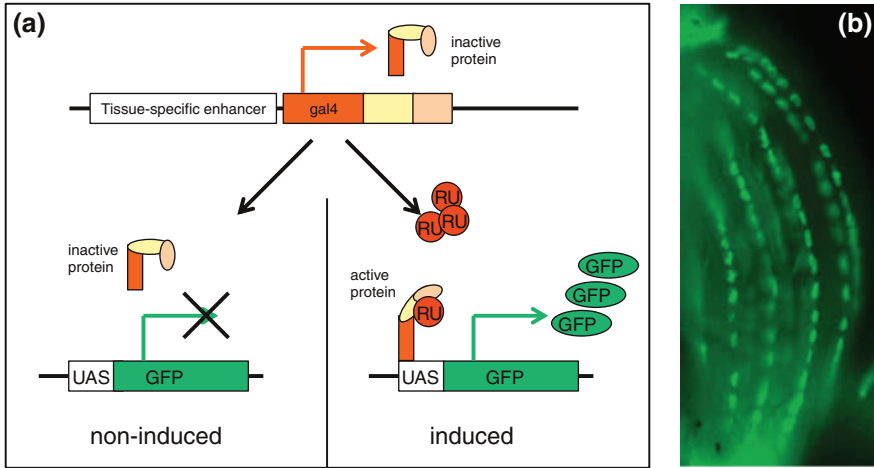


Fig. 1 The GeneSwitch GAL4 system. **a** The GeneSwitch-*Gal4* gene is expressed in the target tissue(s), according to the upstream tissue-specific promoter/enhancer (*upper panel*). In the absence of the activator RU486 (RU, red circle), the GeneSwitch-GAL4 protein remains transcriptionally inactive and cannot activate the downstream reporter gene, for example, encoding green fluorescent protein (GFP), which is linked to an upstream activating sequence (UAS) that responds to GAL4 (uninduced, *left panel*). However, by spiking food with RU486 (induced, *lower right panel*), the GeneSwitch-GAL4 becomes transcriptionally active, and the downstream UAS-linked gene is activated (modified after 15). **b** UAS-Kugeln-GFP (*green*) is expressed in the nuclei of adult fruit fly leg muscle cells using the muscle-specific GeneSwitch-myosin heavy chain (MHC) promoter

2.1 Transgenic Systems for Longevity Analysis

D. melanogaster is a valuable model organism for the investigation of aging and age-related human diseases because its short life span of 4–8 weeks (depending on temperature and diet) allows the studies to be completed rapidly. Large numbers of flies can be cultivated in small bottles, so maintenance is straightforward and inexpensive. The high fecundity of the species allows large numbers of genetically homogeneous animals to be produced rapidly, which is essential for survival assays (Table 1).

It is possible to investigate gene function in fruit flies by conditional transgene overexpression. For lifespan studies, conditional gene expression systems have several advantages, for example, transgene expression is triggered in the Tet-on system by spiking food with the drug doxycycline, and in the GeneSwitch system transgene expression is similarly triggered using the drug RU486/mifepristone [12–18]. The GeneSwitch system combines several advantages (Fig. 1). First, it provides powerful control over genetic background effects on longevity, because flies overexpressing the transgene of interest have an identical genetic background to control flies, differing only in the presence or absence of the inducer. Second, it allows the tissue-specific control of transgene expression, such as expression in the

nervous system or muscles, and also ubiquitous expression using an actin driver line [18]. Third, transgene expression can be limited to specific lifecycle stages such as larval development or adulthood, which is required, for example, to circumvent lethal effects during development [12–16].

2.2 Multipotent Adult Stem Cells in *D. melanogaster*

Adult stem cells are tissue-restricted cells with the unique ability to self-renew and to differentiate into all the specific cell types of a particular tissue (reviewed in Ref. [19]). As a result, they provide a continuous supply of differentiated cells in their tissue compartment. The renewal of differentiated cells is particularly important for tissue homeostasis in adult organisms, because this maintains adult organs and facilitates repair after injury or disease [20, 21]. The capacity of adult stem cells for cellular renewal and tissue homeostasis is thought to decline with age. This functional decline may be responsible for many tissue-specific phenotypes associated with aging (reviewed in Refs. [22 and 23]). In contrast to mammals, most adult *D. melanogaster* tissues are thought to be postmitotic. However, the aging of *D. melanogaster* stem cells, for example, in the midgut epithelium and the gonads, provides excellent models for the study of stem cell renewal and aging.

The aging of adult stem cells in the *D. melanogaster* gonad causes a loss of fecundity that becomes more severe with age [24]. The rate of adult stem cell division in the male gonad declines significantly with age, and this correlates with a reduction in the number of somatic hub cells that contribute to the stem cell niche. Interestingly, the stem cell division rate does not decline in *methuselah* (*mth*) mutant flies, which have a prolonged lifespan and greater stress resistance [25].

The digestive systems of vertebrate and invertebrate species show extensive similarities in terms of development, cellular architecture, and genetic regulation. Enterocytes form the majority of the intestinal epithelial cells and are interspersed with hormone-producing enteroendocrine cells. Human intestinal cells are continuously replenished by adult stem cells, and the deregulation of this process may underlie some common digestive diseases and cancers [21]. Recently, somatic stem cells have also been discovered in the midgut of the adult fruit fly, and like their vertebrate counterparts these proliferating progenitor cells reside within the midgut epithelium [20, 21]. Genetic mosaic analysis and lineage labeling has shown that differentiated midgut epithelial cells arise from a common lineage [20, 21]. These adult stem cells are multipotent, and Notch signaling is required to produce the correct proportion of enteroendocrine cells. Furthermore, the Notch signaling pathway is necessary for homeostatic proliferation in the midgut epithelium. The hyperactivation of Notch signaling suppresses adult stem cell proliferation whereas the inhibition of Notch signaling induces proliferation [20, 21]. Choi et al. [23] reported an age-related increase in the number and activity of adult stem cells in the *D. melanogaster* midgut. Furthermore, oxidative stress induced by

N,N'-dimethyl-4,4'-bipyridinium dichloride (Paraquat) or the loss of catalase activity mimicked the changes associated with aging in the midgut, and this was associated with the overexpression of PVF2 (*D. melanogaster* PDGF/VEGF-like factor 2), which was required for the age-related changes in midgut adult stem cells. Goulas and colleagues [26] found that the integrin-dependent adhesion of stem cells to the basement membrane was responsible for the asymmetric segregation of the signaling factors Par-3, Par-6, and atypical protein kinase C (aPKC) to the daughter cells. Perturbing this mechanism or altering the orientation of stem cell division resulted in the formation of tumors in the intestinal epithelium [26]. The identification and characterization of *D. melanogaster* midgut stem cells with striking similarities to their vertebrate counterparts will facilitate the genetic analysis of normal and age-related abnormal intestinal functions in humans.

2.3 Dietary Restriction

Dietary restriction extends the lifespan of many different organisms including yeasts, worms, and flies, as well as mammals [24]. Dietary restriction can increase the longevity of *D. melanogaster* by up to 30 % and reduce the reproduction rate, for example, by maintaining adults on a cornmeal–sugar–agar diet topped with a dilute concentration of yeast [27, 28]. However, adult flies maintained on highly restricted diets are short-lived and infertile. Therefore, longevity is only maximized by providing an intermediate diet in which restricted food intake is combined with adequate nutrition (reviewed in Ref. [28]).

It is now clear that specific nutrients rather than calories mediate longevity. Therefore *D. melanogaster* mutants that show no extension of lifespans on restricted diets should help to identify the genetic pathways through which dietary restriction controls aging. However, the genetic analysis of dietary restriction is difficult because longevity tests across a range of diets must be carried out using genetic screens [28]. Wang and colleagues showed that a transporter of Krebs cycle intermediates, encoded by the *I'm not dead yet (Indy)* gene, interacts with dietary restriction mechanisms to increase longevity [28, 29]. Although dietary restriction extends the lifespan of numerous species, the precise mechanisms have not been determined for any of these organisms. It is therefore unclear whether dietary restriction reflects evolutionary conservation or convergence [24].

3 Using *D. melanogaster* to Model Human Diseases

Age-related diseases are becoming increasingly prevalent in industrialized societies due to the greater average life expectancies. The biological aging process is one of the major risk factors for virtually all of the common diseases of developed societies, including Alzheimer's disease, Parkinson's disease, stroke, age-related

macular degeneration, type 2 diabetes mellitus, osteoporosis, sarcopenia, arteriosclerosis, and most types of cancer [30]. More than 100 years of *D. melanogaster* research has provided a wealth of genetic, genomic, cellular, and developmental data, as well as tools, techniques, and reagents, resulting in a well-characterized system that is easy to manipulate but complex enough to be relevant as a model for human diseases [30]. Many basic biological, physiological, and neurological characteristics are conserved between flies and mammals, and the *D. melanogaster* genome sequence shows that more than 60 % of human genes (including disease genes) have functional orthologues in the fruit fly [31–34], but the fly genome has only minimal genetic redundancy which makes it much easier to study gene function [35]. *D. melanogaster* has therefore become a popular model organism for the investigation of human diseases [35–38].

3.1 Alzheimer's Disease

Alzheimer's disease is a neurodegenerative disorder characterized by the functional impairment and destruction of neurons, resulting in a progressive loss of memory and other cognitive functions, leading to dementia [39]. Despite the much greater complexity of the human brain, the *D. melanogaster* central nervous system generates complex behaviors, including learning and memory, and comprises neurons and glia that operate on the same fundamental principles as their vertebrate counterparts; many neurotransmitter systems, including dopamine, glutamate, and acetylcholine, are conserved between flies and humans [40].

The pathology of Alzheimer's disease includes the formation of neuritic plaques, which are extracellular deposits primarily comprising the protein amyloid- β ($A\beta$), and internal neurofibrillary tangles primarily comprising aggregates of the neuronal microtubule-associated protein Tau [39]. $A\beta$ is 40 or 42 amino acids in length and is formed by the proteolytic cleavage of the larger amyloid precursor protein (APP) [41]. The N-terminus of $A\beta$ is generated by β -secretase activity whereas γ -secretase activity defines its length, with $A\beta$ 40 being more common and $A\beta$ 42 representing the more fibrillogenic and neurotoxic form. The activity of γ -secretase activity depends on four components: Presenilin, Nicastrin, Anterior pharynx-defective 1 (APH-1), and Presenilin enhancer 2 (PEN-2). In contrast, β -secretase activity has been attributed to the individual protein β -site APP-cleaving enzyme 1 (BACE1) [42, 43].

A typical strategy for establishing a human disease model in *D. melanogaster* is to investigate whether the gain or loss of function of a given gene known to be involved in the disease can enhance or suppress the disease phenotype in the fly. Two complementary approaches are often implemented: (i) the candidate gene approach tests a specific hypothesis that a given gene or genetic pathway plays an important role in a particular disease process; or (ii) genetic screens can be used to conduct unbiased surveys for genetic modifiers.

D. melanogaster neurons are sensitive to $A\beta$ toxicity. The targeted expression of $A\beta_{42}$ in flies causes neurodegenerative phenotypes, amyloid deposits, and learning defects, whereas the targeted expression of $A\beta_{40}$ only induces learning defects [44, 45]. Human APP expressed in *D. melanogaster* is cleaved by endogenous γ -secretase activity because the fly contains homologues of APP and all four components of the γ -secretase complex. The *D. melanogaster* homologues of *presenilin* and *nicastrin* were both identified in genetic screens for mutations that produce *Notch*-like phenotypes, and both proteins are required for the proteolytic cleavage and release of the *Notch* intracellular fragment [46–49].

Mutations in the human *tau* gene, encoding the protein found in Alzheimer's neurofibrillary tangles, are associated with familial frontotemporal dementia syndromes. A *tau* homologue has been identified in *D. melanogaster* [50], and the expression of human *tau* in the fly causes progressive neurodegeneration as well as a truncated lifespan. Unlike human *tau*-related diseases, neurodegeneration in the fly can occur without Tau aggregating into neurofibrillary tangles [51]. This suggests that Tau acquires its toxic properties before it forms macromolecular aggregations, and therapies could be developed that target pretangle forms of Tau [40].

3.2 *D. melanogaster* Age-Related Cardiovascular Disease Model

Cardiac dysfunction is the most common cause of death among the elderly in industrialized societies, and it is therefore useful to develop models that provide insight into the progression and genetic control of age-related changes in heart function [52]. The fruit fly is the only invertebrate genetic model organism with a heart. The genetic basis of cardiac dysfunction associated with age and disease in the fruit fly has been studied by developing heart function assays using high-speed video cameras to capture heart wall movements in semi-intact preparations with the fly heart surgically exposed [52]. Like the human heart, the performance of the fly heart deteriorates with age; that is, there is a progressive increase in electrical pacing-induced heart failure and arrhythmias [52]. These defects are exacerbated in *DmeKCNQ* deletion mutants, which experience episodes of prolonged heart contraction and fibrillation aggravated by age [52]. Therefore, despite the anatomical differences between flies and humans, the *D. melanogaster* heart is an emerging and promising genetic model of age-dependent cardiovascular deterioration.

4 *D. melanogaster* Premature-Aging Models

The molecular mechanisms underlying human aging have been investigated by considering progeroid syndromes such as Hutchinson–Gilford progeria syndrome (HGPS), in which a dominant point mutation in the *LMNA* gene (encoding lamin A, a component of the nuclear lamina) causes a premature accelerated aging-like

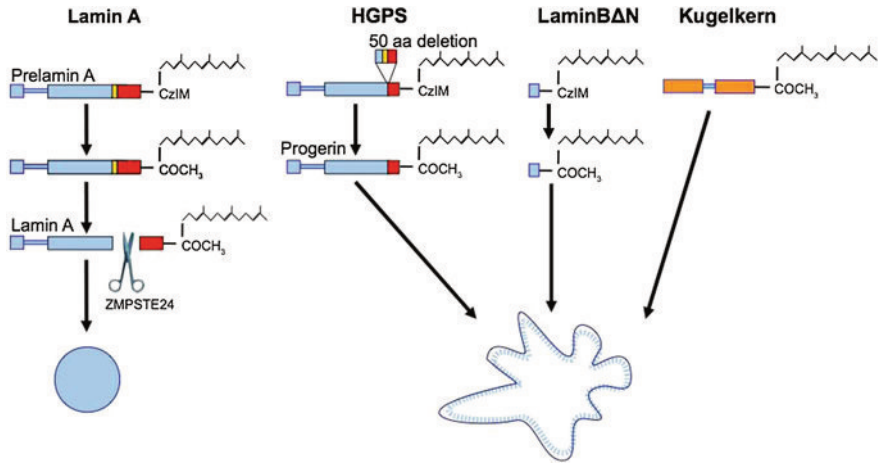


Fig. 2 Farnesylated nuclear proteins induce nuclear shape changes. The premature Prelamin A protein is farnesylated. The C-terminal region, including the farnesyl residue (red), is cleaved by the endoprotease ZMPSTE24 at the endoprotease binding site (yellow). In HGPS cells, a point mutation leads to the activation of a cryptic splicing site resulting in a 150-bp deletion, removing 50 amino acids including the endoprotease binding site. The resulting protein (Progerin) is permanently farnesylated and induces aging-like phenotypes as related nuclear shape changes, DNA damage, and reduced heterochromatin. A highly truncated form of Lamin B (LaminB Δ N) can induce similar phenotypes [62, 68, 69]. LaminB Δ N comprises only the C-terminal region of Lamin B, including the nuclear localization signal and the farnesylation site. The *D. melanogaster* protein Kugelkern contains a putative coiled-coil region (small blue bar), a nuclear localization signal, and a C-terminal farnesylation site but no other conserved features (orange). Even so, Kugelkern can induce aging-like phenotypes similar to those described for Progerin and LaminB Δ N

disorder in children [53, 54]. Affected children appear normal at birth, but soon develop symptoms and pathologies associated with normal human aging. Children with HGPS generally die from myocardial infarction or cerebrovascular accidents at an average age of 13 years [55, 56].

The mutation responsible for HGPS influences the splicing of the primary *LMNA* transcript such that a normally rare splicing variant is produced constitutively (Fig. 2). The normal splicing variant loses its farnesyl group and partly relocates from the nuclear lamina to the nucleoplasm, but the rare variant (known as Progerin) retains its farnesyl group and is permanently inserted into the nuclear lamina where it affects nuclear shape, DNA integrity, and chromatin architecture [55, 56]. Even in healthy individuals, this cryptic splicing site is sporadically active and Progerin is present in aged human cells. Although *progerin* mRNA is only found at low levels, the protein accumulates in the skin in a subset of dermal fibroblasts [57], and in coronary arteries [58], thus participating in the physiological aging process [59]. Inhibiting the *progerin* splicing variant can reverse the nuclear defects observed in aging cells [53, 54, 59–61].

HGPS is characterized by lobulated wrinkled nuclei, but these are also present in healthy aging humans, in nematodes, and also in *D. melanogaster* [59, 62, 63].

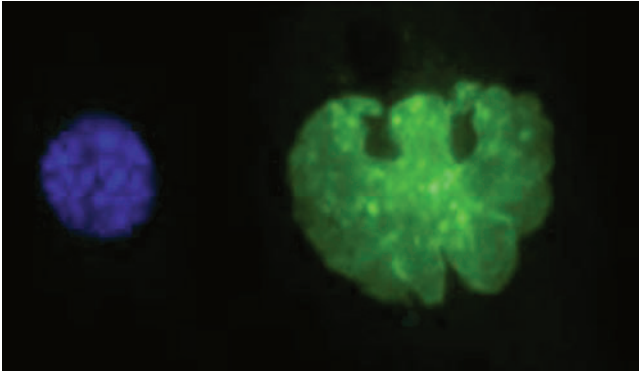


Fig. 3 The nucleus in aging fibroblasts. Mouse fibroblasts transfected with *D. melanogaster kuk* (green, right panel) undergo nuclear shape changes similar to those observed in aging fibroblasts and HGPS cells. Untransfected control cells have round and smooth nuclei (blue, left panel)

In wildtype flies, the nuclei of flight-muscle cells become larger with age and they adopt an aberrant shape [62]. This aging-like phenotype can be prematurely induced by expressing farnesylated lamina proteins (Figs. 2, 3). The overexpression of genes encoding *Lam* (*D. melanogaster* Lamin B) or Kugelkern (*kuk*) induces aberrant nuclear shapes early in adult life and reduces the fly lifespan, correlating with an early decline in age-dependent locomotor behavior [62]. Lobulation of the nuclear membrane induced by the insertion of farnesylated nuclear proteins can lead to premature aging-like phenotypes in cultured mammalian cells and in adult flies [62].

5 The Role of *D. melanogaster* in Drug Discovery

Understanding the molecular mechanisms of aging may facilitate the development of novel strategies to attenuate or delay the process in humans. Research using popular vertebrate model organisms such as mice (*Mus musculus*) and zebrafish (*Danio rerio*) has provided important insights into vertebrate aging [64, 65]. However, both species live for 3 years or longer under laboratory conditions, making longevity screens time-consuming and expensive. In contrast, small and prolific organisms with a lifespan of only few weeks, such as the fruit fly and the nematode *Caenorhabditis elegans* provide the basis for large and unbiased screens allowing the investigation of novel genes and substances that influence aging in a physiological context [66].

Drug discovery usually begins with the identification of a target protein implicated in the disease, followed by high-throughput screens of chemical compound libraries to identify substances that interact with the targets and alter

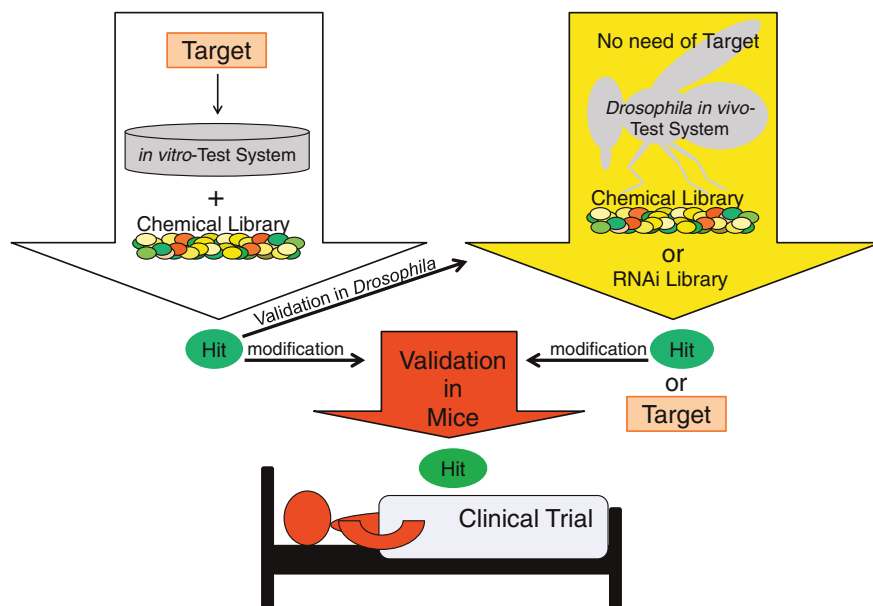


Fig. 4 A schematic view of two alternative drug discovery pathways based on high-throughput screens. The *white arrow* shows the traditional drug discovery process, which is based on the identification of a Target (e.g., enzyme, receptor, or ion channel) implicated in a human disease. High-throughput screening of a large chemical library is carried out to identify Hits, but these large-scale screens are typically based on in vitro cell culture, biochemical assays, or receptor binding assays (in vitro Test System). Hits are optimized by medicinal chemistry (modification) and subsequently tested in rodent models (*red arrow*, Validation in Mice) before clinical development (Clinical Trial). Alternatively, the high-throughput screens are performed in whole-animal models (*Yellow arrow*; *D. melanogaster* in vivo-Test System). This also allows the screening of large libraries based on chemical compounds, RNAi, or genetic modifiers. Furthermore, genetic manipulation can be used to produce a phenotype, for example, by expressing the disease-causing human protein in the fly. Depending on the purpose of the screen, the appropriate output parameter can be chosen (e.g., biochemical, cellular, tissue, behavioral parameters, or even longevity). The outcome of such a screen can be a positive compound (Hit) or a novel gene implicated in the disease or aging process (Target) revealing new molecular mechanisms. *D. melanogaster* may also bridge the gap between traditional high-throughput screening and validation in mammalian models (Validation in *D. melanogaster*)

their activity (Fig. 4). Traditionally, these large-scale screens have involved in vitro cell culture, biochemical assays, or receptor-binding assays. Positive compounds (hits) are optimized by medicinal chemistry and then tested in rodent models. Despite significant investment, most drug candidates fail before they reach the market, for example, due to unpredicted toxicity, off-target effects, or clinical inefficacy (reviewed in Ref. [35]). The attrition rate is high because of the poor selectivity of hits in the initial test systems, which have only limited predictive value for clinical performance because they cannot take into account the complexity of living organisms. To address this challenge it would be useful to develop

primary drug screening methods applied directly in whole animals, where all relevant systems are present and functioning together in a manner that is more relevant to human pathology. However, it is infeasible to use the common rodent models for whole-animal primary screening because millions of animals would be required to screen tens of thousands of small molecules in each experiment, and in the case of aging-relevant compounds this would also take many years. Innovative new screening platforms are therefore required to identify hits relevant to aging-related disease targets [35].

Recently, small invertebrate animal models such as *D. melanogaster* and *C. elegans* have been used for high-throughput drug screening [67]. *D. melanogaster* in particular allows whole-animal, high-throughput screening in a model that is relevant to humans, so that unbiased primary screens can be carried out without requiring the prior identification of a target protein [38]. The genetic and physiological conservation between invertebrates and humans suggests that human diseases can be modeled in flies and worms, although anatomical differences mean that only a partial picture of the human aging process/disease can be achieved. The use of a model organism such as the fly offers speed and high-throughput screens in the whole animal, and significantly reduces overall costs that together should result in enhanced drug discovery rates [38].

Acknowledgments We thank K. Grikscheit, and D. T. Brandt for critical reading of the manuscript. The authors acknowledge funding by the Hessian Ministry for Science and Art via the LOEWE research focus “Translational pharmaceutical research”.

References

1. Oeppen J, Vaupel JW (2002) Demography. Broken limits to life expectancy. *Science* 296(5570):1029–1031
2. Partridge L (2011) Some highlights of research on aging with invertebrates, 2010. *Aging Cell* 1:5–9
3. Partridge L, Gems D (2002) The evolution of longevity. *Curr Biol* 16:R544–R546
4. Eleftherianos I, Castillo JC (2012) Molecular mechanisms of aging and immune system regulation in *Drosophila*. *Int J Mol Sci* 13(8):9826–9844
5. Manev H, Dimitrijevic N (2004) *Drosophila* model for in vivo pharmacological analgesia research. *Eur J Pharmacol* 491(2–3):207–208
6. Arias AM (2008) *Drosophila melanogaster* and the development of biology in the twentieth century. *Methods Mol Biol* 420:1–25
7. Matthews KA, Kaufman TC, Gelbart WM (2005) Research resources for *Drosophila*: the expanding universe. *Nat Rev Genet* 3:179–193
8. De Velasco B, Shen J, Go S, Hartenstein V (2004) Embryonic development of the *Drosophila* corpus cardiacum, a neuroendocrine gland with similarity to the vertebrate pituitary, is controlled by *sine oculis* and *glass*. *Dev Biol* 274(2):280–294
9. Venken KJ, Bellen HJ (2005) Emerging technologies for gene manipulation in *Drosophila melanogaster*. *Nat Rev Genet* 3:167–178
10. Matsushima Y, Adán C, Garesse R, Kaguni LS (2007) Functional analysis by inducible RNA interference in *Drosophila melanogaster*. *Methods Mol Biol* 372:207–217

11. Drysdale R (2008) FlyBase: a database for the *Drosophila* research community. FlyBase Consortium. *Methods Mol Biol* 420:45–59
12. Osterwalder T, Yoon KS, White BH, Keshishian H (2001) A conditional tissue-specific transgene expression system using inducible GAL4. *Proc Natl Acad Sci USA* 98(22):12596–12601
13. Roman G, Davis RL (2002) Conditional expression of UAS-transgenes in the adult eye with a new gene-switch vector system. *Genesis* 34(1–2):127–131
14. Ford D, Hoe N, Landis GN, Tozer K, Luu A, Bhole D, Badrinath A, Tower J (2007) Alteration of *Drosophila* life span using conditional, tissue-specific expression of transgenes triggered by doxycycline or RU486/Mifepristone. *Exp Gerontol* 6:483–497
15. Nicholson L, Singh GK, Osterwalder T, Roman GW, Davis RL, Keshishian H (2008) Spatial and temporal control of gene expression in *Drosophila* using the inducible GeneSwitch GAL4 system. I. Screen for larval nervous system drivers. *Genetics* 178:215–234
16. Poirier L, Shane A, Zheng J, Seroude L (2008) Characterization of the *Drosophila* gene-switch system in aging studies: a cautionary tale. *Aging Cell* 7:758–770
17. Brandt A, Krohne G, Grosshans J (2008) The farnesylated nuclear proteins KUGELKERN and LAMIN B promote aging-like phenotypes in *Drosophila* flies. *Aging Cell* 4:541–551
18. Shen J, Curtis C, Tavaré S, Tower J (2009) A screen of apoptosis and senescence regulatory genes for life span effects when over-expressed in *Drosophila*. *Aging* 1(2):191–211
19. Takashima S, Hartenstein V (2012) Genetic control of intestinal stem cell specification and development: a comparative view. *Stem Cell Rev* 8(2):597–608
20. Micchelli CA, Perrimon N (2006) Evidence that stem cells reside in the adult *Drosophila* midgut epithelium. *Nature* 439(7075):475–479
21. Ohlstein B, Spradling A (2006) The adult *Drosophila* posterior midgut is maintained by pluripotent stem cells. *Nature* 439(7075):470–474
22. Van Zant G, Liang Y (2003) The role of stem cells in aging. *Exp Hematol* 8:659–672
23. Choi NH, Kim JG, Yang DJ, Kim YS, Yoo MA (2008) Age-related changes in *Drosophila* midgut are associated with PVF2, a PDGF/VEGF-like growth factor. *Aging Cell* 3:318–334
24. Partridge L (2007) Some highlights of research on aging with invertebrates, 2006–2007. *Aging Cell* 6(5):595–598
25. Wallenfang MR, Nayak R, DiNardo S (2006) Dynamics of the male germline stem cell population during aging of *Drosophila melanogaster*. *Aging Cell* 4:297–304
26. Goulas S, Conder R, Knoblich JA (2012) The par complex and integrins direct asymmetric cell division in adult intestinal stem cells. *Cell Stem Cell* 11(4):529–540
27. Chippindale AK, Leroi AM, Kim SB, Rose MR (1993) Phenotypic plasticity and selection in *Drosophila* life-history evolution. I. Nutrition and the cost of reproduction. *J Evol Biol* 6:171–193
28. Tatar M (2011) The plate half-full: status of research on the mechanisms of dietary restriction in *Drosophila melanogaster*. *Exp Gerontol* 46(5):363–368
29. Wang P-Y, Neretti N, Whitaker R, Hosier S, Chang C, Lu D, Rogina B, Helfand SL (2009) Long-lived Indy and calorie restriction interact to extend life span. *Proc Natl Acad Sci* 106:9262–9267
30. Staveley BE (2012) Successes of modelling parkinson disease in drosophila. In: Dushanova J (ed) *Mechanism in Parkinson's disease—models and treatments* ISBN: 978-953-307-876-2, InTech p 233–248
31. Bernards A, Hariharan IK (2001) Of flies and men—studying human disease in *Drosophila*. *Curr Opin Genet Dev* 11(3):274–278
32. Celniker SE, Rubin GM (2003) The *Drosophila melanogaster* genome. *Annu Rev Genomics Hum Genet* 4:89–117
33. Bier E (2005) *Drosophila*, the golden bug, emerges as a tool for human genetics. *Nat Rev Genet* 6(1):9–23
34. Reiter LT, Potocki L, Chien S, Gribskov M, Bier E (2001) A systematic analysis of human disease-associated gene sequences in *Drosophila melanogaster*. *Genome Res* 11(6):1114–1125

35. Pandey UB, Nichols CD (2011) Human disease models in *Drosophila melanogaster* and the role of the fly in therapeutic drug discovery. *Pharmacol Rev* 63(2):411–436
36. Botas J (2007) *Drosophila* researchers focus on human disease. *Nat Genet* 39(5):589–591
37. Doronkin S, Reiter LT (2008) *Drosophila* orthologues to human disease genes: an update on progress. *Prog Nucleic Acid Res Mol Biol* 82:1–32
38. Giacomotto J, Ségalat L (2010) High-throughput screening and small animal models, where are we? *Br J Pharmacol* 160(2):204–216
39. Götz J, Matamales M, Götz NN, Ittner LM, Eckert A (2012) Alzheimer's disease models and functional genomics—how many needles are there in the haystack? *Front Physiol* 3:320. doi: [10.3389/fphys.2012.00320](https://doi.org/10.3389/fphys.2012.00320)
40. Shulman JM, Feany MB (2003) Genetic modifiers of tauopathy in *Drosophila*. *Genetics* 165(3):1233–1242
41. Glenner GG, Wong CW (1984) Alzheimer's disease: initial report of the purification and characterization of a novel cerebrovascular amyloid protein. *Biochem Biophys Res Commun* 120(3):885–890
42. Edbauer D, Winkler E, Regula JT, Pesold B, Steiner H, Haass C (2003) Reconstitution of gamma-secretase activity. *Nat Cell Biol* 5(5):486–488
43. Vassar R, Bennett BD, Babu-Khan S, Kahn S, Mendiaz EA, Denis P, Teplow DB, Ross S, Amarante P, Loeloff R, Luo Y, Fisher S, Fuller J, Edenson S, Lile J, Jarosinski MA, Biere AL, Curran E, Burgess T, Louis JC, Collins F, Treanor J, Rogers G, Citron M (1999) Beta-secretase cleavage of Alzheimer's amyloid precursor protein by the transmembrane aspartic protease BACE. *Science* 286(5440):735–741
44. Finelli A, Kelkar A, Song HJ, Yang H, Konsolaki M (2004) A model for studying Alzheimer's Aβ42-induced toxicity in *Drosophila melanogaster*. *Mol Cell Neurosci* 26(3):365–375
45. Greeve I, Kretzschmar D, Tschäpe JA, Beyn A, Brellinger C, Schweizer M, Nitsch RM, Reifegerste R (2004) Age-dependent neurodegeneration and Alzheimer-amyloid plaque formation in transgenic *Drosophila*. *J Neurosci* 24(16):3899–3906
46. Chung HM, Struhl G (2001) Nicastrin is required for Presenilin-mediated transmembrane cleavage in *Drosophila*. *Nat Cell Biol* 3(12):1129–1132
47. Ye Y, Lukinova N, Fortini ME (1999) Neurogenic phenotypes and altered Notch processing in *Drosophila* Presenilin mutants. *Nature* 398(6727):525–529
48. Struhl G, Greenwald I (1999) Presenilin is required for activity and nuclear access of notch in *Drosophila*. *Nature* 398:522–525
49. Struhl G, Greenwald I (2001) Presenilin-mediated transmembrane cleavage is required for notch signal transduction in *Drosophila*. *Proc Natl Acad Sci USA* 98:229–234
50. Ocorr K, Akasaka T, Bodmer R (2007) Age-related cardiac disease model of *Drosophila*. *Mech Ageing Dev* 128(1):112–116
51. Hidary G, Fortini ME (2001) Identification and characterization of the *Drosophila* tau homolog. *Mech Dev* 108:171–178
52. Wittmann CW, Wszolek MF, Shulman JM et al (2001) Tauopathy in *Drosophila* 2001 neurodegeneration without neurofibrillary tangles. *Science* 293:711–714
53. De Sandre-Giovannoli A, Bernard R, Cau P, Navarro C, Amiel J, Boccaccio I, Lyonnet S, Stewart CL, Munnich A, Le Merrer M, Levy N (2003) Lamin A truncation in Hutchinson-Gilford progeria. *Science* 300(5628):2055
54. Eriksson M, Brown WT, Gordon LB, Glynn MW, Singer J, Scott L, Erdos MR, Robbins CM, Moses TY, Berglund P, Dutra A, Pak E, Durkin S, Csoka AB, Boehnke M, Glover TW, Collins FS (2003) Recurrent de novo point mutations in lamin A cause Hutchinson-Gilford progeria syndrome. *Nature* 423:293–298
55. Goldman RD, Shumaker DK, Erdos MR, Eriksson M, Goldman AE, Gordon LB, Gruenbaum Y, Khuon S, Mendez M, Varga R, Collins FS (2004) Accumulation of mutant lamin A causes progressive changes in nuclear architecture in Hutchinson-Gilford progeria syndrome. *Proc Natl Acad Sci USA* 101:8963–8968

56. Hennekam RC (2006) Hutchinson-Gilford progeria syndrome: review of the phenotype. *Am J Med Genet A* 140(23):2603–2624
57. McClintock D, Ratner D, Lokuge M, Owens DM, Gordon LB, Collins FS, Djabali K (2007) The mutant form of lamin A that causes Hutchinson-Gilford progeria is a biomarker of cellular aging in human skin. *PLoS One* 2(12):e1269
58. Olive M, Harten I, Mitchell R, Beers JK, Djabali K, Cao K, Erdos MR, Blair C, Funke B, Smoot L, Gerhard-Herman M, Machan JT, Kutys R, Virmani R, Collins FS, Wight TN, Nabel EG, Gordon LB (2010) Cardiovascular pathology in Hutchinson-Gilford progeria: correlation with the vascular pathology of aging. *Arterioscler Thromb Vasc Biol* 11:2301–2309
59. Scaffidi P, Misteli T (2006) Lamin A-dependent nuclear defects in human *Science* 312:1059–1063
60. Scaffidi P, Misteli T (2005) Reversal of the cellular phenotype in the premature aging disease Hutchinson-Gilford progeria syndrome. *Nat Med* 11:440–445
61. Capell BC, Collins FS (2006) Human laminopathies: nuclei gone genetically awry. *Nat. Rev. Genet* 7:940–952
62. Brandt A, Krohne G, Grosshans J (2008) The farnesylated nuclear proteins KUGELKERN and LAMIN B promote aging-like phenotypes in *Drosophila* flies. *Aging Cell* 7(4):541–551
63. Haithcock E, Dayani Y, Neufeld E, Zahand AJ, Feinstein N, Mattout A, Gruenbaum Y, Liu J (2005) Age-related changes of nuclear architecture in *Caenorhabditis elegans*. *Proc Natl Acad Sci USA* 102:16690–16695
64. Kishi S, Bayliss PE, Uchiyama J, Koshimizu E, Qi J, Nanjappa P, Imamura S, Islam A, Neuberger D, Amsterdam A, Roberts TM (2008) The identification of zebrafish mutants showing alterations in senescence-associated biomarkers. *PLoS Genet* 4(8):e1000152
65. Hasty P, Campisi J, Hoeijmakers J, van Steeg H, Vijg J (2003) Aging and genome maintenance: lessons from the mouse? *Science* 299(5611):1355–1359
66. Bauer JH, Goupil S, Garber GB, Helfand SL (2004) An accelerated assay for the identification of lifespan-extending interventions in *Drosophila melanogaster*. *Proc Natl Acad Sci USA* 101(35):12980–12985
67. Spindler SR, Li R, Dhahbi JM, Yamakawa A, Sauer F (2012) Novel protein kinase signaling systems regulating lifespan identified by small molecule library screening using *Drosophila*. *PLoS One* 7(2):e29782
68. Prüfert K, Vogel A, Krohne G (2004) The lamin CxxM motif promotes nuclear membrane growth. *J Cell Sci* 117:6105–6116
69. Brandt A, Papagiannouli F, Wagner N, Wilsch-Bräuninger M, Braun M, Furlong EE, Loserth S, Wenzl C, Pilot F, Vogt N, Lecuit T, Krohne G, Grosshans J (2006) Developmental control of nuclear size and shape by Kugelkern and Kurzkern. *Curr Biol* 16(6):543–552

Tribolium castaneum as a whole-animal screening system for the detection and characterization of neuroprotective substances

Annely Brandt^{1,2}  | Gerrit Joop³ | Andreas Vilcinskas^{1,3} 

¹Department of Bioresources, Fraunhofer Institute of Molecular Biology and Applied Ecology, Giessen, Germany

²LLH-Bee Institute Kirchhain, Kirchhain, Germany

³Institute for Insect Biotechnology, Justus-Liebig-University of Giessen, Giessen, Germany

Correspondence

Annely Brandt, LLH Bee Institute Kirchhain, Erlenstr. 9, 35274 Kirchhain, Germany.
Email: annely.brandt@llh-hessen.de

Funding information

Hessen State Ministry of Higher Education, Research and the Arts (HMWK) via the LOEWE Research Center "Insect Biotechnology and Bioresources"

Abstract

Parkinson's disease (PD) is a movement disorder caused by the progressive loss of dopaminergic neurons. Natural antioxidants and plant extracts with neuroprotective properties offer a promising new therapeutic approach for PD patients, but a suitable large-scale screening system is required for their discovery and preclinical analysis. Here we used the red flour beetle (*Tribolium castaneum*) as a whole-animal screening system for the detection and characterization of neuroprotective substances. Paraquat was added to the diet of adult beetles to induce PD-like symptoms, which were quantified using a novel positive geotaxis behavioral assay. These paraquat-induced behavioral changes were reduced in beetles fed on diets supplemented with L-dihydroxyphenylalanine, ascorbic acid, curcumin, hemp-seed flour, or the Chinese herb gou-teng. *T. castaneum* is, therefore, a valuable model for the screening of neuroprotective substances in chemical libraries and plant extracts and could be developed as a model for the preclinical testing of therapeutic candidates for the treatment of neurodegenerative diseases, such as PD.

KEYWORDS

drug development, in vivo screening, model insect, neurodegenerative diseases, red flour beetle

1 | INTRODUCTION

The prevalence of age-related neurodegenerative diseases is increasing as the world's population becomes older. Parkinson's disease (PD) is a progressive neurodegenerative disorder clinically characterized by bradykinesia (slow movement), resting tremor, rigidity, and postural instability, often accompanied by nonmotor symptoms such as olfactory deficit, sleep impairment, and dementia (Braak, Ghebremedhin, Rüb, Bratzke, & Del Tredici, 2004; Chaudhuri & Sauerbier, 2015; Jankovic & Aguilar, 2008; Klingelhofer & Reichmann, 2015; Lees, Hardy, & Revesz, 2009). The symptoms of PD reflect the loss of 50–70% of the dopaminergic neurons in the substantia nigra, lower levels of the neurotransmitter dopamine in the striatum, and cytoplasmic inclusions of insoluble protein aggregates known as Lewy bodies (Cuervo, Wong, & Martinez-Vicente, 2010).

PD is a multifactorial disorder (Betarbet et al., 2000; Chaudhuri, Healy, & Schapira, 2006; Gorell, Johnson, Rybicki, Peterson, & Richardson, 1998). More than 90% of cases are sporadic, whereas only 5–10% are caused by mutations underlying the familial forms of the disease (Bonilla-Ramirez, Jimenez-Del-Rio, & Velez-Pardo, 2011). Four principal pathogenic events that eventually lead to PD have been identified: oxidative stress, protein aggregation, inflammation, and excitotoxicity (Blesa, Trigo-Damas, Quiroga-Varela, & Jackson-Lewis, 2015; Dawson, Ko, & Dawson, 2010). Oxidative stress caused by the redox-active herbicide paraquat has been identified as one of the etiological agents responsible for sporadic PD in humans (Dinis-Oliveira et al., 2006; Thiruchelvam, Brockel, Richfield, Baggs, & Cory-Slechta, 2000), and this compound can, therefore, be used to induce PD-like symptoms in other animals (Bonilla, Medina-Leendertz, Villalobos, Molero, & Bohórquez, 2006; Brooks, Chadwick, Gelbard, Cory-Slechta, & Federoff, 1999; Dixit et al., 2013; Feany & Bender, 2000; McCormack, Thiruchelvam, & Manning-Bog, 2002; Pienaar, Götz, & Feany, 2010; Rappold et al., 2011; Hosamani & Muralidhara, 2013; Mehdi & Qamar, 2013).

There is no known cure for PD and current therapeutic approaches focus on symptomatic relief by replenishing striatal dopamine levels, which can be achieved by the oral administration of the dopamine precursor L-dihydroxyphenylalanine (L-DOPA), inhibitors of dopamine-degrading enzymes (e.g., entacapone or selegiline) or dopamine receptor agonists (e.g., pergolide). The inhibition of oxidative stress in dopaminergic neurons is a promising target for new drugs (Mythri & Bharathm, 2012; Santos, 2012). However, large compound libraries must be screened to identify promising candidates, and ideally, this requires a model organism that displays the main features of PD and is also suitable for large-scale screening *in vivo*. Although the anatomy and structural organization of the insect dopaminergic system differs from that of vertebrates, many fundamental cellular and molecular features of neuronal development and activity are conserved (Bicker & Menzel, 1989; Whitworth, Wes, & Pallanck, 2006). Paraquat can, therefore, be used to induce PD-like symptoms in insects allowing the development of a PD model in which to screen for new drugs and other protective substances, including natural antioxidants found in plant extracts.

The red flour beetle *Tribolium castaneum* is potentially suitable for the characterization of neuroprotective substances because it combines the general advantages of insect models (easy and inexpensive to rear in large numbers, lack of ethical issues that affect vertebrate models, fully sequenced genome, and a diet that enables the oral administration of test compounds; Denell, 2008; Grünwald, Adam et al., 2013; Grünwald, Stellzig et al., 2013; Knorr & Vilcinskas, 2011; Bingsohn, Knorr, & Vilcinskas, 2016; Knorr, Bingsohn, Kanost, & Vilcinskas, 2013; Mukherjee, Twyman, & Vilcinskas, 2015; Schmitt-Engel et al., 2015) with unique features that facilitate PD research. Specifically, *T. castaneum* beetles feign death when attacked (a behavioral phenomenon known as tonic immobility) and the duration of the response correlates with brain dopamine levels (Miyatake et al., 2004; Nakayama & Miyatake, 2010). This behavior is accessible to pharmacological intervention, for example, when the dopamine agonist caffeine is added to the diet, the duration of tonic immobility is short (Nishi, Sasaki, & Miyatake, 2010).

We, therefore, took advantage of the unique pharmacological readout afforded by red flour beetles by feeding adult beetles on a flour diet supplemented with or without candidate neuroprotective substances and with or

without paraquat (to induce PD-like symptoms) in a fully factorial set-up. To test potentially neuroprotective substances and to investigate the usefulness and applicability of *T. castaneum* as a high-throughput whole-animal screening system for the discovery and characterization of neuroprotective substances.

2 | MATERIALS AND METHODS

2.1 | Insects and culture

The *T. castaneum* strain pBA19 (kindly provided by G. Bucher; Trauner et al., 2009) was used for our experiments because it climbs more quickly in negative geotaxis assays than the San Bernardino and GA2 strains (pers. observation). The beetles were reared on wholemeal flour (Alnatura, Germany) enriched with 5% Brewer's yeast (Leiber GmbH, Bramsche, Germany), and were housed in a chamber (Binder, Tuttlingen, Germany) maintained at 32°C and 70% relative humidity without artificial light.

2.2 | Pretreatment with test substances

Adult beetles (7 days old, both sexes) were exposed to the test substances for two weeks, before the paraquat treatment. To ensure a homogenous distribution of the active ingredients in the flour, we dissolved most active substances (paraquat, L-DOPA, ascorbic acid, curcumin, gou-teng, for details see below) and added the same volume of the spiked solutions to the flour, to ensure that every little flour grain was completely soaked in the spiked solution. This mesh was mixed thoroughly and subsequently dried. Only hempseed flour was directly added to the normal wheat flour and, here, we could not rule out that beetles maybe avoided the hemp.

In detail, the beetles were pretreated with candidate substances to prevent PD-like symptoms in 770-ml glass jars closed with tissues fixed with a rubber band. Curcumin is an antioxidant with reported anti-inflammatory and anticancer effects in mammalian models, and it has been shown to minimize cell death and neuronal loss in cellular and animal models of Alzheimer's disease, Huntington's disease, and stroke, as well as PD (Cole, Teter, & Frautschy, 2007). For curcumin pretreatment, each jar contained 30 g rearing medium supplemented with 30 mg curcumin. The curcumin powder was dissolved in pure ethanol (1 mg/ml) and 30 ml of the curcumin solution was poured onto the 30 g rearing medium to achieve an at least visually even distribution. Subsequently, the spiked flour was dried at 60°C for 4 hr. To control for the potential influence of ethanol, control beetles were placed on food treated with equivalent amounts of ethanol without curcumin.

For pretreatment with hempseed flour, the rearing medium contained 20% hempseed flour (Rapunzel, Germany), 5% yeast and 75% wholemeal flour. In contrast, control jars contained 95% wholemeal flour and 5% yeast. For gou-teng pretreatment, a gou-teng tea was prepared from 210 g gou-teng (dried *Uncaria rhynchophylla* twigs and thorns, internet-apotheke Freiburg, Germany; Watanabe et al., 2003) by simmering in 1.5 L distilled water for 1 hr. Subsequently, the tea was sieved and 30 ml of the solution was mixed with 30 g rearing medium to achieve an even distribution before drying for 24 hr at 60°C. Control jars were treated with distilled water only.

L-DOPA powder ($\geq 98\%$; Sigma-Aldrich, St. Louis, MO) was dissolved in 30 ml distilled water to a concentration of 1 mM, based on a previous *D. melanogaster* PD model (Pendleton, Parvez, Sayed, & Hillman, 2002), then poured onto the 30 g of rearing medium (wt/wt) and dried at 60°C for 24 hr. The ascorbic acid powder was dissolved in 30 ml distilled water to a concentration of 1.4 mM (Pendleton et al., 2002), poured onto the 30 g of rearing medium and dried at 60°C for 24 hr. In control jars, only water was added to the flour.

For all experiments, approximately 500 beetles were placed in each jar and the pretreatment was carried out for 2 weeks in a chamber maintained at 32°C and 70% relative humidity without artificial light.

2.3 | Paraquat treatment

Paraquat treatment (to induce PD-like symptoms) was carried out in 68-ml polystyrene vials closed with ceapren plugs (Greiner Bio-One, Kremsmünster, Austria). The vials contained 3 g wholemeal flour enriched with 5% Brewer's yeast as the food supply. A paraquat stock solution (1:6,000) was prepared in water and filled to 3 ml with pure ethanol before pouring onto the 3 g food mixture to achieve an even distribution throughout the flour. For control vials, 3 ml of pure ethanol was used to account for any potential effect of ethanol. The ethanol was evaporated over 3 days under a flow hood, and 100 beetles were then placed in each vial and kept for 4 days in a chamber at 32°C and 70% relative humidity without artificial light.

2.4 | Treatment categories

The tonic immobility and negative geotaxis assays below were done in a fully factorial experimental set up; that is, beetles of the treatments categories "test substance" (control, curcumin, hempseed, gou-teng, and L-DOPA) and "paraquat" (control, paraquat), alone and in combination with each other, were tested in all experiments. Apoptosis assay were conducted only on some chosen test substances.

2.5 | Negative geotaxis assay

At least 2 hr before the test, the vials containing beetles were placed on a heating plate at 35°C in daylight. Moving or shaking the vials was strictly avoided to prevent the undesirable agitation of the beetles. For the negative geotaxis assay, a paper strip (4 × 45 cm) with a printed scale in cm was placed inside the vials, and the beetles were allowed to climb up. To prevent the beetles from moving to the back of the paper strip, both sides of the strip were blocked with glossy scotch tape (tesa Werk, Hamburg, Germany). After 1 min, the beetles on the paper strip were photographed and the number of beetles that had reached each centimeter marker was counted. In each experiment, six vials, each containing 100 beetles, were used per treatment category.

2.6 | Observation of tonic immobility

At least 2 hr before the test, each beetle was placed in a well of a 48-well tissue culture plate (Greiner Bio-One) to prevent disturbance by other beetles, which reduces the duration of tonic immobility (Miyatake et al., 2004). The plate was placed on a heating surface at 35°C (Leica HI1220, Germany). Each beetle was gently placed on its back inside the 48-well plate. Tonic immobility was induced by touching the abdomen of the beetle with blunt steel forceps (Neolab, Heidelberg, Germany). A trial consisted of provoking tonic immobility and recording its duration with a stopwatch. The duration was defined as the length of time between the forceps touching the beetle and detection of the first visible movement of the legs. If the beetle did not freeze, the touch was repeated twice. Three or four independent experiments were conducted per treatment category.

2.7 | Apoptosis assay

Apoptotic cells were identified using the DeadEnd Fluorometric TUNEL System (Promega, Fitchburg). The beetles (all treatment categories) were cold anesthetized, submerged in precooled Schneider cell medium (Invitrogen, Waltham, MA) and the brains were removed and fixed in 5% formaldehyde in phosphate buffered saline (PBS) for 1 hr at room temperature. Fixed brains were washed in PBS and permeabilized in PBS containing 0.5% Triton X-100 for 1–2 hr. The brains were immersed in terminal deoxynucleotidyl transferase dUTP nick-end labeling (TUNEL) equilibration buffer and then in the terminal deoxynucleotidyltransferase/fluorescent nucleotide staining mixture for 1 hr at 37°C with agitation, according to the manufacturer's instructions. After washing three times in PBS for

15 min, the brains were stained with 4',6-diamidino-2-phenylindole ($\geq 98\%$; Sigma-Aldrich) and mounted in Aqua-Poly/Moun (Polyscience, Eppelheim, Germany). The total number of fluorescent cells was determined in whole mount preparations of the brains under a fluorescence microscope (Leica DM 5000B). Apoptotic cells in the retina and lamina were excluded from the counts because these structures were not present in all dissected brains.

2.8 | Statistics

Three or four independent experiments were conducted per test method and treatment category. The death feigning and negative geotaxis data were analyzed using an analysis of variance with a Bonferroni corrected Tukey HSD post hoc analysis. For the apoptosis data, each parameter was compared between treatment groups using Kruskal-Wallis (KW) tests followed by post hoc pairwise comparisons with Mann-Whitney U (MWU) tests. All statistical tests were processed in SPSS v20 for Windows (IBM Corp., Armonk).

3 | RESULTS

3.1 | Tonic immobility

Beetles were exposed to oxidative stress by spiking their food with paraquat. After 4 days on this diet, the duration of tonic immobility was measured (Figure 1a, Table 1). Even the beetles exposed to only 60 mM paraquat showed a significant increase in the duration of tonic immobility compared with controls. Beetles exposed to 100 or 1,000 mM paraquat showed an even greater increase in the duration of this behavior (KW test, $p < 0.0001$; MWU test, control ($n = 189$) versus 60 mM ($n = 189$, $p < 0.0001$), 100 mM ($n = 183$, $p < 0.0001$), and 1,000 mM ($n = 48$, $p = 0.0127$)).

To evaluate the accuracy of our insect model compared with existing PD animal models, we tested the effect of test substances on the duration of tonic immobility (Figure 1b, Table 1). All of our test substances, if fed before paraquat, did reduce the paraquat effect (100 mM) on tonic immobility. However, if applied only on their own all test substances besides gou-teng also increased tonic immobility compared with the controls to some extent, coming with some side effects so to say. For numbers in the individual treatments please compare Table 1.

3.2 | Negative geotaxis

We established a negative geotaxis assay for *T. castaneum* to determine whether test compounds could reduce the mobility deficits induced by paraquat.

All test substances indeed did reduce the negative paraquat-effect on negative geotaxis (Figure 2a, Table 2), where some test substances (curcumin, gou-teng) alone even increased the climbing ability of the beetles. For numbers in the individual treatments please compare Table 2.

3.3 | Pretreatment with curcumin or hempseed flour prevents paraquat-induced apoptosis

To evaluate the effects of paraquat on neuronal survival in the beetle brain, a TUNEL assay was used to label DNA strand breaks that occur during apoptosis. A clear increase in TUNEL-positive cells was observed in beetles that were treated with paraquat for 21 days (Figure 3a,b) compared with the control animals (MWU test, $U_A = 0$, $z = 2.78$, $p = 0.0027$). To evaluate the effects of potential neuroprotective compounds, we pretreated the beetles for 2 weeks with curcumin or hempseed flour, before the paraquat treatment of 21 days. Curcumin showed a strong antiapoptotic effect if fed before paraquat (Figure 3a,b) because the beetles pretreated with curcumin featured significantly fewer apoptotic cells compared with those treated with paraquat alone (MWU test, $U_A = 0$, $z = 3.31$; $p_{(1)} = 0.0005$). Similar

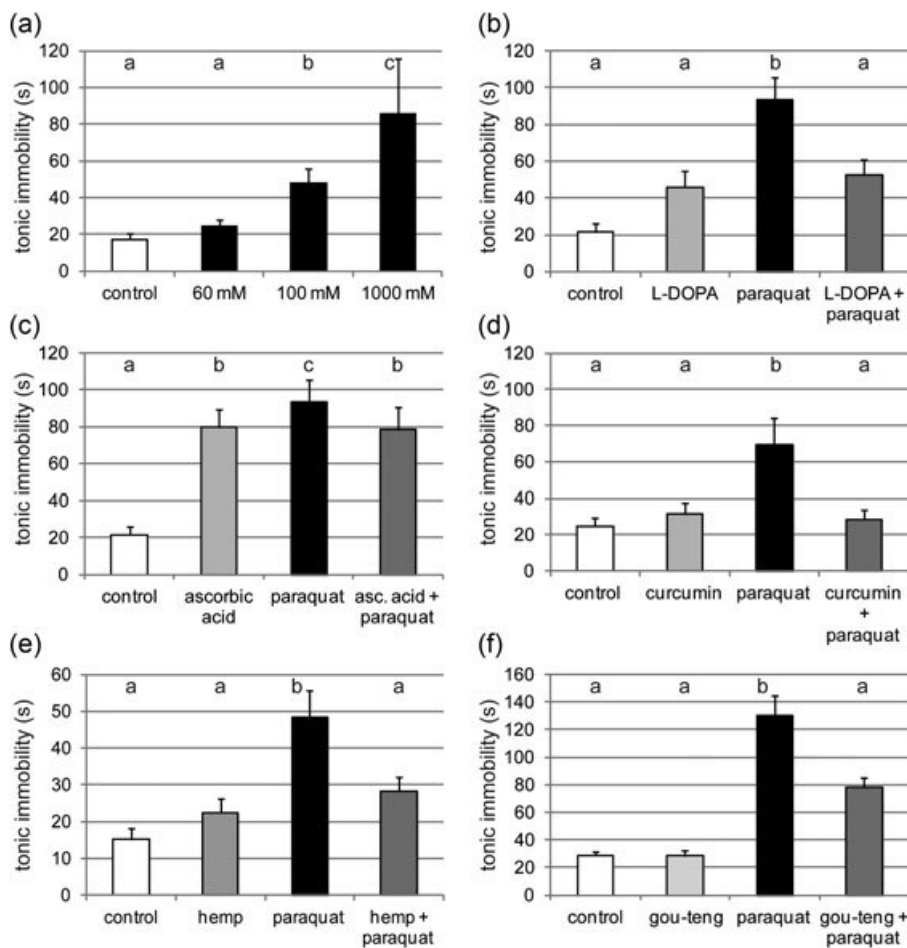


FIGURE 1 Paraquat prolonged the duration of tonic immobility, but pretreatment with drugs and natural compounds alleviated the effect. Tonic immobility was provoked by touching the ventral side of the abdomen. Paraquat increased the duration of tonic immobility (a). Two weeks of Pretreatment with L-DOPA (b) ascorbic acid (c) curcumin (d) hempseed flour (e) or the Chinese herb gou-teng (f) could prevent the paraquat-induced (100 mM) loss of climbing activity. Bars show means with standard errors, treatments with different letters differ statistically significantly from each other

neuroprotective effects were observed for hempseed flour prefed to the paraquat (Figure 3a,b), again resulting in the formation of fewer apoptotic cells in the brain (MWU test, $U_A = 2$, $z = 2.85$, $p = 0.0022$). Interestingly, pretreatment with curcumin, as well as with hempseed flour, reduced the number of apoptotic cells even in comparison with the control animals (curcumin: MWU test, $U_A = 3$, $z = 2.5$, $p = 0.0062$; hempseed: MWU test, $U_A = 3$, $z = 2.1$, $p = 0.0179$).

4 | DISCUSSION

We have demonstrated that the red flour beetle *T. castaneum* is ideal as a whole-animal screening system for the detection and characterization of neuroprotective substances. Our results suggest that paraquat induces apoptosis in the brain and mimics the motor impairments associated with PD, thus providing an amenable *in vivo* testing system for potential neuroprotective substances and drug candidates for the treatment of PD. Furthermore, using

TABLE 1 Tonic immobility behavior, presenting sample size and statistical test results

A	Number of beetles	p values		
		Control	Paraquat 60 mM	Paraquat 100 mM
Control	189	–		
Paraquat 60 mM	179	1.000	–	
Paraquat 100 mM	48	0.004	0.056	–
Paraquat 1,000 mM	48	0.000	0.000	0.045
B	Number of beetles	Control	L-DOPA	Paraquat
Control	144	–		
L-DOPA	1,100	0.352	–	
Paraquat	144	0.000	0.001	–
L-DOPA+Paraquat	1,100	0.99	1.000	0.009
C	Number of beetles	Control	Ascorbic acid	Paraquat
Control	144	–		
Ascorbic acid	144	0.000	–	
Paraquat	144	0.000	0.043	–
Ascorbic acid+paraquat	144	0.001	0.480	0.05
D	Number of beetles	Control	Curcumin	Paraquat
Control	145	–		
Curcumin	144	1.000	–	
Paraquat	143	0.001	0.012	–
Curcumin+paraquat	145	1.000	1.000	0.004
E	Number of beetles	Control	Hemp	Paraquat
Control	189	–		
Hemp	189	1.000	–	
Paraquat	183	0.000	0.001	–
Hemp+paraquat	242	0.267	1.000	0.011
F	Number of beetles	Control	Gou-teng	Paraquat
Control	144	–		
Gou-teng	144	1.000	–	
Paraquat	144	0.000	0.000	–
Gou-teng+paraquat	141	0.276	0.238	0.000

Note. Adult red flour beetles were fed on a flour diet supplemented with or without candidate neuroprotective substances and with or without paraquat (to induce PD-like symptoms) in a fully factorial set-up. Certain compounds and plant extracts reversed the paraquat-induced behavior tonic immobility. The data were analyzed using an analysis of variance with a Bonferroni corrected Tukey HSD post hoc analysis.

the *T. castaneum* testing system we provide experimental evidence for the neuroprotective activity of curcumin, hempseed flour, and gou-teng tea, all of which are natural products containing antioxidants (Cole et al., 2007; Mythri & Bharathm, 2012; Pendleton et al., 2002).

Neurological diseases can be modeled in animals to simulate specific pathogenic events and behavioral symptoms (Blesa et al., 2015). The oxidative stress induced by paraquat is mediated by redox cycling, which generates reactive oxygen species that damage lipids, proteins, RNA, and DNA (Blesa et al., 2015; Bonilla et al., 2006; Feany & Bender, 2000; Hosamani & Muralidhara, 2013; Rappold et al., 2011). In fruit fly models, dopaminergic neurons in the dorsomedial cluster are particularly susceptible to paraquat (Faust et al., 2009; Jahromi, Haddadi, Shivanandappa,

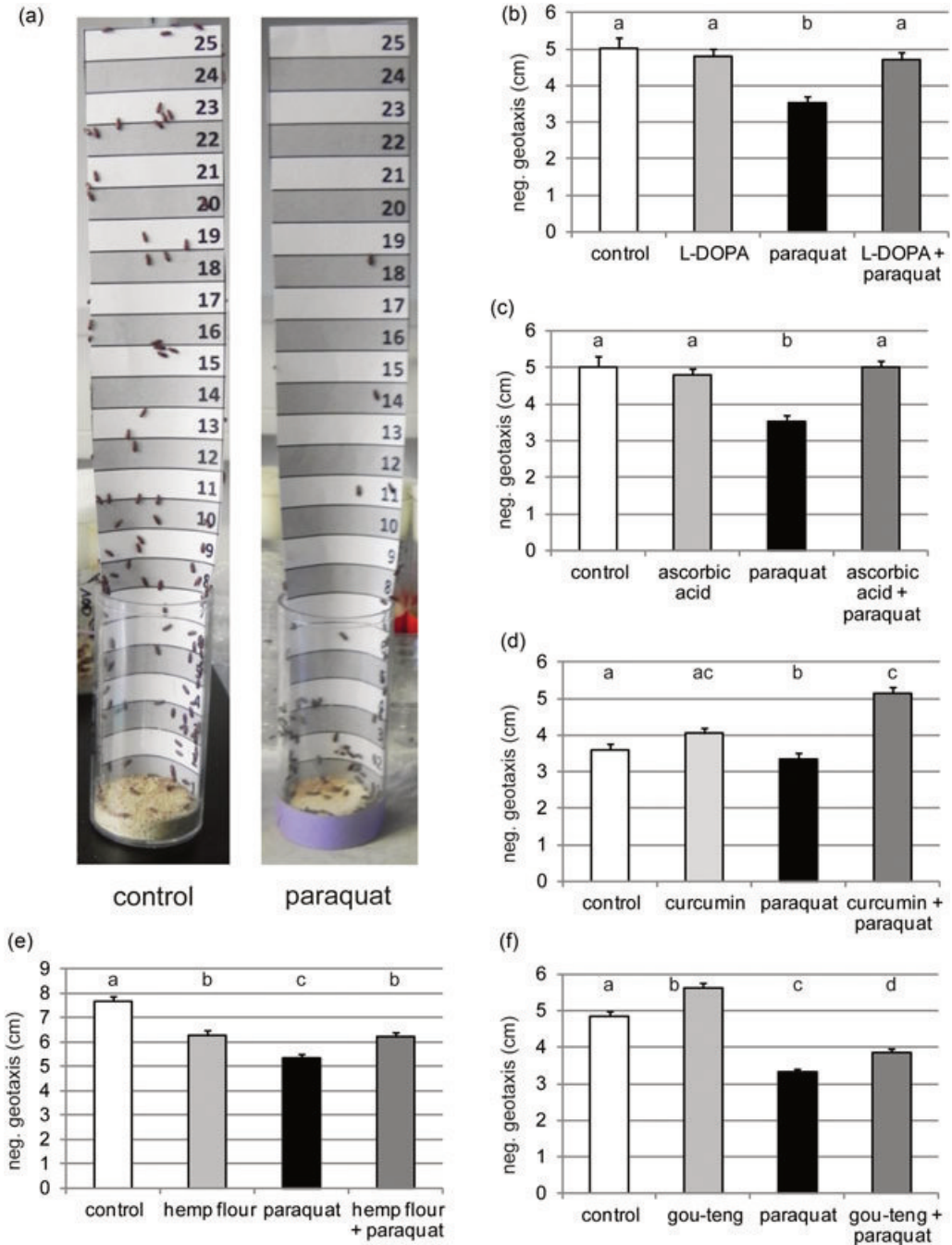


FIGURE 2 Paraquat treatment reduced negative geotaxis, but pretreatment with drugs or natural compounds alleviated the effect. (a–f) Beetles were allowed to climb upon a paper strip for 60 s. In this period of time, only a few beetles reached the top of the paper strip and no beetle fell down. They never climbed up the walls of the plastic vials. Paraquat reduced the climbing activity. Two weeks of pretreatment with L-DOPA (b) ascorbic acid (c) curcumin (d) hempseed flour (e) or the Chinese herb gou-teng (f) prevented the paraquat-induced loss of climbing activity. Bars show means with standard errors, treatments with different letters differ statistically significantly from each other

TABLE 2 Negative geotaxis behavior, presenting sample size and statistical test results

B	Number of beetles	p values		
		Control	L-DOPA	Paraquat
Control	700	-		
L-DOPA	1,100	1.000	-	
Paraquat	1,100	0.000	0.000	-
L-DOPA+Paraquat	1,100	1.000	1.000	0.000
C	Number of beetles	Control	Ascorbic acid	Paraquat
Control	700	-		
Ascorbic acid	1,000	1.000	-	
Paraquat	1,100	0.000	0.002	-
Ascorbic acid+paraquat	1,100	1.000	0.888	0.000
D	Number of beetles	Control	Curcumin	Paraquat
Control	1,500	-		
Curcumin	1,700	0.257	-	
Paraquat	1,300	0.000	0.000	-
Curcumin+paraquat	1,700	0.013	0.230	0.000
E	Number of beetles	Control	Hemp	Paraquat
Control	1,500	-		
Hemp	1,400	0.000	-	
Paraquat	1,200	0.000	0.006	-
Hemp+paraquat	1,700	0.000	1.000	0.008
F	Number of beetles	Control	Gou-teng	Paraquat
Control	1,100	-		
Gou-teng	1,500	0.000	-	
Paraquat	1,500	0.000	0.000	-
Gou-teng+paraquat	1,500	0.000	0.000	0.043

Note. In a fully factorial set-up, adult red flour beetles were fed on a flour diet supplemented with or without candidate neuroprotective substances and with or without paraquat (to induce PD-like symptoms). Certain compounds and plant extracts reversed the paraquat-induced negative geotaxis behavior. The data were analyzed using an analysis of variance with a Bonferroni corrected Tukey HSD post hoc analysis.

& Ramesh, 2013). Likewise, we found that paraquat increased the number of apoptotic cells in the brains of red flour beetles, although it was not possible to directly show that the apoptotic cells were dopaminergic neurons because dual TH and TUNEL staining is not technically feasible.

In fruit flies, paraquat induces PD-like symptoms such as climbing deficits, resting tremor, bradykinesia, rotational behavior, and postural instability (Niveditha, Ramesh, Shivanandappa, 2017). We also observed profound motor impairments in paraquat-treated red flour beetles, that is, the climbing deficits in the negative geotaxis assay and the prolonged tonic immobility. A strong genetic correlation between tonic immobility/locomotor activity levels and brain dopamine levels has been reported in this species, suggesting tonic immobility can be used as an indirect measure of dopamine levels (Miyatake et al., 2004; Nakayama, Sasaki, Matsumura, Lewis, & Miyatake, 2012).

Geographical genetic variations in red flour beetle populations are known to affect the duration of tonic immobility (Prohammer & Wade, 1981). Beetles selected for brief tonic immobility have higher concentrations of dopamine in the brain than those selected for prolonged tonic immobility (Miyatake et al., 2004). Furthermore, the

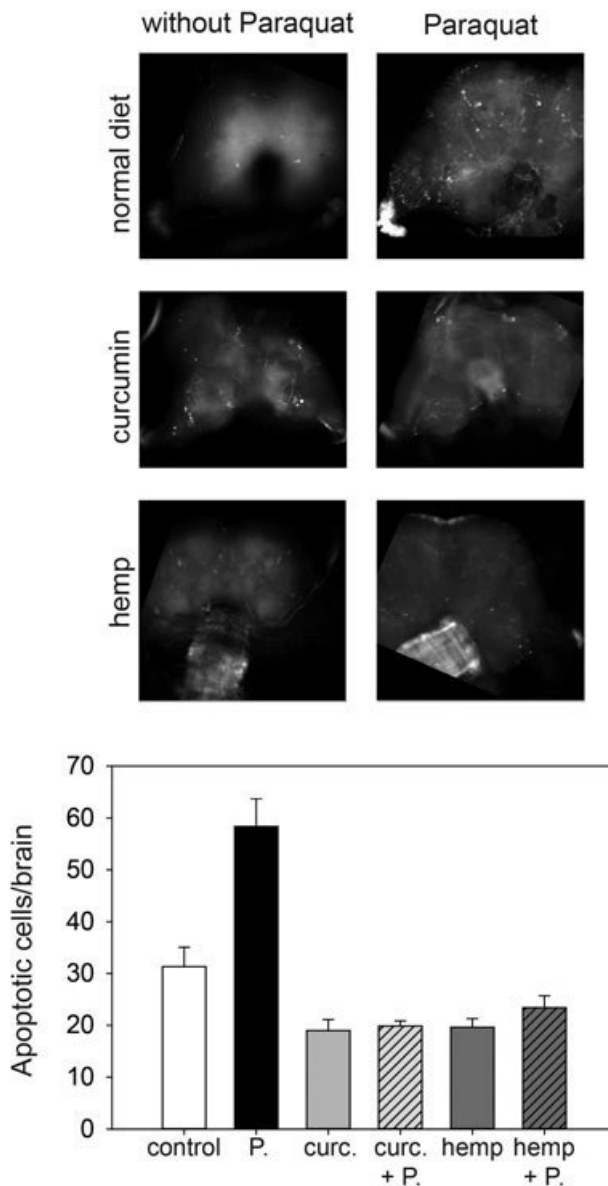


FIGURE 3 Paraquat treatment induced apoptosis in the brain, but pretreatment with curcumin or hempseed flour alleviated the effect. (a) Apoptotic cells (white or red, compiled pictures) were visualized by TUNEL-staining in the brain (blue=DAPI-stained nuclei). Beetles exposed to paraquat (100 mM) featured a higher number of apoptotic cells than the untreated controls. (a,b) Two weeks of pretreatment with curcumin or hempseed flour was able to prevent the paraquat-induced cell death. Columns depict mean-values with standard errors ($n = 8$ individuals per treatment group). DAPI: 4',6-diamidino-2-phenylindole; TUNEL: terminal deoxynucleotidyl transferase dUTP nick-end labeling

duration of tonic immobility can be reduced by the injection of dopamine in a dose-dependent manner or by treatment with caffeine, a known dopamine receptor agonist, showing that this PD model is accessible for pharmacological intervention (Fredholm, Bättig, Holmén, Nehlig, & Zvartau, 1999; Trauner et al., 2009). Accordingly, we were able to influence the duration of tonic immobility by feeding beetles with the dopamine precursor L-DOPA, or natural substances, such as ascorbic acid, curcumin, hempseed flour, and gou-teng.

We found that the dopamine precursor L-DOPA and several natural antioxidants were neuroprotective in our beetle model of PD. When added to the standard diet, all these supplements reduced paraquat-induced motor impairments and limited the duration of tonic immobility, achieving results comparable with previous studies involving fruit fly and rodent models. Most PD therapies currently aim to replenish striatal dopamine, and although drugs such as L-DOPA provide symptomatic relief during the early stages of PD, many patients develop motor complications with long-term treatment, and the underlying neurodegeneration is not prevented (Mythri & Bharathm, 2012).

Several epidemiological studies have suggested that antioxidant-rich diets may reduce the likelihood of oxidative damage (Blesa et al., 2015; Jahromi et al., 2013). Accordingly, in vitro and in vivo studies of endogenous and natural antioxidants such as coenzyme Q10, vitamins A, C and E, and polyphenols have shown protective effects against oxidative stress-induced neuronal death in PD models (Miyasaki, Martin, Suchowersky, Weiner, & Lang, 2002; Mythri & Bharathm, 2012; Santos, 2012). Likewise, we found that the antioxidant ascorbic acid (vitamin C) had a positive impact on paraquat-induced motor impairments and tonic immobility. Curcumin also reduced the effect of paraquat-induced motor impairments and tonic immobility and counteracted the induction of apoptosis in our model. Curcumin is a polyphenol extracted from turmeric (*Curcuma longa*), which is widely used as a dietary spice and herbal medicine (Mythri & Bharathm, 2012). Curcumin binds directly to α -synuclein in vitro and protects against α -synuclein-induced cell death in cultured cells by inhibiting the formation of reactive oxygen species and preventing mitochondrial toxicity (Liu, Yu, Li, Ross, & Smith, 2011). In a toxin-induced mouse model of PD, curcumin reverses neurodegeneration by preventing mitochondrial dysfunction and apoptosis (Eckert et al., 2013). In agreement with data from rodent PD models and studies in humans, our results showed that L-DOPA, curcumin, and ascorbic acid had neuroprotective effects in our insect model of PD. This strongly supports our assumption that a compound with positive effects in an insect model is likely to be beneficial in rodent models or even in human patients.

We also tested natural substances whose effects have yet to be documented in rodent models. Hempseed flour reduced the impact of paraquat on climbing ability and the duration of tonic immobility in *T. castaneum*. Hempseed flour was shown to act as an antioxidant in a fruit fly PD model, although no beneficial effects on the locomotion phenotype were observed (Lee et al., 2011). Gou-teng tea also reduced the impact of paraquat on climbing ability and the duration of tonic immobility. Gou-teng tea is made from the dried twigs and thorns of *Uncaria rhynchophylla*. Extracts of the plant (*Uncariae uncinis cum ramulus*) have had a long history of use in traditional Chinese medicine for vascular dementia (Watanabe et al., 2003).

5 | CONCLUSIONS

Given that oxidative stress is a fundamental factor in the etiology and progression of PD and other neurodegenerative diseases such as Alzheimer's disease, amyotrophic lateral sclerosis, and Huntington's disease, there is a growing interest in neuroprotective substances such as natural antioxidants that may prevent degeneration (Mythri & Bharathm, 2012; Santos, 2012). The aim of preventive medicine is to develop neuroprotective drugs that can be administered before the onset of advanced symptoms, thus slowing down disease progression as early as possible.

To identify novel neuroprotective compounds, a well-defined model system is required that allows a large number of substances to be evaluated. *T. castaneum* is a genetically and pharmacologically tractable insect model system (Denell, 2008; Grünwald, Adam et al., 2013; Grünwald, Stellzig et al., 2013; Knorr & Vilcinskis, 2011; Knorr, Bingsohn, 2013; Mukherjee et al., 2015; Bingsohn et al., 2016) that can be used to screen for substances that can ameliorate a toxin-induced PD-like phenotype. At this stage, the behavioral assays described are admittedly laborious and time consuming, which can easily be overcome by the development of automated assays. It is a powerful insect model of neurodegenerative disease, which is less expensive and time consuming than vertebrate

models but more ethically acceptable, providing a useful first-level screening platform for the detection and testing of neuroprotective compounds and extracts.

ACKNOWLEDGMENTS

The authors acknowledge financial support from the Hessen State Ministry of Higher Education, Research and the Arts (HMWK) via the collaborative research projects granted under the LOEWE Centers for "Insect Biotechnology and Bioresources." We thank H. Dembeck and J. Dudzik for technical assistance and Ch. Kollewe and E. Knorr for technical assistance and discussions. The authors thank Dr. Richard M. Twyman for editing the manuscript.

CONFLICTS OF INTEREST

The authors declare that they have no conflicts of interest.

AUTHOR CONTRIBUTIONS

A. B. designed the methods and experiments, carried out the laboratory experiments, analyzed the data, interpreted the results, and wrote the manuscript. G. J. supported the statistical analysis and participated in writing the manuscript. A. V. defined the research theme and helped to draft the manuscript. All authors read and approved the final version of the manuscript.

ORCID

Annelly Brandt  <http://orcid.org/0000-0002-2583-3530>

Andreas Vilcinskas  <http://orcid.org/0000-0001-8276-4968>

REFERENCES

- Betarbet, R., Sherer, T. B., MacKenzie, G., Garcia-Osuna, M., Panov, A. V., & Greenamyre, J. T. (2000). Chronic systemic pesticide exposure reproduces features of Parkinson's disease. *Nature Neuroscience*, 3, 301–306.
- Bicker, G., & Menzel, R. (1989). Chemical codes for the control of behaviour in arthropods. *Nature*, 337, 33–39.
- Bingsohn, L., Knorr, E., & Vilcinskas, A. (2016). The model beetle *Tribolium castaneum* can be used as an early warning system for transgenerational epigenetic side effects caused by pharmaceuticals. *Comparative Biochemistry and Physiology. C, Toxicology & Pharmacology*, 185–186, 57–64.
- Blesa, J., Trigo-Damas, I., Quiroga-Varela, A., & Jackson-Lewis, V. R. (2015). Oxidative stress and Parkinson's disease. *Frontiers in Neuroanatomy*, 9, 91. <https://doi.org/10.3389/fnana.2015.00091>
- Bonilla, E., Medina-Leendertz, S., Villalobos, V., Molero, L., & Bohórquez, A. (2006). Paraquat-induced oxidative stress in *Drosophila melanogaster*: Effects of melatonin, glutathione, serotonin, minocycline, lipoic acid, and ascorbic acid. *Neurochemical Research*, 31, 1425–1432.
- Bonilla-Ramirez, L., Jimenez-Del-Rio, M., & Velez-Pardo, C. (2011). Acute and chronic metal exposure impairs locomotion activity in *Drosophila melanogaster*: A model to study Parkinsonism. *BioMetals*, 24, 1045–1057. <https://doi.org/10.1007/s10534-011-9463-0>
- Braak, H., Ghebremedhin, E., Rüb, U., Bratzke, H., & Del Tredici, K. (2004). Stages in the development of Parkinson's disease-related pathology. *Cell and Tissue Research*, 318, 121–134.
- Brooks, A. I., Chadwick, C. A., Gelbard, H. A., Cory-Slechta, D. A., & Federoff, H. J. (1999). Paraquat elicited neurobehavioral syndrome caused by dopaminergic neuron loss. *Brain Research*, 823, 1–10.
- Chaudhuri, K. R., & Sauerbier, A. (2015). Parkinson disease: Unravelling the nonmotor mysteries of Parkinson disease. *Nature Reviews Neurology*, 12, 10–11. <https://doi.org/10.1038/nrneurol.2015.236>
- Chaudhuri, K. R., Healy, D. G., & Schapira, A. H. (2006). Non-motor symptoms of Parkinson's disease: Diagnosis and management. *Lancet Neurology*, 5, 235–245.

- Cole, G. M., Teter, B., & Frautschy, S. A. (2007). Neuroprotective effects of curcumin. *Advances in Experimental Medicine and Biology*, 595, 197–212. https://doi.org/10.1007/978-0-387-46401-5_8
- Cuervo, A. M., Wong, E. S. P., & Martinez-Vicente, M. (2010). Protein degradation, aggregation, and misfolding. *Movement Disorders*, 25, S49–S54. <https://doi.org/10.1002/mds.22718>
- Dawson, T. M., Ko, H. S., & Dawson, V. L. (2010). Genetic Animal Models of Parkinson's Disease. *Neuron*, 5, 646–651.
- Denell, R. (2008). Establishment of *Tribolium* as a genetic model system and its early contributions to Evo-Devo. *Genetics*, 180, 1779–1786.
- Denis-Oliveira, R. J., Remião, F., Carmo, H., Duarte, J. A., Navarro, A. S., Bastos, M. L., & Carvalho, F. (2006). Paraquat exposure as an etiological actor of Parkinson's disease. *Neurotoxicology*, 27, 1110–1122.
- Dixit, A., Srivastava, G., Verma, D., Mishra, M., Singh, P. K., Prakash, O., & Singh, M. P. (2013). Minocycline, levodopa, and MnTMPyP induced changes in the mitochondrial proteome profile of MPTP and maneb and paraquat mice models of Parkinson's disease. *Biochimica et Biophysica Acta*, 1832, 1227–1240. <https://doi.org/10.1016>
- Eckert, G. P., Schiborr, C., Hagl, S., Abdel-Kader, R., Müller, W. E., Rimbach, G., & Frank, J. (2013). Curcumin prevents mitochondrial dysfunction in the brain of the senescence-accelerated mouse-prone 8. *Neurochemistry International*, 62, 595–602. <https://doi.org/10.1016/j.neuint.2013.02.014>. Epub 2013 Feb 17
- Faust, K., Gehrke, S., Yang, Y., Yang, L., Beal, M. F., & Lu, B. (2009). Neuroprotective effects of compounds with antioxidant and anti-inflammatory properties in a *Drosophila* model of Parkinson's disease. *BioMed Central Neuroscience*, 10, 109. <https://doi.org/10.1186/1471-2202-10-109>
- Feany, M. B., & Bender, W. W. (2000). A *Drosophila* model of Parkinson's disease. *Nature*, 404, 394–398.
- Fredholm, B. B., Bättig, K., Holmén, J., Nehlig, A., & Zvartau, E. E. (1999). Actions of caffeine in the brain with special reference to factors that contribute to its widespread use. *Pharmacological Reviews*, 51, 83–133.
- Gorell, J. M., Johnson, C. C., Rybicki, B. A., Peterson, E. L., & Richardson, R. J. (1998). The risk of Parkinson's disease with exposure to pesticides, farming, well water, and rural living. *Neurology*, 50, 1346–1350.
- Grünwald, S., Adam, I. V., Gurmai, A. M., Bauer, L., Boll, M., & Wenzel, U. (2013). The red flour beetle *Tribolium castaneum* as a model to monitor food safety and functionality. *Advances in Biochemical Engineering/Biotechnology*, 135, 111–122.
- Grünwald, S., Stellzig, J., Adam, I. V., Weber, K., Binger, S., Boll, M., ... Wenzel, U. (2013). Longevity in the red flour beetle *Tribolium castaneum* is enhanced by broccoli and depends on nrf-2, jnk-1, and foxo-1 homologous genes. *Genes and Nutrition*, 8, 439–448.
- Hosamani, R., & Muralidhara, L. (2013). Acute exposure of *Drosophila melanogaster* to paraquat causes oxidative stress and mitochondrial dysfunction. *Archives of Insect Biochemistry and Physiology*, 83, 25–40. <https://doi.org/10.1002/arch.21094>
- Jahromi, S. R., Haddadi, M., Shivanandappa, T., & Ramesh, S. R. (2013). Neuroprotective effect of *Decalepis hamiltonii* in paraquat-induced neurotoxicity in *Drosophila melanogaster*: *Neurochemical Research*, 38, 2616–2624. <https://doi.org/10.1007/s11064-013-1179-9>
- Jankovic, J., & Aguilar, R. (2008). Are adenosine antagonists, such as istradefylline, caffeine, and chocolate, useful in the treatment of Parkinson's disease? *Annals of Neurology*, 63, 267–269. <https://doi.org/10.1002/ana.21348>
- Klingelhoefer, L., & Reichmann, H. (2015). Pathogenesis of Parkinson disease—the gut-brain axis and environmental factors. *Nature Reviews Neurology*, 11, 625–636. <https://doi.org/10.1038/nrneuro.2015.197>
- Knorr, E., & Vilcinskas, A. (2011). Post-embryonic functions of HSP90 in *Tribolium castaneum* include regulation of compound eye development. *Development Genes and Evolution*, 211, 357–362.
- Knorr, E., Bingsohn, L., Kanost, M. R., & Vilcinskas, A. (2013). *Tribolium castaneum* as a model for high-throughput RNAi screening. *Advances in Biochemical Engineering/Biotechnology*, 136, 163–178.
- Lee, M. J., Park, S. H., Han, J. H., Hong, Y. K., Hwang, S., Lee, S., ... Cho, K. S. (2011). The effects of hempseed meal intake and linoleic acid on *Drosophila* models of neurodegenerative diseases and hypercholesterolemia. *Molecules and Cells*, 31, 337–342. <https://doi.org/10.1007/s10059-011-0042-6>
- Lees, A. J., Hardy, J., & Revesz, T. (2009). Parkinson's disease. *Lancet*, 73, 2055–2066.
- Liu, Z., Yu, Y., Li, X., Ross, C. A., & Smith, W. W. (2011). Curcumin protects against A53T alpha-synuclein-induced toxicity in a PC12 inducible cell model for Parkinsonism. *Pharmacological Research*, 63, 439–444. <https://doi.org/10.1016/j.phrs.2011.01.004>
- McCormack, A. L., Thiruchelvam, M., Manning-Bog, A. B., Thiffault, C., Langston, J. W., Cory-Slechta, D. A., & Di Monte, D. A. (2002). Environmental risk factors and Parkinson's disease: Selective degeneration of nigral dopaminergic neurons caused by the herbicide paraquat. *Neurobiology of Disease*, 10, 119–127.
- Mehdi, S. H., & Qamar, A. (2013). Paraquat-induced ultrastructural changes and DNA damage in the nervous system is mediated via oxidative-stress-induced cytotoxicity in *Drosophila melanogaster*. *Toxicological Sciences*, 134, 355–365. <https://doi.org/10.1093/toxsci/kft116>
- Miyasaki, J. M., Martin, W., Suchowersky, O., Weiner, W. J., & Lang, A. E. (2002). Practice parameter: Initiation of treatment for Parkinson's disease: An evidence-based review: Report of the Quality Standards Subcommittee of the American Academy of Neurology. *Neurology*, 58, 11–17.

- Miyatake, T., Katayama, K., Takeda, Y., Nakashima, A., Sugita, A., & Mizumoto, M. (2004). Is death-feigning adaptive? Heritable variation in fitness difference of death-feigning behavior. *Proceedings of the Royal Society of London*, 271(1554), 2293–2296.
- Mukherjee, K., Twyman, R. M., & Vilcinskas, A. (2015). Insects as models to study the epigenetic basis of disease. *Progress in Biophysics and Molecular Biology*, 118, 69–78.
- Mythri, R. B., & Bharath, M. M. (2012). Curcumin: A potential neuroprotective agent in Parkinson's disease. *Current Pharmaceutical Design*, 18, 91–99.
- Nakayama, S., & Miyatake, T. (2010). Genetic trade-off between abilities to avoid attack and to mate: A cost of tonic immobility. *Biology Letters*, 6, 18–20. <https://doi.org/10.1098/rsbl.2009.0494>
- Nakayama, S., Sasaki, K., Matsumura, K., Lewis, Z., & Miyatake, T. (2012). Dopaminergic system as the mechanism underlying personality in a beetle. *Journal of Insect Physiology*, 58, 750–755. <https://doi.org/10.1016/j.jinsphys.2012.02.011>
- Nishi, Y., Sasaki, K., & Miyatake, T. (2010). Biogenic amines, caffeine, and tonic immobility in *Tribolium castaneum*. *Journal of Insect Physiology*, 56, 622–628. <https://doi.org/10.1016/j.jinsphys.2010.01.002>
- Niveditha, S., Ramesh, S. R., Shivanandappa, T. (2017). Paraquat-Induced Movement Disorder in Relation to Oxidative Stress-Mediated Neurodegeneration in the Brain of *Drosophila melanogaster*. *Neurochemistry Research*, 42, 3310–3320. <https://doi.org/10.1007/s11064-017-2373-y>
- Pendleton, R. G., Parvez, F., Sayed, M., & Hillman, R. (2002). Effects of pharmacological agents upon a transgenic model of Parkinson's disease in *Drosophila melanogaster*. *The Journal of Pharmacology and Experimental Therapeutics*, 300, 91–96.
- Pienaar, I. S., Götz, J., & Feany, M. B. (2010). Parkinson's disease: Insights from non-traditional model organisms. *Progress in Neurobiology*, 92, 558–571.
- Prohammer, L. A., & Wade, M. J. (1981). Geographic and genetic variation in death-feigning behavior in the flour beetle. *Tribolium castaneum*. *Behavior genetics*, 11, 395–401.
- Rappold, P. M., Cui, M., Chesser, A. S., Tibbett, J., Grima, J. C., Duan, L., ... Tieu, K. (2011). Paraquat neurotoxicity is mediated by the dopamine transporter and organic cation transporter-3. *Proceedings of the National Academy of Sciences of the United States of America*, 108, 20766–20771.
- Santos, C. M. (2012). New agents promote neuroprotection in Parkinson's disease models. *CNS & Neurological Disorders-Drug Targets*, 11, 410–418.
- Schmitt-Engel, C., Schultheis, D., Schwirz, J., Ströhlein, N., Troelenberg, N., Majumdar, U., ... Bucher, G. (2015). The iBeetle large-scale RNAi screen reveals gene functions for insect development and physiology. *Nature Communications*, 6, 7822. <https://doi.org/10.1038/ncomms8822>
- Thiruchelvam, M., Brockel, B. J., Richfield, E. K., Baggs, R. B., & Cory-Slechta, D. A. (2000). Potentiated and preferential effects of combined paraquat and maneb on nigrostriatal dopamine systems: Environmental risk factors for Parkinson's disease? *Brain Research*, 873, 225–234.
- Trauner, J., Schinko, J., Lorenzen, M. D., Shippy, T. D., Wimmer, E. A., Beeman, R. W., ... Brown, S. J. (2009). Large-scale insertional mutagenesis of a coleopteran stored grain pest, the red flour beetle *Tribolium castaneum*, identifies embryonic lethal mutations and enhancer traps. *BMC Biology*, 7, 73. <https://doi.org/10.1186/1741-7007-7-73>
- Watanabe, H., Zhao, Q., Matsumoto, K., Tohda, M., Murakami, Y., Zhang, S. H., ... Takayama, H. (2003). Pharmacological evidence for antidementia effect of Choto-san (Gouteng-san), a traditional Kampo medicine. *Pharmacology, Biochemistry, and Behavior*, 75, 635–643.
- Whitworth, A. J., Wes, P. D., & Pallanck, L. J. (2006). *Drosophila* models pioneer a new approach to drug discovery for Parkinson's disease. *Drug Discovery Today*, 11, 119–126.

How to cite this article: Brandt A, Joop G, Vilcinskas A. *Tribolium castaneum* as a whole-animal screening system for the detection and characterization of neuroprotective substances. *Arch. Insect Biochem. Physiol.* 2019;1–14. <https://doi.org/10.1002/arch.21532>

Gerd Bicker · Mario Naujock · Annely Haase

Cellular expression patterns of acetylcholinesterase activity during grasshopper development

Received: 22 January 2004 / Accepted: 21 April 2004 / Published online: 23 June 2004
© Springer-Verlag 2004

Abstract We examined the expression of acetylcholinesterase (AChE) in the nervous system and epidermal body structures during embryonic and larval development of two grasshopper species: *Locusta migratoria* and *Schistocerca americana*. Histochemical labelling was blocked by the enzyme inhibitors eserine and BW284c51, but not by iso-OMPA, showing that the staining reflected true AChE activity. The majority of staining was localized on the cell surface but granular intracellular staining was also visible in many cell bodies. In both species, the cellular expression of AChE followed a similar but complex spatiotemporal staining pattern. Initially, mainly epidermal tissue structures were stained in the various body appendages (stages 25%–30%). Labelling subsequently appeared in outgrowing neurons of the central nervous system (CNS) and in the nerves innervating the limbs and dorsal body wall (stages 30%–40%). The latter staining originated in motoneurons of the ventral nerve cord. In a third phase (after 45%), the somata of certain identified mechanosensory neurons started to express AChE activity, presumably reflecting cholinergic differentiation. Staining was also found in repo-positive glial cells of the CNS, longitudinal glia of connectives, glia of the stomatogastric nervous system and glial cells ensheathing peripheral nerves. Glial cells remained AChE-positive during larval to adult development, whereas motoneurons lost their AChE expression. The expression pattern in non-neuronal cells and glutamatergic motoneurons and the developmental appearance of AChE prior to synaptogenesis in the CNS suggest non-cholinergic functions of AChE during grasshopper embryogenesis.

Keywords Acetylcholinesterase · Mechanosensory neurons · Motoneurons · Glial cells · Growth cone · *Locusta migratoria* · *Schistocerca americana* (Insecta)

Introduction

The function and development of cholinergic neurotransmission in the insect central nervous system (CNS) has been the focus of intense research. In tissue concentration, the insect CNS is second only to *Torpedo* electric organ with regard to the number of nicotinic acetylcholine receptors (AChR) per unit protein (Dudai 1979). The most reliable marker of cholinergic neurons is the presence of choline acetyltransferase (ChAT), the enzyme catalysing the synthesis of ACh. In *Drosophila*, cholinergic neurons have been localized by using antibodies against ChAT, in situ hybridization techniques to detect the transcript and staining for a reporter gene fused to the regulatory sequence of the ChAT gene (Buchner et al. 1986; Yasuyama and Salvaterra 1999). The histochemical detection of cholinergic pathways has also been achieved by mapping for the various molecular components of the cholinergic system, such as autoradiographic studies of choline uptake, immunocytochemical staining of the choline transporter or distribution of binding sites for radiolabelled ligands (Buchner and Rodrigues 1983; Treherne and Smith 1965; Knipper et al. 1989). Once released into the synaptic cleft, ACh binds briefly to its postsynaptic receptors before being hydrolysed by acetylcholinesterase (AChE). An understanding of the organization of nicotinic cholinergic pathways can also be derived from AChE histochemistry by using the method of Karnovsky and Roots (1964).

The ligand-binding region of the AChE molecule is composed of two moieties, the esteratic subsite containing the active site serine and the peripheral anionic subsite (reviewed in Soreq and Seidman 2001). The former is involved in the hydrolytic cleavage of its substrate, the latter is thought to bind the quaternary ammonium residue of ACh. However, the biological function of AChE is not

Financial support was provided by the Deutsche Forschungsgemeinschaft (Bi 262/7-1 and 262/11-1)

G. Bicker (✉) · M. Naujock · A. Haase
Cell Biology, School of Veterinary Medicine Hannover,
Bischofsholer Damm 15,
30173 Hannover, Germany
e-mail: gerd.bicker@tiho-hannover.de
Tel.: +49-511-8567765
Fax: +49-511-8567687

limited to its classical role of inactivating the transmitter ACh. High concentrations of this enzyme have also been found outside cholinergic pathways in regions of non-neuronal cells, such as blood, cartilage and germ cells (Grisaru et al. 1999). A wealth of experimental evidence points towards additional roles of AChE as a multifunctional molecule with morphogenetic properties that are not dependent upon its enzymatic activity (Soreq and Seidman 2001).

In contrast to the many molecular forms that have been described in vertebrates, only globular forms of AChE have been found in insects (Toutant 1989; Massoulie et al. 1993). Insects may thus provide attractive preparations for investigating the various roles of AChE in the development, function and maintenance of the nervous system. In *Drosophila*, only one enzyme has cholinesterase activity. Its corresponding gene locus (*Ace*) has been mapped and cloned (J.C. Hall and Kankel 1976; L.M. Hall and Spierer 1986). Studies involving enzyme histochemistry and antibody staining in postembryonic *Drosophila* have demonstrated that AChE is present on the axons of many neurons in the ventral nerve cord and in the developing visual system and brain (J.C. Hall et al. 1980; Buchner et al. 1986; Wolfgang and Forte 1989). Histochemical staining for AChE has also been detected in differentiating neuronal cell clusters prepared from dissociated early gastrula-stage *Drosophila* (Salvaterra et al. 1987). Genetic mutations of the *Ace* locus that eliminate AChE activity lead to embryonic lethality, providing evidence that AChE is indeed required for normal development (J.C. Hall et al. 1980). Mosaic analyses have shown that the loss of AChE function causes gross disruption of nervous system structure and function (Greenspan et al. 1980). However, in embryonic *Drosophila*, the detailed histochemical distribution of AChE activity has not been investigated.

In this paper, we focus on the expression of AChE activity during the formation of the nervous system in the grasshopper embryo, a commonly used preparation of developmental neurobiology (Goodman and Bate 1981; Burrows 1996). We follow the temporal and spatial appearance of AChE activity during grasshopper development. Histochemical staining of whole-mount embryos and primary neuronal cell cultures indicates that AChE is synthesized largely as a cell surface molecule. We have also analysed AChE expression in non-neural body tissue, in longitudinal and peripheral glial cells and in motoneurons of the skeletal muscles. The staining patterns together with the sequence homologies to certain cell-adhesion molecules described in the literature suggest non-cholinergic functions of AChE during grasshopper embryogenesis. Thus, the aim in this paper is to provide an anatomical framework for future investigations of cultured embryos developing under the influence of site-specific AChE inhibitors.

Materials and methods

Animals

Egg pods of *Locusta migratoria* and *Schistocerca americana* were obtained from crowded laboratory cultures. *S. americana* embryogenesis lasts approximately 20 days, whereas embryonic development of *L. migratoria* is completed within about 12 days at 30°C and 60% humidity. Staging of the *Schistocerca* embryos was based on the system of Bentley et al. (1979), with additional criteria for the older stages of *Locusta* embryos (Ball and Truman 1998).

AChE histochemistry

Embryos were freed from the eggshell and yolk and dissected in Leibovitz L-15 cell culture medium (Gibco). All embryonic membranes and the midgut were removed to ensure access of solutions. The embryos were fixed in PIPES-FA (100 mM PIPES, 2.0 mM EGTA, 1 mM MgSO₄, 4% paraformaldehyde, pH 7.4) for 30 min. Subsequently, the fixed embryos were permeabilized in 0.3% saponin in phosphate-buffered saline (PBS), pH 7.4, for 30–60 min. To stain the stomatogastric nervous system, 60%–95% embryos were opened dorsally and the gut and the brain were dissected out together and then treated as whole-mount embryos.

To locate AChE activity, we used the classical staining technique of Karnovsky and Roots (1964), which employs acetylthiocholine iodide as the substrate for the detection of cholinesterases. The product of cholinesterase activity, viz. thiocholine, is believed to reduce ferricyanide to ferrocyanide, which precipitates as copper ferrocyanide directly at the site of enzymatic activity. After being washed several times in 0.1 M TRIS–maleate buffer (pH 6.2), the embryos were incubated in AChE staining solution composed of 3.46 mM acetylthiocholine iodide, 5 mM sodium citrate, 3 mM cupric sulphate, and 500 μM potassium ferricyanide in TRIS–maleate buffer at 4°C. For preparations that were stained for longer than 12 h, the acetylthiocholine iodide concentration was reduced to 0.346 mM. After repeated washes in PBS, the embryos were cleared and mounted in a solution of 90% glycerol in PBS or alternatively processed for immunocytochemical staining. For the staining of larval instars and adult locusts, animals were immobilized by cooling to 4°C and then restrained in Sylgard chambers. After fixation in PIPES-FA for 1 h and dissection, the preparations were processed for AChE histochemistry as described for the embryos above. To inactivate AChE in the extracellular space and for better visibility of intracellular staining (Wallace and Gillon 1982), embryos in some experiments were preincubated with 50 μM echothiophate in L-15 medium for 1 h before fixation.

Controls

To test for the specificity of the histochemical staining, a number of pharmacological compounds were tested for their ability to inhibit the AChE activity in fixed embryos. Eserine, iso-OMPA and BW284c51 were obtained from Sigma; echothiophate was from Ayerst Laboratories (New York). These compounds were added to the staining solution at the concentration given in Table 1. Control embryos were incubated under identical conditions, but without inhibitors. The incubation period lasted 4 h at room temperature, after which time the embryos were washed, cleared and compared for a reduction in the amount of AChE staining.

Immunocytochemistry

For the following immunocytochemical procedure, AChE-stained whole-mount embryos were blocked in 5% normal goat serum in PBT (PBS + 0.5% Triton). The rabbit polyclonal antiserum against

Table 1 Summary of the enzyme inhibitors used to test for the specificity of AChE staining

Enzyme inhibitor	Concentration	Inhibition
iso-OMPA	10 μ M	–
	25 μ M	–
	100 μ M	–
Eserine	10 μ M	+
	30 μ M	+
	100 μ M	+
BW284c51	5 μ M	+
	10 μ M	+
	50 μ M	+
Echothiophate	10 μ M	+
	100 μ M	+

the glial repo-protein (Halter et al. 1995, courtesy Dr. G. Technau) was applied at 4°C overnight at a dilution of 1:250 in 5% normal goat serum in PBT. Subsequently, the embryos were rinsed in PBT and exposed to a biotinylated goat anti-rabbit antibody (Vector; diluted 1:250). Immunoreactivity was visualized by streptavidin-Cy3 (Sigma; diluted 1:250). The tissue was cleared in a glycerol series (50%, 90% in PBS) and mounted in Vectashield.

To resolve fine tissue details, some AChE-stained whole-mount embryos were cryoprotected in 30% sucrose in PBS, embedded in Tissue-Tec (Sakura) and sectioned at a thickness of 12–15 μ m in a cryostat. These cryosections were mounted on chrome-alumn-coated slides and processed for repo-immunocytochemistry as described above.

Stained preparations were photographed on a Zeiss Axioskop equipped with Nomarski optics. Images were captured with a ProgRes/3008 camera, arranged in Adobe Photoshop and slightly contrast-enhanced.

AChE cytochemistry in primary cell culture

Dissociated cells were obtained from embryonic thoracic ganglia at various developmental stages by using the cell culture method of Kirchoff and Bicker (1992). L-15+1% penicillin/streptomycin (Sigma; L-15+P/S) cell culture medium was used throughout the following steps. After dissection of the ganglia in sterile culture medium, they were transferred into a collagenase/dispase (Boehringer, Mannheim) solution (1 mg/ml medium) for 1 h to allow for digestion of the extracellular matrix. After being washed, the ganglia were dissociated by gentle trituration in 100 μ l medium with a siliconized Eppendorf pipette tip. Cells were then plated in 35 mm plastic culture dishes (Falcon). After 30 min of adhesion, they were incubated in cell culture medium at 28°C in humidified air.

Following 24 h in culture, the cells were fixed in 4% paraformaldehyde in PBS (pH 7.4) for 20 min on ice, followed by several rinses in PBS. To permeabilize the cells for the staining solution, the fixed cells were treated with 0.3% saponin/PBS for 15 min. After two rinses in PBS, the cells were incubated in the substrate solution overnight at 4°C. The staining reaction was stopped by three rinses with PBS. For each dissociated nerve cord, about 500 cells were examined by light-microscopic evaluation for the expression of the AChE reaction product. Control cultures were incubated without the substrate acetylthiocholine iodide, resulting in no staining.

Larval cell cultures were also prepared according to the protocol of Kirchoff and Bicker (1992). Cells were cultured for 3 days to allow for neurite outgrowth. The cultures were fixed in 4% formalin/PIPES for 20 min, washed in buffer, incubated for 5 h at 4°C in the AChE substrate solution (with 0.346 mM acetylthiocholine iodide), washed and examined with a Zeiss Axiovert 35 microscope. To demonstrate the presence of extracellular AChE activity, the culture

medium in some experiments was simply replaced by the substrate solution and the cultures were left in the substrate solution.

Results

We followed the expression of AChE staining in *L. migratoria* during the complete embryonic development of the nervous system, including some observations of larval and adult stages. By means of whole-mount histochemistry, AChE activity could be monitored in segmentally arranged body appendages, in their innervation, and in the central nervous system up to the 55% stage of development. Because of the penetration barrier of the hardening cuticle, AChE staining in later stages was performed on the dissected CNS. To reveal enzyme activity in glial cells, cryosections were processed for AChE histochemistry and for immunofluorescence to the glial marker repo (Halter et al. 1995). For comparison, embryos of *S. americana* were also examined for AChE staining during their main period of neuronal differentiation, ranging from 30% to 75% development. The following description applies to both species; specific exceptions are mentioned.

Specificity of AChE staining

Since acetylthiocholine may not only be hydrolysed by AChE but also by other cholinesterases, the specificity of AChE staining was determined on fixed grasshopper embryos between 40% and 55% of embryogenesis. Cholinesterases vary in their sensitivity to inhibition by different pharmacological compounds, a property that has been useful in segregating the activity of non-specific esterases from specific AChE. So called “true” AChE enzymes do not hydrolyse butyrylcholine and are sensitive to inhibition by BW284c51, eserine, or echothiophate, an irreversible cell-impermeant inhibitor. Conversely, iso-OMPA selectively inhibits butyrylcholinesterase (BuChE) activity, without affecting AChE.

A number of drugs that selectively inhibit various forms of cholinesterases were tested to determine whether they could eliminate the staining for AChE activity. In each experiment ($n=4$ for *Schistocerca*; $n=2$ for *Locusta*), concentrations of eserine, echothiophate and BW284c51 in the micromolar range were all found to inhibit completely the deposition of AChE reaction product in both CNS neuropile and non-neuronal cellular patches of body wall and appendages (Table 1). The concentrations of the inhibitors used were similar to those reported for inhibition of cholinesterase activities in other invertebrates (Wallace and Gillon 1982; Braun and Mulloney 1994). Exposure of embryos to up to 100 μ M iso-OMPA did not reduce levels of histochemical staining. Together, these inhibitor studies showed that the grasshopper cholinesterase was specific for ACh and could thus be considered as true AChE activity.

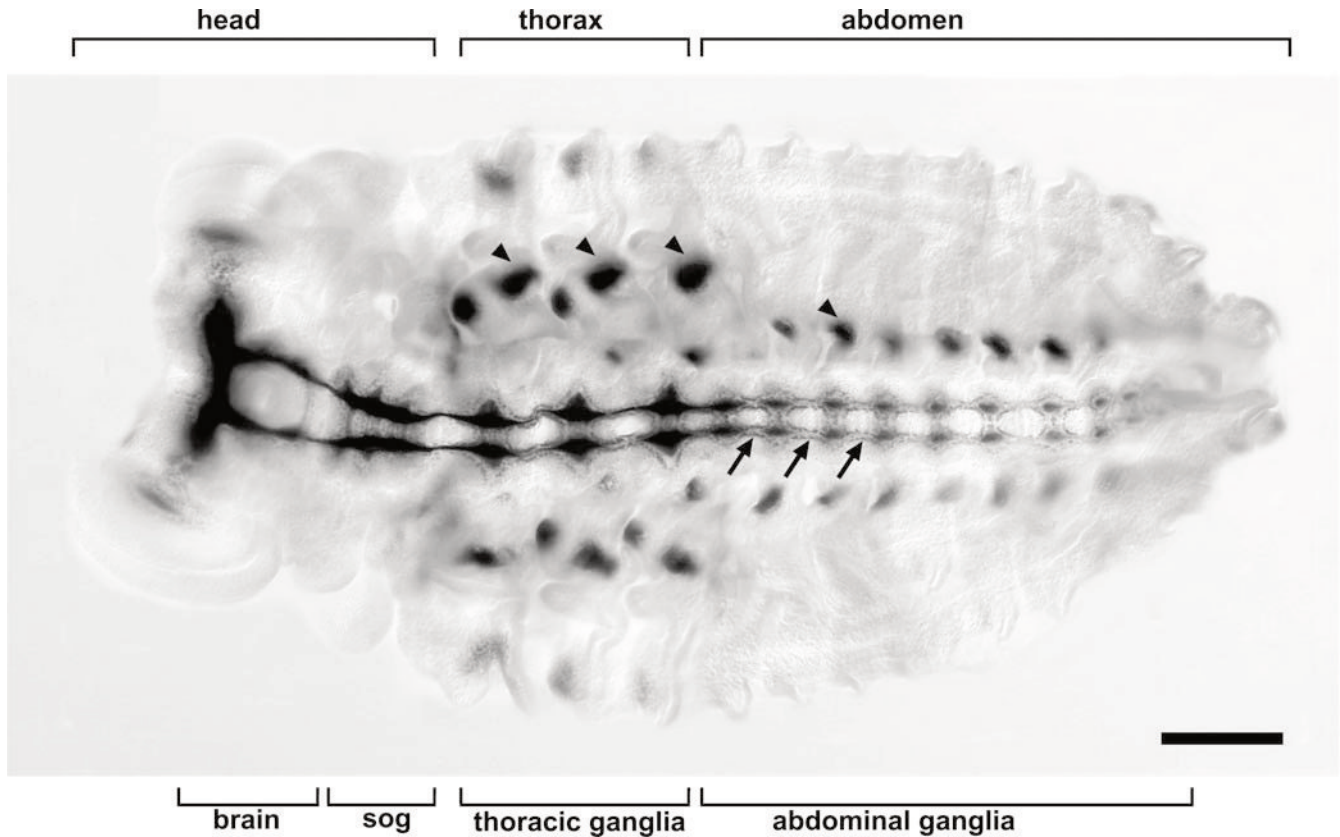


Fig. 1 AChE activity in the embryonic *L. migratoria* at 45%–50% of development. The whole-mount staining of the grasshopper embryo provides an overview of AChE expression. The whole neuropile of the brain and the suboesophageal ganglion shows dense AChE staining. The neuropile is surrounded by stained somata. Staining in the ventral nerve cord is characterized by a developmental gradient of AChE activity. The more anterior ganglia show intense AChE activity in cells of the soma rind, the neuropile and the connectives, whereas in the abdominal ganglia, staining of the connectives is still absent and only weak labelling of the neuropile

and few somata is apparent. Prominent AChE staining is found in the longitudinal glia covering the connectives (examples are indicated by *arrows*). At this stage of development, the staining of epidermal patches is conspicuous. Apart from staining in the dorsal body wall, prominent AChE activity is found in the ventral body wall (*arrowheads*). For better visualization, legs and pleuropodia have been removed. This compound micrograph of the whole-mounted embryo is composed from 41 pictures arranged in Adobe Photoshop (*sog* suboesophageal ganglion). Bar 400 μm

Synopsis of AChE expression during the first half of embryonic development

In embryos younger than 30% of embryonic development, we did not detect any AChE staining in the proliferating neuroblasts and differentiating cells of the CNS. However, non-neuronal AChE expression appeared even at the 30% stage in segmentally arranged cell patches of the dorsal thoracic body wall. As shown in the overview of Fig. 1, this non-neuronal AChE activity was also prominent at 45%–50% of development. It seemed to be developmentally regulated, peaking around 40%–50% and eventually declining at later stages. The time course of developmental AChE expression in the nervous system and in non-neuronal tissue is summarized in Fig. 2. Non-neuronal staining was not only apparent in the body wall but appeared in dorsal and ventral patches of mesodermal cells in the proximal lumen of each limb bud. Staining in this region was first detected at around the 32% stage of development and increased in intensity with embryonic development.

At about 33% (when neuroblasts and their neuronal progeny form glial-bound proliferative clusters in each brain hemisphere; Boyan et al. 1995), the first weak AChE staining became evident in the nervous system. AChE staining could be seen in a few neuronal cell bodies in central brain areas. The deposition of the histochemical reaction product in the cell bodies appeared punctate and did not satisfactorily resolve the shapes of the somata. The boundaries of these cell clusters were delineated by repro-

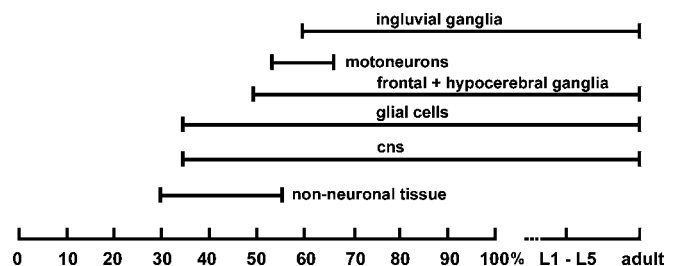


Fig. 2 Time table of the expression of AChE activity during the development of the grasshopper embryo

positive glial cells that did not show AChE activity. At 35%, the number of AChE-positive cell bodies in the protocerebral and deutocerebral brain areas increased. At the 40% stage, the first repo-positive glial cells began to show AChE activity (Fig. 3 A, B). However, double labelling for AChE activity and repo immunoreactivity indicated that the majority of glial cells surrounding the various regions of the brain remained unstained.

In the postoral parts of the CNS, AChE activity became first visible at 35% of embryonic development. At this stage, neuronal cell bodies of the suboesophageal ganglion and the first thoracic ganglion became labelled. Staining was still absent in the mesothoracic, metathoracic and all abdominal ganglia, reflecting an antero-posterior gradient of segmental differentiation.

At the 40% stage, the preoral and postoral commissures had formed around the gut and linked the brain hemispheres. A massive amount of axonal outgrowth and fasciculation had occurred in the brain. Tracts, commissures and descending pathways had increased enormously in size and complexity (Boyan et al. 1995). Concurrently, at 40% of embryonic development, there was a rapid increase in the number of AChE-positive cells. AChE activity was mainly confined to neuronal cell bodies and glial cells, with hardly any discrete staining in the developing neuropile.

At 45% of embryonic development, the three anterior brain neuromeres had become visible as discrete structures. The protocerebral neuropile appeared as a uniformly unstructured mass and exhibited dense AChE staining. It was lined by a layer of AChE-positive glial cells, separating the neuropile from the external cell body rind. The neuropile of the deutocerebrum and tritocerebrum showed no AChE staining at this stage. However, the unstained neuropile of these neuromeres and the circum-oesophageal connectives were surrounded by AChE-stained somata, some of which were glial cells (Fig. 3A, B).

In the ventral ganglia, hardly any staining was visible prior to the 35% stage. Faint staining subsequently became apparent along the surface of most, if not all, axonal projections. At 40%, we could detect AChE staining in neuronal cell bodies and glial cells in the prothoracic ganglion and later in the mesothoracic ganglion. In the metathoracic ganglion, the first weak AChE staining appeared in the soma rind, whereas staining was absent in the abdominal ganglia.

The development of AChE staining in the ventral nerve cord progressed in a well-defined sequence. Initially, AChE staining could be detected in cells with large somata lying near the midline. Subsequently, neurons at the lateral outer surface of the soma rind and some of the surface-associated glial cells (Ito et al. 1995) showed AChE staining. Moreover, the repo-positive longitudinal glia covering the connectives also expressed prominent staining (Fig. 3C, D). As development continued, the number of AChE-stained neuronal cell bodies and the density of staining in the neuropile and in the connectives increased.

At 40%, the connectives between the thoracic ganglia, followed by the commissures, showed AChE staining (Fig. 3C). After 40% of embryonic development, a gradient of AChE staining began to extend along the complete ventral nerve cord eventually reaching the posterior abdominal ganglia. This expression pattern of AChE staining, which was probably caused by the developmental delay in the more posterior body segments, was also visible in whole-mount preparations (Fig. 1).

AChE expression in the stomatogastric nervous system

The stomatogastric nervous system forms as a network of small peripheral ganglia that innervate the muscles of the mouth cavity, foregut and midgut (Hartenstein 1997). The development of the grasshopper stomatogastric nervous system has been described by Ganfornina et al. (1996). In the stomatogastric nervous system, AChE-specific staining first appeared at the 50%–55% stage in the neuropile of the unpaired frontal ganglion and the nerves connecting the tritocerebrum with the frontal ganglion. At 60%–65%, other components of the stomatogastric nervous system, such as the hypocerebral ganglion and the two ingluvial ganglia (Fig. 3E), also expressed prominent AChE labelling. Staining was found in the neuropile and in the ganglionic soma rind. At 65%, the foregut epithelium showed two prominent areas of AChE staining in the floor and the bottom of the foregut (Fig. 3E).

Only a few neurons in the foregut plexus acquired AChE activity. At 65%, all glial cells ensheathing the recurrent and oesophageal nerve showed prominent AChE staining. Double labelling for AChE expression (Fig. 3E) and repo immunocytochemistry (Fig. 3F) demonstrated that some glial cells covering the oesophageal nerves and the foregut plexus were AChE-positive. However, the majority of the glial cells of the foregut plexus showed no AChE activity (Fig. 3E, F). At 80%, the glial cells ensheathing the oesophageal nerves and the nerves of the foregut plexus were clearly labelled (see below). No AChE activity was found in the migrating neurons or glial cells that formed the midgut plexus (Ganfornina et al. 1996).

AChE expression in motoneurons and sensory organs

Starting from 40% of embryonic development, a complex pattern of AChE activity developed in the peripheral nervous system. In *S. americana*, AChE staining became apparent in the segmental and intersegmental nerves. Moreover, AChE-expressing growth cones that extended across the skeletal muscle fibres could be clearly resolved at the peripheral endings of both nerves (Fig. 4A, B).

This earlier labelling of the peripheral nerves was attributable to efferent motoneuronal projections. Because of the position of their somata in the ventral ganglia, some of these motoneurons were most probably RP cells, which

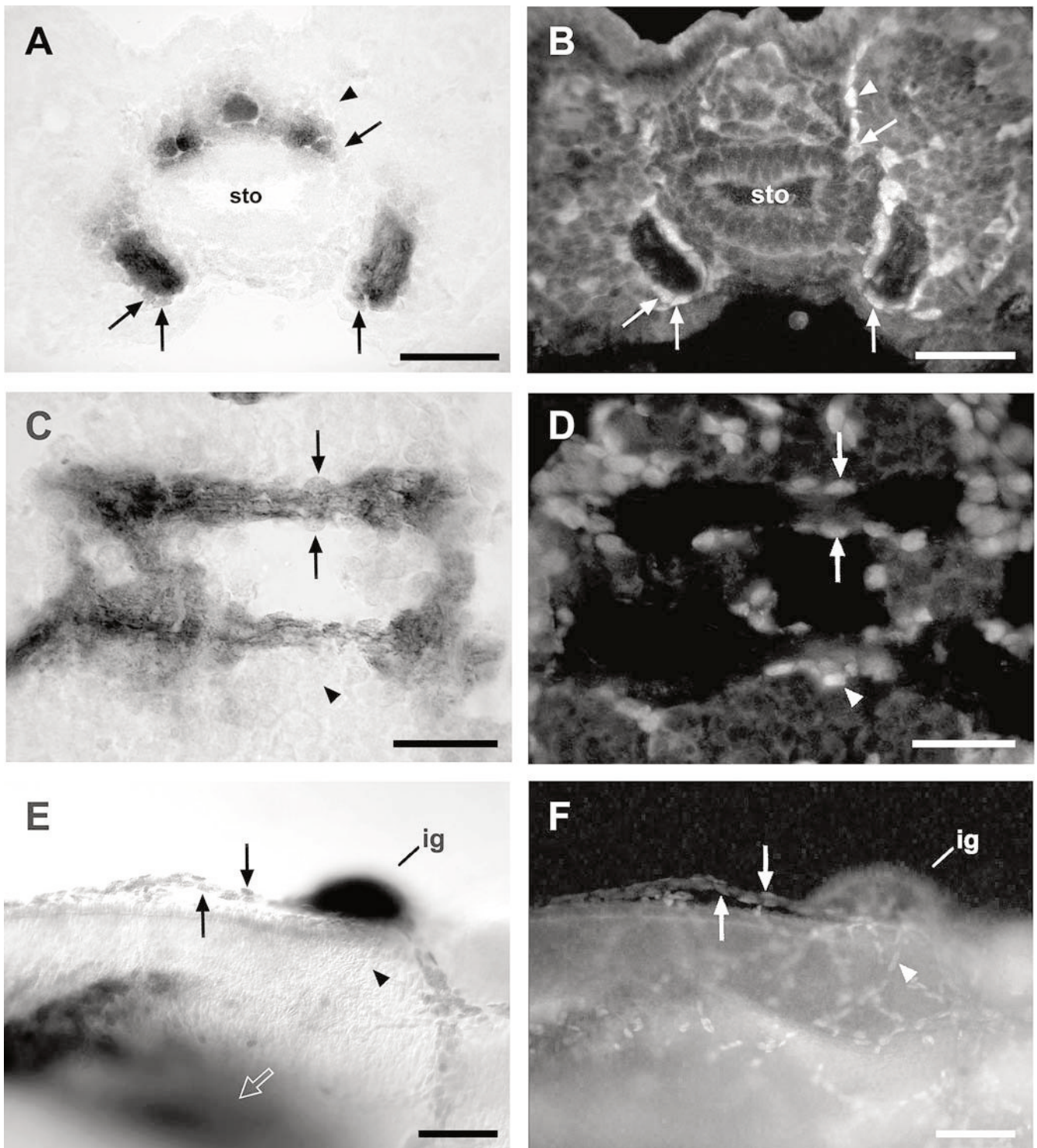


Fig. 3A–F AChE staining of repo-immunoreactive glial cells in the CNS and stomatogastric nervous system. Examples of AChE-positive glial cells as revealed by double labelling of cryosections are indicated by *arrows*. **A** Histochemical staining of cryosection through the brain at 40% development. AChE-stained glial cells (*arrows*) and neurons surrounding the preoral neuropile and the suboesophageal connectives. The stomodeum (*sto*) anterior is to the *top*. **B** Immunofluorescence of the same section as in **A** showing repo-positive glial cells that express AChE (*arrows*). The *arrowhead* indicates an AChE-negative glia cell. **C** Histochemical staining of a horizontal cryosection through the ventral nerve cord at 40% development. Ganglionic neuropile, cell bodies and axons in the connectives show AChE staining (*arrows* AChE-positive longitudinal glial cells covering the connective, *arrowhead* see **D**). **D**

Immunofluorescence of the same section as in **C** showing repo-positive glial cells that express AChE (*arrows*). The *arrowhead* indicates an AChE-negative glia cell. At this stage, the majority of glial cells show no AChE activity (*arrowhead*). **E** AChE staining in the stomatogastric nervous system of a whole-mount preparation at 65% development in side view. The ingluvial ganglion (*ig*) shows prominent staining of the neuropile and soma rind. **F** Immunofluorescence of the same whole-mount preparation as in **E** showing repo-positive glial cells that express AChE (*arrows*). All glial cells covering the oesophageal nerves (*arrows*) are AChE-positive. Most of the glial cells of the foregut plexus show no AChE activity (see *arrowhead* in **E**). At this stage, non-neuronal AChE staining is found in the epidermis of the foregut (*white open arrow* in **E**). Bars 50 μm (**A–D**), 100 μm (**e, F**)

send their axons across the midline and out through the intersegmental nerves to the periphery (Sink and Whittington 1991). The motoneuronal expression pattern of AChE activity was also found in *L. migratoria*; however, the earliest indication of staining here could first be resolved later at 50%. Both in *Locusta* and *Schistocerca*, the appearance of AChE activity in motoneurons was only transient (Fig. 2). The majority of motoneurons of the skeletal muscles are thought to use glutamate as the excitatory neurotransmitter and, correspondingly, no indication of AChE activity could be detected at later developmental stages of the grasshopper.

In the body wall, intense staining developed in sensory cells, possibly indicating the beginning of a cholinergic differentiation in afferent mechanosensory projections. In *Schistocerca*, cell bodies and the dendritic arborization of sensory neurons, such as the wing-hinge stretch receptor, its segmental homologues, and the pleural chordotonal organs, started to stain for AChE around 50%–55% (Fig. 4C, D). In contrast to the transient motoneuronal staining, the mechanosensory neurons in both species were continuously labelled. Eventually, AChE activity could also be found in sensory organs and nerves of the limbs. For example, Fig. 4G demonstrates AChE staining, at the 70% stage, in axons of the limb nerves and the chordotonal organ of the metathoracic leg. AChE activity was also present in the subgenual organ (Fig. 4H).

Extraneuronal staining added to the complexity of the peripheral AChE expression pattern. Between 40% and 50% of embryonic development, the segmentally arranged body patches (Fig. 4E) had increased in AChE staining intensity. We wondered whether this staining was related to the position of the developing sensory neurons in the body wall. However, double labelling for AChE activity (Fig. 4E) and the neuronal horseradish peroxidase (HRP) antigen (Fig. 4F) clearly demonstrated that the location of extraneuronal staining was unrelated to the mechanosensory cell bodies that emerge adjacent to the posterior margin of the epidermal AChE patches. After 55% of development, the embryo possesses a non-permeable cuticle that later acquires pigmentation. For these reasons, it was uncertain whether epidermal AChE activity continued during later stages.

Non-neuronal AChE staining was not only found in the body wall, but also in anterior body structures. In the head capsule, prominent depositions of AChE reaction product were localized to regions of the ocellar Anlagen (Fig. 5A). Pronounced furrows in the epidermis divided the antennae into annular segments, which showed circumferential bands of AChE activity in epithelial cells (Fig. 5E). In the lumen of the antennae, moderate staining was also associated with parts of the mesodermal tissue but we could not discern any staining in the developing sensory neurons. AChE expression was also found in distally located epithelial regions of the developing labral, labial, mandibular and maxillary mouth parts. In addition to the various body appendages and the dorsal body wall, the cercal tips expressed conspicuous AChE staining (Fig. 5F). Strong AChE activity was also found in the

pleuropodia (embryonic structures of the first abdominal segment).

Synopsis of AChE expression during the second half of embryonic development

At 50%, the whole neuropile of the brain (Fig. 5A) and the ventral ganglia (Fig. 4A) appeared to be strongly labelled. A characteristic feature of the AChE expression pattern was the monolayer of stained glial cells and multiple layers of AChE-stained neuronal cell bodies surrounding the neuropiles of brain and ventral ganglia. In the optic lobes, the outer chiasma and the adjacent neurons of the lamina and the medulla showed AChE activity.

As embryogenesis progressed beyond the 60% stage, a large number of the neurons in the CNS became AChE-positive; this was accompanied by intense staining in the neuropile. Because of the combination of punctate intracellular and abundant extracellular staining, it was not possible to count the exact numbers of AChE-stained cell bodies during development.

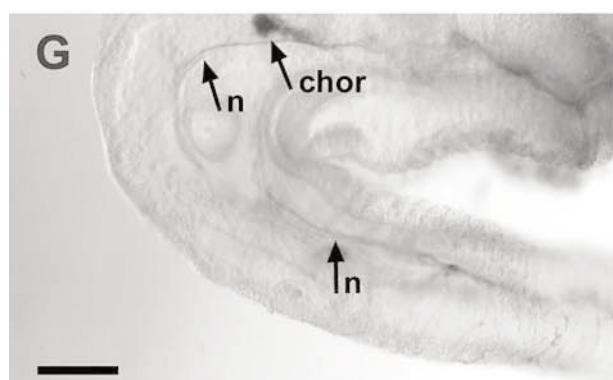
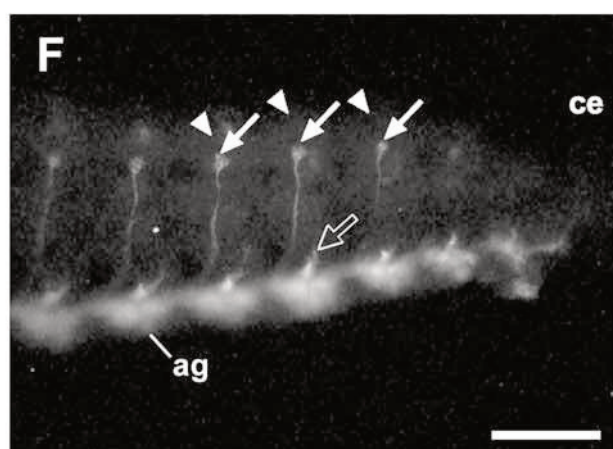
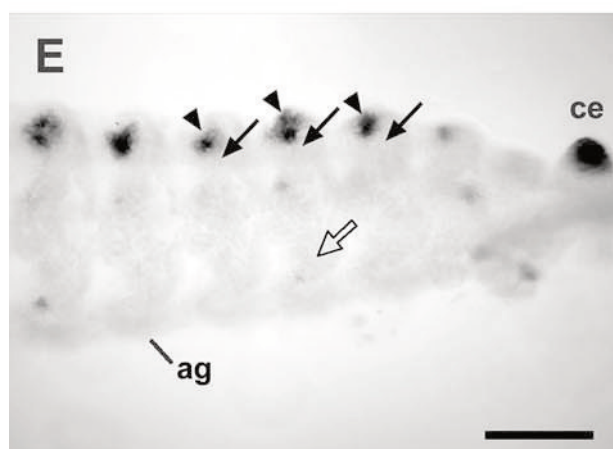
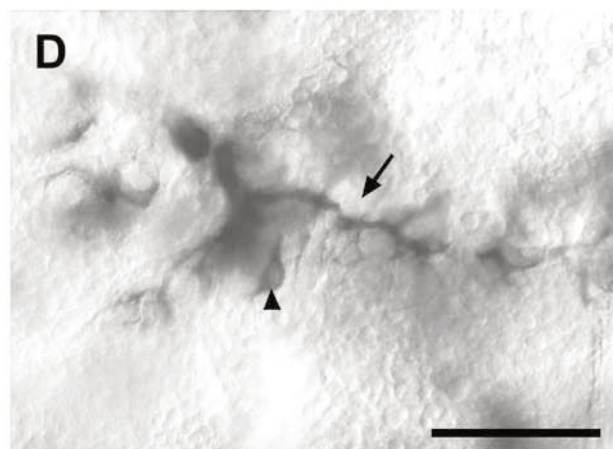
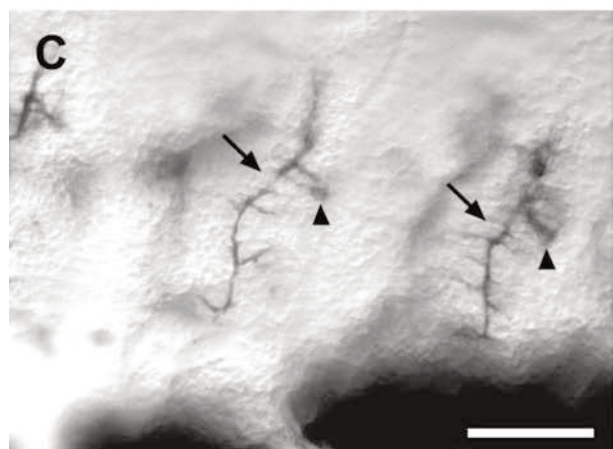
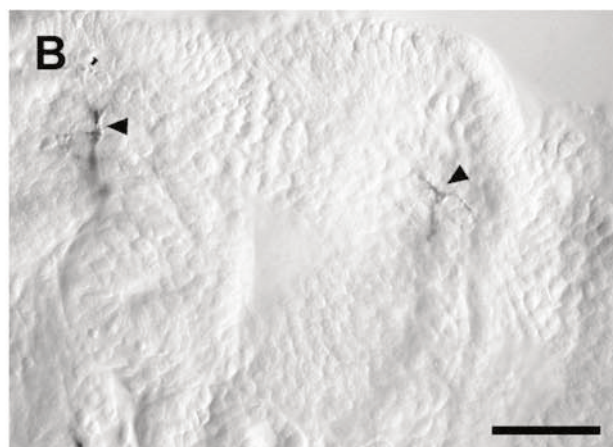
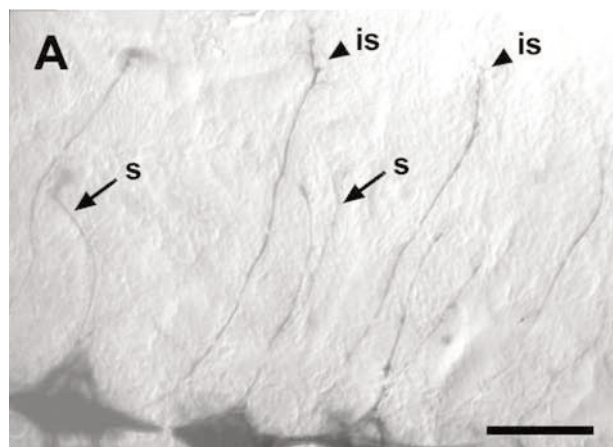
Larval stages and adult animals

During the second half of embryonic development and in the larval and adult stages, AChE-positive glial cells ensheathed the peripheral nerves (Fig. 5D). The longitudinal glia and glial cells covering the ganglia continuously expressed AChE activity throughout larval development and adulthood. AChE staining in the CNS of embryos older than 80% appeared similar to the labelling pattern in instars or adult animals.

In the larval stomatogastric nervous system, the distribution of AChE activity was similar to that in 70%–100% embryos. The frontal and hypocerebral ganglion and the ingluvial ganglia showed high levels of AChE activity. AChE staining was found in the recurrent and oesophageal nerve and the neurons of the foregut plexus. In the first instar, some neurons of the midgut plexus showed AChE activity. In later stages, AChE staining was difficult to resolve because of the endogenous pigmentation of the gut.

AChE expression in primary cell culture

To visualize the subcellular expression patterns of AChE, we prepared primary cell cultures from the ventral nerve cord of *Locusta* larval stages. The somata of the larval neurons are larger than the embryonic cells, thereby enabling more detailed resolution of the staining. Moreover, the cultured cells were directly accessible to the staining solution without any prior fixation. The culture medium was replaced by substrate solution and the histochemical reaction was allowed to proceed for several hours. Labelled neurons showed intense deposition of the reaction product on the surface of the cell body and on



◀ **Fig. 4 A–D, H** AChE activity in whole-mount preparations of the peripheral nervous system. *Schistocerca* embryos were permeabilized at 4°C for 12 h in 0.5% saponin in PBS and incubated overnight at 4°C in a staining solution containing only 0.01% acetylthiocholine iodide. **A** 45% embryo showing staining in the ganglia of the ventral nerve cord (*bottom*) and the nerves innervating the body wall. Between 45% and 55%, motoneurons of the segmental (*arrows s*) and intersegmental (*arrowheads is*) nerve express AChE activity. Anterior is *left*. **B** Enlarged view of **A** showing details of AChE-positive growth cones of motoneurons (*arrowheads*). At this stage, no staining is visible in sensory neurons. **C** At 50–55%, stretch receptor neurons of the body wall show AChE activity. The somata (*arrowheads*) and the neurites (*arrows*) exhibit prominent staining. Anterior is *top*. **D** Enlarged view of the AChE-positive body wall stretch receptor showing the cell body (*arrowhead*) and neurites (*arrow*). **E** Side view of *Locusta* abdominal segments at 40%. All segments exhibit conspicuous AChE staining in the dorsal body wall (*arrowheads*), including the cerci (*ce*). **F** Anti-HRP immunofluorescent staining of identical whole-mount as in **E**. Anti-horseradish peroxidase (HRP)-stained sensory neurons send their axons to the abdominal ganglia (*ag* in **E**, **F**). The somata of the sensory neurons (*arrows* in **E**, **F**) emerge adjacent to the posterior margin of the AChE staining (*arrowheads*). The outgrowing motoneurons (*open arrow* in **E**, **F**) send their axons into the periphery. At this early stage, the outgrowing motor axons show no AChE activity. **G** Staining in femoral–tibial joint region of the metathoracic leg of a 70% *Schistocerca* embryo. AChE activity is found in the femoral chordotonal organ (*chor*) and in the leg nerves (*n*). To facilitate penetration of fixation and staining solutions into the lumen of the leg, the proximal part of the femur and distal part of the tibia were clipped away. **H** Enlarged view of tibia showing AChE staining in the subgenual organ (*subg*). *Bars* 100 µm (**A**, **C**), 50 µm (**B**, **D**), 300 µm (**E**, **F**), 100 µm (**G**), 25 µm (**H**)

processes (Fig. 6A) demonstrating the extracellular localization of AChE. When cell cultures were fixed prior to histochemical staining, the reaction product was again localized on the cell surface but stained intracellular granular compartments also became visible (Fig. 6B).

To obtain an estimate of AChE-positive cells in the embryonic nervous system, we used primary cultures of the ventral nerve cord at various stages of development. As in the primary cultures prepared from adult or laval animals (Kirchhof and Bicker 1992), the dissociated embryonic neurons extended neurites on uncoated plastic Petri dishes (Fig. 6C). Examples of dissociated cell cultures stained for AChE activity at different embryonic stages are shown in transillumination (Fig. 7A, C) and under phase-contrast optics (Fig. 7B, D). An increase in AChE staining is clearly visible. The quantitative evaluation of the cytochemical staining (Fig. 8) showed an increase in AChE-positive somata from 2% (at the 35% stage) to 83% (at the 95%–100% stage), with a conspicuous rise between the 60% and 65% stage.

Discussion

Staining pattern

The enzyme AChE terminates neurotransmission at cholinergic synapses by hydrolysing the transmitter molecule ACh. In this paper, we have shown a complex pattern of AChE expression in the nervous system and in epidermal body structures during the embryonic and larval develop-

ment of the grasshopper species *L. migratoria* and *S. americana*. The sensitivity of the histochemical staining to inhibition by eserine and BW284c51, but not by iso-OMPA, showed that the staining reflected true AChE activity (Table 1). In embryonic grasshoppers, the development of a given abdominal segment significantly lags behind its anterior neighbour. Hence, by traversing posteriorly down the abdomen, we have been able to examine ganglia that are at progressively earlier stages in their anatomical and neurochemical differentiation program (e.g. Ball and Truman 1998). This antero-posterior developmental gradient is also visible in the embryonic differentiation of AChE staining (Fig. 1). The timing of AChE expression and its appearance in non-neuronal cells provides evidence for its non-cholinergic function(s) during grasshopper development.

Staining appeared to be localized mainly at the cell surface but, in many somata, punctate intracellular staining was also visible (Figs. 3C, D, 4H), with some mechanosensory neurons showing intense cytoplasmic soma labelling (Fig. 4C, D). To inactivate extracellular AChE, we used echothiophate, a membrane-impermeant inhibitor of AChE (Brimijoin et al. 1978). This method has also been used in other invertebrate preparations to probe selectively for extracellular AChE (Wallace and Gillon 1982; Braun and Mulloney 1994). In ganglia that had been pretreated by echothiophate and then stained for AChE, the intracellular labelling of axonal projections and selective regions of the neuropile could be resolved against the unstained tissue background (Fig. 5B). Using a cell culture approach, we were able directly to demonstrate the extracellular deposition of the AChE reaction product, simply by replacing the culture medium by substrate solution. Labelled neurons showed intense deposition of the reaction product on the surface of the cell body and on the processes (Fig. 6A).

Staining was found not only in the developing neurons, but also in repo-positive glial cells of the CNS, in the longitudinal glia of the connectives, in the enteric nervous system and in glial cells ensheathing peripheral nerves (Figs. 3, 5D). AChE-stained glial cells were commonly positioned around neuropilar regions (Fig. 3A, B) but the AChE expression on connectives (Fig. 3C, D) and peripheral nerves (Fig. 5D) clearly could not be linked to synaptic functions. Glial cells of the vertebrate nervous system also contain BuChE, which may have a role in cell proliferation and differentiation of the cellular phenotype (Robitzki et al. 2000). Since there is no evidence for the expression of BuChE in the insect nervous systems, the existence of glial-specific forms of AChE enzymes outside synaptic areas remains a distinct possibility. The electron-microscopical localization of eserine-sensitive AChE staining has also been reported in the glial sheath of cercal nerves and in glial folds around perikarya of the last abdominal ganglion of the adult cockroach (Smith and Treherne 1965). The glial cells of the grasshopper remain AChE-positive during larval to adult development, whereas the motoneurons lose their AChE expression. Prominent non-neuronal staining is also found in tissue

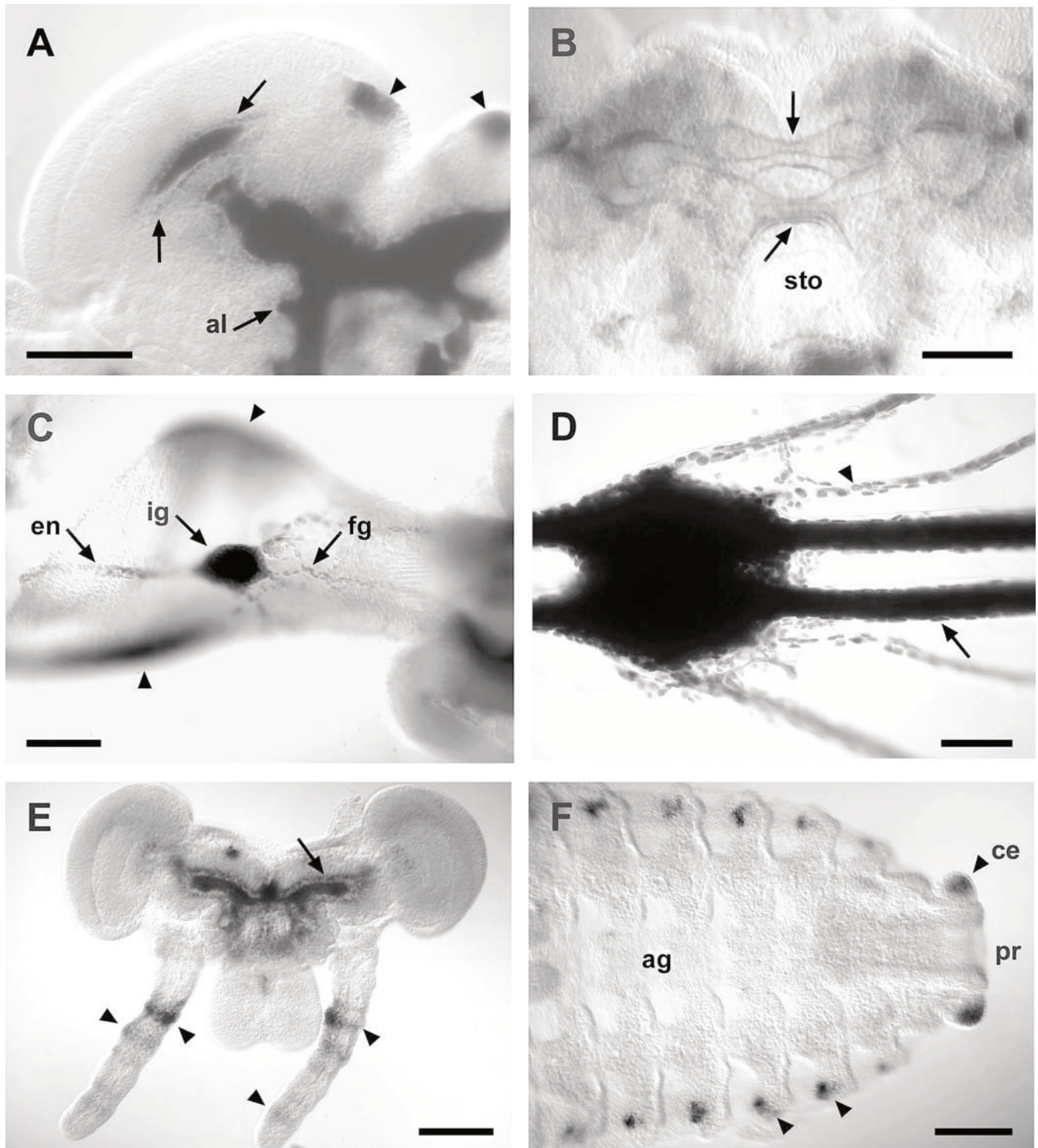


Fig. 5A–F AChE histochemistry in whole-mount preparations. **A** At 50%, the entire neuropile of the protocerebrum, surrounded by lightly stained cell bodies, expresses dense AChE staining. In the developing optic lobe, the intense neuropilar staining and the staining of adjacent cell bodies (*arrows*) are clearly distinct. Three prominent spots of AChE staining, one in the midline and the others lateral to the midline (*arrowheads*) are located in the anterior protocerebrum. These structures appear to represent the primordia of the ocelli. Dense staining is also found in deutocerebral (*al* antennal lobe) and tritocerebral neuropile. **B** AChE expression in the brain of a 55% *Schistocerca* embryo pretreated with echothiophate to reduce extracellular AChE activity (*sto* stomodeum). This method reveals discrete labelling of interhemispheric axon bundles (*arrows*). **C** Whole-mount preparation of the foregut at 80% in a side view showing the area around the intensely labelled ingluvial ganglion

(*ig*). The glia cells ensheathing the oesophageal nerve (*en*) and the nerves of the foregut plexus (*fg*) are AChE-positive. The foregut epithelium shows two prominent areas of AChE staining in the floor and the roof regions (*arrowheads*). **D** Stained abdominal ganglion of a third instar. The surface of the ganglion, the connective (*arrow*) and the peripheral nerves (*arrowhead*) are covered by AChE-stained glial cells. **E** Whole-mount of the head at 40% development. The neuropile of the brain is covered by a monolayer of glial cells (*arrow*). Pronounced furrows in the epidermis divide the antennae into annular segments that show circumferential bands of AChE activity (*arrowheads*). **F** Ventral view of the abdomen. At 35%–40% development, all segments show conspicuous AChE staining in the dorsal body wall (*arrowheads*), including the cerci (*ce*) but there is no staining in the abdominal ganglia (*ag*) or proctodeum (*pr*). *Bars* 200 μ m (**A**, **D–F**), 100 μ m (**B**, **C**)

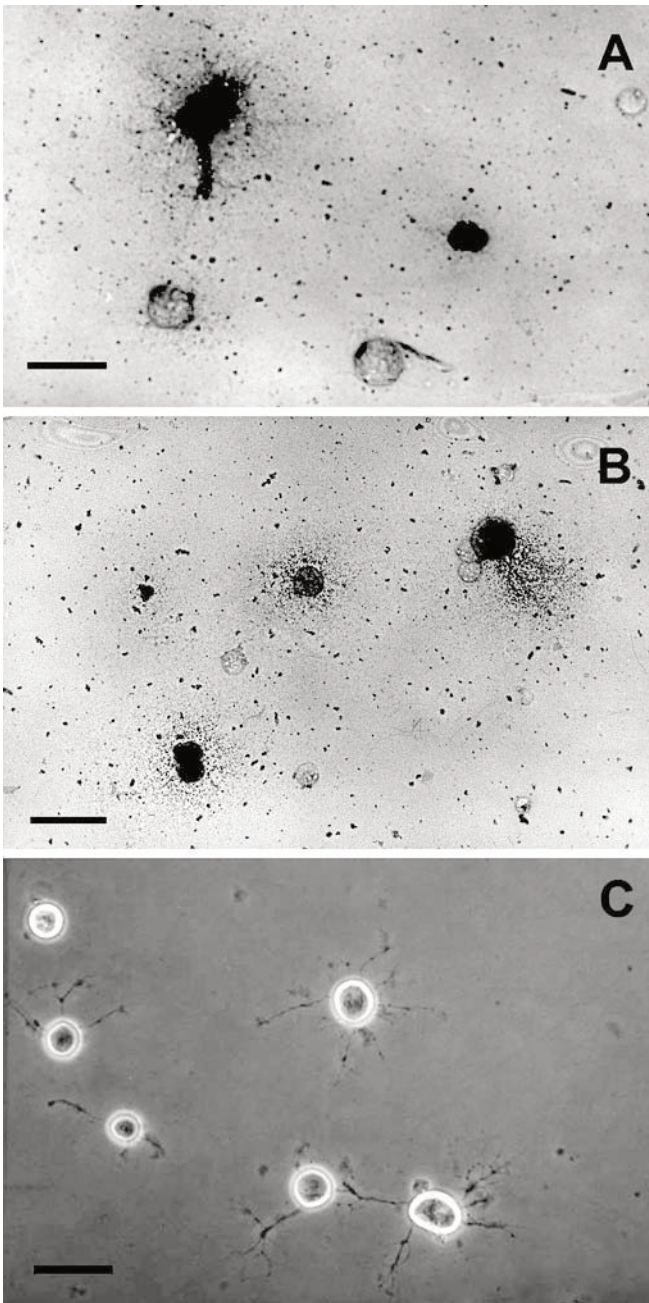


Fig. 6A–C Dissociated cell cultures of *Locusta* thoracic ganglia viewed by transillumination. AChE staining of third larval stage neurons. **A** Culture medium was replaced by substrate solution and the histochemical reaction was allowed to take place for 5 h at 4°C. Labeled neurons show intense staining on the cell surface and on processes. **B** Prior fixation results in both cell surface and intracellular granular staining. **C** Primary cell culture of 80% stage embryos viewed with phase-contrast optics. Bars 25 μm (A, B), 30 μm (C)

patches of the developing body wall (Fig. 1) and appendages, suggesting novel non-classical functions of AChE outside of the grasshopper nervous system. Presumably, these functions are not related to the differentiation of the nervous system, because our double-labelling experiments have clearly shown that the strong

expression of AChE does not co-localize with the position of the HRP-immunopositive sensory neurons (Fig. 4E, F).

Because of the extracellular AChE activity, a clear distinction among stained and unstained cell bodies was difficult to discern in whole-mount preparations. To visualize the expression of AChE in somata of the CNS, dissociated cell cultures were prepared from the ventral nerve cord; this facilitated the direct demonstration of AChE activity in the extracellular space (Fig. 6A, B). Cell cultures also allowed the quantitative evaluation of AChE-positive cells. During embryonic development, AChE staining increased from 2% of the neuronal cell bodies at the 35% stage to 83% of the neuronal cell bodies at larval hatching (Fig. 8). A rapid increase in stained cell bodies was found between the 60% and 65% stages (Fig. 8). Presumably, this rapid rise after an initial phase of low-level expression might be related to cellular differentiation to a cholinergic-transmitter phenotype in the CNS. The high percentage of AChE-stained neurons at the end of grasshopper embryogenesis corresponds well to the finding that, in cultures of embryonic *Drosophila* CNS, about 80% of the neurons stain for the cholinergic marker enzyme ChAT (Lee and O'Dowd 1999). Thus, a large number of cholinergic central neurons appears to be a general feature of hemimetabolous and holometabolous insect nervous systems.

In insects, sensory neurons are thought to use predominantly ACh as a neurotransmitter (Sattelle and Breer 1990) and many sensory neurons of the adult locust stain with an antibody against ChAT (Lutz and Tyrer 1987). Here, we show that mechanosensory neurons of the body wall (Meier and Reichert 1990), such as the segmentally arranged stretch receptors, stain for AChE (Fig. 4C, D). During early embryogenesis, no AChE staining could be detected in the pioneer neurons, guidepost cells or developing sensory neurons of the antennal and limb buds (Bate 1976). However, in legs from embryos older than 70%, the sensory neurons of the chordotonal and subgenual organs expressed strong AChE activity (Fig. 4G, H) indicating differentiation of the cholinergic phenotype.

Timing of AChE expression and synaptogenesis

Electrophysiological investigations have shown that insect motoneurons are mainly glutamatergic (Usherwood 1969; Jan and Jan 1976); this has also been demonstrated by immunocytochemical staining (Bicker et al. 1988; Watson 1988). The detection of AChE activity on certain motor axons in the grasshopper embryo provides evidence that AChE expression in embryonic neurons is not strictly correlated with the future cellular transmitter phenotype and may have a function in the embryo other than in ACh metabolism. This hypothesis receives further support from the finding that AChE expression in motoneurons and their growth cones is only transient.

A comparison of the timing of AChE expression with the formation of synapses in the nervous system of the

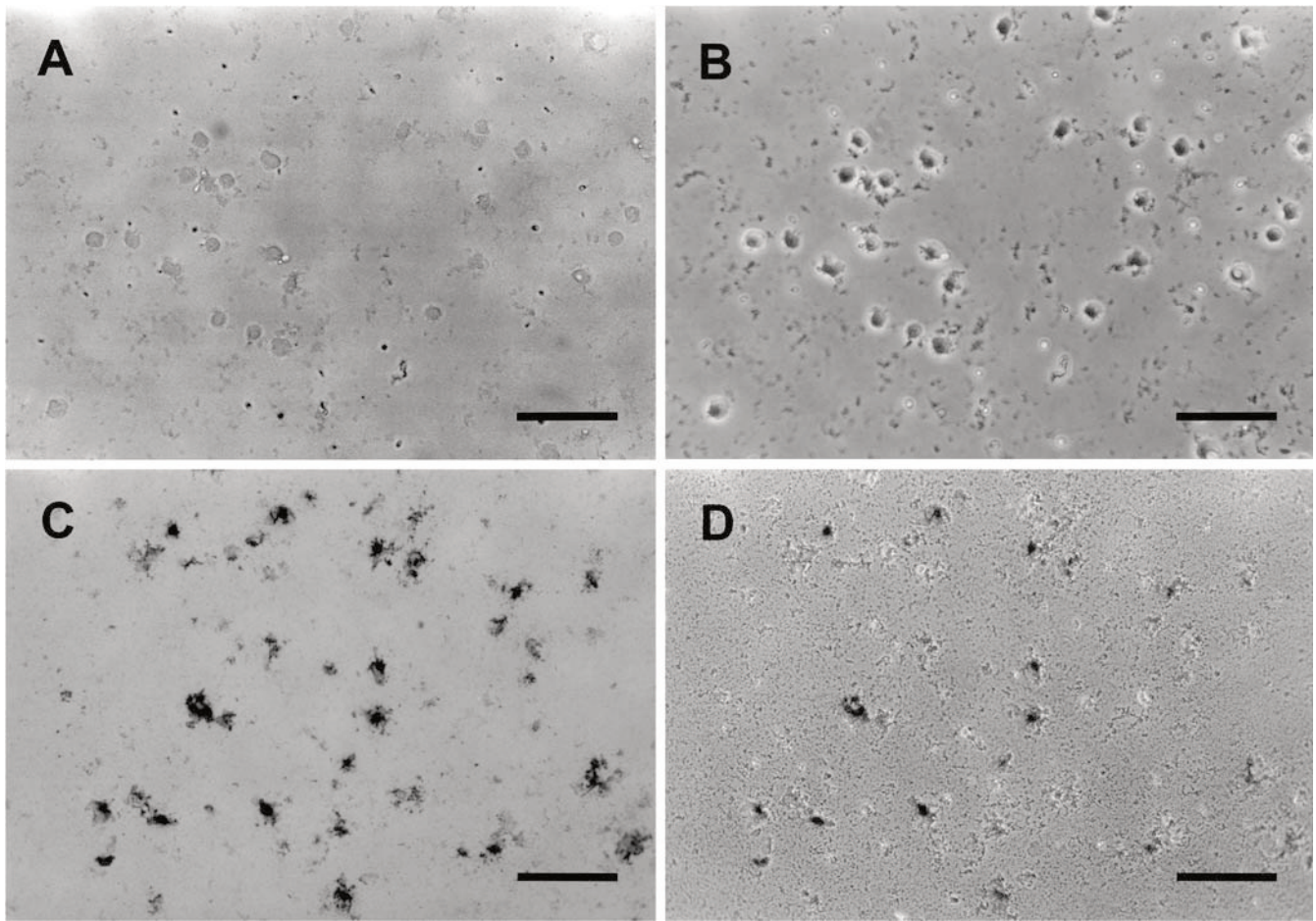


Fig. 7A–D AChE staining of embryonic cultures. Transillumination reveals the dramatic increase in AChE-positive cells from 35% (A) to 80% (C) embryonic development. To reveal unstained cells at

the 35% (B) and 80% (D) stages, identical fields of view are presented under phase-contrast optics. Bars 50 μm (A, B), 200 μm (C, D)

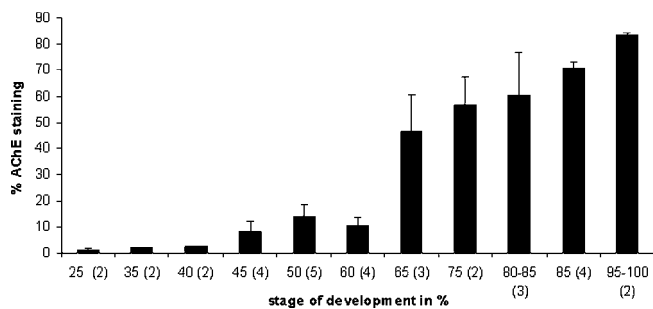


Fig. 8 Quantitative evaluation of the increase in AChE-positive cells during embryonic development of the ventral nerve cord. The percentage of stained cells was counted in dissociated cultures of various developmental stages. The number of evaluated embryos is given in brackets (error bars SEM)

grasshopper is of interest. A detailed electron-microscopic and electrophysiological study has been performed to follow synaptogenesis in an identifiable population of thoracic local neurons (Leitch et al. 1992). In the adult animal, these neurons receive direct input from leg mechanosensory afferents and, in turn, make output synapses on motoneurons and interneurons. Morphologically recognizable synapses with vesicles and presynaptic

bars are first evident at 70%–75% development, coincident with the time when these neurons become electrically excitable and synaptic potentials can first be recorded. At this stage, many of the leg sensory neurons also establish functional synaptic connections in the CNS (Burrows 1996). Another indicator of synaptogenesis is the distribution of immunoreactivity to an α -bungarotoxin binding ACh-receptor protein that has been isolated and characterized in the adult locust (Breer et al. 1985). In the grasshopper embryo, immunoreactivity for this acetylcholine receptor-like antigen appears during the outgrowth of the earliest differentiating neurons between 30% and 35% (Watkins et al. 1995). Initially, the developing neuropile is uniformly labelled. However at 75%, a more mature pattern of immunostaining emerges, in which synaptic regions are distinctly labelled, whereas tracts and commissures are not. Taken together, these studies indicate that, in the CNS, most synaptic connectivity becomes functional around 70%–75%. This corresponds to the rise in AChE-labelled central neurons at 65% (Fig. 8). In the peripheral nervous system, muscle twitches have been elicited by electrical nervous stimulation from the 70% stage on, with a significant increase in contraction time after 80% of development (Tyrer 1969). We consider it

unlikely that the initial AChE expression of grasshopper motoneurons at 40%–50% reflects transmitter switching between cholinergic and glutamatergic phenotypes. The development of neuromuscular synaptic physiology has been investigated in great detail in embryonic and larval *Drosophila* (Bate and Broadie 1995) and indicates that motoneurons use glutamate as a fast transmitter from the start.

The expression of AChE in the non-cholinergic grasshopper motoneurons finds a parallel in the developing visual system of *Drosophila* in which AChE appears in photoreceptor cells prior to the establishment of functional connections (Wolfgang and Forte 1989). Because the retinula cells have not yet established synaptic connections at the time when AChE is first detected, AChE cannot be performing its standard catalytic function. Subsequently, the retinula cells of the imaginal *Drosophila* compound eye use histamine, the transmitter of arthropod photoreceptors (Stuart 1999), showing that cellular expression of AChE during insect development does not predict a cholinergic phenotype.

In vertebrates, a large body of evidence supports non-cholinergic functions of AChE. In neuronal cell cultures and in the nerve-growth-factor-stimulated differentiation of PC12 cells, AChE has been shown to facilitate neurite growth (Layer 1990; Layer and Willbold 1995; Grifman et al. 1998; Grisaru et al. 1999). A potential neurite growth-promoting role of AChE derives from sequence homologies to cell-surface molecules carrying serine-esterase-like domains. Examples of cell adhesion molecules with AChE-like extracellular domains are *Drosophila* neurotactin (Barthalay et al. 1990; de la Escalera et al. 1990; Hortsch et al. 1990), glutactin (Olson et al. 1990), gliotactin (Auld et al. 1995) and the neuroligins cloned from rat (Ichtchenko et al. 1995). Neuroligins serve as ligands for beta-neurexins, highly polymorphic cell-surface molecules. Interactions between neuroligins and neurexins are candidates for neuronal cell recognition mechanisms (Soreq and Seidman 2001).

In *Drosophila*, mutations that affect the *Ace* locus and AChE expression lead to a disrupted nervous system architecture (J.C. Hall et al. 1980; Greenspan et al. 1980; Chase and Kankel 1988). In an ultrastructural study of wildtype and *Ace*-mutant developmental stages, Chase and Kankel (1988) have suggested that AChE is required for the maintenance rather than formation of the nervous system. However, the absence of cellular studies of *Ace*-mutant neurons has precluded the elucidation of the mechanisms that connect the loss of AChE function with defects in neuronal development. The picture emerging from our histochemical study reveals the developmental appearance, in the CNS, of AChE that largely precedes synaptogenesis. Expression in non-neural cells, glutamatergic motoneurons and peripheral glial cells and the sequence homologies to certain cell-adhesion molecules all point towards the non-cholinergic function(s) of AChE, at least during early stages of grasshopper embryogenesis. The expression pattern of AChE activity in the embryo and its localization at the cell surface are indicators that

AChE participates in modulating cellular interactions with other cells or the extracellular matrix. Moreover, AChE is expressed on the growth cones of motoneurons, indicative of the potential role of this cell-surface molecule in cell motility.

Research on vertebrate AChE has taken advantage of natural occurring peptide ligands that have been isolated from snake venom and that bind to the peripheral anionic site of AChE. An influence of AChE on cell culture morphology, independent of catalytic function, has been demonstrated by using these ligands to cover the peripheral anionic subsite (Blasina et al. 2000). We are currently employing these ligands to investigate effects on neurite outgrowth in cultured grasshopper neurons. This could reveal whether AChE is also involved in morphogenetic interactions during the development of an insect nervous system.

Acknowledgements This work was initiated in the laboratory of David Bentley, UC Berkeley, with Wesley Chang. G.B. is grateful to David Bentley for his hospitality and to Wesley Chang for joint experiments and discussions during the beginning of this study. We thank Gerd Technau for the gift of the repo-antiserum.

References

- Auld VJ, Fetter RD, Broadie K, Goodman CS (1995) Gliotactin, a novel transmembrane protein on peripheral glia, is required to form the blood–nerve barrier in *Drosophila*. *Cell* 81:757–767
- Ball EE, Truman JW (1998) Developing grasshopper neurons show variable levels of guanylyl cyclase activity on arrival at their targets. *J Comp Neurol* 394:1–13
- Barthalay Y, Hipeau-Jacquotte R, Escalera S de la, Jimenez F, Piovant M (1990) *Drosophila* neurotactin mediates heterophilic cell adhesion. *EMBO J* 9:3603–3609
- Bate CM (1976) Pioneer neurones in an insect embryo. *Nature* 260:54–56
- Bate M, Broadie K (1995) Wiring by fly: the neuromuscular system of the *Drosophila* embryo. *Neuron* 15:513–525
- Bentley D, Keshishian H, Shankland M, Toroian-Raymond A (1979) Quantitative staging of embryonic development of the grasshopper, *Schistocerca nitens*. *J Embryol Exp Morphol* 54:47–74
- Bicker G, Schäfer S, Ottersen OP, Storm-Mathisen J (1988) Glutamate-like immunoreactivity in identified neuronal populations of insect nervous systems. *J Neurosci* 8:2108–2122
- Blasina MF, Faria AC, Gardino PF, Hokoc JN, Almeida OM, Mello FG de, Arruti C, Dajas F (2000) Evidence for a noncholinergic function of acetylcholinesterase during development of chicken retina as shown by fasciculins. *Cell Tissue Res* 299:173–184
- Boyan G, Therianos S, Williams JLD, Reichert H (1995) Axogenesis in the embryonic brain of the grasshopper *Schistocerca gregaria*: an identified cell analysis of early brain development. *Development* 121:75–86
- Braun G, Mulloney B (1994) Acetylcholinesterase activity in neurons of crayfish abdominal ganglia. *J Comp Neurol* 350:272–280
- Breer H, Kleene R, Hinz G (1985) Molecular forms and subunit structure of the acetylcholine receptor in the central nervous system of insects. *J Neurosci* 5:3386–3392
- Brimijoin S, Skau K, Wiermaa MJ (1978) On the origin and fate of external acetylcholinesterase in peripheral nerve. *J Physiol (Lond)* 285:143–158

- Buchner E, Rodrigues V (1983) Autoradiographic localization of [³H]choline uptake in the brain of *Drosophila melanogaster*. *Neurosci Lett* 42:25–31
- Buchner E, Buchner S, Crawford G, Mason TW, Salvaterra PM, Sattelle DB (1986) Choline acetyltransferase-like immunoreactivity in the brain of *Drosophila melanogaster*. *Cell Tissue Res* 246:57–62
- Burrows M (1996) The neurobiology of an insect brain. Oxford University, Oxford
- Chase BA, Kankel DR (1988) On the role of normal acetylcholine metabolism in the formation and maintenance of the *Drosophila* nervous system. *Dev Biol* 125:361–380
- Dudai Y (1979) Cholinergic receptors in insects. *Trends Biochem Sci* 2:40–44
- Escalera S de la, Bockamp EO, Moya F, Piovant M, Jimenez F (1990) Characterization and gene cloning of neurotactin, a *Drosophila* transmembrane protein related to cholinesterases. *EMBO J* 9:3593–3601
- Ganformina MD, Sanchez D, Bastiani MJ (1996) Embryonic development of the enteric nervous system of the grasshopper *Schistocerca americana*. *J Comp Neurol* 372:581–596
- Goodman CS, Bate CM (1981) Neuronal development in the grasshopper. *Trends Neurosci* 4:163–169
- Greenspan RJ, Finn JA Jr, Hall JC (1980) Acetylcholinesterase mutants in *Drosophila* and their effects on the structure and function of the central nervous system. *J Comp Neurol* 189:741–774
- Grifman M, Galyam N, Seidman S, Soreq H (1998) Functional redundancy of acetylcholinesterase and neuroigin in mammalian neuritogenesis. *Proc Natl Acad Sci USA* 95:13935–13940
- Grisaru D, Sternfeld M, Eldor A, Glick D, Soreq H (1999) Structural roles of acetylcholinesterase variants in biology and pathology. *Eur J Biochem* 264:672–686
- Hall JC, Kankel DR (1976) Genetics of acetylcholinesterase in *Drosophila melanogaster*. *Genetics* 83:517–535
- Hall JC, Alahiotis SN, Strumpf DA, White K (1980) Behavioral and biochemical defects in temperature-sensitive acetylcholinesterase mutants of *Drosophila melanogaster*. *Genetics* 96:939–965
- Hall LM, Spierer P (1986) The Ace locus of *Drosophila melanogaster*: structural gene for acetylcholinesterase with an unusual 5' leader. *EMBO J* 5:2949–2954
- Halter DA, Urban J, Rickert C, Ner SS, Ito K, Travers AA, Technau GM (1995) The homeobox gene repo is required for the differentiation and maintenance of glia function in the embryonic nervous system of *Drosophila melanogaster*. *Development* 121:317–332
- Hartenstein V (1997) Development of the insect stomatogastric nervous system. *Trends Neurosci* 20:421–427
- Hortsch M, Patel NH, Bieber AJ, Traquina ZR, Goodman CS (1990) *Drosophila* neurotactin, a surface glycoprotein with homology to serine esterases, is dynamically expressed during embryogenesis. *Development* 110:1327–1340
- Ichtchenko K, Hata Y, Nguyen T, Ullrich B, Missler M, Moomaw C, Sudhof TC (1995) Neuroigin 1: a splice site-specific ligand for beta-neurexins. *Cell* 81:435–443
- Ito K, Urban J, Technau G (1995) Distribution, classification, and development of *Drosophila* glial cells in the late embryonic and early larval ventral nerve cord. *Roux's Arch Biol* 204:284–307
- Jan LY, Jan YN (1976) L-Glutamate as an excitatory transmitter at the *Drosophila* larval neuromuscular junction. *J Physiol (Lond)* 262:215–236
- Karnovsky MJ, Roots L (1964) A "direct-coloring" thiocholine method for cholinesterases. *J Histochem Cytochem* 12:219–221
- Kirchhof B, Bicker G (1992) Growth properties of larval and adult locust neurons in primary cell culture. *J Comp Neurol* 323:411–422
- Knipper M, Strotmann J, Madler U, Kahle C, Breer H (1989) Monoclonal-antibodies against the high-affinity choline transport system. *Neurochem Int* 14:217–222
- Layer PG (1990) Cholinesterases preceding major tracts in vertebrate neurogenesis. *Bioessays* 12:415–420
- Layer PG, Willbold E (1995) Novel functions of cholinesterases in development, physiology and disease. *Prog Histochem Cytochem* 29:1–94
- Lee D, O'Dowd DK (1999) Fast excitatory synaptic transmission mediated by nicotinic acetylcholine receptors in *Drosophila* neurons. *J Neurosci* 19:5311–5321
- Leitch B, Laurent G, Shepherd D (1992) Embryonic development of synapses on spiking local interneurons in locust. *J Comp Neurol* 324:213–236
- Lutz EM, Tyrer NM (1987) Immunohistochemical localization of choline acetyltransferase in the central nervous system of the locust. *Brain Res* 407:173–179
- Massoulie J, Pezzementi L, Bon S, Krejci E, Vallette FM (1993) Molecular and cellular biology of cholinesterases. *Prog Neurobiol* 41:31–91
- Meier T, Reichert H (1990) Embryonic development and evolutionary origin of the orthopteran auditory organs. *J Neurobiol* 21:592–610
- Olson PF, Fessler LI, Nelson RE, Sterne RE, Campbell AG, Fessler JH (1990) Glutactin, a novel *Drosophila* basement membrane-related glycoprotein with sequence similarity to serine esterases. *EMBO J* 9:1219–1227
- Robitzki A, Doll F, Richter-Landsberg C, Layer PG (2000) Regulation of the rat oligodendroglia cell line OLN-93 by antisense transfection of butyrylcholinesterase. *Glia* 31:195–205
- Salvaterra PM, Bourmias-Vardiabasis N, Nair T, Hou G, Lieu C (1987) In vitro neuronal differentiation of *Drosophila* embryo cells. *J Neurosci* 7:10–22
- Sattelle DB, Breer H (1990) Cholinergic nerve terminals in the central nervous system of insects. *J Neuroendocrinol* 2:241–256
- Sink H, Whittington PM (1991) Pathfinding in the central nervous system and periphery by identified embryonic *Drosophila* motor axons. *Development* 112:307–316
- Smith DS, Treherne JE (1965) The electron microscopic localization of cholinesterase activity in the central nervous system of an insect, *Periplaneta americana* L. *J Cell Biol* 26:445–465
- Soreq H, Seidman S (2001) Acetylcholinesterase—new roles for an old actor. *Nat Rev Neurosci* 2:294–302
- Stuart AE (1999) From fruit flies to barnacles, histamine is the neurotransmitter of arthropod photoreceptors. *Neuron* 22:431–433
- Toutant JP (1989) Insect acetylcholinesterase: catalytic properties, tissue distribution and molecular forms. *Prog Neurobiol* 32:423–446
- Treherne JE, Smith DS (1965) The metabolism of acetylcholine in the intact central nervous system of an insect (*Periplaneta americana* L.). *J Exp Biol* 43:441–454
- Tyrer NM (1969) Time course of contraction and relaxation in embryonic locust muscle. *Nature* 224:815–817
- Usherwood PN (1969) Glutamate sensitivity of denervated insect muscle fibres. *Nature* 223:411–413
- Wallace BG, Gillon JW (1982) Characterization of acetylcholinesterase in individual neurons in the leech central nervous system. *J Neurosci* 2:1108–1118
- Watkins BL, Leitch B, Burrows M, Knowles BH (1995) Localization of a nicotinic acetylcholine receptor-like antigen in the thoracic nervous system of embryonic locusts, *Schistocerca gregaria*. *J Comp Neurol* 351:134–144
- Watson AH (1988) Antibodies against GABA and glutamate label neurons with morphologically distinct synaptic vesicles in the locust central nervous system. *Neuroscience* 26:33–44
- Wolfgang WJ, Forte MA (1989) Expression of acetylcholinesterase during visual system development in *Drosophila*. *Dev Biol* 131:321–330
- Yasuyama K, Salvaterra PM (1999) Localization of choline acetyltransferase-expressing neurons in *Drosophila* nervous system. *Microsc Res Tech* 45:65–79

SCIENTIFIC REPORTS



OPEN

Temporal dynamics of whole body residues of the neonicotinoid insecticide imidacloprid in live or dead honeybees

Matthias Schott^{1,2}, Gabriela Bischoff³, Gerrit Eichner⁴, Andreas Vilcinskas^{2,5}, Ralph B uchler⁶, Marina Doris Meixner⁶ & Annelly Brandt^{5,6}

In cases of acute intoxication, honeybees often lay in front of their hives for several days, exposed to sunlight and weather, before a beekeeper can take a sample. Beekeepers send samples to analytical laboratories, but sometimes no residues can be detected. Temperature and sun light could influence the decrease of pesticides in bee samples and thereby residues left for analysis. Moreover, samples are usually sent via normal postal services without cooling. We investigated the temporal dynamics of whole-body residues of imidacloprid in live or dead honeybees following a single-meal dietary exposure of 41 ng/bee under various environmental conditions, such as freezing, exposure to UV light or transfer of individuals through the mail system. Immobile, “dead” looking honeybees recovered from paralysis after 48 hours. The decrease of residues in living but paralysed bees was stopped by freezing (= killing). UV light significantly reduced residues, but the mode of transport did not affect residue levels. Group feeding increased the variance of residues, which is relevant for acute oral toxicity tests. In conclusion, elapsed time after poisoning is key for detection of neonicotinoids. Freezing before mailing significantly reduced the decrease of imidacloprid residues and may increase the accuracy of laboratory analysis for pesticides.

Honeybees (*Apis mellifera* L.) and wild bees are primary pollinators of wild plants and cultivated crops and therefore essential for ecosystem function and agriculture^{1–3}. Over the past decade there has been a serious decline in bee populations reported in parts of the world, including the European Union (EU)^{4–9}. A multitude of causative factors is being discussed, such as parasites and pathogens, diet quantity, quality, diversity, and the exposure to pesticides^{9–15}. In particular the application of neonicotinoid insecticides has been suspected to represent a major threat to honeybee survival^{16–21}. Especially three neonicotinoids, frequently used as seed dressings (imidacloprid, thiamethoxam, and clothianidin), are discussed in the context of bee declines, which led to a moratorium of these substances in the EU²².

Neonicotinoids are neurotoxins that act as agonists of the nicotinic acetylcholine receptor. The disruption of the neuronal cholinergic signal transduction causes abnormal behavior, immobility, and death of target insect pests^{23–25}. Frequently, also non-target insects like honeybees are exposed to these insecticides^{12, 19, 26–28}, since forager bees transport neonicotinoid-contaminated pollen, nectar, dust, or guttation fluids to their colonies, where they can be frequently detected in honey and bee bread^{12, 13, 29–31}. Imidacloprid, one of the most commonly used insecticides³², is highly toxic to honeybees and other beneficial insects such as wild bees^{12, 20, 33}. Frequently, honeybees are exposed to lower concentrations of neonicotinoids, leading to sublethal effects, like impaired learning or homing behaviour, or suppressed immune defence^{34–37}. Whether sublethal effects of neonicotinoids are reversible or even low-level dietary residues can accumulate to be lethal is controversial^{38–43}.

¹Institute for Zoology, University of Cologne, Cologne, Germany. ²Institute for Insectbiotechnology, Justus-Liebig University of Giessen, Giessen, Germany. ³Julius Kühn-Institut - Federal Research Centre for Cultivated Plants, Institute for Bee Protection, Berlin, Germany. ⁴Mathematical Institute, Justus-Liebig University of Giessen, Giessen, Germany. ⁵Fraunhofer Institute for Molecular Biology and Applied Ecology, Department of Bioresources, Giessen, Germany. ⁶LLH Bee Institute, Erlenstr. 9, 35274, Kirchhain, Germany. Correspondence and requests for materials should be addressed to A.B. (email: annely.brandt@llh.hessen.de)

Direct lethal effects of neonicotinoids occur only rarely, mostly caused by accidental exposure of forager bees to acute toxic concentrations of neonicotinoids⁴⁴. In such cases, when a high number of bees are found in front of the hives, beekeepers can send a sample of bees for residue analysis to a laboratory to test for pesticide residues, including neonicotinoids and their metabolites. In Germany, the recommended practice is to send the samples via standard postal routes without extra cooling. During transportation, samples can be exposed to fluctuations in temperature and humidity, depending on climate, season, and weather, which could influence the decrease of imidacloprid, and thereby the level of residues left for analysis upon arrival at the analytical laboratory.

In this study, we investigated the temporal dynamics of whole-body residues of imidacloprid in live or dead honeybees following a single-meal dietary exposure (acute dose paradigm) under various environmental conditions, such as freezing of individuals, exposure to UV light or transfer of individuals through the mail system. Under field conditions, it is often not clear whether immobile bees found in front of the hives are really dead or only have been paralysed by the pesticides. Therefore, we wanted to test, (1) if rapidly freezing (= killing) of the bees can prevent or slow down the decrease of imidacloprid residues. Beekeepers do not check on their colonies on a daily basis, thus intoxicated honeybees may lie in front of their hives for several days, exposed to sun and weather. Since neonicotinoids are known to be sensitive to photolytic degradation⁴⁵ by sunlight, we wanted to test (2), whether exposure to UV light might affect the decrease of whole-body residues in honeybee samples. (3) To test if the mode of transportation affects the decrease of imidacloprid, we examined whether rapid transportation of dead bees on dry ice can preserve the level of residues left for analysis. According to the OECD guideline⁴⁶, oral toxicity tests are conducted in cages with groups of ten bees exposed to test substances. To examine whether the group feeding influences the residue level in honeybee, (4) we compared imidacloprid residues in single fed bees compared to bees that were fed in groups.

Results

To study the dynamic decrease of whole-body imidacloprid residues in live or dead honeybees, we individually fed worker bees with a single dose of 41 ng imidacloprid. Some bees were exposed to intensive UV light (RT24UV). Subsequently, after one (RT1, RT1mail), 24 (RT24, RT24UV), and 48 (RT48) hours after the feeding, the bees were frozen. The samples ($n = 150$ individuals per treatment group) were either transported at ambient temperature via normal postal mail service (RT1mail) or on dry ice via express service to the analytical laboratory (all other samples).

Immediately after the intake of the imidacloprid spiked feeding solution (41 ng/bee), honeybees showed spasms and appeared immobile and lifeless in the centrifuge tubes one hour after the feeding took place. However, bees that were kept at room temperature after dosing (RT48 treatment) recovered and walked up and down the tubes 48 hours after ingesting treated syrup.

Impact of time at room temperature. Under field conditions, it is often not clear, whether immobile bees are dead or only paralysed by a toxin. Hence, active cellular detoxification may take place even in “dead” looking bees. Therefore, we wanted to test, whether killing the bees by freezing can slow down or stop the decrease of imidacloprid residues. Indeed, the period of time elapsed before freezing significantly affected the amount of imidacloprid detected in the samples (Fig. 1). The regression analysis yielded a significant time main effect with a half-life of imidacloprid of about 22 hours (with a 95%-confidence interval from 18.6 to 26.8 hours, see statistical report in supplement). The hive experimental bees originated from did not show a significant influence in the regression model.

We detected $33.2 \pm 2.2\%$ (mean \pm relative standard error) of the ingested imidacloprid dose in the RT1 sample, $17.6 \pm 1.4\%$ in the RT24 sample and $7.8 \pm 0.9\%$ in the RT48 sample. The degradation process and recovery rate were investigated in more detail by quantifying the imidacloprid metabolites 5-hydroxy-imidacloprid and imidacloprid-olefin (Fig. 1). For 5-hydroxy-imidacloprid residue levels we observed a significant main effect of the hive the bees originated from as well as a significant main effect of time (elapsed after ingestion), and a significant interaction between hive and time (see statistical report in supplement). The levels of Imidacloprid-olefin were similar in RT1, RT24 and RT48 samples. Hive and time before freezing had no significant impact on olefin residues, but the interaction between hive and time had a significant impact on the detectable Imidacloprid-olefin amount (see statistical report in supplement).

Impact of transport method. To test whether the transport of the samples to the analytical laboratory influences imidacloprid residue levels, bees were individually exposed to imidacloprid and frozen one hour after the feeding. All bee samples were frozen at -20°C . One treatment group (RT1mail) was only frozen for one hour at -20°C , but subsequently stored at 4°C as it is recommended practice for beekeepers to store bee samples in the refrigerator. Later, the bees of the treatment group RT1mail were sent for analysis using a standard parcel delivery service at ambient temperatures. For these samples, we chose a selection of dispatch dates, including the days before weekends and bank holidays, so the delivery took between one and six days. All other samples were sent by express delivery on dry ice and arrived on the same day at the analytical laboratory.

The transport at ambient temperature via standard postal service did not significantly reduce the amount of imidacloprid compared to samples sent on dry ice (Fig. 2; RT1 vs. RT1mail, multiple comparisons using Dunnett contrasts, $p = 0.093$, see statistical report in supplement), although the samples were exposed to ambient temperature over long periods, with a maximum shipping duration of 144 hours. The residues in the RT24 and RT48 samples were significantly lower ($p = 0.0218$ and $p < 0.001$, respectively) than those of the RT1mail group. The hives the bees originated from and the interaction between hive and treatment (mailing) had no significant effect on the detectable imidacloprid values.

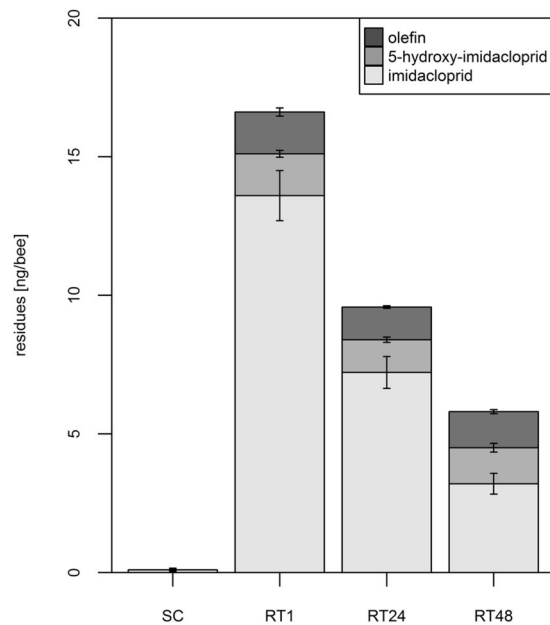


Figure 1. Whole-body imidacloprid residues decrease in honeybee samples over time. Individual honeybees were fed with a sugar syrup control (SC), containing only the solvent acetone but no imidacloprid or a dosage of 41 ng/bee imidacloprid ($n = 150$ bees/group). The honeybees were frozen after one hour (SC and RT1), 24 hours (RT24), or 48 hours (RT48) at room temperature. LC/MS/MS was used to quantify residue levels of imidacloprid, 5-hydroxy-imidacloprid, and imidacloprid-olefin. Error bars indicate standard error. The imidacloprid residue level was only significantly influenced ($p < 0.001$) by the time passed after ingestion. The residue level of 5-hydroxy-imidacloprid was influenced by the time the bees originated from, the time passed after ingestion and interaction effects between both (all $p < 0.001$). The residue level of imidacloprid-olefin was only influenced by the interaction effects between the hive the bees originated and the time passed after ingestion ($p < 0.001$, see statistical report in supplement).

Impact of UV radiation. Exposure to UV light significantly reduced the imidacloprid concentration ($p = 0.0163$ comparing RT24 and RT24UV using Dunnett contrasts, Fig. 2). The concentration in RT24UV was not significantly different from the one observed in RT48.

Impact of feeding condition. Compared to individually fed bees, bees that were fed in groups of ten had significantly higher imidacloprid residues (Fig. 3, RT1 vs. RT24GF, Dunnett contrasts, $p = 0.0128$; RT24 vs. RT24GF, Dunnett contrasts, $p < 0.001$; RT48 vs. RT24GF, Dunnett contrasts, $p < 0.001$, see statistical report in supplement). We assessed the “quality” of the obtained data using the Bartlett-, the Fligner-Killeen- and the F-test to compare variances of the residue levels. Only if we neglected the hive the bees originated from, variances of RT24 and RT48 were significantly different from the variance in RT24GF.

Dose-dependent effects on locomotory behavior. In order to assess the effect of different dosages of imidacloprid on the bee’s mobility, individual bees were exposed to different imidacloprid dosages and observed for 72 hours. Bees of the control group showed a decline in activity over the observation period (Fig. 4 and Supplementary Fig. 1). Bees fed with a dosage of 3.7 ng (corresponding to $LD50_{oral\ 48h}^{47}$, showed normal activity until 24 hours after exposure. At 36 hours, a steep decline in activity began. At 72 hours, most bees (80%) were completely immobile. In contrast, the bees fed with a dosage of 41 ng (corresponding to the dosage used in the experiments described above), showed cramps, uncoordinated movements, or paralysis one hour after exposure. At 36 hours most bees (78.9%) were completely immobile. Strikingly, after 48 hours only 26.3% of the bees were immobile, 47.3% of the bees exhibited some movement of body parts and 26.3% showed coordinated movements, e.g. walking or ventilation (Supplementary Figure 1). After this peak, activity declined again at 72 hours. In consequence to the uncoordinated movements most bees were not able to feed properly (pers. observation) and the experiment was stopped.

Discussion

Here, we provide data on the decrease of whole-body residues of imidacloprid in acutely poisoned bees and explore the effects of various environmental conditions, such as freezing of individuals, exposure to UV light or routes of shipping on the whole-body residue levels measured. The results allow recommending a standard sampling and shipping procedure to beekeepers in cases of suspected acute poisoning with imidacloprid. Thus, they contribute to a decrease of uncertainty in interpretation of analysis results and eventually to strengthen the confidence of beekeepers in extension and communication services.

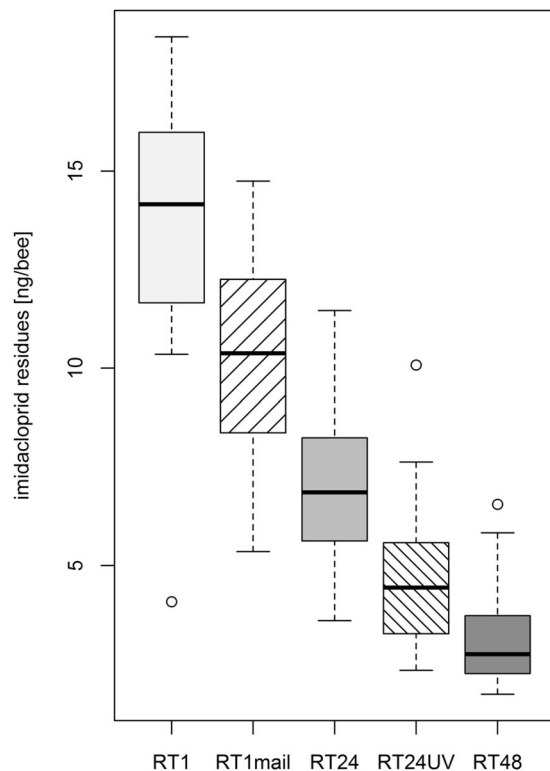


Figure 2. UV light accelerated the decrease of whole-body imidacloprid residues in honeybees, transportation on ice had no significant effect. Individual honeybees were fed with a dosage of 41 ng/bee. The honeybees were frozen after one hour (RT1, RT1mail), 24 hours (RT24, RT24UV), or 48 hours at room temperature. The samples of RT1, RT24, RT24UV, and RT48 were sent on dry ice with express delivery, RT1mail samples were sent without cooling via standard parcel service to the analytical laboratory (n = 150 bees/group). The mode of transport did not significantly affect imidacloprid residue levels (Comparison RT1 vs. RT1mail: $p = 0.093$). Intensive UV-light (RT24UV) significantly accelerated the decrease of imidacloprid (comparison RT24 vs. RT24UV: $p = 0.0163$; RT48 vs. RT24UV: $p = 0.1637$, see statistical report in supplement).

To study the temporal dynamics of the decrease of whole-body residues that takes place in imidacloprid exposed bees, we analysed the residue levels in individual bees one, 24, and 48 hours after exposure. We used a high dosage of imidacloprid (41 ng/bee) to ensure that a measurable level of imidacloprid was left for detection after 48 hours. In the assessment of risks from imidacloprid to bees, the EFSA considered the median lethal dose ($LD_{50_{48h}}$) at 3.7 ng/bee⁴⁷. However, reports of the oral acute $LD_{50_{48h}}$ range up to >81 ng⁴⁸. Surprisingly, a decrease of whole-body residues took place even in motionless, “dead” looking bees. Supporting these findings, poisoned, motionless bees partially recovered after approx. 48 hours post administration of 41 ng imidacloprid. The bees in our study became active again, when imidacloprid was degraded to a level of approx. 4 ng/bee.

Neonicotinoids act as neurotoxins. Whether the interactions of imidacloprid with its target site in the nervous system – the nicotinic acetylcholine receptor – is reversible or not is an academic controversy which has practical implications for the risk assessment of neonicotinoids^{38–43}. In case bees would fail to fully clear ingested pesticides from their bodies, the persistence of even small daily intakes could eventually build up to harmful or even lethal levels over time. Some scientists argue that imidacloprid irreversibly blocks the nicotinic acetylcholine receptors^{40–42}. Indeed, the lethality of imidacloprid to insects appears to be dependent on the time of exposure: the longer the exposure time, the less amount of total chemical is needed to kill honeybees^{40, 49, 50}. However, imidacloprid and its metabolites are rapidly metabolised by detoxification enzymes in bees and a partial or full recovery from imidacloprid-induced sublethal effects on bees has been observed^{38, 51, 52}. In support of the reversibility-hypothesis, our data clearly indicate, that a recovery from the paralyzing neurotoxic effects of a high dose of imidacloprid is possible. Strikingly, we found a non-linear dose-response relationship: the lower dose ($LD_{50_{48h}}$ 3.7 ng/bee) had a greater impact on bee immobility/death than the higher dose of 41 ng (48 hours after ingestion). Apparently, lethal effects are delayed in bees paralysed by a high dose of imidacloprid. Non-linear dose-response relationships of toxins have been reported before^{53, 54}. This raises the question, what the ultimate physiological cause of death by neonicotinoids is in honeybees. Further studies are needed to elucidate this relevant question.

In small invertebrates it is hard to measure brain waves, heartbeat, or respiration; hence it is difficult to define the exact moment of death. The OECD guideline defines mortality/death in honeybees as when an animal is “completely immobile”⁴⁶. This is an important criterion, since in acute oral toxicity tests required for regulatory risk assessment procedures, the LD_{50} is defined as a single dose of a substance that can cause death (= immobility) in 50% of animals⁴⁶. The possibility that honeybees can recover from an immobile state has not been considered before in the OECD guideline. Based on our observation of honeybees recovering from a completely immobile

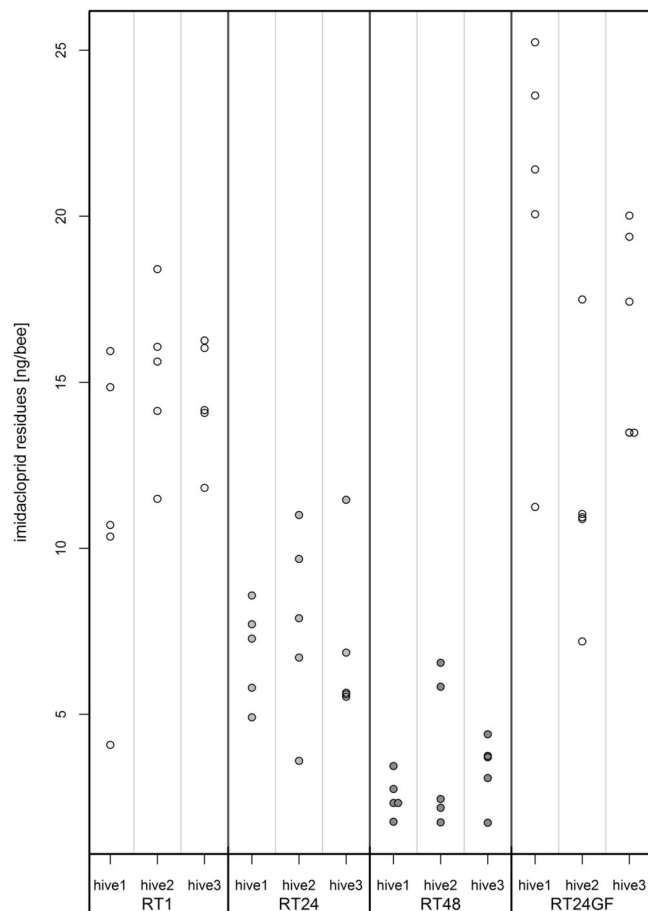


Figure 3. Group feeding resulted in significantly higher whole-body imidacloprid residues compared to the individually fed honeybees. Individual honeybees were fed with a single dosage of 41 ng/bee (RT1, RT24, RT48). Alternatively, groups of ten honeybees per cage were fed with 410 ng/cage imidacloprid (RT24GF). One dot indicates imidacloprid value of one sample of ten bees. Five samples of each hive are presented in one column ($n = 150$ bees/group). Statistical comparison with an ANOVA yielded a significant effect of the applied treatment ($p < 0.001$) and multiple comparisons using Dunnett contrasts resulted in RT1 vs. RT24GF: $p = 0.0128$; RT24 vs. RT 24GF: $p < 0.001$; RT48 vs. RT24GF: $p < 0.001$ (see statistical report in supplement).

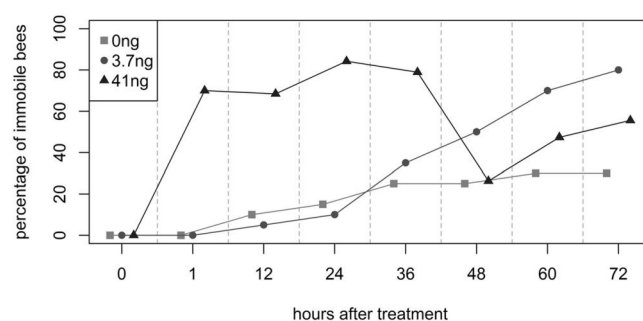


Figure 4. Imidacloprid-exposed bees partly recovered from paralysis after 48 hours. Individual honeybees were fed with a single dose of sugar syrup control or a dosage of 3.7 and 41 ng/bee imidacloprid (20 bees per treatment group, single experiment). After one, 12, 24, 36, 48, 60, and 72 hours bees were examined for activity. Non-moving bees were counted as immobile. After one hour, 70% of the bees of the 41 ng treatment were immobile, but recovered to the same level of immobility as the control after 48 hours.

state, the definition of “mortality” by the OECD may need to be reconsidered. Up to now, immobile, “dead” looking bees have to be removed daily and are usually discarded; hence there was no chance to observe a potential recovery from paralyzing toxins. In field realistic conditions however, this question is less relevant since most foragers which come into contact with extremely toxic, paralyzing substances may become easy prey and are lost to the colony.

In cases of suspected acute poisoning, beekeepers can send honeybee samples to certified laboratories for residue analysis. Sometimes, no residues can be detected in such samples, but it is often unclear whether no substance was present from the beginning or whether contaminant residue levels decreased in the time that passed since the poisoning event or during shipping. Beekeepers usually do not inspect their bee yards daily, thus poisoned honeybees may lay in front of their hives for several days before a sample can be taken. Consequently, the chances of finding any dead bees decreases with time, since immobilised bees may become easy prey for birds or ants.

From controlled laboratory studies it is known that whole-body imidacloprid residues can rapidly decrease^{38, 51, 52, 55}. Hardly any data exist, however, on the breakdown of the substance under conditions that may apply to a field situation where bees are acutely poisoned and become immobilised (and are taken for dead), or in bee samples during shipping to analytic facilities. Thus, a reliable interpretation of residue analyses results is often difficult and may be hampered by substantial uncertainty. After a single feeding of imidacloprid, honeybees eliminate the neonicotinoid from their body within 24 hours mostly through metabolic degradation rather than by excretion of the compound^{51, 52}. Our data confirm the rapid decrease of whole-body imidacloprid residues in honeybees^{38, 51, 52}. Even though we used a relatively high dose of imidacloprid, only small amounts of the two imidacloprid metabolites tested, imidacloprid-olefin and 5-hydroxy-imidacloprid, were detectable after 48 hours. However, for a complete picture of the dynamics of the decrease of imidacloprid residues in honeybee samples, it would be necessary to quantify all known metabolites^{20, 33}.

While the decrease of whole-body imidacloprid residues continuously progressed, even in bees that appeared dead, freezing the bees for a short time significantly slowed down this process. In cases where immobilised bees are found in an apiary and the beekeeper suspects poisoning by neonicotinoids, we therefore recommend instantaneous short freezing of the samples to stop possible cellular detoxification processes. Provided the decrease of whole-body residues has been slowed or stopped by freezing, our data show that no further significant decrease of imidacloprid occurs during standard shipping, compared to the transport on dry ice. Thus, the mode of transport does not affect the residue levels of imidacloprid in honeybee samples, and beekeepers can continue to send their samples without cooling via standard postal routes.

In the field, poisoned honeybees laying in front of their hive may eventually be exposed to sunlight which could further contribute to the decrease of detectable residues. A previous study demonstrates that imidacloprid is photodegradable by UV-irradiation⁴⁵, however, the data were generated using *in vitro* assays and did not involve live organisms or bees. In live bees or dead bees, the cuticle or the melanisation of the body may provide protection against UV radiation and may prevent photolytic degradation processes. In fact, in our experiment a moderately accelerated decrease of whole-body imidacloprid residues was observed after intensive UV irradiation. However, although the applied amount of UV radiation corresponded to the amount of UV light during two cloudless weeks at the equator, its effect on the residue degradation was less pronounced than that of an additional 24 hours of room temperature (see RT24UV and RT48, Fig. 2). In consequence, we consider photolytic degradation a less important factor affecting the detectable level of imidacloprid residues in honeybee samples.

In accordance with regulatory guidelines for pesticide risk assessments, acute oral toxicity tests are conducted with caged bees, where groups of ten bees per cage are exposed to the test compound⁴⁶. When applying imidacloprid under group feeding conditions, we observed a high variance and a significantly higher amount of residue level compared to individually fed bees. Our data suggest that some individuals may have consumed more than others and therefore the bees in a cage may not have been equally exposed to the test substance, confirming observations from Brodschneider *et al.*⁵⁶ who demonstrated by radioactively labelled markers that differences in food intake exist within caged bees that eventually may lead to differential exposure in toxicity tests. Since a worker bee which consumes the spiked sugar syrup becomes immobile after a few minutes, it has only little chances to share the food by trophallaxis with its cage mates. Thus, maybe only few individuals of a cage consume most of the contaminated food and others receive less. In this case, the variance in the recovery rates between the cages may result from the variable number of individuals which had direct contact to the syrup. The individuals that ate most of the contaminated food could not have been able to detoxify as fast as the single fed bees that really received the planned concentrations per individual. In contrast to the OECD guidelines⁴⁶, where a minimum of 100 µl sugar syrup for one cage is proposed, we only gave them 50 µl of the feeding solution. Thus, in an experiment performed exactly conforming to the guideline, the variance between cages might be lower, since more bees would be in direct contact to the test substance. However, our findings of the impact of feeding condition are not only relevant for immediately paralyzing test substances like imidacloprid, but for all substances (e.g. neurotoxins), which might interfere with the trophalactic exchange of food. We should therefore consider whether social insects like honeybees should always be monitored at group level. This may depend on the aim of the study. Under field conditions intoxications occur first on an individual level. Trophallaxis will only occur later if the bees are able to fly back to the hive. Group feeding does not account for the estimation of the detoxification process in full hive situation. The processes there are more complex and can hence be only evaluated by full hive studies.

Conclusion

The metabolism and toxicokinetics of imidacloprid has been intensively investigated^{33, 38, 51, 52, 55, 57}. Our data complement the knowledge of the temporal dynamics imidacloprid residues under field relevant conditions. Our study indicates that a short freezing of bee samples stops the decrease of whole-body residues and further shipping time does not change the amount of traceable residues. Importantly, when bees appear immobile or dead a fast decrease of the ingested pesticides could still occur. Therefore, we recommend freezing honeybee samples as fast as possible, before sending them via standard postal routes to the analytical laboratories. However, honeybees come in to contact with many different chemical compounds used in agriculture. In beebread-samples regularly more than 70 different active compounds can be found (on average 5.2 active compounds per hive), some of them highly toxic for insects^{29, 58}. In cases of suspected honeybee poisoning a high number of pesticides are analyzed to identify and quantify the relevant substance. Yet, about the metabolism, degradation rates and possible synergistic

Name	Treatment	Feeding condition	Time before freezing	Storage temperature before transport	Transport temperature	UV-exposure
SC	Sugar control	individual	1 h	freezer (ca. -80°C)	dry ice (ca. -80°C)	—
RT1	41 ng imidacloprid/bee	individual	1 h	freezer (ca. -80°C)	dry ice (ca. -80°C)	—
RT24	41 ng imidacloprid/bee	individual	24 h	freezer (ca. -80°C)	dry ice (ca. -80°C)	—
RT48	41 ng imidacloprid/bee	individual	48 h	freezer (ca. -80°C)	dry ice (ca. -80°C)	—
RT1mail	41 ng imidacloprid/bee	individual	1 h	fridge (ca. 4°C)	ambient temperature	—
RT24UV	41 ng imidacloprid/bee	individual	24 h	freezer (ca. -80°C)	dry ice (ca. -80°C)	+
RT24GF	410 ng imidacloprid/ten bees	group	24 h	freezer (ca. -80°C)	dry ice (ca. -80°C)	—

Table 1. Treatment conditions of experimental groups.

interactions⁵⁹ of the majority of these compounds only very little is known. Our work gives new insights into an important aspect of residue analysis in honeybees and contributes to the ongoing discussion among scientist, beekeepers, and stakeholders about the impact of pesticides on honeybee health and survival.

Experimental Procedures

Specimens. Honeybee worker bees were collected from brood combs of a colony of Carnolian bees located at the Fraunhofer Institute, Giessen, Germany (suburban landscape, in immediate vicinity to an arboreous environmental protection area), and at two field sites at the Bee Institute, Kirchhain, Germany (suburban landscape) in early September 2014 and 2015. At this time of the year, agricultural applications of neonicotinoids are uncommon in this region. All source colonies were briefly inspected, were healthy and showed no symptoms of bacterial, fungal, or viral disease.

Feeding solution. We spiked 999 μl of a 50% sugar/water feeding solution with 1 μl acetone (GC Ultra Grade, Carl Roth, Germany). The sugar control group (sample SC) received feeding solutions spiked with pure acetone, whereas the other groups were presented with feeding solutions spiked with acetone containing imidacloprid (Sigma-Aldrich, St Louis, MO, USA), resulting in a 8.2 ng imidacloprid per μl feeding solution. For the individual feeding experiments, bees were isolated in 15 ml centrifuge tubes (SLG, Gauting, Germany) and starved for 1.5 h. The caps of the tubes were spotted with 5 μl of the feeding solution, representing a total imidacloprid dosage of 41 ng per bee. The starved bees ingested all of the solution immediately after the presentation. For the group feeding experiment, 10 worker bees were transferred to standard metal cages ($8.5 \times 6.5 \times 4$ cm) and starved for 1.5 h. Subsequently, caps with 50 μl of the feeding solution were placed into the cages, representing a total imidacloprid dosage of 410 ng per cage and 41 ng per bee, respectively. Since the treatments groups sugar control, RT1, and RT1mail were frozen one hour after the feeding of the single dose of imidacloprid, there was no need to provide them with additional food. The bees of the other treatment groups were paralysed and appeared to be “dead” until they became mobile again (approx. 46–48 hours after the feeding) but they received no additional food.

Experimental design. We assigned 50 worker bees to each treatment. Each experiment (see Table 1) was carried out three times, and each repetition involved bees from a different hive. Each treatment was therefore applied to 150 bees in total.

Impact of time at room temperature. In the initial degradation experiment, three groups of individually fed bees were frozen after different periods of exposure to room temperature (ca. 21°C , Table 1): one hour (sample RT1), 24 hours (sample RT24), and 48 hours (sample RT48). Until freezing, tubes and cages containing the bees were placed on laboratory benches; direct sunlight was avoided.

Impact of transport method. Bees were individually exposed to imidacloprid, frozen for one hour (-20°C), but subsequently stored in a fridge (-4°C). Later, they were sent for analysis using a standard German parcel delivery service (DHL Paket GmbH, Bonn, Germany) at ambient temperatures (sample RT1mail). For these samples, we chose a selection of dispatch dates, including the days before weekends and bank holidays, so the delivery took between 1 and 6 days.

All other samples were sent by express delivery (TNT Express GmbH, Troisdorf, Germany) on dry ice and arrived on the same day at the analytical laboratory.

Impact of UV radiation. A group of individually fed bees were exposed to 20 J/cm² UV light one hour after feeding and were frozen after 24 hours at room temperature (sample RT24UV).

Impact of feeding condition. In all our previous experiments bees were fed individually to minimise “dilution”-effects by trophallaxis (transfer of food droplets from one bee to another). In this experiment (sample RT24GF), the bees were kept in cages of 10 individuals and had access to the ten-fold volume (50 μl) of the imidacloprid spiked sugar solution. Every other factor was kept similar. After feeding, these bees were left at room temperature for 24 hours (comparable to RT24).

Dose-dependent effects on locomotory behavior. To assess the effect of different dosages of imidacloprid, including the LD50_{oral 48h} (3.7 ng/bee) on the bee’s mobility, individual bees were placed in petri dishes (20 bees per treatment group, one replicate). After a starving period of 1.5 hours, the bees were exposed to 5 μl of

feeding solution representing a total imidacloprid dosage of 0 ng, 3.7 ng, or 41 ng per bee. After one hour, bees were fed a 50% sucrose/water solution (v/v) *ad libitum* with a perforated Eppendorf tube through a hole in the lid of the petri dish. At different time points (one hour before exposure, one, 12, 24, 36, 48, 60, and 72 hours after exposure), the activity was examined. Immobility was defined as absence of any visible movements of body parts (including ventilation of the abdomen) or coordinated activity (e.g. standing, hanging, waking, etc.). Bees were observed for 30 seconds at each time interval.

Chemical residue analysis. *Preparation of samples for residue analysis of worker bees.* A sample of worker bees (10 individuals, about 1 g) was weighed in a centrifuge tube made of glass (100 ml), and 50 µl of a surrogate standard solution (acetamiprid-d3, used to evaluate the analysis, not used for calculations) and 30 ml of a acetone/water-mixture (2/1, v/v) were added to every sample. The tubes were closed and left to stand for 30 minutes. The samples were homogenized for 3 minutes with a disperser and then centrifuged (10 minutes at 3,000 rpm). After centrifugation, 15 ml of the extract were removed and after addition of 5 ml sodium chloride-solution (20%) to this aliquot transferred onto a disposable cartridge filled with diatomaceous earth (ChemElut® cartridges, 20 ml, unbuffered, Agilent). After a waiting time of 15 minutes the samples were eluted with dichloromethane (2 × 50 ml). The eluates were evaporated to approximately 2 ml by using a rotary evaporator, then transferred to a graduated tube and evaporated to dryness with nitrogen, using a metal block thermostat with nitrogen blow device. The residual extract was taken up with 1 ml of a methanol/water mixture (1/1, v/v) containing the internal standards (imidacloprid-d4, clothianidin-d3), dissolved using an ultrasonic liquid mixer (30 seconds) and then put into the freezer (−18 °C) over night. On the next day, the samples were filtered cold (syringe filter: 0.2 µm).

Identification and quantification of imidacloprid and its main metabolites. LC-MS/MS was used for the identification and quantification of the substances in the samples. The system used was a Prominence UFLC XR HPLC (SHIMADZU) coupled to a triple quadrupole mass spectrometer 4000 Q TRAP® (AB SCIEX) equipped with an electrospray ionization (ESI) source. Imidacloprid was measured in positive ion mode and its main metabolites imidacloprid-5-hydroxy and imidacloprid-olefin were measured in negative ion mode. All three substances were identified by their retention time and three MRM-transitions. The residues in the samples were quantified with reference standards in matrix (concentrations: 0.05, 0.1, 0.5, 1, 5, 10, 25, 50 and 100 pg/µl). The quantification was carried out by the internal standard method. Certified pesticide standards were purchased from Dr. Ehrenstorfer (Augsburg, Germany, now LGC Standards, Wesel, Germany), except imidacloprid-5-hydroxy ([6-Chloro-3-pyridinyl)methyl]-4,5-dihydro-2-(nitroamino)-1H-imidazol-5-ol) that was obtained from Bayer Crop Science (Frankfurt am Main, Germany). All solvents used were classified as highly pure for residue analysis and LC/MS. The residue values shown for the samples are averages of measurements out of duplicate injections of the sample extracts. The limit of detection (LOD) was determined as the lowest concentration tested in which the peak signal of the main MRM, which was used for quantification, was three times higher than the background noise of the chromatogram. The limit of quantification (LOQ) was 1 pg/µl for imidacloprid, 0.5 pg/µl for imidacloprid-5-hydroxy, and 5 pg/µl for imidacloprid-olefin, this refers to 2 µg/kg, 1 µg/kg and 10 µg/kg taking into account an initial sample weight of 1 g and the terms of the described residue analysis.

Statistical analysis. To investigate

- (1) Whether rapid transportation on dry ice can preserve the level of residue left for analysis, linear regression models of residue-concentrations on time (in hours exposed to room temperature before freezing) and hives were used (including a potential interaction between time and hive).
- (2) If the degradation process can be slowed down by short freezing, a two-factorial ANOVA for the imidacloprid-concentration on treatment and hive (including their interaction) was employed, followed by multiple comparisons with a reference group (here RT1 mail) and calculation of simultaneous confidence intervals for the respective differences.
- (3) Whether exposure to UV light affects residue degradation in honeybee samples, the same analyses were applied as in (2).
- (4) If imidacloprid residues in individually fed bees are different from those in bees that were fed in groups, the analysis was two-fold: Bartlett's several samples test for homogeneity of variances of imidacloprid concentrations in combinations of the RT24 and RT24GF treatments and hives was used to see if measurement quality is affected by feeding. To determine if quantified residue levels are affected by the feeding method, the same analyses were applied as in (2) but with RT24GF as reference.

In all analyses a decadic (base 10) log-transformation of the respective response variable was considered and used if model diagnostics (like q-q-plots and scale-location-plots for the model residuals) suggested it to achieve homoscedastic normality for the data.

All statistical calculations and analyses were performed using R 3.3.1 (R Core Team, 2016) including the packages car (Fox and Weisberg, 2011; for q-q-plots with confidence intervals) and multcomp (Hothorn *et al.*, 2008; for multiple pairwise comparisons).

References

1. Fontaine, C., Dajoz, I., Meriguet, J. & Loreau, M. Functional Diversity of Plant/Pollinator Interaction Webs Enhances the Persistence of Plant Communities. *PLoS Biol* **4**, e1, doi:10.1371/journal.pbio.0040001 (2005).
2. Bascompte, J., Jordano, P. & Olesen, J. M. Asymmetric Coevolutionary Networks Facilitate Biodiversity Maintenance. *Science* **312**, 431–433, doi:10.1126/science.1123412 (2006).

3. Klein, A.-M. *et al.* Importance of pollinators in changing landscapes for world crops. *Proceedings of the Royal Society of London B: Biological Sciences* **274**, 303–313, doi:10.1098/rspb.2006.3721 (2007).
4. van Engelsdorp, D., Tarry, D. R., Lengerich, E. J. & Pettis, J. S. Idiopathic brood disease syndrome and queen events as precursors of colony mortality in migratory beekeeping operations in the eastern United States. *Preventive veterinary medicine* **108**, 225–233, doi:10.1016/j.prevetmed.2012.08.004 (2013).
5. Potts, S. G. *et al.* Global pollinator declines: trends, impacts and drivers. *Trends in ecology & evolution* **25**, 345–353, doi:10.1016/j.tree.2010.01.007 (2010).
6. Potts, S. G. *et al.* Declines of managed honey bees and beekeepers in Europe. *Journal of Apicultural Research* **49**, 15–22, doi:10.3896/ibra.1.49.1.02 (2010).
7. van der Zee, R., Gray, A., Pisa, L. & de Rijk, T. An Observational Study of Honey Bee Colony Winter Losses and Their Association with Varroa destructor, Neonicotinoids and Other Risk Factors. *PLoS one* **10**, e0131611, doi:10.1371/journal.pone.0131611 (2015).
8. Goulson, D., Nicholls, E., Rotheray, E. & Botias, C. Qualifying pollinator decline evidence-response. *Science* **348**, 982, doi:10.1126/science.348.6238.982 (2015).
9. Goulson, D., Nicholls, E., Botias, C. & Rotheray, E. L. Bee declines driven by combined stress from parasites, pesticides, and lack of flowers. *Science* **347**, 1255957, doi:10.1126/science.1255957 (2015).
10. Alaux, C. *et al.* Interactions between Nosema microspores and a neonicotinoid weaken honeybees (*Apis mellifera*). *Environmental microbiology* **12**, 774–782, doi:10.1111/j.1462-2920.2009.02123.x (2010).
11. Brodschneider, R. & Crailsheim, K. Nutrition and health in honey bees. *Apidologie* **41**, 278–294, doi:10.1051/apido/2010012 (2010).
12. Blacquiere, T., Smaghe, G., van Gestel, C. A. & Mommaerts, V. Neonicotinoids in bees: a review on concentrations, side-effects and risk assessment. *Ecotoxicology* **21**, 973–992, doi:10.1007/s10646-012-0863-x (2012).
13. Genersch, E. *et al.* The German bee monitoring project: a long term study to understand periodically high winter losses of honey bee colonies. *Apidologie* **41**, 332–352 (2010).
14. Di Pasquale, G. *et al.* Variations in the Availability of Pollen Resources Affect Honey Bee Health. *PLoS one* **11**, e0162818, doi:10.1371/journal.pone.0162818 (2016).
15. Williams, G. R. *et al.* Neonicotinoid pesticides severely affect honey bee queens. *Scientific reports* **5**, 14621, doi:10.1038/srep14621 (2015).
16. Goulson, D. REVIEW: An overview of the environmental risks posed by neonicotinoid insecticides. *Journal of Applied Ecology* **50**, 977–987, doi:10.1111/1365-2664.12111 (2013).
17. Vanbergen, A. J. & Initiative, the Insect Pollinators. Threats to an ecosystem service: pressures on pollinators. *Frontiers in Ecology and the Environment* **11**, 251–259, doi:10.1890/120126 (2013).
18. Dively, G. P., Embrey, M. S., Kamel, A., Hawthorne, D. J. & Pettis, J. S. Assessment of chronic sublethal effects of imidacloprid on honey bee colony health. *PLoS one* **10**, e0118748, doi:10.1371/journal.pone.0118748 (2015).
19. Pisa, L. W. *et al.* Effects of neonicotinoids and fipronil on non-target invertebrates. *Environmental science and pollution research international* **22**, 68–102, doi:10.1007/s11356-014-3471-x (2015).
20. Simon-Delso, N. *et al.* Systemic insecticides (neonicotinoids and fipronil): trends, uses, mode of action and metabolites. *Environmental science and pollution research international* **22**, 5–34, doi:10.1007/s11356-014-3470-y (2015).
21. van der Sluijs, J. P. *et al.* Conclusions of the Worldwide Integrated Assessment on the risks of neonicotinoids and fipronil to biodiversity and ecosystem functioning. *Environmental science and pollution research international* **22**, 148–154, doi:10.1007/s11356-014-3229-5 (2015).
22. European Commission. Bee health: EU-wide restrictions on pesticide use to enter into force. *Brussels* (2013).
23. Elbert, A., Haas, M., Springer, B., Thielert, W. & Nauen, R. Applied aspects of neonicotinoid uses in crop protection. *Pest management science* **64**, 1099–1105, doi:10.1002/ps.1616 (2008).
24. Matsuda, K. *et al.* Neonicotinoids: insecticides acting on insect nicotinic acetylcholine receptors. *Trends in pharmacological sciences* **22**, 573–580 (2001).
25. Tomizawa, M. & Casida, J. E. Unique neonicotinoid binding conformations conferring selective receptor interactions. *Journal of agricultural and food chemistry* **59**, 2825–2828, doi:10.1021/jf1019455 (2011).
26. Desneux, N., Decourtye, A. & Delpuech, J. M. The sublethal effects of pesticides on beneficial arthropods. *Annual review of entomology* **52**, 81–106, doi:10.1146/annurev.ento.52.110405.091440 (2007).
27. Cresswell, J. E. A meta-analysis of experiments testing the effects of a neonicotinoid insecticide (imidacloprid) on honey bees. *Ecotoxicology* **20**, 149–157, doi:10.1007/s10646-010-0566-0 (2011).
28. van der Sluijs, J. P. *et al.* Neonicotinoids, bee disorders and the sustainability of pollinator services. *Current Opinion in Environmental Sustainability* **5**, 293–305, doi:10.1016/j.cosust.2013.05.007 (2013).
29. Rosenkranz, P. *et al.* Schlussbericht: Deutsches Bienenmonitoring – “DeBiMo” 2011–2013 (2014).
30. Reetz, J. E. *et al.* Uptake of Neonicotinoid Insecticides by Water-Foraging Honey Bees (Hymenoptera: Apidae) Through Guttation Fluid of Winter Oilseed Rape. *Journal of economic entomology* **109**, 31–40, doi:10.1093/jeet/tov287 (2015).
31. Rundlof, M. *et al.* Seed coating with a neonicotinoid insecticide negatively affects wild bees. *Nature* **521**, 77–80, doi:10.1038/nature14420 (2015).
32. Jeschke, P., Nauen, R., Schindler, M. & Elbert, A. Overview of the status and global strategy for neonicotinoids. *Journal of agricultural and food chemistry* **59**, 2897–2908, doi:10.1021/jf101303g (2011).
33. Suchail, S., Guez, D. & Belzunces, L. P. Discrepancy between acute and chronic toxicity induced by imidacloprid and its metabolites in *Apis mellifera*. *Environmental toxicology and chemistry/SETAC* **20**, 2482–2486 (2001).
34. Yang, E. C., Chuang, Y. C., Chen, Y. L. & Chang, L. H. Abnormal foraging behavior induced by sublethal dosage of imidacloprid in the honey bee (Hymenoptera: Apidae). *Journal of economic entomology* **101**, 1743–1748 (2008).
35. Henry, M. *et al.* A common pesticide decreases foraging success and survival in honey bees. *Science* **336**, 348–350, doi:10.1126/science.1215039 (2012).
36. Di Prisco, G. *et al.* Neonicotinoid clothianidin adversely affects insect immunity and promotes replication of a viral pathogen in honey bees. *Proceedings of the National Academy of Sciences of the United States of America* **110**, 18466–18471, doi:10.1073/pnas.1314923110 (2013).
37. Brandt, A., Gorenflo, A., Siede, R., Meixner, M. & Büchler, R. The Neonicotinoids Thiacloprid, Imidacloprid and Clothianidin affect the immunocompetence of Honey Bees (*Apis mellifera* L.). *Journal of insect physiology* **86**, 40–47 (2016).
38. Cresswell, J. E., Robert, F. X., Florance, H. & Smirnov, N. Clearance of ingested neonicotinoid pesticide (imidacloprid) in honey bees (*Apis mellifera*) and bumblebees (*Bombus terrestris*). *Pest management science* **70**, 332–337, doi:10.1002/ps.3569 (2014).
39. Laycock, I. & Cresswell, J. E. Repression and recuperation of brood production in *Bombus terrestris* bumble bees exposed to a pulse of the neonicotinoid pesticide imidacloprid. *PLoS one* **8**, e79872, doi:10.1371/journal.pone.0079872 (2013).
40. Rondeau, G. *et al.* Delayed and time-cumulative toxicity of imidacloprid in bees, ants and termites. *Scientific reports* **4**, 5566, doi:10.1038/srep05566 (2014).
41. Tennekes, H. A. & Sanchez-Bayo, F. The molecular basis of simple relationships between exposure concentration and toxic effects with time. *Toxicology* **309**, 39–51, doi:10.1016/j.tox.2013.04.007 (2013).
42. Tennekes, H. A. The significance of the Druckrey-Küpfmüller equation for risk assessment—the toxicity of neonicotinoid insecticides to arthropods is reinforced by exposure time. *Toxicology* **276**, 1–4 (2010).

43. Maus, C. & Nauen, R. Response to the publication: Tennekes, H. A. (2010): The significance of the Druckrey–Küpfmüller equation for risk assessment—The toxicity of neonicotinoid insecticides to arthropods is reinforced by exposure time. *Toxicology* **280**, 176–177, doi:10.1016/j.tox.2010.11.014 (2011).
44. Pistorius, J., B. G., Heimbach, U. & Stähler, M. In *10th international symposium of the ICP-BR Bee Protection Group: Hazards of pesticides to bees* Vol. Julius-Kühn-Archiv 423 p 118–126 (Ooman, P. A. & Thompsons, H. M., Quedlinburg, 2009).
45. Zheng, W., Liu, W. P., Wen, Y. Z. & Lee, S. J. Photochemistry of insecticide imidacloprid: direct and sensitized photolysis in aqueous medium. *Journal of environmental sciences (China)* **16**, 539–542 (2004).
46. OECD/OCDE. Honeybees, Acute Oral Toxicity Test. *OECD Guidelines for the Testing of Chemicals*: 213 (1998).
47. Hertfordshire, U. O. The Pesticide Properties DataBase (PPDB) developed by the Agriculture & Environment Research Unit (AERU). *University of Hertfordshire, 2006–2013* (2013).
48. Nauen, R., Ebbinghaus-Kintscher, U. & Schmuck, R. Toxicity and nicotinic acetylcholine receptor interaction of imidacloprid and its metabolites in *Apis mellifera* (Hymenoptera: Apidae). *Pest management science* **57**, 577–586, doi:10.1002/ps.331 (2001).
49. Tasei, J.-N., Lerin, J. & Ripault, G. Sub-lethal effects of imidacloprid on bumblebees, *Bombus terrestris* (Hymenoptera: Apidae), during a laboratory feeding test. *Pest management science* **56**, 784–788, doi:10.1002/1526-4998 (2000).
50. Moncharmont, F.-X. D., Decourtye, A., Hennequet-Hantier, C., Pons, O. & Pham-Delègue, M.-H. Statistical analysis of honeybee survival after chronic exposure to insecticides. *Environmental Toxicology and Chemistry* **22**, 3088–3094, doi:10.1897/02-578 (2003).
51. Suchail, S., De Sousa, G., Rahmani, R. & Belzunces, L. P. *In vivo* distribution and metabolisation of 14C-imidacloprid in different compartments of *Apis mellifera* L. *Pest management science* **60**, 1056–1062, doi:10.1002/ps.895 (2004).
52. Suchail, S., Debrauwer, L. & Belzunces, L. P. Metabolism of imidacloprid in *Apis mellifera*. *Pest management science* **60**, 291–296, doi:10.1002/ps.772 (2004).
53. Calabrese, E. J. Biphasic dose responses in biology, toxicology and medicine: accounting for their generalizability and quantitative features. *Environmental pollution (Barking, Essex: 1987)* **182**, 452–460, doi:10.1016/j.envpol.2013.07.046 (2013).
54. Kaiser, J. H. Sipping from a poisoned chalice. *Science* **302**, 376–379, doi:10.1126/science.302.5644.376 (2003).
55. Alburaki, M. *et al.* Performance of honeybee colonies located in neonicotinoid-treated and untreated cornfields in Quebec. *Journal of Applied Entomology* **141**, 112–121, doi:10.1111/jen.12336 (2017).
56. Brodschneider, R., Libor, A., Kupelwieser, V. & Crailsheim, K. Food consumption and food exchange of caged honey bees using a radioactive labelled sugar solution. *PloS one* **12**, e0174684, doi:10.1371/journal.pone.0174684 (2017).
57. Cresswell, J. E. *et al.* Differential sensitivity of honey bees and bumble bees to a dietary insecticide (imidacloprid). *Zoology* **115**, 365–371, doi:10.1016/j.zool.2012.05.003 (2012).
58. Mullin, C. A. *et al.* High Levels of Miticides and Agrochemicals in North American Apiaries: Implications for Honey Bee Health. *PloS one* **5**, e9754, doi:10.1371/journal.pone.0009754 (2010).
59. Iwasa, T., Motoyama, N., Ambrose, J. T. & Roe, R. M. Mechanism for the differential toxicity of neonicotinoid insecticides in the honey bee, *Apis mellifera*. *Crop Protection* **23**, 371–378, doi:10.1016/j.cropro.2003.08.018 (2004).

Acknowledgements

We gratefully thank S. Backhaus, E. Leider, Ch. Wehrenfennig, and T. Gasch for technical support and K. Petzold-Treibert, and U. Hubbe for assistance in beekeeping and all team members of the Bee Institute Kirchhain for support. Special thanks go to K. Jaenicke from Julius Kühn-Institute in Berlin for careful carrying out residue analysis and T. Reinhardt for comments on an earlier version of the manuscript. This research was supported by the Land Hessen “Förderung von Maßnahmen zur Verbesserung der Erzeugung und Vermarktung von Honig in Hessen” and the Hessen State Ministry of Higher Education, Research and the Arts (HMWK) via the LOEWE Research Center “Insect Biotechnology and Bioresources”.

Author Contributions

M.S. and A.B. designed the methods and experiments, carried out the honeybee experiments, analyzed the data, interpreted the results and wrote the manuscript. G.B. conducted the chemical analysis and helped to interpret the results. G.E. and M.S. conducted the statistical analysis. M.D.M., A.V., and R.B. helped to interpret the results and to edit the manuscript. All authors read and approved the final version of the manuscript.

Additional Information

Supplementary information accompanies this paper at doi:10.1038/s41598-017-06259-z

Competing Interests: The authors declare that they have no competing interests.

Publisher's note: Springer Nature remains neutral with regard to jurisdictional claims in published maps and institutional affiliations.



Open Access This article is licensed under a Creative Commons Attribution 4.0 International License, which permits use, sharing, adaptation, distribution and reproduction in any medium or format, as long as you give appropriate credit to the original author(s) and the source, provide a link to the Creative Commons license, and indicate if changes were made. The images or other third party material in this article are included in the article's Creative Commons license, unless indicated otherwise in a credit line to the material. If material is not included in the article's Creative Commons license and your intended use is not permitted by statutory regulation or exceeds the permitted use, you will need to obtain permission directly from the copyright holder. To view a copy of this license, visit <http://creativecommons.org/licenses/by/4.0/>.

© The Author(s) 2017



The neonicotinoids thiacloprid, imidacloprid, and clothianidin affect the immunocompetence of honey bees (*Apis mellifera* L.)



Annelly Brandt*, Anna Gorenflo, Reinhold Siede, Marina Meixner, Ralph Büchler

LLH Bee Institute, Erlenstr. 9, 35274 Kirchhain, Germany

ARTICLE INFO

Article history:

Received 22 June 2015

Received in revised form 7 January 2016

Accepted 8 January 2016

Available online 8 January 2016

Keywords:

Honey bee

Neonicotinoid

Immune system

Hemocyte

Encapsulation

Wound healing

Antimicrobial activity

ABSTRACT

A strong immune defense is vital for honey bee health and colony survival. This defense can be weakened by environmental factors that may render honey bees more vulnerable to parasites and pathogens. Honey bees are frequently exposed to neonicotinoid pesticides, which are being discussed as one of the stress factors that may lead to colony failure. We investigated the sublethal effects of the neonicotinoids thiacloprid, imidacloprid, and clothianidin on individual immunity, by studying three major aspects of immunocompetence in worker bees: total hemocyte number, encapsulation response, and antimicrobial activity of the hemolymph. In laboratory experiments, we found a strong impact of all three neonicotinoids. Thiacloprid (24 h oral exposure, 200 µg/l or 2000 µg/l) and imidacloprid (1 µg/l or 10 µg/l) reduced hemocyte density, encapsulation response, and antimicrobial activity even at field realistic concentrations. Clothianidin had an effect on these immune parameters only at higher than field realistic concentrations (50–200 µg/l). These results suggest that neonicotinoids affect the individual immunocompetence of honey bees, possibly leading to an impaired disease resistance capacity.

© 2016 Elsevier Ltd. All rights reserved.

1. Introduction

Honey bees provide vital pollination services to crops and wild plants and are thus important components for food security and the maintenance of biodiversity (Bascompte et al., 2006; Fontaine et al., 2006; Klein et al., 2007). Recent reports on global pollinator declines (Biesmeijer et al., 2006; Potts et al., 2010a; Cameron et al., 2011) are alarming, especially with respect to the increasing demands for pollination services (Klein et al., 2007; Aizen and Harder, 2009). Honey bees are the most economically valuable pollinators (Klein et al., 2007). However, the number of managed honey bees decreased by one fourth in Europe between 1985 and 2005 (Potts et al., 2010b; Goulson et al., 2015) and by more than one half in North America between 1947 and 2005 (vanEngelsdorp et al., 2008; Goulson et al., 2015; National Research Council, 2007).

Several stress factors are suspected to negatively affect the survival of honey bee colonies. There is consensus on the involvement of multiple causal factors, parasites and pathogens are among the main candidates (Genersch et al., 2010), but diet quantity, quality, and diversity (Alaux et al., 2010; Brodschneider and Crailsheim,

2010; Di Pasquale et al., 2013) as well as exposure to pesticides may also affect colony survival (Sandrock et al., 2014; Goulson et al., 2015). In particular the application of neonicotinoid insecticides, which has increased substantially on a global scale over the last decade (Elbert et al., 2008; Mullin et al., 2010; Jeschke et al., 2011; van der Sluijs et al., 2013; Goulson et al., 2015), has been suspected to represent a major threat to honey bee survival (Desneux et al., 2007; Goulson, 2013; Pisa et al., 2015; Vanbergen and the Insect Pollinators Initiative, 2013).

Neonicotinoids are neurotoxins that act as agonists of the nicotinic acetylcholine receptor by disrupting the neuronal cholinergic signal transduction, leading to abnormal behavior, immobility and death of target insect pests (Matsuda et al., 2001; Tomizawa and Casida, 2005; Elbert et al., 2008). Frequently, non-target insects, like honey bees, come into contact with these insecticides (Pisa et al., 2015). Neonicotinoids are referred to as “systemic” as they are absorbed by plants and spread to all tissues through their vascular system (Elbert et al., 2008). Thus, pollen, nectar and also guttation fluids can contain neonicotinoids (Desneux et al., 2007; Cresswell, 2011; Blacquière et al., 2012; Goulson, 2013; van der Sluijs et al., 2013; EASAC, 2015). Thus, forager bees can come into contact with neonicotinoid-contaminated pollen and nectar and transport them to the hive, where they are frequently detected in honey and bee bread (Genersch et al., 2010; Blacquière et al., 2012; Rosenkranz et al., 2014).

* Corresponding author at: Bee Institute Kirchhain, Erlenstr. 9, D-35274 Kirchhain, Germany.

E-mail address: annely.brandt@ilh.hessen.de (A. Brandt).

Direct lethal effects of neonicotinoids, caused by accidental exposure of forager bees to acute toxic concentrations of neonicotinoids, occur only rarely (Pistorius et al., 2009). More commonly, honey bees are exposed to lower concentrations of neonicotinoids, leading to sublethal effects, like impaired learning or homing behavior (Yang et al., 2008, 2012; Han et al., 2010; Henry et al., 2012; Decourtye et al., 2004). Some neonicotinoids like thiacloprid are applied as sprays on flowering crops, e.g. oil seed rape. Others, like imidacloprid, clothianidin, or thiamethoxam are mainly applied as seed dressings or soil applications. Recently, these latter three neonicotinoids have been temporarily banned by the European Commission (2013), because of growing concerns about the risk they may pose on honey bees and other pollinators (Gross, 2013; EFSA, 2013a,b,c, 2014).

Colony losses are often associated with high infection levels of pathogens and parasites (Neumann and Carreck, 2010; Ratnieks and Carreck, 2010). This suggests a causal link between external stress factors and reduced immune function (Gregory et al., 2005; Yang and Cox-Foster, 2005). The immune defense depends on several internal and external factors such as the nutritional state or the age of honey bees (Wilson-Rich et al., 2008; Di Pasquale et al., 2013; Mao et al., 2013; Frias et al., 2015; Negri et al., 2015). Moreover, there is evidence that the invasive ectoparasite *Varroa destructor* Anderson and Trueman (2000) impairs the immune defense of honey bees by reducing the expression of immune-relevant genes and boosting viral replication, thereby affecting lifespan and disease resistance (Yang and Cox-Foster, 2005; Nazzi et al., 2012).

The immune defense of honey bees may also be affected by pesticides (for review see James and Xu, 2012). The exposure to sublethal dosages of neonicotinoids is often associated with a higher pathogenic impact, including the prevalent gut-parasite *Nosema* spp. and viruses typically associated with *V. destructor*, such as deformed wing virus (DWV) (Alaux et al., 2010; Aufauvre et al., 2012; Pettis et al., 2012; Fauser-Misslin et al., 2014; Doublet et al., 2015). Di Prisco et al. (2013) demonstrated that the neonicotinoid clothianidin adversely affects a member of the gene family NF- κ B and promotes the replication of the deformed wing virus in honey bees bearing a covert infection. Due to its central role in insect immunity (Evans et al., 2006; Schlüns and Crozier, 2007), pesticide induced changes in NF- κ B-related signaling may also affect other immune responses, like encapsulation, wound healing, or antimicrobial defense. However, the effect of neonicotinoids on these functional traits of honey bee immunity has not been investigated so far (for review see Collison et al., 2015).

In this study, we examined whether general immune defense mechanisms of adult worker honey bees are affected by sublethal concentrations of neonicotinoids. Neonicotinoid exposure was performed in laboratory cage experiments, including field realistic concentrations found in bee products. Since disease resistance is difficult to measure (Luster et al., 1993; Keil et al., 2001; Adamo, 2004; Rantala and Roff, 2005; Wilson-Rich et al., 2008), we selected three established parameters of immunity to analyze honey bee immunocompetence, namely total hemocyte count, encapsulation response, and antimicrobial activity of the hemolymph.

2. Material and methods

2.1. Neonicotinoid exposure in laboratory cage experiments

Worker bees were collected from six *A. m. carnica* colonies. All colonies were regularly inspected for symptoms of diseases. Prior to the experiments, samples of adult bees from each colony were tested for the presence of Chronic Bee Paralysis Virus (CBPV) as

described by Amiri et al. (2014), and deformed wing virus (DWV), acute bee paralysis virus (ABPV), and sacbrood virus (SBV; Genersch et al., 2010; Rosenkranz et al., 2014). Only healthy colonies were used. For all experiments, single frames of late stage capped brood were brought to the laboratory and incubated in the dark at 32 °C (Binder, Tuttlingen, Germany; humidity provided by open water jars). Newly emerged bees (≤ 24 h) were collected and transferred to standard metal cages (8.5 × 6.5 × 4 cm, 10 bees per cage) containing water and pollen (collected at the Bee Institute Kirchhain or obtained from Imkereibedarf Bährle, Aschaffenburg, Germany), and *ad libitum* sugar syrup (Apiinvert, Mannheim, Germany) diluted to a 60% solution with distilled water in a 5 ml syringe (Carl Roth, Karlsruhe, Germany). Cages were kept in an incubator in the dark at 32 °C (Williams et al., 2013).

Neonicotinoid stock solutions were diluted in sugar syrup (60% Apiinvert) and fed *ad libitum* in the following concentrations: 200 μ g/l thiacloprid, 2000 μ g/l thiacloprid, 1 μ g/l imidacloprid, 10 μ g/l imidacloprid, 10 μ g/l clothianidin, 50 μ g/l clothianidin, 100 μ g/l clothianidin, and 200 μ g/l clothianidin. Control bees received sugar syrup *ad libitum* (60% Apiinvert) containing the same concentration of the solvent (acetone) as the neonicotinoid-treated groups. Worker bees in each cage were exposed to one of these concentrations for 24 h. On the next day, their immunocompetence was evaluated by one of the methods: quantification of hemocytes, antimicrobial activity of the hemolymph, or encapsulation response.

2.2. Hemolymph collection

Worker bees were anesthetized on ice before hemolymph was collected by inserting a microinjection needle (Hartenstein, Würzburg, Germany) into the proximal abdomen. Any fluid which appeared yellow or brown was discarded and excluded from further analysis as this was likely not hemolymph but gastric fluid (Wilson-Rich et al., 2008).

2.3. Total hemocyte count

For total hemocyte counts, 1 μ l of hemolymph was transferred to a PCR-tube (Biozym, Hessisch Oldendorf, Germany) containing 3 μ l PBS (Sigma, pH 7.4) and 1 μ l of DAPI-staining solution (4',6-diamidino-2-phenylindole; 1:100 dilution of an 5 mg/ml DAPI stock solution; lifetechnologies). Immediately after collection, the diluted hemolymph solution was transferred to a Bürker hemocytometer chamber (Carl Roth, Karlsruhe, Germany), where hemocytes were counted (average of five chambers per bee) under a phase contrast/fluorescent microscope (Leica DMIL, Leica camera DFC 420C). To verify the cellular character of the observed structures, the DAPI staining was used as counterstaining of nuclear DNA. On rare occasions, obviously cell-like structures, which did not contain a DAPI-stained nucleus, were observed. These cell-like structures were included in the total hemocyte count. Each experiment was repeated at least three times with 30–45 individuals per treatment group.

2.4. Encapsulation response

We provoked an encapsulation response by inserting a nylon filament into the abdomen, thus mimicking the behavior of *V. destructor* (Cox-Foster and Stehr, 1994; Allander and Schmid-Hempel, 2000; Wilson-Rich et al., 2008). A nylon fishing line (0.2 mm diameter, Nexos, Naila, Germany) was cut with a razor blade into approximately 2 mm long segments and sterilized in 100% pure ethanol (Roth). Honey bees were first anesthetized on ice, and a nylon filament was implanted in the abdomen through the intersegmental membrane between the 3rd and 4th tergum

(Allander and Schmid-Hempel, 2000; Wilson-Rich et al., 2008). This provokes the encapsulation of the filament within the hemocoel as well as the closure of the wound. The strength of the immune reaction was measured by the degree of melanization on the filament. Nylon filaments were implanted in such a way that approximately 1 mm of the filament remained outside the body wall. After implantation, bees were transferred to a 2 ml microcentrifuge tube (Eppendorf) with holes poked through cap and sidewalls. This prevented bees from grooming themselves such that the implant remained in place, while maintaining access to air. A small amount of sugar candy (Apiinvert) was placed inside the cap to provide food during the four-hour incubation period. Afterwards, the nylon filament was removed, fixed in Formaldehyde (4% in PBS, Carl Roth), rinsed three times in PBS, counterstained in DAPI-staining solution and mounted in Aquapolymount (Polysciences). Each experiment was repeated at least three times (11–58 individuals per treatment group).

A segment of each explanted filament was photographed at 100× magnification using a Leica phase contrast/fluorescence microscope and image capturing software (Leica, LASV4.4). Three pictures per explant were taken at different focal depths to quantify a three-dimensional mechanism using two-dimensional tools (Rantala et al., 2000; Rantala and Kortet, 2003; Contreras-Garduño et al., 2006; Kapari et al., 2006; Wilson-Rich et al., 2008). The mean grey value per filament served as a measure of melanization and was quantified for the inserted portion of the filament using image analysis software (Allander and Schmid-Hempel, 2000; Rantala et al., 2000; Wilson-Rich et al., 2008; ImageJ 1.34s, National Institutes of Health, USA). Mean grey values of the inserted portions were subtracted from the mean grey value of an unimplanted filament which served as background value (Allander and Schmid-Hempel, 2000; Rantala et al., 2000; Wilson-Rich et al., 2008).

2.5. Inhibition-zone assay

The worker bees were exposed to neonicotinoids for 48 h. After the first 24 h, the immune system was challenged by the injection of 1 µl of heat-inactivated *Escherichia coli* (grown to OD 0.5). For inhibition-zone assays, 2–3 µl of hemolymph were collected, stored in PCR-tubes and kept frozen at –20 °C until the assay was conducted. Antibacterial test plates (ø 9 cm) were prepared by adding 0.3 ml of live *Micrococcus flavus* bacteria suspension (OD 0.5) to 150 ml of sterile broth medium (48 °C, 1.5 g Agar No. 1, Oxoid; 3.75 g nutrient broth, Applichem). Per test plate, five holes (ø 1 mm) were punched into the medium and 1 µl of hemolymph solution was added to each one. The plates were then incubated at 38 °C overnight and the diameter of inhibition zones were measured with a digital slide caliper. The areas of these zones of inhibition were used as a measure of the strength of antibacterial activity in the hemolymph. Each experiment was repeated at least three times with 30–40 individuals per treatment group.

2.6. Statistical methods

Total hemocyte counts, melanization/mean grey values and mean diameters of inhibition zones were not normally distributed and hence non-parametric statistics were used. Each immunocompetence measure was compared between groups treated with neonicotinoids and untreated control bees using Kruskal–Wallis tests followed by post hoc pairwise comparisons with Mann–Whitney *U* tests. All statistical tests were run with the computer program SPSS for Windows (v. 20).

3. Results

3.1. Total hemocyte counts

Total hemocyte counts (THC) were performed as an indirect measurement of baseline cellular immunocompetence (Wilson et al., 2002; Lee et al., 2006; Wilson-Rich et al., 2008). Exposure to all three neonicotinoids significantly reduced the total hemocyte counts of young adult worker bees (Fig. 1A–C). The median total hemocyte counts were lower in thiacloprid treated worker bees than in control bees (Fig. 1A, K.–W. test, $p < 0.0001$). Untreated control bees displayed a higher hemocyte density than bees treated with 200 µg/l thiacloprid (M.–W. *U* test, $p = 0.003$; control: median = 8200 hemocytes/µl (h/µl), $n = 37$; 200 µg/l thiacloprid: median = 6200 h/µl, $n = 45$), or treated with 2000 µg/l thiacloprid (M.–W. *U* test, $p < 0.0001$, median = 3100 h/µl, $n = 34$). The exposure to thiacloprid reduced the hemocyte density in a dose dependent manner: THC was significantly lower in worker bees exposed to 2000 µg/l than in bees exposed to 200 µg/l thiacloprid (M.–W. *U* test, $p = 0.007$). Total hemocyte counts of bees treated with imidacloprid was lower than in control workers (Fig. 1B, K.–W. test, $p = 0.049$), with control bees displaying a higher hemocyte density than bees treated with 1 µg/l imidacloprid (M.–W. *U* test, $p = 0.035$; control: median = 6835 h/µl, $n = 34$; 1 µg/l imidacloprid: median = 3800 h/µl, $n = 35$), or treated with 10 µg/l imidacloprid (median = 4500 h/µl, $n = 34$, M.–W. *U* test, $p = 0.032$).

However, clothianidin reduced THC only when applied in higher than field relevant concentrations (Fig. 1C; 100 µg/l). Untreated control bees displayed a higher hemocyte density than bees treated with 100 µg/l clothianidin (K.–W. test, $p = 0.029$, M.–W. *U* test, $p = 0.002$; control: median = 6835 h/µl, $n = 34$; 100 µg/l clothianidin: median = 3200 h/µl, $n = 18$), but not than bees treated with 50 µg/l clothianidin (median = 5800 h/µl, $n = 22$), or 10 µg/l clothianidin (median = 4600 h/µl, $n = 34$). The THC was lower in bees exposed to 100 µg/l than in bees exposed to 50 µg/l clothianidin (M.–W. *U* test, $p = 0.041$).

3.2. Encapsulation response

Compared to control bees, the encapsulation response of bees treated with neonicotinoids was significantly reduced (Fig. 2A–C). The encapsulation response was reduced in thiacloprid treated bees (Fig. 2B, K.–W. test, $p = 0.013$; M.–W. *U* test, control vs. 200 µg/l thiacloprid: $p = 0.028$, control vs. 2000 µg/l thiacloprid: $p = 0.004$; control: median = 115.01% grey value (gv), $n = 39$; 200 µg/l thiacloprid: median = 52.93% gv, $n = 38$; 2000 µg/l thiacloprid: median = 58.38% gv, $n = 43$). Encapsulation responses of workers that were treated with imidacloprid were lower than in control bees (Fig. 2C, K.–W. test, $p < 0.0001$).

Control bees showed a stronger melanization reaction than bees treated with imidacloprid (M.–W. *U* test, control vs. 1 µg/l imidacloprid: $p = 0.016$, control vs. 10 µg/l imidacloprid: $p < 0.0001$; control: median = 113.02% gv, $n = 34$; 1 µg/l imidacloprid: median = 68.62% gv, $n = 34$; 10 µg/l imidacloprid: median = 35% gv, $n = 25$).

Encapsulation response was also reduced in clothianidin treated worker bees (Fig. 2D, K.–W. test, $p < 0.001$) with melanization of control bees being significantly higher than of bees fed with 50 µg/l and 200 µg/l, but not of bees exposed to 10 µg/l clothianidin (M.–W. *U* test, control vs. 50 µg/l clothianidin: $p = 0.08$, control vs. 200 µg/l clothianidin: $p < 0.0001$; control: median = 115.01% gv, $n = 58$; 10 µg/l clothianidin: median = 113.05% gv, $n = 27$; 50 µg/l clothianidin: median = 51.05% gv, $n = 23$; 200 µg/l clothianidin: median = 27.21% gv, $n = 63$).

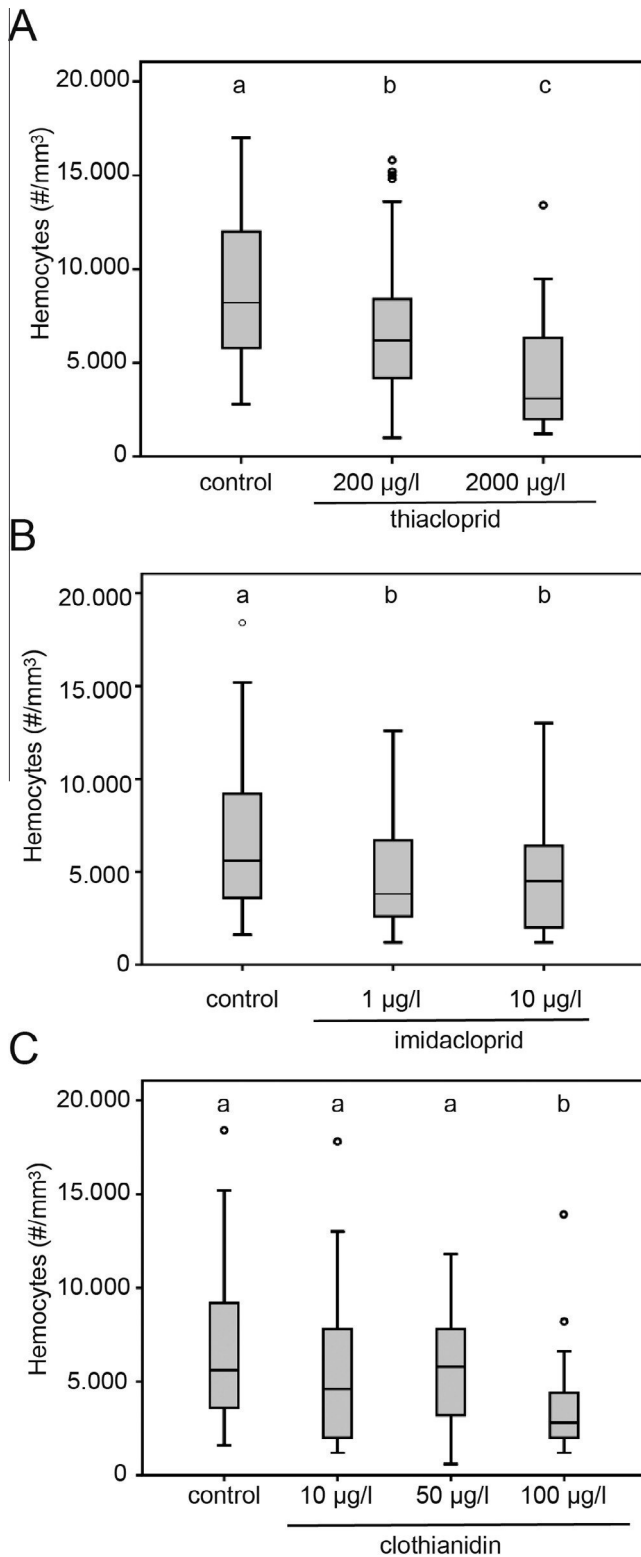


Fig. 1. Cage experiments: exposure to neonicotinoids reduces total hemocyte counts. The 24 h-treatment of newly hatched worker bees with thiacloprid (A; control: $n = 37$, 200 mg/l: $n = 45$, 2000 mg/l: $n = 34$), imidacloprid (B; control: $n = 34$; 1 µg/l: $n = 35$; 10 µg/l: $n = 34$), or clothianidin (C; control: $n = 34$; 10 µg/l: $n = 34$; 50 µg/l: $n = 22$; 100 µg/l: $n = 18$) reduced the total hemocyte counts compared to control bees. Boxes show 1st and 3rd interquartile range with black lines denoting medians. Whiskers encompass 95% of the individuals, beyond which outliers (circles) reside. Treatments with different letters differ significantly from each other.

3.3. Antimicrobial activity of the hemolymph

The antimicrobial activity of the hemolymph, measured as the size of the inhibition zones, was significantly reduced in bees treated with thiacloprid, imidacloprid, or clothianidin compared to control bees (Fig. 3, K–W. test, $p < 0.0001$). The post hoc pairwise analysis revealed that the control group was significantly different to all neonicotinoid treatments and concentrations (M.–W. U test: $p < 0.0001$; control: median = 20.8 mm, $n = 40$; thiacloprid 200 µg/l: median = 18.5 mm, $n = 38$; thiacloprid 2000 µg/l: median = 17.2 mm, $n = 40$; imidacloprid 1 µg/l: median = 18.0 mm, $n = 38$; imidacloprid 10 µg/l: median = 19.2 mm, $n = 40$; clothianidin 10 µg/l: median = 15.8 mm, $n = 37$; clothianidin 200 µg/l: median = 15.6 mm, $n = 30$). For additional statistical analysis see [Supp. Table 1](#).

4. Discussion

In this paper we report effects of three neonicotinoids on general immune parameters of honey bees. As measures of individual immunocompetence we used three different aspects of honey bee immunity, total hemocyte count, encapsulation/wound healing response, and antimicrobial activity of the hemolymph. Our results indicate that all three aspects of immunity are affected by sublethal concentrations of neonicotinoids.

Total hemocyte counts provide an indirect measure of basal cellular immunocompetence. In our cage experiments, exposure to thiacloprid and imidacloprid resulted in significant effects on total hemocyte counts, even in concentrations as low as those reported from pollen samples collected by bees (highest concentrations of thiacloprid: 498 µg/kg and 240 µg/kg, in 2012 and 2013 respectively ([Rosenkranz et al., 2014](#)); imidacloprid 5.7 µg/kg, ([Chauzat, 2006](#)); clothianidin: 2.59 µg/kg, ([Cutler and Scott-Dupree, 2007](#))). Although the lethal dosages of imidacloprid and clothianidin are in the same order of magnitude, exposure to clothianidin reduced total hemocyte counts only at much higher than field-realistic concentrations (100 µg/l). On the other hand, the profound impact of thiacloprid at field realistic concentrations was unexpected, since its acute toxicity is much lower than that of imidacloprid or clothianidin (thiacloprid: oral acute $LD_{50_{48h}} = 17.32$ µg/bee, imidacloprid: oral acute $LD_{50_{48h}} = 0.0037$ µg/bee, clothianidin: oral acute $LD_{50_{48h}} = 0.004$ µg/bee; [University of Hertfordshire, 2013](#)).

The strong effects of imidacloprid on total hemocyte counts in our experiments are in contrast to a previous study reporting no significant effect of exposure to this neonicotinoid ([Alaux et al., 2010](#)). However, in this previous study all experimental bees, including control bees, were already infected with low levels of *Nosema* spp. spores. This may indicate that honey bees bearing an infection react differently to neonicotinoids compared to healthy ones. Further studies are needed to investigate the effect of pesticides on diseased honey bees ([Collison et al., 2015](#)).

Hemocytes are key components of cellular immune defense of insects, since they are responsible for phagocytosis and participate in the encapsulation of pathogens and in the closure of wounds ([Gupta, 1986](#); [Tanada and Kaya, 1993](#); [Alaux et al., 2012](#)). An altered hemocyte density following neonicotinoid exposure could thus influence immune defense and increase a bee's susceptibility towards pathogens. By measuring THC, we only investigated the effect of neonicotinoids on the overall number of free ranging hemocytes, without specifying subclasses in detail ([Van Steenkiste, 1988](#)). It would be interesting to find out whether a differential effect on the subclasses of hemocytes exists. Hemocyte density of worker bees also varies with development ([Schmid et al.,](#)

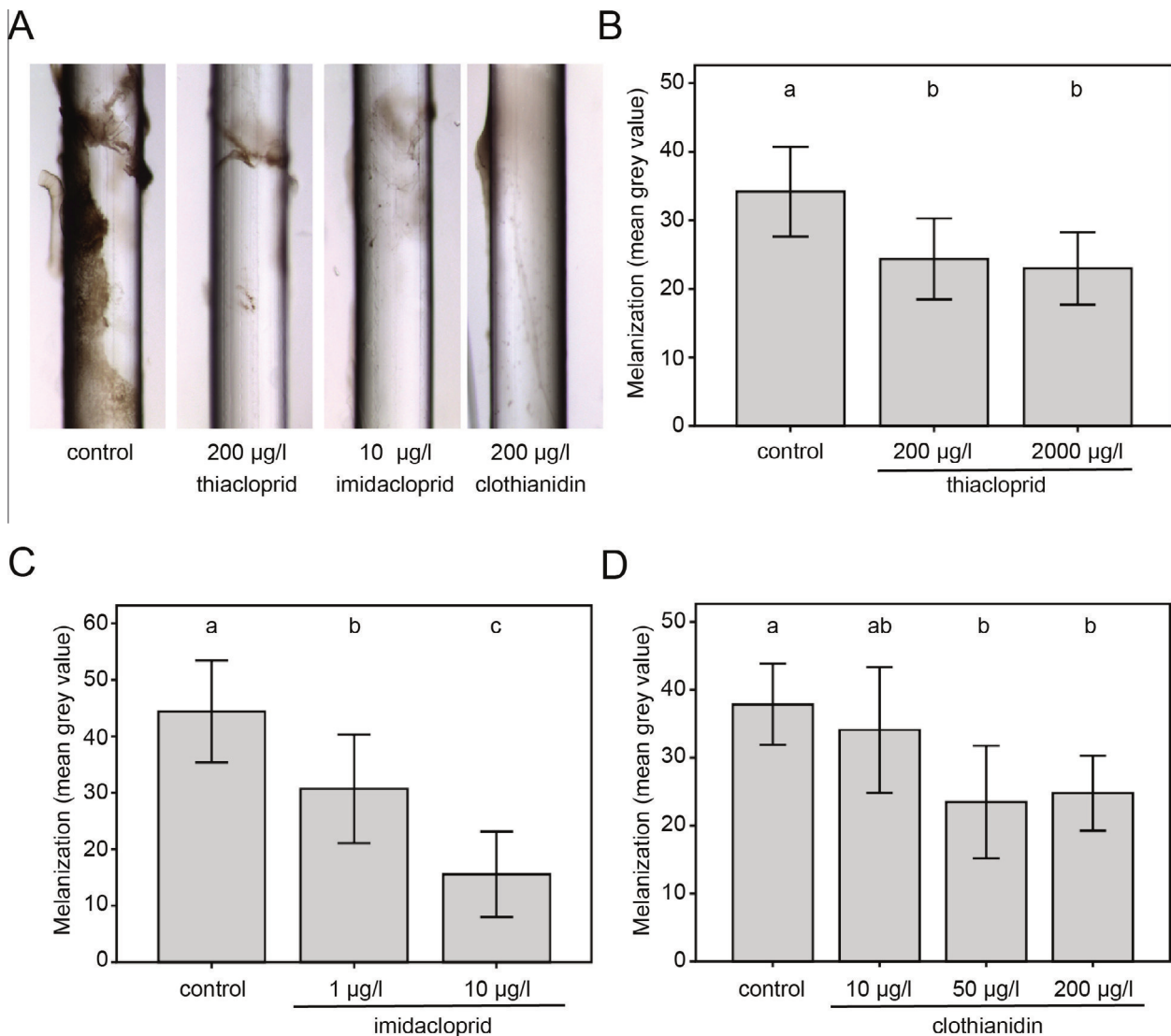


Fig. 2. Encapsulation response is reduced by neonicotinoids. (A) Implanted nylon filaments were encapsulated by dark brown melanin (melanization). (B–D) The 24 h-treatment with neonicotinoids in cage experiments reduced melanization. (B) Thiacloprid (control: $n = 39$; 200 µg/l: $n = 38$; 2000 µg/l: $n = 43$). (C) Imidacloprid (control: $n = 34$; 1 µg/l: $n = 38$; 10 µg/l: $n = 40$). (D) Clothianidin (control: $n = 58$; 10 µg/l: $n = 27$; 50 µg/l: $n = 23$; 200 µg/l: $n = 63$). Error bars denote standard deviations; treatments with different letters differ significantly from each other.

2008; Wilson-Rich et al., 2008), infection status (Gilliam and Shimanuki, 1967), or diet (Szymaś and Jędruszek, 2003). The consequences of altered hemocyte density for the survival and the disease susceptibility of honey bees as a reaction towards external stress factors are not yet fully understood.

One central immune defense mechanism mediated by hemocytes is the encapsulation and melanization of intruding pathogens. The melanization reaction is catalyzed by phenoloxidase, whose precursor (prophenoloxidase) is produced by hemocytes and activated by serine proteases (Evans et al., 2006). In our study, we observed a significantly reduced encapsulation response after treatment with all three neonicotinoids and all tested concentrations, except clothianidin 10 µg/l. A reduced encapsulation response may be caused by (a) reduced numbers of total hemocytes, (b) a reduced proportion of hemocytes that engage in aggregation, (c) a reduced production of prophenoloxidase, or (d) a combination of all three.

A possible molecular link between neonicotinoids and immunity was reported by Di Prisco et al. (2013) showing an immunosuppressive effect of clothianidin by up-regulating an inhibitor of

a member of the gene family NF-κB within the TOLL pathway and promoting the replication of the deformed wing virus in honey bees. Since the NF-κB gene family is involved in central aspects of insect immunity, e.g. the transcriptional regulation of AMP expression (abaecin, hymenoptaecin; Schlüns and Crozier, 2007), as well as in the clotting reaction of hemocytes, and in melanization of foreign objects (Evans et al., 2006), its inhibition could be a possible explanation for our results regarding reduced encapsulation.

The ability to encapsulate a foreign body correlates positively with the resistance to viral infections (Washburn et al., 1996; Trudeau et al., 2001), parasitoids (Carton and David, 1983; Kraaijeveld et al., 2001) and parasites (Doums and Schmid-Hempel, 2000). Wound closure involves similar mechanisms as encapsulation and plays an important role for reducing virus transfer between bees (Chen, 2011). Antimicrobial peptides (AMPs) which combat pathogens are produced by fat body cells and their production is triggered by the TOLL and Imd pathways (Evans et al., 2006; Schlüns and Crozier, 2007). In our cage experiments, we showed that challenge with thiacloprid, imidacloprid, or clothianidin significantly reduced the antimicrobial activity of the

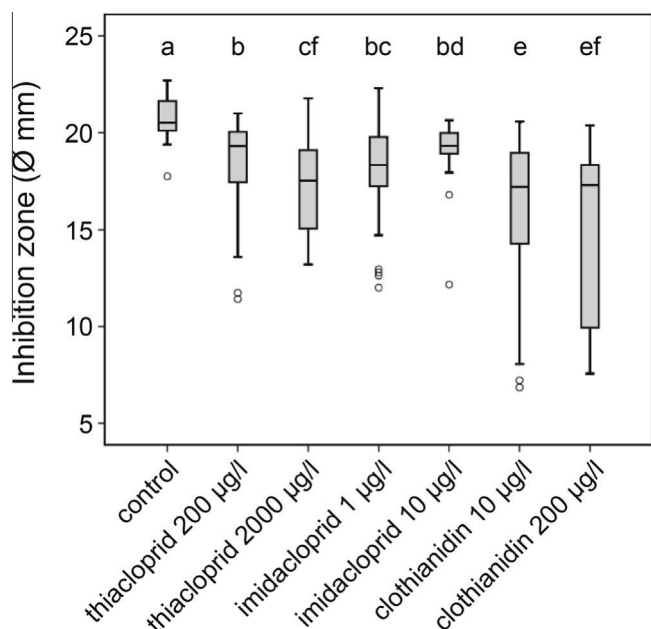


Fig. 3. Neonicotinoid exposure reduced antimicrobial activity of hemolymph. The hemolymph inhibited the growth of grampositive bacteria (*M. flavus*) on agar plates. The 24 h-treatment with thiacloprid (200 µg/l: $n = 38$; 2000 µg/l: $n = 40$), imidacloprid (1 µg/l: $n = 38$; 10 µg/l $n = 40$), or clothianidin (10 µg/l: $n = 37$; 200 µg/l: $n = 30$) reduced the antimicrobial activity of the hemolymph, the diameter of the inhibition zones being smaller than in control bees ($n = 40$). Boxes show 1st and 3rd interquartile range with black lines denoting medians. Whiskers encompass 95% of the individuals, beyond which outliers reside (circles). Significant differences indicated with letters.

hemolymph, together with a decrease of the encapsulation response. These findings may be interpreted as impairment of disease resistance capacities of honey bees in consequence of exposure to neonicotinoids. Our results may be especially important in light of the continuous threat to the health of honey bees by the parasitic varroa mite, in particular due to its central role as a vector of viruses (Genersch et al., 2010; Le Conte et al., 2010; Rosenkranz et al., 2010; Di Prisco et al., 2011; Nazzi et al., 2012). The investigation of additional parameters of immunocompetence, like fat body weight or immune gene expression profiles (Schmehl et al., 2014) and of other developmental stages (larvae and pupae, Gättschenberger et al., 2013) and castes (drones and queens) would add to a comprehensive understanding of the effect of neonicotinoids.

4.1. Conclusion

This study shows a clear impact of neonicotinoids at field realistic concentrations on immunocompetence in adult worker honey bees. However, it remains to be shown whether the observed alterations of the immune system have consequences for the disease resistance capacity of honey bees. Two of the neonicotinoids tested, imidacloprid and clothianidin, are temporarily banned by the EU moratorium until the end of 2015. The third substance, thiacloprid, is frequently being used as spray application on flowering crops and was found in more than 50% of bee bread samples (Genersch et al., 2010; Rosenkranz et al., 2014). Interestingly, thiacloprid, which is classified as “not harmful for bees” due to its much lower acute toxicity, showed similar sublethal effects on immune parameters at a field realistic concentration. Our findings add a significant piece of information to the ongoing discussion of the role of neonicotinoid insecticides in colony losses. The results we report clearly indicate the need for more detailed laboratory and long-term field studies, aiming to assess how insecticides interfere with pathogen propagation and disease susceptibility.

Conflict of interest

The authors have no financial and personal relationships that might bias or be seen to bias their work.

Acknowledgments

We gratefully thank A. von Gall and S. Backhaus for technical support, Ch. Fingerhut, U. Hubbe, K. Petzold-Treibert, D. Schuller, V. Strasser, and M. Gabel for assistance in beekeeping and all team members of the Bee Institute Kirchhain for support and fruitful discussions. This research was supported by the EU and Land Hessen, “Förderung von Maßnahmen zur Verbesserung der Erzeugung und Vermarktung von Honig in Hessen”.

Appendix A. Supplementary data

Supplementary data associated with this article can be found, in the online version, at <http://dx.doi.org/10.1016/j.jinsphys.2016.01.001>.

References

- Adamo, S.A., 2004. How should behavioural ecologists interpret measurements of immunity? *Anim. Behav.* 68, 1443–1449.
- Aizen, M.A., Harder, L.D., 2009. The global stock of domesticated honey bees is growing slower than agricultural demand for pollination. *Curr. Biol.* 19, 915–918.
- Alaux, C., Brunet, J.-L., Dussaubat, C., Mondet, F., Tchamitchan, S., Cousin, M., Brillard, J., Baldy, A., Belzunces, L.P., Le Conte, Y., 2010. Interactions between *Nosema* microspores and a neonicotinoid weaken honeybees (*Apis mellifera*). *Environ. Microbiol.* 12, 774–782.
- Alaux, C., Kemper, N., Kretzschmar, A., Le Conte, Y., 2012. Brain, physiological and behavioral modulation induced by immune stimulation in honeybees (*Apis mellifera*): a potential mediator of social immunity? *Brain Behav. Immun.* 26, 1057–1060.
- Allander, K., Schmid-Hempel, P., 2000. Immune defence reaction in bumble-bee workers after a previous challenge and parasitic coinfection. *Funct. Ecol.* 14, 711–717.
- Amiri, E., Meixner, M., Büchler, R., Kryger, P., 2014. Chronic bee paralysis virus in honeybee queens: evaluating susceptibility and infection routes. *Viruses* 6, 1188–1201.
- Anderson, D.L., Trueman, J.W., 2000. *Varroa jacobsoni* (Acari: Varroidae) is more than one species. *Exp. Appl. Acarol.* 24, 165–189.
- Aufauvre, J., Biron, D.G., Vidau, C., Fontbonne, R., Roudel, M., Diogon, M., Vignes, B., Belzunces, L.P., Delbac, F., Blot, N., 2012. Parasite–insecticide interactions: a case study of *Nosema ceranae* and fipronil synergy on honeybee. *Sci. Rep.*, 2.
- Bascompte, J., Jordano, P., Olesen, J.M., 2006. Asymmetric coevolutionary networks facilitate biodiversity maintenance. *Science* 312, 431–433.
- Biesmeijer, J.C., Roberts, S.P.M., Reemer, M., Ohlemueller, R., Edwards, M., Peeters, T., Schaffers, A.P., Potts, S.G., Kleukers, R., Thomas, C.D., Settele, J., Kunin, W.E., 2006. Parallel declines in pollinators and insect-pollinated plants in Britain and the Netherlands. *Science* 313, 351–354.
- Blacquière, T., Smaghe, G., van Gestel, C.A.M., Mommaerts, V., 2012. Neonicotinoids in bees: a review on concentrations, side-effects and risk assessment. *Ecotoxicology* 21, 973–992.
- Brodtschneider, R., Crailsheim, K., 2010. Nutrition and health in honey bees. *Apidologie* 41, 278–294.
- Cameron, S.A., Lozier, J.D., Strange, J.P., Koch, J.B., Cordes, N., Solter, L.F., Griswold, T. L., 2011. Patterns of widespread decline in North American bumble bees. *Proc. Natl. Acad. Sci. U.S.A.* 108, 662–667.
- Carton, Y., David, J.R., 1983. Reduction of fitness in *Drosophila* adults surviving parasitization by a cynipid wasp. *Experientia* 39, 231–233.
- Chauzat, M., 2006. A survey of pesticide residues in pollen loads collected by honey bees in France. *J. Econ. Entomol.* 99, 253–262.
- Chen, Y., 2011. Viruses and viral diseases of the honey bee, *Apis mellifera*. In: Liu, T.-X., Kang, L. (Eds.), *Recent Advances in Entomological Research: From Molecular Biology to Pest Management*. Springer–Higher Education Press, China, pp. 105–120.
- Collison, E., Hird, H., Cresswell, J., Tyler, C., 2015. Interactive effects of pesticide exposure and pathogen infection on bee health – a critical analysis. *Biol. Rev. Camb. Philos. Soc.* 6. <http://dx.doi.org/10.1111/brv.12206>.
- Contreras-Garduño, J., Canales-Lazcano, J., Córdoba-Aguilar, A., 2006. Wing pigmentation, immune ability, fat reserves and territorial status in males of the rubyspot damselfly, *Hetaerina americana*. *J. Ethol.* 24, 165–173.
- Cox-Foster, D.L., Stehr, J.E., 1994. Induction and localization of FAD-glucose dehydrogenase (GLD) during encapsulation of abiotic implants in *Manduca sexta* larvae. *J. Insect Physiol.* 40, 235–249.

- Cresswell, J.E., 2011. A meta-analysis of experiments testing the effects of a neonicotinoid insecticide (imidacloprid) on honey bees. *Ecotoxicology* 20, 149–157.
- Cutler, G.C., Scott-Dupree, C.D., 2007. Exposure to clothianidin seed-treated canola has no long-term impact on honey bees. *J. Econ. Entomol.* 100, 765–772.
- Decourtye, A., Armengaud, C., Renou, M., Devillers, J., Cluzeau, S., Gauthier, M., Pham-Deleugue, M.H., 2004. Imidacloprid impairs memory and brain metabolism in the honeybee (*Apis mellifera* L.). *Pestic. Biochem. Physiol.* 78, 83–92.
- Desneux, N., Decourtye, A., Delpuech, J.-M., 2007. The sublethal effects of pesticides on beneficial arthropods. *Annu. Rev. Entomol.* 52, 81–106.
- Di Pasquale, G., Salignon, M., Le Conte, Y., Belzunces, L.P., Decourtye, A., Kretzschmar, A., Suchail, S., Brunet, J.-L., Alaux, C., 2013. Influence of pollen nutrition on honey bee health: do pollen quality and diversity matter? *PLoS ONE* 8, e72016.
- Di Prisco, G., Zhang, X., Pennacchio, F., Caprio, E., Li, J., Evans, J.D., DeGrandi-Hoffman, G., Hamilton, M., Chen, Y.P., 2011. Dynamics of persistent and acute deformed wing virus infections in honey bees, *Apis mellifera*. *Viruses* 3, 2425–2441. <http://dx.doi.org/10.3390/v3122425>.
- Di Prisco, G., Cavaliere, V., Annoscia, D., Varricchio, P., Caprio, E., Nazzi, F., Gargiulo, G., Pennacchio, F., 2013. Neonicotinoid clothianidin adversely affects insect immunity and promotes replication of a viral pathogen in honey bees. *Proc. Natl. Acad. Sci. U.S.A.* 110, 18466–18471.
- Doublet, V., Labarussias, M., de Miranda, J.R., Moritz, R.F.A., Paxton, R.J., 2015. Bees under stress: sublethal doses of a neonicotinoid pesticide and pathogens interact to elevate honey bee mortality across the life cycle. *Environ. Microbiol.* 17, 969–983.
- Doums, C., Schmid-Hempel, P., 2000. Immunocompetence in workers of a social insect, *Bombus terrestris* L., in relation to foraging activity and parasitic infection. *Can. J. Zool.* 78, 1060–1066.
- EASAC, European Academies Science Advisory Council, 2015. Policy report 26: ecosystem services, agriculture and neonicotinoids.
- EFSA, European Food Safety Authority, 2013a. Conclusion on the peer review of the pesticide risk assessment for bees for the active substance clothianidin. *EFSA J.* 11, 3066.
- EFSA, European Food Safety Authority, 2013b. Conclusion on the peer review of the pesticide risk assessment for bees for the active substance imidacloprid. *EFSA J.* 11, 3068.
- EFSA, European Food Safety Authority, 2013c. Conclusion on the peer review of the pesticide risk assessment for bees for the active substance thiamethoxam. *EFSA J.* 11, 3067.
- EFSA, European Food Safety Authority, 2014. Towards an integrated environmental risk assessment of multiple stressors on bees: review of research projects in Europe, knowledge gaps and recommendations. *EFSA J.* 12, 3594.
- Elbert, A., Haas, M., Springer, B., Thielert, W., Nauen, R., 2008. Applied aspects of neonicotinoid uses in crop protection. *Pest Manag. Sci.* 64, 1099–1105.
- European Commission, 2013. Bee health: EU-wide restrictions on pesticide use to enter into force. European Commission, Brussels.
- Evans, J.D., Aronstein, K., Chen, Y.P., Hetru, C., Imler, J.L., Jiang, H., Kanost, M., Thompson, G.J., Zou, Z., Hultmark, D., 2006. Immune pathways and defence mechanisms in honey bees *Apis mellifera*. *Insect Mol. Biol.* 15, 645–656.
- Frias, B., Barbosa, C., Barbosa, C.D., Lourenço, A.P., 2015. Pollen nutrition in honey bees (*Apis mellifera*): impact on adult health. *Apidologie*. <http://dx.doi.org/10.1007/s13592-015-0373-y>.
- Fausser-Misslin, A., Sadd, B.M., Neumann, P., Sandrock, C., 2014. Influence of combined pesticide and parasite exposure on bumblebee colony traits in the laboratory. *J. Appl. Ecol.* 51, 450–459.
- Fontaine, C., Dajoz, I., Meriguet, J., Loreau, M., 2006. Functional diversity of plant-pollinator interaction webs enhances the persistence of plant communities. *PLoS Biol.* 4, 129–135.
- Gätschenberger, H., Azzami, K., Tautz, J., Beier, H., 2013. Antibacterial immune competence of honey bees (*Apis mellifera*) is adapted to different life stages and environmental risks. *PLoS ONE* 8, e66415.
- Genersch, E., von der Ohe, W., Kaatz, H., Schroeder, A., Otten, C., Buechler, R., Berg, S., Ritter, W., Muehlen, W., Gisder, S., Meixner, M., Liebig, G., Rosenkranz, P., 2010. The German bee monitoring project: a long term study to understand periodically high winter losses of honey bee colonies. *Apidologie* 41, 332–352.
- Gilliam, M., Shimanuki, H., 1967. *In vitro* phagocytosis of *Nosema apis* spores by honey-bee hemocytes. *J. Invertebr. Pathol.* 9, 387–389.
- Goulson, D., 2013. REVIEW: an overview of the environmental risks posed by neonicotinoid insecticides. *J. Appl. Ecol.* 50, 977–987.
- Goulson, D., Nicholls, E., Botias, C., Rotheray, E.L., 2015. Bee declines driven by combined stress from parasites, pesticides, and lack of flowers. *Science* 347, 1255957.
- Gregory, P.G., Evans, J.D., Rinderer, T., de Guzman, L., 2005. Conditional immune-gene suppression of honeybees parasitized by Varroa mites. *J. Insect Sci.*, 5
- Gross, M., 2013. EU ban puts spotlight on complex effects of neonicotinoids. *Curr. Biol.* 23, R462–R464.
- Gupta, A.P., 1986. Hemocytic and Humoral Immunity in Arthropods. John Wiley and Sons, Chichester, 536.
- Han, P., Niu, C.-Y., Lei, C.-L., Cui, J.-J., Desneux, N., 2010. Quantification of toxins in a Cry1Ac+CPt cotton cultivar and its potential effects on the honey bee *Apis mellifera* L. *Ecotoxicology* 19, 1452–1459.
- Henry, M., Beguin, M., Requier, F., Rollin, O., Odoux, J.-F., Aupinel, P., Aptel, J., Tchamitchian, S., Decourtye, A., 2012. A common pesticide decreases foraging success and survival in honey bees. *Science* 336, 348–350.
- James, R.R., Xu, J., 2012. Mechanisms by which pesticides affect insect immunity. *J. Invertebr. Pathol.* 109, 175–182.
- Jeschke, P., Nauen, R., Schindler, M., Elbert, A., 2011. Overview of the status and global strategy for neonicotinoids. *J. Agric. Food Chem.* 59, 2897–2908.
- Kapari, L., Haukioja, E., Rantala, M.J., Ruuhola, T., 2006. Defoliating insect immune defense interacts with induced plant defense during a population outbreak. *Ecology* 87, 291–296.
- Keil, D., Luebke, R.W., Pruett, S.B., 2001. Quantifying the relationship between multiple immunological parameters and host resistance: probing the limits of reductionism. *J. Immunol.* 167, 4543–4552.
- Klein, A.-M., Vaissiere, B.E., Cane, J.H., Steffan-Dewenter, I., Cunningham, S.A., Kremen, C., Tschamtker, T., 2007. Importance of pollinators in changing landscapes for world crops. *Proc. R. Soc. B-Biol. Sci.* 274, 303–313.
- Kraaijeveld, A.R., Hutcheson, K.A., Limentani, E.C., Godfray, H.C.J., 2001. Costs of counterdefenses to host resistance in a parasitoid of *Drosophila*. *Evolution* 55, 1815–1821.
- Le Conte, Y., Ellis, M., Ritter, W., 2010. *Varroa* mites and honey bee health: can *Varroa* explain part of the colony losses? *Apidologie* 41, 353–363.
- Lee, K.P., Cory, J.S., Wilson, K., Raubenheimer, D., Simpson, S.J., 2006. Flexible diet choice offsets protein costs of pathogen resistance in a caterpillar. *Proc. R. Soc. B-Biol. Sci.* 273, 823–829.
- Luster, M.I., Portier, C., Pait, D.G., Rosenthal, G.J., Germolec, D.R., Corsini, E., Blaylock, B.L., Pollock, P., Kouchi, Y., Craig, W., White, K.L., Munson, A.E., Comment, C.E., 1993. Risk assessment in immunotoxicology. 2. Relationships between immune and host-resistance tests. *Fundam. Appl. Toxicol.* 21, 71–82.
- Mao, W., Schuler, M.A., Berenbaum, M.R., 2013. Honey constituents up-regulate detoxification and immunity genes in the western honey bee *Apis mellifera*. *Proc. Natl. Acad. Sci. U.S.A.* 110 (22), 8842–8846. <http://dx.doi.org/10.1073/pnas.1303884110>.
- Matsuda, K., Buckingham, S.D., Kleier, D., Rauh, J.J., Grauso, M., Sattelle, D.B., 2001. Neonicotinoids: insecticides acting on insect nicotinic acetylcholine receptors. *Trends Pharmacol. Sci.* 22, 573–580.
- Mullin, C.A., Frazier, M., Frazier, J.L., Ashcraft, S., Simonds, R., vanEngelsdorp, D., Pettis, J.S., 2010. High levels of miticides and systemic agrochemicals in North American beehives: implications for honey bee health. *PLoS ONE* 5, e9754.
- National Research Council, 2007. Status of Pollinators in North America. National Academies Press, Washington, DC.
- Nazzi, F., Brown, S.P., Annoscia, D., Del Piccolo, F., Di Prisco, G., Varricchio, P., Della Vedova, G., Cattonaro, F., Caprio, E., Pennacchio, F., 2012. Synergistic parasite-pathogen interactions mediated by host immunity can drive the collapse of honeybee colonies. *PLoS Pathog.* 8, e1002735.
- Negri, P., Maggi, M.D., Ramirez, L., De Feudis, L., Szwarski, N., Quintana, S., Eguaras, M.J., Lorenzo Lamattina, L., 2015. Abscisic acid enhances the immune response in *Apis mellifera* and contributes to the colony fitness. *Apic. Res.* 49, 542–557.
- Neumann, P., Carreck, N.L., 2010. Honey bee colony losses. *J. Apic. Res.* 49, 1–6.
- Pettis, J.S., vanEngelsdorp, D., Johnson, J., Dively, G., 2012. Pesticide exposure in honey bees results in increased levels of the gut pathogen *Nosema*. *Naturwissenschaften* 99, 153–158.
- Pisa, L.W., Amaral-Rogers, V., Belzunces, L.P., Bonmatin, J.M., Downs, C.A., Goulson, D., Kreuzweiser, D.P., Krupke, C., Liess, M., McField, M., Morrissey, C.A., Noome, D.A., Settele, J., Simon-Delso, N., Stark, J.D., Van der Sluijs, J.P., Van Dyck, H., Wiemers, M., 2015. Effects of neonicotinoids and fipronil on non-target invertebrates. *Environ. Sci. Pollut. Res.* 22, 68–102.
- Pistorius, J., Bischoff, G., Heimbach, U., Stähler, M., 2009. Bee poisoning incidents in Germany in spring 2008 caused abrasion of active substance from treated seeds during sowing of maize. In: Ooman, P.A., Thompsons, H.M. (Eds.), Hazards of Pesticides to Bees. 10th International Symposium of the ICP-BR Bee Protection Group (Julius-Kühn-Archiv 423), Julius Kühn-Institut, Bundesforschungsanstalt für Kulturpflanzen, Quedlinburg, 118–126.
- Potts, S.G., Biesmeijer, J.C., Kremen, C., Neumann, P., Schweiger, O., Kunin, W.E., 2010. Global pollinator declines: trends, impacts and drivers. *Trends Ecol. Evol.* 25, 345–353.
- Potts, S.G., Roberts, S.P.M., Dean, R., Marris, G., Brown, M.A., Jones, R., Neumann, P., Settele, J., 2010. Declines of managed honey bees and beekeepers in Europe. *J. Apic. Res.* 49, 15–22.
- Rantala, M.J., Koskimäki, J., Taskinen, J., Tynkynen, K., Suhonen, J., 2000. Immunocompetence, developmental stability and wingspot size in the damselfly *Calopteryx splendens* L. *Proc. R. Soc. B-Biol. Sci.* 267, 2453–2457.
- Rantala, M.J., Kortet, R., 2003. Courtship song and immune function in the field cricket *Gryllus bimaculatus*. *Biol. J. Linn. Soc.* 79, 503–510.
- Rantala, M.J., Roff, D.A., 2005. An analysis of trade-offs in immune function, body size and development time in the Mediterranean Field Cricket, *Gryllus bimaculatus*. *Funct. Ecol.* 19, 323–330.
- Ratnieks, F.L.W., Carreck, N.L., 2010. Clarity on honey bee collapse? *Science* 327, 152–153.
- Rosenkranz, P., Aumeier, P., Ziegelmann, B., 2010. Biology and control of *Varroa destructor*. *J. Invertebr. Pathol.* 103, 596–119.
- Rosenkranz, P., von der Ohe, W., Moritz, R.F.A., Genersch, E., Buechler, R., Berg, S. and Otten, C. (2014) Schlussbericht: Deutsches Bienenmonitoring – “DeBiMo”, 2011–2013.
- Sandrock, C., Tanadini, M., Tanadini, L.G., Fausser-Misslin, A., Potts, S.G., Neumann, P., 2014. Impact of chronic neonicotinoid exposure on honeybee colony performance and queen supersedure. *PLoS ONE* 9, e103592.
- Schlüns, H., Crozier, R.H., 2007. Relish regulates expression of antimicrobial peptide genes in the honeybee, *Apis mellifera*, shown by RNA interference. *Insect Mol. Biol.* 16, 753–759.

- Schmehl, D.R., Teal, P.E., Frazier, J.L., Grozinger, C.M., 2014. Genomic analysis of the interaction between pesticide exposure and nutrition in honey bees (*Apis mellifera*). *J. Insect Physiol.* 71, 177–190.
- Schmid, M.R., Brockmann, A., Pirk, C.W.W., Stanley, D.W., Tautz, J., 2008. Adult honeybees (*Apis mellifera* L.) abandon hemocytic, but not phenoloxidase-based immunity. *J. Insect Physiol.* 54, 439–444.
- Szymaś, B., Jędruszek, A., 2003. The influence of different diets on haemocytes of adult worker honey bees, *Apis mellifera*. *Apidologie* 34, 97–102.
- Tanada, Y., Kaya, H.K., 1993. *Insect Pathology*. Academic Press, San Diego, USA.
- Tomizawa, M., Casida, J.E., 2005. Neonicotinoid insecticide toxicology: mechanisms of selective action. *Annu. Rev. Pharmacol. Toxicol.* 45, 247–268.
- Trudeau, D., Washburn, J.O., Volkman, L.E., 2001. Central role of hemocytes in *Autographa californica* M nucleopolyhedrovirus pathogenesis in *Heliothis virescens* and *Helicoverpa zea*. *J. Virol.* 75, 996–1003.
- University of Hertfordshire, 2013. The Pesticide Properties DataBase (PPDB) developed by the Agriculture & Environment Research Unit (AERU), University of Hertfordshire, 2006–2013.
- Vanbergen, A.J., Insect Pollinators Initiative, 2013. Threats to an ecosystem service: pressures on pollinators. *Front. Ecol. Environ.* 11, 251–259.
- van der Sluijs, J.P., Simon-Delso, N., Goulson, D., Maxim, L., Bonmatin, J.-M., Belzunces, L.P., 2013. Neonicotinoids, bee disorders and the sustainability of pollinator services. *Curr. Opin. Environ. Sustainability* 5, 293–305.
- vanEngelsdorp, D., Hayes Jr., J., Underwood, R.M., Pettis, J., 2008. A survey of honey bee colony losses in the US, fall 2007 to spring 2008. *PLoS ONE* 3, e4071.
- Van Steenkiste, D., 1988. De hemocyten van de honingbij (*Apis mellifera* L.): typologie, bloedbeeld en cellulair verdedigingsreacties, Ph.D. thesis, University of Ghent.
- Washburn, J.O., Kirkpatrick, B.A., Volkman, L.E., 1996. Insect protection against viruses. *Nature* 383, 767–767.
- Williams, G.R., Alaux, C., Costa, C., Csaki, T., Doublet, V., Eisenhardt, D., Fries, I., Kuhn, R., McMahon, D.P., Medrzycki, P., Murray, T.E., Natsopoulou, M.E., Neumann, P., Oliver, R., Paxton, R.J., Pernal, S.F., Shutler, D., Tanner, G., van der Steen, J.J.M., Brodschneider, R., 2013. Standard methods for maintaining adult *Apis mellifera* in cages under in vitro laboratory conditions. In: Dietemann, V., Ellis J.D., Neumann, P. (Eds.), *The COLOSS BEEBOOK*, Vol. 1. Standard methods for *Apis mellifera* research. *Journal of Apicultural Research*, 52.
- Wilson, K., Thomas, M.B., Blanford, S., Doggett, M., Simpson, S.J., Moore, S.L., 2002. Coping with crowds: density-dependent disease resistance in desert locusts. *Proc. Natl. Acad. Sci.* 99, 5471–5475.
- Wilson-Rich, N., Dres, S.T., Starks, P.T., 2008. The ontogeny of immunity: development of innate immune strength in the honey bee (*Apis mellifera*). *J. Insect Physiol.* 54, 1392–1399.
- Yang, X.L., Cox-Foster, D.L., 2005. Impact of an ectoparasite on the immunity and pathology of an invertebrate: evidence for host immunosuppression and viral amplification. *Proc. Natl. Acad. Sci. U.S.A.* 102, 7470–7475.
- Yang, E.C., Chuang, Y.C., Chen, Y.L., Chang, L.H., 2008. Abnormal foraging behavior induced by sublethal dosage of imidacloprid in the honey bee (Hymenoptera: Apidae). *J. Econ. Entomol.* 101, 1743–1748.
- Yang, E.-C., Chang, H.-C., Wu, W.-Y., Chen, Y.-W., 2012. Impaired olfactory associative behavior of honeybee workers due to contamination of imidacloprid in the larval stage. *PLoS ONE* 7, e49472.

SCIENTIFIC REPORTS



OPEN

Immunosuppression in Honeybee Queens by the Neonicotinoids Thiacloprid and Clothianidin

Anneli Brandt¹, Katharina Grikscheit², Reinhold Siede¹, Robert Grosse², Marina Doris Meixner ¹ & Ralph Büchler¹

Queen health is crucial to colony survival of honeybees, since reproduction and colony growth rely solely on the queen. Queen failure is considered a relevant cause of colony losses, yet few data exist concerning effects of environmental stressors on queens. Here we demonstrate for the first time that exposure to field-realistic concentrations of neonicotinoid pesticides can severely affect the immunocompetence of queens of western honeybees (*Apis mellifera* L.). In young queens exposed to thiacloprid (200 µg/l or 2000 µg/l) or clothianidin (10 µg/l or 50 µg/l), the total hemocyte number and the proportion of active, differentiated hemocytes was significantly reduced. Moreover, functional aspects of the immune defence namely the wound healing/melanisation response, as well as the antimicrobial activity of the hemolymph were impaired. Our results demonstrate that neonicotinoid insecticides can negatively affect the immunocompetence of queens, possibly leading to an impaired disease resistance capacity.

Honeybees are highly eusocial insects that build colonies of several thousand individuals which contain only one fertile female, the queen¹. This queen is responsible for all egg laying and brood production within the colony; consequently, her integrity and health is crucial for the colony's performance and survival, and any impairment can result in adverse effects on colony fitness. In the worst case, if the workers are unable to replace a failing queen, the colony will perish²⁻⁴. Recently, queen failure has been proposed as an important driver of honeybee colony mortality^{2,4-6}. While the natural lifespan of a honeybee queen is two to four years¹, recent reports from the U.S.A. show high rates of early queen failure, with 50% or more being replaced in colonies within the first six months^{3,3}. This extremely high rate of queen failure coincides with high mortality rates of colonies in the U.S.A., where in some years more than 50% of colonies are dying^{2,7}.

Several stress factors are suspected to negatively affect survival of honeybee colonies. Parasites and pathogens are among the main factors⁴, but diet quantity, quality, and diversity⁸⁻¹⁰ as well as exposure to pesticides may also affect colony survival^{5,6,11}. In particular, the widespread application of neonicotinoid insecticides¹²⁻¹⁸, has been suspected to represent a major threat to honeybee survival^{11,19-22}. Neonicotinoids are neurotoxins that act as agonists of the nicotinic acetylcholine receptor. They disrupt the neuronal cholinergic signal transduction, leading to abnormal behaviour, immobility and death of target pests^{12,23,24}. Frequently, non-target insects like honeybees also come into contact with these systemic insecticides²¹. Exposure of bees to neonicotinoids is mostly through ingestion of residues in the pollen and nectar of contaminated plants^{11,19}. These pesticide residues are taken by the forager bees to their colonies and remain stored in bee bread or honey until they are fed to larvae, workers, drones, or the queen^{4,25}.

The study of lethal and sub-lethal effects of neonicotinoid pesticides on social bees has largely focused on worker bees and, to a lesser extent, on overall colony function^{18,25-28}. Although reports of colony losses due to high rates of queen failure exist, only few studies address direct or indirect physiological effects in queens caused by pesticide exposure^{2,5,29,30}. Most studies focused on only three neonicotinoid insecticides, clothianidin, imidacloprid, and thiamethoxam, which are currently subject to a moratorium in the European Union³¹. Here, we also include thiacloprid, a cyano-substituted neonicotinoid which is considered as non-harmful for bees due to its much lower acute toxicity compared to other neonicotinoids. Thiacloprid is widely used in agriculture, for instance as spray application in fruit trees or directly into flowering oil seed rape during bee flight. It is the most

¹LLH Bee Institute, Erlenstr. 9, 35274, Kirchhain, Germany. ²Institute of Pharmacology, Biochemical-Pharmacological Center (BPC), University of Marburg, 35032, Marburg, Germany. Correspondence and requests for materials should be addressed to A.B. (email: anneli.brandt@llh.hessen.de)

abundant insecticide in beebread samples and has been detected in more than 60% of the samples analysed in the German Bee Monitoring Project³².

A strong immune defence is vital for honeybee health and colony survival. The strength of the individual immune defence depends on internal factors such as the nutritional state, the age, and the caste affiliation of the exposed individuals^{10, 33–37}. In addition, the invasive ectoparasite *Varroa destructor*³⁸ impairs the immune defence of honeybees by reducing expression of immune-relevant genes and boosting viral replication, thereby affecting lifespan and disease resistance^{11, 39–41}. The individual immunocompetence can also be weakened by environmental factors like pesticides that may render honeybees more vulnerable to parasites and pathogens^{41–44}.

The exposure to pesticides is often associated with an increased pathogenic load, including the prevalent gut-parasite *Nosema* spp. and viruses typically associated with *V. destructor*, such as deformed wing virus (DWV)^{8, 11, 43, 45, 46}. Neonicotinoids have been shown to affect the individual immunocompetence of honeybee workers. They negatively modulate NF- κ B immune signalling and promote the replication of DWV⁴⁴. Neonicotinoids have been shown to reduce hemocyte density as well as functional aspects of insect immunity as the melanisation of foreign objects, and the antimicrobial activity of the hemolymph⁴⁷ in worker bees. However, there is only little information available about the individual immunity of honeybee queens. In queens, phenoloxidase (PO) enzyme levels continuously increase with age and reach levels twice as high as those found in workers⁴⁸. Gättschenberger and colleagues⁴⁹ examined the antimicrobial defence systems of queens and found that reactions of young queens to bacterial immune challenges resemble those of worker bees. In this study we examine the effects of pesticide exposure on young queens. Our main question is whether general immune defence mechanisms are affected by sublethal concentrations of the neonicotinoids thiacloprid or clothianidin. Since disease resistance is difficult to measure directly³³, we selected established functional parameters of immunity to analyse honeybee immunocompetence, namely total and differential hemocyte counts, melanisation response, and antimicrobial activity of the hemolymph.

Results

Sublethal effects and exposure. To date, acute toxicity tests are solely performed with worker bees^{5, 25}. To determine whether the dosages of neonicotinoids used in the immune assays are indeed sublethal to queens, the number of dead queens was recorded after seven days of exposure. We found no significant difference between the treatment groups regarding the survival of the queens (Supplementary Fig. S1, Supplementary Table S2). Thiacloprid exposure had no lethal effect on worker bees. However, there was a significant effect of clothianidin on worker bee mortality (χ^2 -test; $p = 0.009$). Hence, the highest concentration of clothianidin (200 μ g/l) was excluded from immune tests.

To estimate the exposure level to neonicotinoids, the food consumption was measured. We found no significant difference between the treatment groups regarding the consumption of sugar solution or pollen (Supplementary Fig. S2, Supplementary Table S2). Moreover, the behaviour of the bees was observed regularly. When the food was changed, the queens were surrounded by attending workers and fed via trophallaxis. During these short observations, we never saw a queen directly feeding at the syringe containing the spiked sugar solution.

The wellbeing of a queen depends on the care and the adequate supply with food (royal jelly and honey¹) by the attending worker bees. However, neonicotinoids have been shown to reduce the size of the hypopharyngeal gland (HPG) of nurse bees. To examine, whether thiacloprid or clothianidin affected the HPG size of the attending worker bees in our experiments, the acinus diameter of age defined worker bees were measured. Interestingly, no significant difference was found in the HPG size of worker bees after seven days of exposure in a cage, attending to a queen (Supplementary Fig. S3, Supplementary Table S2; KWT, $p > 0.05$).

Total and differential hemocyte counts. Exposure to relevant concentrations of both neonicotinoids significantly reduced the total hemocyte counts of young queens (Fig. 1a,b). The median total hemocyte counts of thiacloprid treated queens were lower than those of control queens (Fig. 1a, Kruskal–Wallis test (KWT), $p = 0.011$). Untreated control queens displayed a higher hemocyte density than queens treated with 200 μ g/l thiacloprid (59% of control value; Supplementary Table S1; MWU, $p = 0.022$; control: median = 4250 hemocytes/ μ l (h/ μ l), $n = 19$; 200 μ g/l thiacloprid: median = 2500 h/ μ l, $n = 16$), or treated with 2000 μ g/l thiacloprid (47% of control value; MWU, $p = 0.024$, median = 2000 h/ μ l, $n = 19$).

Total hemocyte counts of queens treated with clothianidin were lower than in control queens (Fig. 1b, KWT, $p = 0.0005$), with control queens displaying a higher hemocyte density than queens treated with 10 μ g/l clothianidin (53% of control value; MWU, $p = 0.015$; control: median = 4250 h/ μ l, $n = 19$; 10 μ g/l clothianidin: median = 2250 h/ μ l, $n = 15$), or treated with 50 μ g/l clothianidin (47% of control value; median = 2000 h/ μ l, $n = 14$, MWU, $p = 0.014$).

To evaluate changes in the composition of subclasses in the hemocyte population, the cells were classified using the morphological characteristics described by Negri *et al.*^{36, 50}, supported by phalloidin staining of the actin cytoskeleton and DAPI staining of the nuclear DNA (Fig. 2a–d). W1-like hemocytes⁵⁰ contained a large oval or irregular shaped nucleus and prominent vesicle-like structures. These granulocyte-like hemocytes^{36, 50} had a well-developed actin cytoskeleton marked by intensive f-actin staining, and showed extreme cellular spreading as indicated by lamellipodia and numerous filopodia-like structures (Fig. 2a,b). The hemocytes of the subclass W2 had large, round or oval shaped nuclei with decondensed chromatin, but did not contain vesicle-like structures (Fig. 2a,c,d). Some W2-like hemocytes showed spreading with an intensively stained actin cytoskeleton, lamellipodia formation, and filopodia-like structures (Fig. 2c). Hemocytes of the W3-like subclass were the most abundant ones. They were small, of oval or round shape and contained small nuclei with highly condensed chromatin. In contrast to the other cell types, W3-like cells showed no spreading and had only very weak

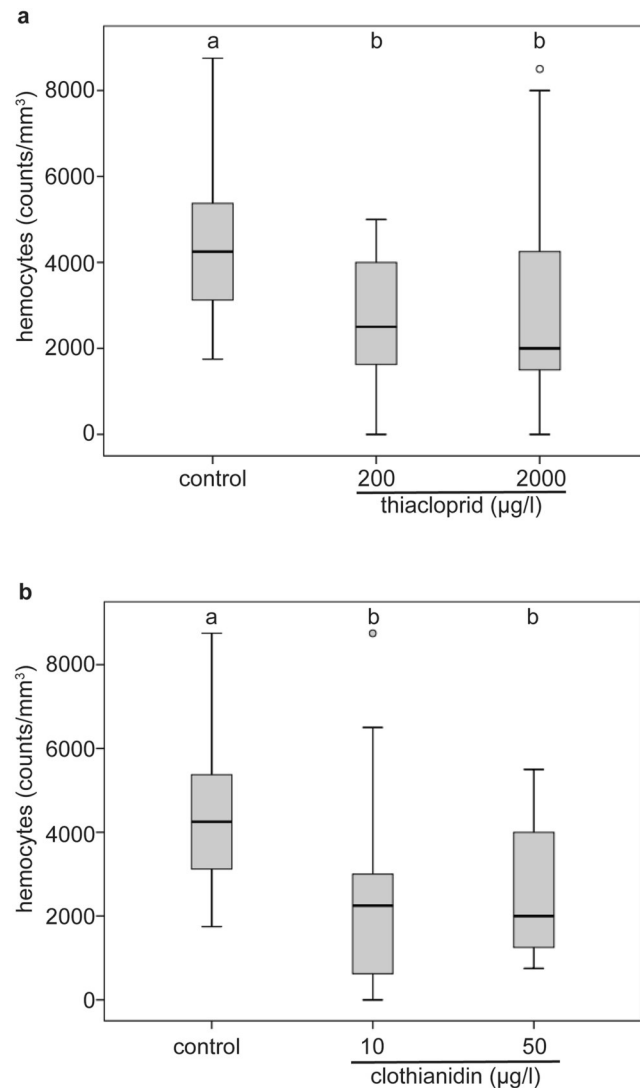


Figure 1. Exposure to thiacloprid or clothianidin reduced total hemocyte counts. The seven day-treatment of young honeybee queen with thiacloprid (**a**); control: $n = 19$, $200 \mu\text{g/l}$: $n = 16$, $2000 \mu\text{g/l}$: $n = 19$, or clothianidin (**b**); control: $n = 19$; $10 \mu\text{g/l}$: $n = 15$; $50 \mu\text{g/l}$: $n = 14$) reduced the total hemocyte counts compared to control queens. Boxes show 1st and 3rd interquartile range with black lines denoting medians. Whiskers encompass 95% of the individuals, beyond which outliers (circles) reside. Treatments with different letters differ significantly from each other.

f-actin staining (Fig. 2a,b,d). Queen hemocytes classified as W4-like had a spindle-shaped morphology with well-developed actin cytoskeleton and small, elongated or irregular shaped nuclei (Fig. 2a,d).

Pesticide treatment differentially affected the relative abundance of hemocyte subclasses. Exposure to $200 \mu\text{g/l}$ thiacloprid and $10 \mu\text{g/l}$ clothianidin reduced the percentage of W1-like cells in treated queens compared to controls (Fig. 2e, KWT, $p = 0.0005$; MWU, control vs. $200 \mu\text{g/l}$ thiacloprid: $p = 0.002$, control vs. $10 \mu\text{g/l}$ clothianidin: $p = 0.034$; control: average = 3.356%, $n = 9$; $200 \mu\text{g/l}$ thiacloprid: average = 1.980%, $n = 9$; clothianidin: average = 0.394%, $n = 8$). Exposure to $10 \mu\text{g/l}$ clothianidin produced a detectable reduction of W2-like hemocytes (Fig. 2e, KWT, $p = 0.0384$; MWU, control vs. $200 \mu\text{g/l}$ thiacloprid: $p > 0.05$, control vs. clothianidin: $p = 0.06$; control: average = 14.17%; $200 \mu\text{g/l}$ thiacloprid: average = 7.97%; clothianidin: average = 6.67%). Clothianidin treated queens showed a relative increase of undifferentiated, W3-like hemocytes (Fig. 2e, KWT, $p = 0.0408$; MWU, control vs. $200 \mu\text{g/l}$ thiacloprid: $p > 0.05$, control vs. clothianidin: $p = 0.077$; control: average = 69.06%; $200 \mu\text{g/l}$ thiacloprid: average = 72.73%; clothianidin: average = 83.27%). There was no significant difference between the treatment groups regarding the spindle-shaped W4-like hemocytes.

Melanisation. Compared to control queens, the melanisation response of queens treated with neonicotinoids was significantly reduced at all concentrations tested (Fig. 3). The melanisation in thiacloprid treated queens was reduced to 41% ($200 \mu\text{g/l}$) or 23% ($2000 \mu\text{g/l}$) of the control value (Fig. 3a, KWT, $p = 0.001$; MWU, control vs. $200 \mu\text{g/l}$ thiacloprid: $p = 0.016$, control vs. $2000 \mu\text{g/l}$ thiacloprid: $p = 0.003$; control: median = 23.83% grey value

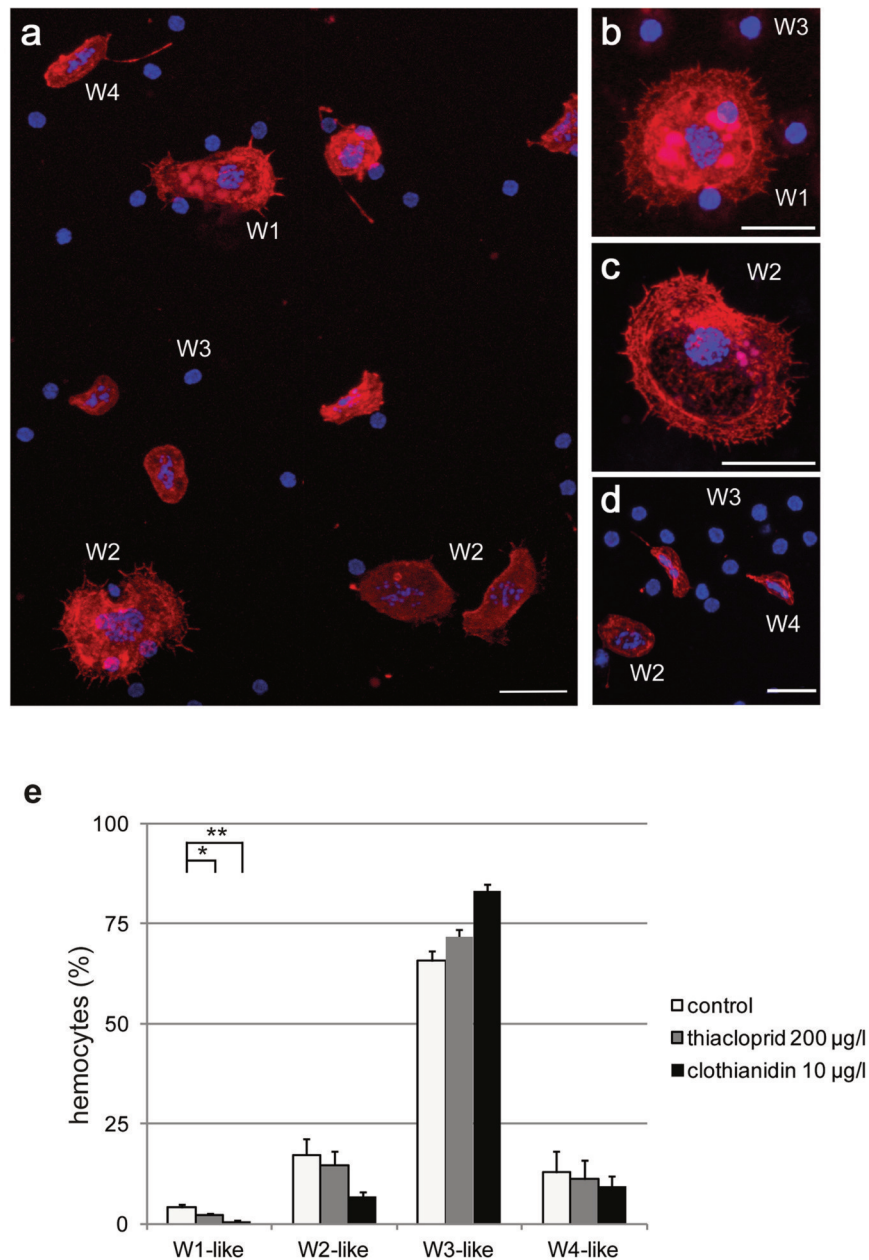


Figure 2. Exposure to neonicotinoids differentially affected hemocyte subclasses. (a–e) Queen hemocytes showing staining of the filamentous actin cytoskeleton (red: phalloidin-staining) and nuclear DNA (blue: DAPI-staining). (a) Compound image. W1-like hemocytes contained vesicle-like structures and showed extreme cellular spreading, lamellipodia formation, and filopodia-like structures with a well developed cytoskeleton marked by intensive f-actin staining (a,b; W1). W2-like hemocytes contained no vesicle-like structures, but also showed spreading and strong f-actin staining (a,c; W2). The nuclei of W1- or W2-like hemocytes were large and contained decondensed chromatin. W3-like hemocytes were oval/round and had only very weak f-actin staining. Nuclear chromatin of W3 like cells was highly condensed (a,b,d; W3). W4-like hemocytes had a spindle-shaped morphology and showed intensive f-actin staining of the cytoskeleton and elongated nuclei (a,d; W4). (e) Thiacloprid (200 µg/l) or clothianidin (10 µg/l) treatment affected the composition of the hemocyte population (8 to 9 individuals per treatment group, at least 350 cells per individual counted). Thiacloprid or clothianidin exposure significantly reduced the number of W1-type hemocytes. Clothianidin treated queens had a lower percentage of W2-like cells and a higher percentage of W3-like cells compared to control queens (error bars = s.e.m; * $p \leq 0.05$; ** $p \leq 0.01$; scale bar 10 µm).

(gv), $n = 20$; 200 µg/l thiacloprid: median = 10% gv, $n = 17$; 2000 µg/l thiacloprid: median = 5.5% gv, $n = 15$). The melanisation in clothianidin treated queens was reduced to 31% (10 µg/l) or 29% (50 µg/l) of the control value (Fig. 3b, KWT, $p < 0.0001$). Control queens showed a stronger melanisation than queens treated with clothianidin

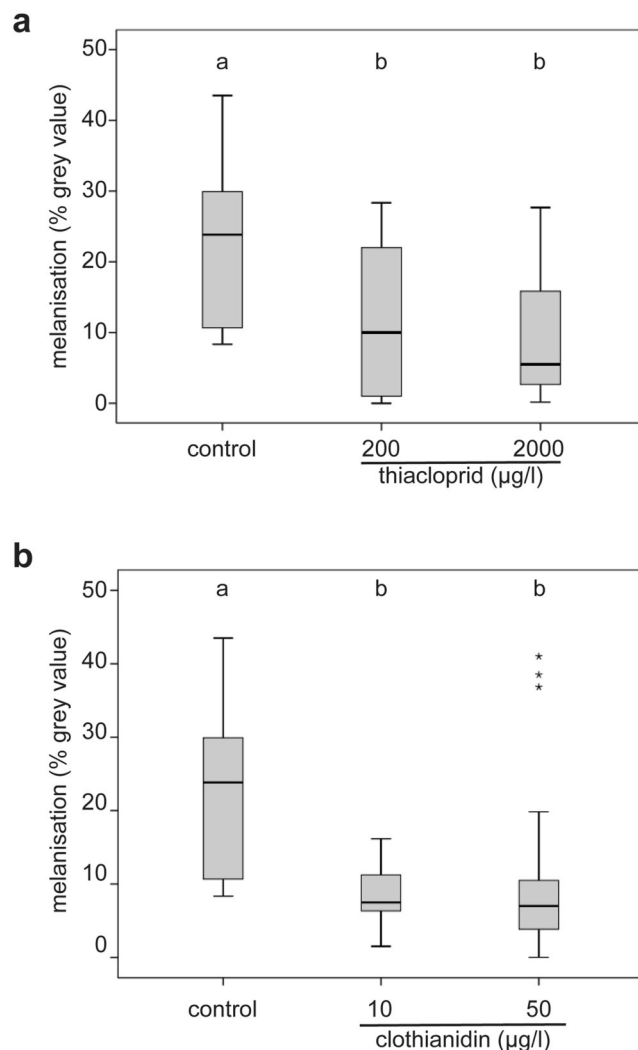


Figure 3. Exposure to thiacloprid or clothianidin reduced melanisation response. The seven day-exposure of young honeybee queens to thiacloprid ((a); control: n = 20, 200 µg/l: n = 17, 2000 µg/l: n = 15), or clothianidin ((b); control: n = 20; 10 µg/l: n = 19; 50 µg/l: n = 18) reduced the melanisation of an implanted nylon filament compared to control queens. Boxes show 1st and 3rd interquartile range with black lines denoting medians. Whiskers encompass 95% of the individuals, beyond which outliers (asterisks) reside. Treatments with different letters differ significantly from each other.

(Mann–Whitney U test (MWU), control vs. 10 µg/l clothianidin: $p < 0.0001$, control vs. 50 µg/l clothianidin: $p = 0.002$; control: median = 23.83% gv, n = 20; 10 µg/l clothianidin: median = 7.5% gv, n = 19; 50 µg/l clothianidin: median = 7.00% gv, n = 18).

Antimicrobial activity of the hemolymph. The antimicrobial activity of the hemolymph, measured as the size of the inhibition zones, was significantly reduced in queens treated with all concentrations of thiacloprid or clothianidin compared to control queens (Fig. 4, KWT, $p = 0.002$). Inhibition zones of queens exposed to thiacloprid were significantly smaller than in control queens (89% of control value; MWU, $p = 0.008$; control: median = 19.37 mm, n = 15; 200 µg/l thiacloprid: median = 17.25 mm, n = 16), or treated with 2000 µg/l thiacloprid (84% of control value; MWU, $p = 0.003$, median = 16.42 mm, n = 15). Inhibition zones of queens treated with clothianidin were significantly smaller than in control queens (Fig. 4b, KWT, $p < 0.001$), with control queens displaying a larger inhibition zone than queens treated with 10 µg/l clothianidin (89% of control value; MWU, $p < 0.001$, median = 17.26 mm, n = 14), or treated with 50 µg/l clothianidin (85% of control value; MWU, $p < 0.001$, median = 16.54 mm, n = 14).

Discussion

In this paper we report immunosuppressive effects of two neonicotinoid pesticides on general immune parameters of honeybee queens. We employed a broad array of methods to investigate the immune defence competence of queens: total and differential hemocyte counts, wound healing/melanisation, and antimicrobial activity of the hemolymph after immune stimulation. Our results indicate that the tested aspects of individual immunity are

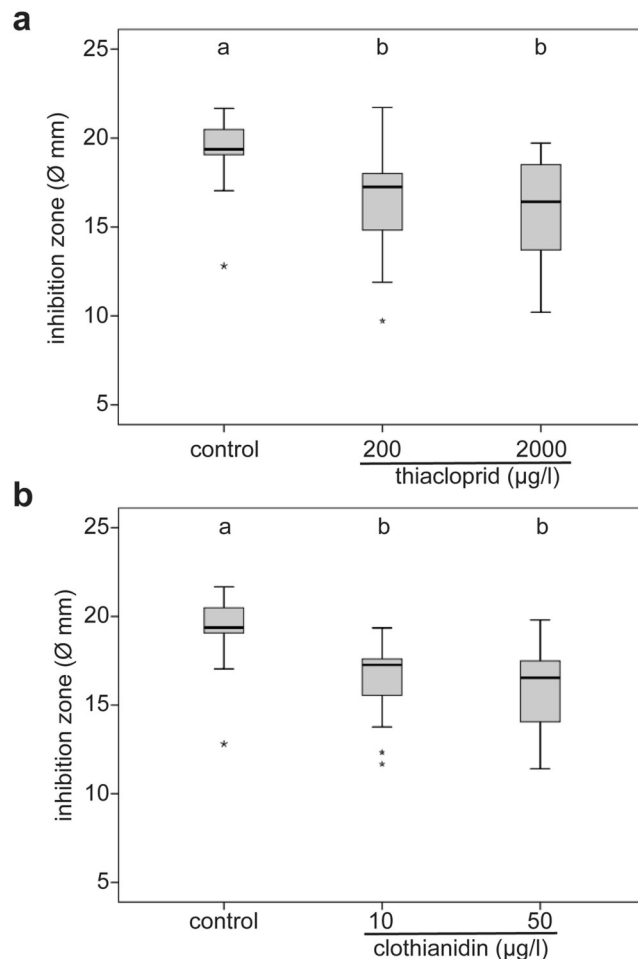


Figure 4. Neonicotinoid exposure reduced antimicrobial activity of hemolymph. The hemolymph inhibited the growth of gram-positive bacteria (*Micrococcus flavus*) on agar plates. The seven-day-treatment with thiacloprid ((a), control: n = 15; 200 µg/l: n = 16; 2000 µg/l: n = 15) or clothianidin ((b), control: n = 15; 10 µg/l: n = 14; 200 µg/l: n = 14) reduced the antimicrobial activity of the hemolymph, the diameter of the inhibition zones being smaller than in control queens. Boxes show 1st and 3rd interquartile range with black lines denoting medians. Whiskers encompass 95% of the individuals, beyond which outliers reside (asterisks). Significant differences indicated with letters.

negatively affected by sublethal, environmentally relevant concentrations of neonicotinoids in newly emerged honeybee queens.

Hemocytes are the key components of insect cellular immune defence. They are responsible for phagocytosis or encapsulation of pathogens and for the closure of wounds^{36,51}. The mechanisms of cellular immunity in honeybees are not yet completely understood, mostly due to limited information about the cellular subtypes, their functions and abundances^{50,52,53}. We found an overall reduction of hemocyte density at all concentrations tested. Based on morphological characterisation, we also observed changes in the abundance of subclasses in the population of hemocytes in clothianidin-exposed queens, which may indicate a severe interference of neonicotinoid treatment with cellular immunity.

The staining of the actin cytoskeleton by phalloidin together with nuclear staining can be used as a valuable tool for hemocyte characterization. Granulocytes are the first type of hemocyte to attach to a foreign object during the encapsulation response⁵⁰. We found a significant reduction in the number of granulocyte-like hemocytes in queens exposed to clothianidin. As in workers⁵⁰, these granulocyte-like cells showed extensive spreading with extensive filopodia and lamellipodia formation and contained numerous vesicle-like structures which may indicate their involvement in phagocytosis^{36,50}. The reduction of granulocyte-like hemocytes may be particularly severe, since this type of active, differentiated hemocyte is considered responsible for the elimination of pathogens and is the first cell type to initiate the encapsulation process^{36,54}. In addition, W2-like hemocytes tended to be reduced in queens treated with clothianidin. The W2 hemocytes have been shown to be the second cell type which adheres to foreign surfaces, a specific function of this cell type has not yet been described⁵⁰.

Hemocytes of the types W3 and W4 are normally freely floating in the hemolymph and interact with adherent granulocytes to form cell agglomerations³⁶. We found a relative increase of W3-like cells in queens exposed to clothianidin. The overall number of W3- or W4-like hemocytes may be underestimated in our study, since most

likely not all of them adhered to the surface of the glass cover slip³⁶. In conclusion, an altered hemocyte density together with a reduction in specific subclasses of active, differentiated hemocytes caused by neonicotinoid exposure could likely impair the cellular immune defence, hence increasing a queen's susceptibility towards pathogens. Nevertheless, honeybee hemocyte typing remains complex and it is difficult to compare the results obtained by different methods^{50,52,53}. More detailed investigations are necessary to bring light into the process of hemocyte differentiation in honeybees, combining the development of reliable cell markers and time-lapse microscopy.

A central immune defence mechanism mediated by hemocytes is the encapsulation and melanisation of intruding pathogens and the closure of wounds. The melanisation reaction is catalysed by the enzyme phenoloxidase whose precursor prophenoloxidase is produced by hemocytes⁵¹. We observed a significantly reduced melanisation after treatment with neonicotinoids in all substances and concentrations tested. The ability to melanise and encapsulate a foreign object is positively correlated with resistance to viral infections, parasitoids, and parasites. Wound closure involves similar mechanisms as encapsulation and melanisation and is important for reducing virus transfer between bees^{51,55}. In addition, we showed that exposure to thiacloprid or clothianidin significantly reduced the antimicrobial activity of the hemolymph. The antimicrobial activity depends on the amount of antimicrobial peptides in the hemolymph, which are produced by hemocytes or fat body cells⁵⁵. Together with the observed decrease in the melanisation response and changes in hemocyte composition and density, our findings may be interpreted as impairments of immune defence and disease resistance capacity of honeybee queens during exposure to neonicotinoids.

In our cage experiments, exposure to thiacloprid and clothianidin significantly affected the immunocompetence of young queens, even in sublethal concentrations as low as those reported from samples collected by honeybees. The thiacloprid or clothianidin concentrations fed over a period of seven days showed no lethal effects on queens and were therefore considered as sublethal for queens. Only the extremely high concentration of 200 µg/l clothianidin increased the mortality of attending worker bees and was therefore excluded from further analysis. According to Sanchez-Bayo and Goka⁵⁶, mean thiacloprid residues are 75.1 µg/kg (max.: 1002 µg/kg, mean prevalence of 17.7%) in pollen, and 6.5 µg/kg in honey (max.: 208 µg/kg, 64% prevalence)⁵⁶. Mean clothianidin residues in pollen were 9.4 µg/kg (max.: 41.2 µg/kg, mean prevalence of 11%) and in honey 1.9 µg/kg (max.: 10.1 µg/kg, mean prevalence of 17%). In the German bee monitoring, the highest observed concentrations of thiacloprid in beebread samples were 498 µg/kg³². Thiacloprid is frequently detected in honey samples, up to concentrations of 200 µg/kg^{4,25}.

In a colony the queen is constantly surrounded by attending worker bees which take care of her wellbeing and constantly supply her with high-quality food such as royal jelly. A queen can survive without worker bees for only a few days. However, this is a non-natural situation with unknown effects on the immune status of a queen. To approximate the natural situation in a laboratory experiment, ten attending bees were placed into each cage to provide for the queen. However, this makes it difficult to discern between the direct effects of neonicotinoids on the immune system of queens and indirect effects that may come from affected worker bees. In the concentrations used in immune assays, the mortality of queens or workers was not increased. Moreover, food consumption of sugar solution or pollen was comparable in all treatment groups, indicating normal feeding behaviour. Interestingly, in the presence of a queen, the neonicotinoids had no significant effect on the size of the HPG compared to controls. The mechanism by which xenobiotics like neonicotinoids, fungicides or varroacides affect HPG size is still unknown. Our findings may imply that the stimulus provided by the queen may counteract the HPG-reducing effects described for neonicotinoids. Although we cannot rule out any possible indirect effect, when considering the normal survival rate, the normal food consumption and the normal size of the HPGs together, we have no indications that our experimental queens may have suffered from a lack of care or feeding.

Adult queens receive mostly royal jelly from nurse bees, possibly with some additional honey^{1, 57}. Contaminated food reaches queens through trophallaxis. The contamination might originate from the transfer of active substances through the mandibular and hypopharyngeal glands located in the heads of nurse bees or by the addition of contaminated honey⁵⁸. Although little is known about pesticide contamination of royal jelly, neonicotinoids can be found in the heads of bees where the glands are located²⁶. Neonicotinoids have also been detected in brood food⁵⁹ and royal jelly when bees were exposed to contaminated pollen⁴⁰. In addition, neonicotinoids can reduce the size of the royal jelly producing hypopharyngeal glands in nurse bees^{60,61}, thus queens may be indirectly affected by altered food quality or quantity.

It is not clear, whether queens in laboratory assays or in the social context of a colony are exposed to the same dosages of pesticides as worker bees. In a honeybee colony, the queen may be shielded from harmful agents like pesticides by the attending workers. Transmission experiments suggest that behavioural patterns are in place to protect the queen from viral infection by symptomatic bees. Either queens avoid direct contact with or uptake of food from diseased workers, or diseased workers try to avoid interaction with the queen⁶². It is not known, whether similar behavioural mechanisms may exist in a colony that prevent or reduce exposure of queens to pesticides.

To estimate the level of exposure to queens, the detoxification of neonicotinoids has also to be taken into account. In case queens failed to fully clear ingested pesticides from their bodies, the persistence of even small daily intakes could eventually accumulate to harmful or even lethal levels over time. Indeed, the lethality of the neonicotinoid imidacloprid to worker bees, ants or termites appears to be dependent on the duration of exposure: the longer the exposure time, the less amount of pesticide is needed to kill the worker⁶³. So far, the temporal dynamics of the decrease of neonicotinoid residues has only been studied in worker bees²⁶. To our knowledge, no data are available concerning the ability of queens to detoxify pesticides.

A honeybee colony represents an environment with a high chance for the spread of infections, because of its highly organised social structure and crowded population density⁶⁴. In honeybees, transmission of viruses can occur horizontally among workers, or vertically, from the queen to her offspring. In queens, numerous viruses

have been detected, e.g. DWV, chronic bee paralysis virus (CBPV), black queen cell virus, Kashmir bee virus, and sacbrood virus⁶⁴. In a recent sanitary survey in Belgium, 75% of the eggs tested had at least one virus present⁶⁵. It appears plausible that a queen with a weakened immune defence may be prone to infections, which she can transmit vertically to her offspring.

In honeybees, like in other insect species, a maternal immune experience can be transmitted to the progeny. This so called trans-generational immune priming has been demonstrated to have a positive impact on offspring resistance and survival of infections^{66,67}. Whether a queen with weakened immune defence can still sufficiently protect her offspring via these mechanisms has yet to be investigated. Since a queen lays between 175.000 or 200.000 eggs annually¹, the health status of a queen is highly relevant for the overall colony health.

A young queen has to master several challenges in the early phase of her life. She has to fight her competitive sisters, perform risky nuptial flights, successfully mate with a sufficient number of drones, and start laying fertilised eggs in an adequate number and quality to be accepted by the colony¹. Especially when the queen gets into contact with drones on her nuptial flights, she is potentially confronted with an additional load of pathogens⁶⁸. We do not know whether the immunosuppressive effect of neonicotinoids may affect the ability of a queen to accomplish these tasks. The impact on the health and fitness of a queen may depend on the phase of life and the duration of the exposure to pesticides. Exposure to neonicotinoid pesticides during larval development of queens can have severe effects on her performance later in life: clothianidin and thiamethoxam treatment during the larval phase affects ovary size and reduces the number and quality of stored spermatozoa within queen spermathecae, which results in reduced egg laying success⁵. In our study, we analysed the immunocompetence of newly hatched queens after only seven days of exposure to neonicotinoids. However, in the field, queens may be exposed to pesticides for several months, including the winter season⁶⁹. Whether queens are susceptible to neonicotinoids during all phases of their life, or whether the immunosuppressive effects are persistent or reversible has yet to be determined.

Immune suppression by pesticides like neonicotinoids opens the way to the spread and abundance of pathogens and parasites, which are the proximate mortality factors of honeybee colonies^{11,36}. Infestation with *Varroa destructor*, the suspected main cause for colony losses, was shown to be promoted by exposing colonies to neonicotinoid treated crops⁷⁰. This study on the immunocompetence of queens complements previous, similar findings on the immunosuppressive effects of neonicotinoids on worker bees^{41,47}. Currently, regulatory requirements for evaluating the safety of pesticides to honeybees do not consider effects on the immune defence on workers, drones, or queens⁷¹. Given the key importance of queens to colony health and survival, the general lack of knowledge concerning both lethal and sub-lethal effects of pesticides on queen physiology is alarming. Our findings highlight the vulnerability of honeybee queens to common neonicotinoid pesticides, and demonstrate the need for future studies to identify relevant measures of queen health and disease susceptibility. Improving the understanding of honeybee immunity could provide new insights into the stress factors and their interactions that threaten honeybee survival and ultimately enable us to design strategies to protect them¹¹.

Material and Methods

Rearing of Queens. Queens were produced using standard honeybee queen-rearing techniques⁷². Briefly, young grafted larvae were introduced into queenless starter colonies. After 5 days, sealed queen cells were transferred to an incubator (35 °C, 65% humidity; Grumbach, Asslar, Germany). Sister queens from eight different maternal lines were distributed equally among the treatment groups. After emergence, queens were visually inspected and transferred into standard metal cages (8.5 × 6.5 × 4 cm,) together with ten attendant workers from healthy experimental colonies that tested negative for virus infections (DWV, acute bee paralysis virus, CBPV, sac brood virus)^{4,62}.

Neonicotinoid exposure in laboratory cage experiments. The cages were supplied with water and pollen (collected at the Bee Institute Kirchhain, Germany), and *ad libitum* sugar syrup (Apiinvert, Mannheim, Germany) diluted to a 50% sugar solution (w/v with ambrosia Bienenfutter, Germany and distilled water) in a 5 ml syringe (Carl Roth, Karlsruhe, Germany). Cages were kept in an incubator (Binder, Tuttingen, Germany; humidity provided by open water jars) in the dark at 33 °C⁷³.

Thiacloprid was obtained from Sigma Aldrich (St. Louis, USA; analytical standards, purity 99.9%). A stock solution of 2 mg/ml thiacloprid in acetone was prepared in a glass flask and stored in the dark at room temperature (~15 °C) until use. A sugar solution (50% w/v) was prepared and thiacloprid stock solution was added to reach a final concentration of 100 or 200 µg/l thiacloprid. The final concentration of acetone in the feeding solutions was adjusted to 0.0086% (v:v) in all thiacloprid treatment groups, including the control. Clothianidin (Sigma Aldrich, analytical standards, purity 99.3%) was dissolved in water and added to the sugar solution (50% w/v) to obtain a final concentration of 10, 50, or 200 µg/l clothianidin. The pollen pastry was prepared from pollen collected at the Bee Institute Kirchhain or obtained from Imkerebedarf Bährle (Aschaffenburg, Germany).

Honeybees of each cage (= a queen with ten worker bees) were exposed to one of these concentrations for seven days. During the phase of exposure, queens remained within the group of the attendant bees in the cages. In that way queens were exposed to the dietary pesticide either directly by taking up contaminated food themselves or indirectly via the food (e.g. royal jelly) received from the attending worker bees. The consumption of food was recorded daily. To quantify the food consumption, the syringes containing the sugar solution and the caps containing the pollen were weighed after 24 hours in the cage. Food consumption was calculated by dividing the total amount of food consumed in 24 hours divided by the number of workers in the cage. Three empty cages contained an evaporation control. Dead individuals were removed every 24 or 48 hours (for details see Supplementary Table S2).

Subsequently, the immunocompetence of the queens was evaluated by one of the methods: quantification of hemocytes, antimicrobial activity of the hemolymph, or melanisation response. Any individual queen was used

for only one single immune test. Each test was replicated at least three times with at least 14 queens per treatment group (details see below and Supplementary Table S1).

Hemolymph collection. Queens were anesthetized on ice before hemolymph was collected by inserting a microinjection needle (Hartenstein, Würzburg, Germany) into the proximal abdomen. Any fluid which appeared yellow or brown was discarded and excluded from further analysis as this was likely not hemolymph but gastric fluid³³.

Total and differential hemocyte counts. Total hemocyte counts were performed as an indirect measurement of cellular immunocompetence³³. For total hemocyte counts, 1 µl of hemolymph was transferred to a PCR-tube (Biozym, Hessisch Oldendorf, Germany) containing 3 µl PBS (pH 7.4; Sigma Aldrich, St. Louis, USA) and 1 µl of DAPI-staining solution (4',6-diamidino-2-phenylindole; 1:100 dilution, lifetechnologies, Carlsbad, California, USA). Immediately after collection, the diluted hemolymph solution was transferred to a Bürker counting chamber (Carl Roth, Karlsruhe, Germany), where hemocytes were counted (average of five squares per queen) under a phase contrast/fluorescent microscope (Leica DMIL, Leica camera DFC 420 C). To verify the cellular character of the observed structures, DAPI staining was used as counterstaining of nuclear DNA⁴⁷. Each experiment was repeated five times with 14 to 19 queens per treatment group.

To analyze whether exposure to pesticides affects the composition of the hemocyte population, differential hemocyte counts were conducted. The hemolymph (3 µl) was placed on sterile glass cover slips in a cell culture 24-multiwell plate (Sigma Aldrich) with distilled water in the spaces between the wells. The multiwell plate was placed in the incubator for 4 hours at 33 °C. Subsequently, the cells were fixed in formaldehyde solution (4% formaldehyde in PBS, Carl Roth) over night at 4 °C, rinsed three times in PBS and permeabilized in PBS + 0.2% Tween-20 (Sigma Aldrich) for 10 min. To visualize the cytoskeleton and the nuclei, cells were stained with Alexa 555-conjugated phalloidin at 1:200 (Invitrogen, Carlsbad, USA) and DAPI at 0.3 µM for 30 min, washed with PBS and mounted in Vectashield (VWR International, Darmstadt, Germany). Queen hemocytes were visualized using a confocal microscope (Zeiss LSM 700, Jena, Germany) or observed under the phase contrast/fluorescent microscope. Following the description and classification of Negri *et al.*⁵⁰, we classified the queen hemocytes using morphological characteristics (eight to nine queens per treatment group, 351 to 530 cells counted per individual; for details see Supplementary Table S1).

Melanisation. To provoke a melanisation response, a nylon filament was partly inserted into the abdomen of a queen, thus mimicking the behaviour of *Varroa destructor* as previously described by Brandt *et al.*⁴⁷. The strength of the immune reaction was measured by the degree of melanisation on the filament. Briefly, a nylon fishing line (0.2 mm diameter, Nexos, Naila, Germany) was cut into approximately 2.5 mm long segments and sterilized in 100% pure ethanol (Roth, Karlsruhe, Germany). Queens were anesthetized on ice, and the nylon filament was implanted in the abdomen through the intersegmental membrane between the 3rd and 4th tergum^{33,74}. After implantation, queens were transferred to a 2 ml microcentrifuge tube (Eppendorf, Hamburg, Germany) with holes poked through cap and sidewalls. After approx. four hours, the nylon filament was extracted, fixed in formaldehyde solution for at least 1 hour, rinsed three times in PBS, and subsequently mounted in glycerol (85%, Carl Roth). Each experiment was repeated four times (17 to 19 queens per treatment group). Three pictures per explant were taken at different focal depths. The mean grey value per filament served as a measure of melanisation and was quantified for the inserted portion of the filament using image analysis software⁷³. The mean grey value of a non-implanted filament that served as background value was subtracted from the mean grey value of the implanted filaments⁴⁷. Each treatment group (for details see Supplementary 15 to 20 queens per treatment group (for details see Supplementary Table S1).

Inhibition-Zone Assay. For inhibition zones assays, queens were exposed to neonicotinoids for seven days. On day six of the exposure, the immune system was challenged by the injection of 1 µl of heat-inactivated *Escherichia coli* (grown to OD 0.5). As previously described⁴⁷, hemolymph was collected and stored at -20 °C until the assay was conducted. Antibacterial test plates (ø 9 cm) were prepared by adding 0.8 ml of live *Micrococcus luteus* bacteria suspension (OD 0.5) to 150 ml of sterile broth medium (48 °C, 1.5 g Agar No. 1, Oxoid; 3.75 g nutrient broth, Applichem). Per test plate, five holes (ø 1 mm) were punched into the medium and 1 µl of hemolymph solution was added to each one. The plates were incubated at 38 °C overnight and the diameter of inhibition zones was measured. Each experiment was repeated three times with 14 to 16 queens per treatment group.

Hypopharyngeal gland size of attendant bees. In order to determine whether caged queens received sufficient food, the HPG size of attending worker bees was measured. To obtain worker bees of defined age, single frames of late stage capped brood were brought to the laboratory and incubated in the dark at 33 °C (humidity provided by open water jars). The frames with worker brood were collected from two institute colonies, which were regularly inspected for symptoms of diseases. Newly emerged bees (≤24 h) were collected, colour marked and returned to the colony of origin. On day seven after emergence, the marked bees were re-collected and placed into the cages containing the queens. After seven days of exposure to neonicotinoids in the laboratory, the workers were immobilized on ice and the HPGs were dissected in ice cold phosphate buffered saline (PBS, pH 7.4). The specimens were fixed in formaldehyde (4% in PBS, Carl Roth), rinsed three times in PBS and mounted in Aquapolymount (Polysciences, Eppelheim; Germany). Three pictures of each gland (only one gland per bee) were photographed using a Leica phase contrast/fluorescence microscope and image capturing software (Leica, LASV4.4, Wetzlar, Germany). To measure the size of the glands, the diameter of 15 acini per bee was measured with ImageJ software (ImageJ 1.490; Image Processing and Analysis in Java, <http://rsb.info.nih.gov/ij/index.html>)⁷⁵. The experiment was repeated three times with 20 to 33 individuals per treatment group (for details see Supplementary Table S2).

Statistical methods. Total hemocyte counts, melanisation/mean grey values, and mean diameters of inhibition zones were not normally distributed, and hence non-parametric statistics were used. Each immunocompetence measure was compared between groups treated with neonicotinoids and untreated control queens using KWT followed by post-hoc pair wise comparisons with Mann–Whitney U tests (MWU). Proportions of cell types were arcsin-transformed before performing statistical testing. The probability levels inferior to 0.05 were corrected for multiple testing according to the Holm's sequential Bonferroni procedure⁷⁶. All statistical tests were run with the computer program SPSS for Windows (v. 20).

References

- Winston, M. L. *The Biology of the Honey Bee*. (Harvard University Press, 1987).
- Pettis, J. S., Rice, N., Joselow, K., vanEngelsdorp, D. & Chaimanee, V. Colony Failure Linked to Low Sperm Viability in Honey Bee (*Apis mellifera*) Queens and an Exploration of Potential Causative Factors. *PLoS one* **11**, e0147220, doi:10.1371/journal.pone.0147220 (2016).
- vanEngelsdorp, D., Tarry, D. R., Lengerich, E. J. & Pettis, J. S. Idiopathic brood disease syndrome and queen events as precursors of colony mortality in migratory beekeeping operations in the eastern United States. *Prev Vet Med* **108**, 225–233, doi:10.1016/j.prevetmed.2012.08.004.pmid:22939774 (2013).
- Genersch, E. *et al.* The German bee monitoring project: a long term study to understand periodically high winter losses of honey bee colonies*. *Apidologie* **41**, 332–352 (2010).
- Williams, G. R. *et al.* Neonicotinoid pesticides severely affect honey bee queens. *Scientific reports* **5**, 14621, doi:10.1038/srep14621 (2015).
- Sandrock, C. *et al.* Impact of chronic neonicotinoid exposure on honeybee colony performance and queen supersedure. *PLoS one* **9**, e103592, doi:10.1371/journal.pone.0103592 (2014).
- Lee, K. V. *et al.* A national survey of managed honey bee 2013–2014 annual colony losses in the USA. *Apidologie* **46**, 292–305 (2015).
- Alaux, C. *et al.* Interactions between *Nosema* microspores and a neonicotinoid weaken honeybees (*Apis mellifera*). *Environmental microbiology* **12**, 774–782, doi:10.1111/j.1462-2920.2009.02123.x (2010).
- Brodtschneider, R. & Crailsheim, K. Nutrition and health in honey bees. *Apidologie* **41**, 278–294, doi:10.1051/apido/2010012 (2010).
- Di Pasquale, G. *et al.* Influence of pollen nutrition on honey bee health: do pollen quality and diversity matter? *PLoS one* **8**, e72016, doi:10.1371/journal.pone.0072016 (2013).
- Sanchez-Bayo, F. *et al.* Are bee diseases linked to pesticides? - A brief review. *Environment international* **89–90**, 7–11, doi:10.1016/j.envint.2016.01.009 (2016).
- Elbert, A., Haas, M., Springer, B., Thielert, W. & Nauen, R. Applied aspects of neonicotinoid uses in crop protection. *Pest management science* **64**, 1099–1105, doi:10.1002/ps.1616 (2008).
- Mullin, C. A. *et al.* High Levels of Miticides and Agrochemicals in North American Apiaries: Implications for Honey Bee Health. *PLoS one* **5**, e9754, doi:10.1371/journal.pone.0009754 (2010).
- Jeschke, P., Nauen, R., Schindler, M. & Elbert, A. Overview of the status and global strategy for neonicotinoids. *Journal of agricultural and food chemistry* **59**, 2897–2908, doi:10.1021/jf101303g (2011).
- van der Sluijs, J. P. *et al.* Neonicotinoids, bee disorders and the sustainability of pollinator services. *Current Opinion in Environmental Sustainability* **5**, 293–305, doi:10.1016/j.cosust.2013.05.007 (2013).
- Goulson, D., Nicholls, E., Botias, C. & Rotheray, E. L. Bee declines driven by combined stress from parasites, pesticides, and lack of flowers. *Science* **347**, 1255957, doi:10.1126/science.1255957 (2015).
- Henry, M. *et al.* Reconciling laboratory and field assessments of neonicotinoid toxicity to honeybees. *Proceedings. Biological sciences/The Royal Society* **282**, doi:10.1098/rspb.2015.2110 (2015).
- Henry, M. *et al.* A common pesticide decreases foraging success and survival in honey bees. *Science* **336**, 348–350, doi:10.1126/science.1215039 (2012).
- Desneux, N., Decourtye, A. & Delpuech, J. M. The sublethal effects of pesticides on beneficial arthropods. *Annual review of entomology* **52**, 81–106, doi:10.1146/annurev.ento.52.110405.091440 (2007).
- Goulson, D. Review: An overview of the environmental risks posed by neonicotinoid insecticides. *Journal of Applied Ecology* **50**, 977–987, doi:10.1111/1365-2664.12111 (2013).
- Pisa, L. W. *et al.* Effects of neonicotinoids and fipronil on non-target invertebrates. *Environmental science and pollution research international* **22**, 68–102, doi:10.1007/s11356-014-3471-x (2015).
- Vanbergen, A. J. & Initiative, T. I. P. Threats to an ecosystem service: pressures on pollinators. *Frontiers in Ecology and the Environment* **11**, 251–259, doi:10.1890/120126 (2013).
- Matsuda, K. *et al.* Neonicotinoids: insecticides acting on insect nicotinic acetylcholine receptors. *Trends in pharmacological sciences* **22**, 573–580 (2001).
- Tomizawa, M. & Casida, J. E. Unique neonicotinoid binding conformations conferring selective receptor interactions. *Journal of agricultural and food chemistry* **59**, 2825–2828, doi:10.1021/jf1019455 (2011).
- Blacquiere, T., Smagghe, G., van Gestel, C. A. & Mommaerts, V. Neonicotinoids in bees: a review on concentrations, side-effects and risk assessment. *Ecotoxicology* **21**, 973–992, doi:10.1007/s10646-012-0863-x (2012).
- Suchail, S., De Sousa, G., Rahmani, R. & Belzunces, L. P. *In vivo* distribution and metabolisation of 14C-imidacloprid in different compartments of *Apis mellifera* L. *Pest management science* **60**, 1056–1062, doi:10.1002/ps.895 (2004).
- Rundlof, M. *et al.* Seed coating with a neonicotinoid insecticide negatively affects wild bees. *Nature* **521**, 77–80, doi:10.1038/nature14420 (2015).
- Whitehorn, P. R., O'Connor, S., Wackers, F. L. & Goulson, D. Neonicotinoid pesticide reduces bumble bee colony growth and queen production. *Science* **336**, 351–352, doi:10.1126/science.1215025 (2012).
- Straub, L. *et al.* Neonicotinoid insecticides can serve as inadvertent insect contraceptives. *Proceedings of the Royal Society B: Biological Sciences* **283**, doi:10.1098/rspb.2016.0506 (2016).
- Kairo, G. *et al.* Drone exposure to the systemic insecticide Fipronil indirectly impairs queen reproductive potential. *Scientific reports* **6**, 31904, doi:10.1038/srep31904 (2016).
- European Commission. Commission implementing Regulation (EU) No 485/2013 of 24 May 2013 amending Implementing Regulation (EU) No 540/2011, as regards the condition of approval of the active substances clothianidin, thiamethoxam and imidacloprid, and prohibiting the use and sale of seeds treated with plant protection products containing those active substances. *Official Journal of the European Union*, L139/12.25.5.2013 (2013).
- Rosenkranz, P. *et al.* Schlussbericht: Deutsches Bienenmonitoring – DeBiMo 2011–2013 (2014).
- Wilson-Rich, N., Dres, S. T. & Starks, P. T. The ontogeny of immunity: development of innate immune strength in the honey bee (*Apis mellifera*). *Journal of insect physiology* **54**, 1392–1399, doi:10.1016/j.jinsphys.2008.07.016 (2008).
- Mao, W., Schuler, M. A. & Berenbaum, M. R. Honey constituents up-regulate detoxification and immunity genes in the western honey bee *Apis mellifera*. *Proceedings of the National Academy of Sciences* **110**, 8842–8846, doi:10.1073/pnas.1303884110 (2013).
- Frias, B., Barbosa, C. & Lourenço, A. Pollen nutrition in honey bees (*Apis mellifera*): impact on adult health. *Apidologie*, 1–11, doi:10.1007/s13592-015-0373-y (2015).

36. Negri, P. *et al.* Cellular immunity in *Apis mellifera*: studying hemocytes brings light about bees skills to confront threats. *Apidologie*, 1–10 (2015).
37. Steinmann, N., Corona, M., Neumann, P. & Dainat, B. Overwintering Is Associated with Reduced Expression of Immune Genes and Higher Susceptibility to Virus Infection in Honey Bees. *PLoS one* **10**, e0129956, doi:10.1371/journal.pone.0129956 (2015).
38. Anderson, D. L. & Trueman, J. W. *Varroa jacobsoni* (Acari: Varroidae) is more than one species. *Exp Appl Acarol* **24**, 165–189 (2000).
39. Guseman, A. J. *et al.* Multi-Drug Resistance Transporters and a Mechanism-Based Strategy for Assessing Risks of Pesticide Combinations to Honey Bees. *PLoS one* **11**, e0148242, doi:10.1371/journal.pone.0148242 (2016).
40. Dively, G. P., Embrey, M. S., Kamel, A., Hawthorne, D. J. & Pettis, J. S. Assessment of chronic sublethal effects of imidacloprid on honey bee colony health. *PLoS one* **10**, e0118748, doi:10.1371/journal.pone.0118748 (2015).
41. Di Prisco, G. *et al.* A mutualistic symbiosis between a parasitic mite and a pathogenic virus undermines honey bee immunity and health. *Proceedings of the National Academy of Sciences of the United States of America* **113**, 3203–3208, doi:10.1073/pnas.1523515113 (2016).
42. James, R. R. & Xu, J. Mechanisms by which pesticides affect insect immunity. *Journal of invertebrate pathology* **109**, 175–182, doi:10.1016/j.jip.2011.12.005 (2012).
43. Aufauvre, J. *et al.* Parasite-insecticide interactions: a case study of *Nosema ceranae* and fipronil synergy on honeybee. *Scientific reports* **2**, 326, doi:10.1038/srep00326 (2012).
44. Di Prisco, G. *et al.* Neonicotinoid clothianidin adversely affects insect immunity and promotes replication of a viral pathogen in honey bees. *Proceedings of the National Academy of Sciences of the United States of America* **110**, 18466–18471, doi:10.1073/pnas.1314923110 (2013).
45. Pettis, J. S., vanEngelsdorp, D., Johnson, J. & Dively, G. Pesticide exposure in honey bees results in increased levels of the gut pathogen *Nosema*. *Die Naturwissenschaften* **99**, 153–158, doi:10.1007/s00114-011-0881-1 (2012).
46. Doublet, V., Labarussias, M., de Miranda, J. R., Moritz, R. F. & Paxton, R. J. Bees under stress: sublethal doses of a neonicotinoid pesticide and pathogens interact to elevate honey bee mortality across the life cycle. *Environmental microbiology*, doi:10.1111/1462-2920.12426 (2014).
47. Brandt, A., Gorenflo, A., Siede, R., Meixner, M. & Büchler, R. The Neonicotinoids Thiacloprid, Imidacloprid and Clothianidin affect the immunocompetence of Honey Bees (*Apis mellifera* L.). *Journal of insect physiology* **86**, 40–47 (2016).
48. Schmid, M. R., Brockmann, A., Pirk, C. W., Stanley, D. W. & Tautz, J. Adult honeybees (*Apis mellifera* L.) abandon hemocytic, but not phenoloxidase-based immunity. *Journal of insect physiology* **54**, 439–444 (2008).
49. Gatschenberger, H., Azzami, K., Tautz, J. & Beier, H. Antibacterial immune competence of honey bees (*Apis mellifera*) is adapted to different life stages and environmental risks. *PLoS one* **8**, e66415, doi:10.1371/journal.pone.0066415 (2013).
50. Negri, P., Maggi, M., Szawarski, N., Lamattina, L. & Eguaras, M. *Apis mellifera* haemocytes *in-vitro*, What type of cells are they? Functional analysis before and after pupal metamorphosis. *Journal of Apicultural Research* **53**, 576–589, doi:10.3896/ibra.1.53.5.11 (2014).
51. Evans, J. D. *et al.* Immune pathways and defence mechanisms in honey bees *Apis mellifera*. *Insect molecular biology* **15**, 645–656, doi:10.1111/j.1365-2583.2006.00682.x (2006).
52. Graaf, D. C. d., Dauwe, R., Walravens, K. & Jacobs, F. J. Flow cytometric analysis of lectin-stained haemocytes of the honeybee (*Apis mellifera*). *Apidologie* **33**, 571–579 (2002).
53. Marringa, W. J., Krueger, M. J., Burritt, N. L. & Burritt, J. B. Honey Bee Hemocyte Profiling by Flow Cytometry. *PLoS one* **9**, e108486, doi:10.1371/journal.pone.0108486 (2014).
54. Negri, P. *et al.* *Apis mellifera* hemocytes generate increased amounts of nitric oxide in response to wounding/encapsulation. *Apidologie* **45**, 610–617, doi:10.1007/s13592-014-0279-0 (2014).
55. Strand, M. R. The insect cellular immune response. *Insect Science* **15**, 1–14, doi:10.1111/j.1744-7917.2008.00183.x (2008).
56. Sanchez-Bayo, F. & Goka, K. Pesticide Residues and Bees – A Risk Assessment. *PLoS one* **9**, e94482, doi:10.1371/journal.pone.0094482 (2014).
57. Haydak, M. H. Honey Bee Nutrition. *Annual review of entomology* **15**, 143–156, doi:10.1146/annurev.en.15.010170.001043 (1970).
58. Davies, A. R. & Shuel, R. W. Distribution of C1-labelled carbofuran and dimethoate in royal jelly, queen larvae and nurse honeybees. *Apidologie* **19**, 37–50 (1988).
59. Giroud, B., Vaucher, A., Vulliet, E., Wiest, L. & Bulete, A. Trace level determination of pyrethroid and neonicotinoid insecticides in beebread using acetonitrile-based extraction followed by analysis with ultra-high-performance liquid chromatography-tandem mass spectrometry. *Journal of chromatography. A* **1316**, 53–61, doi:10.1016/j.chroma.2013.09.088 (2013).
60. Škerl, M. I. S. & Gregorc, A. Heat shock proteins and cell death *in situ* localisation in hypopharyngeal glands of honeybee (*Apis mellifera carnica*) workers after imidacloprid or coumaphos treatment. *Apidologie* **41**, 73–86, doi:10.1051/apido/2009051 (2010).
61. Hatjina, F. *et al.* Sublethal doses of imidacloprid decreased size of hypopharyngeal glands and respiratory rhythm of honeybees *in vivo*. *Apidologie* **44**, 467–480, doi:10.1007/s13592-013-0199-4 (2014).
62. Amiri, E., Meixner, M., Büchler, R. & Kryger, P. Chronic Bee Paralysis Virus in Honeybee Queens: Evaluating Susceptibility and Infection Routes. *Viruses* **6**, 1188–1201, doi:10.3390/v6031188 (2014).
63. Rondeau, G. *et al.* Delayed and time-cumulative toxicity of imidacloprid in bees, ants and termites. *Scientific reports* **4**, 5566, doi:10.1038/srep05566 (2014).
64. Chen, Y. P., Pettis, J. S., Collins, A. & Feldlaufer, M. F. Prevalence and transmission of honeybee viruses. *Applied and environmental microbiology* **72**, 606–611, doi:10.1128/aem.72.1.606-611.2006 (2006).
65. Ravoet, J., De Smet, L., Wenseleers, T. & de Graaf, D. C. Vertical transmission of honey bee viruses in a Belgian queen breeding program. *BMC Veterinary Research* **11**, 61, doi:10.1186/s12917-015-0386-9 (2015).
66. Hernandez Lopez, J., Schuehly, W., Crailsheim, K. & Riessberger-Galle, U. Trans-generational immune priming in honeybees. *Proceedings. Biological sciences/The Royal Society* **281**, 20140454, doi:10.1098/rspb.2014.0454 (2014).
67. Salmela, H., Amdam, G. V. & Freitak, D. Transfer of Immunity from Mother to Offspring Is Mediated via Egg-Yolk Protein Vitellogenin. *PLoS pathogens* **11**, e1005015, doi:10.1371/journal.ppat.1005015 (2015).
68. Amiri, E., Meixner, M. D. & Kryger, P. Deformed wing virus can be transmitted during natural mating in honey bees and infect the queens. *Scientific reports* **6**, 33065, doi:10.1038/srep33065 (2016).
69. Reetz, J. E. *et al.* Uptake of Neonicotinoid Insecticides by Water-Foraging Honey Bees (Hymenoptera: Apidae) Through Guttation Fluid of Winter Oilseed Rape. *J Econ Entomol* **109**, 31–40, doi:10.1093/jee/109/1/31 (2016).
70. Alburaki, M. *et al.* Performance of honeybee colonies located in neonicotinoid, treated and untreated cornfields in Quebec. *Journal of Applied Entomology*, doi:10.1111/jen.12336 (2016).
71. European Food and Safety Authority (EFSA). Guidance on the risk assessment of plant protection products on bees (*Apis mellifera*, *Bombus* spp. and solitary bees). *EFSA Journal* **11**, 3295 (2013).
72. Büchler, R. *et al.* Standard methods for rearing and selection of *Apis mellifera* queens. *Journal of Apicultural Research* **52**, 1–30, doi:10.3896/ibra.1.52.1.07 (2013).
73. OECD. Proposal for a new guideline for the testing of chemicals. Honey bee (*Apis mellifera* L.), chronic oral toxicity test, 10 day feeding test in the laboratory (2016).
74. Allander, K. & Schmid-Hempel, P. Immune defence reaction in bumble-bee workers after a previous challenge and parasitic coinfection. *Functional Ecology* **14**, 711–717, doi:10.1046/j.1365-2435.2000.00476.x (2000).
75. Rasband, W. S. ImageJ. U. S. National Institutes of Health, Bethesda, Maryland, USA, <http://imagej.nih.gov/ij/> (1997–2016).
76. Abdi, H. Holm's sequential Bonferroni procedure. *Encyclopedia of research design* **1** (2010).

Acknowledgements

We gratefully thank W. Strasser for queen rearing, K. Petzold-Treibert for assistance in beekeeping, S. Backhaus, A. Gorenflo, B. Hohnheiser, and Ch. Geßner for technical support, D.T. Brandt for histochemical stainings, and all team members of the Bee Institute Kirchhain for support and fruitful discussions. This research was supported by the EU and Land Hessen “Förderung von Maßnahmen zur Verbesserung der Erzeugung und Vermarktung von Honig in Hessen”.

Author Contributions

A.B. and R.S. designed the study and performed the experiments. K.G. made microscope pictures. A.B. and R.S. analysed the data and wrote the manuscript. All authors edited and approved the manuscript.

Additional Information

Supplementary information accompanies this paper at doi:[10.1038/s41598-017-04734-1](https://doi.org/10.1038/s41598-017-04734-1)

Competing Interests: The authors declare that they have no competing interests.

Publisher's note: Springer Nature remains neutral with regard to jurisdictional claims in published maps and institutional affiliations.



Open Access This article is licensed under a Creative Commons Attribution 4.0 International License, which permits use, sharing, adaptation, distribution and reproduction in any medium or format, as long as you give appropriate credit to the original author(s) and the source, provide a link to the Creative Commons license, and indicate if changes were made. The images or other third party material in this article are included in the article's Creative Commons license, unless indicated otherwise in a credit line to the material. If material is not included in the article's Creative Commons license and your intended use is not permitted by statutory regulation or exceeds the permitted use, you will need to obtain permission directly from the copyright holder. To view a copy of this license, visit <http://creativecommons.org/licenses/by/4.0/>.

© The Author(s) 2017

A Comparison of *Wolbachia* Infection Frequencies in *Varroa* With Prevalence of Deformed Wing Virus

Thorben Grau,¹ Annelly Brandt,² Sara DeLeon,¹ Marina Doris Meixner,²
Jakob Friedrich Strauß,³ Gerrit Joop,^{1,4,*} and Arndt Telschow^{3,*}

¹Institute of Insect Biotechnology, Justus-Liebig University Giessen, Giessen, Germany (thorben.grau@agr.uni-giessen.de; sara.deleon@agr.uni-giessen.de; gerrit.joop@agr.uni-giessen.de), ²LLH Bee Institute, Kirchhain, Germany (annely.brandt@llh.hessen.de; marina.meixner@llh.hessen.de), ³Institute for Evolution and Biodiversity, Westfaelische Wilhelms University Muenster, Muenster, Germany (jfstrauss@gmail.com; atels_01@uni-muenster.de), and ⁴Corresponding author, e-mail: gerrit.joop@agr.uni-giessen.de

*Equally contributing senior authors.

Subject Editor: Sara Goodacre

Received 5 July 2016; Editorial decision 27 March 2017

Abstract

Wolbachia are widely distributed bacterial endosymbionts of arthropods and filarial nematodes. These bacteria can affect host fitness in a variety of ways, such as protecting hosts against viruses and other pathogens. Here, we investigate the possible role of *Wolbachia* in the prevalence of the deformed wing virus (DWV), a highly virulent pathogen of honey bees (*Apis mellifera*) that is transmitted by parasitic *Varroa* mites (*Varroa destructor*). About 180 *Varroa* mites from 18 beehives were tested for infection with *Wolbachia* and DWV. We first screened for *Wolbachia* using two standard primers (*wsp* and 16S rDNA), and found 26% of the mites to be positive for *Wolbachia* using the *wsp* primer and 64% of the mites to be positive using the 16S rDNA primer. Using these intermediate *Wolbachia* frequencies, we then tested for statistical correlations with virus infection frequencies. The analysis revealed a significant positive correlation between DWV and *Wolbachia* using the *wsp* primer, but no significant association between DWV and *Wolbachia* using the 16S rDNA primer. In conclusion, there is no evidence for an anti-pathogenic effect of *Wolbachia* in *V. destructor*, but weak evidence for a pro-pathogenic effect. These results encourage further examination of *Wolbachia*-virus interactions in *Varroa* mites since an increased vector competence of the mites may significantly impact disease outbreaks in honey bees.

Key words: deformed wing virus, honey bee, protective symbiont, *Varroa destructor*, *Wolbachia*

Honey bees (*Apis mellifera* L.), important pollinators of wild plants and cultivated crops, are essential for ecosystem function and global agriculture (Fontaine et al. 2005, Bascompte et al. 2006, Klein et al. 2007). Over the past decade, there has been a serious decline in bee populations reported in the European Union and other parts of the world (EFSA 2008; van Engelsdorp et al. 2009; Potts et al. 2010a,b; van Engelsdorp and Meixner 2010; van der Zee et al. 2012, 2014; Spleen et al. 2013; Steinhauer et al. 2014; Goulson et al. 2015). While a multitude of causative factors, such as parasites, pathogens, diet quantity, quality, diversity and the exposure to pesticides, is being discussed (Alaux et al. 2010; Brodschneider and Crailsheim 2010; Genersch et al. 2010; Blacquièrre et al. 2012; Di Pasquale et al. 2013; Goulson 2013, 2015; Sandrock et al. 2014), infestation with the invasive ectoparasitic mite *Varroa destructor* is now considered the most significant cause for colony losses (Anderson and Trueman 2000, Genersch et al. 2010, Rosenkranz et al. 2010, Dainat et al. 2012a, Martin et al. 2012). *Varroa destructor* is originally a parasite of the Asian *Apis cerana*, in which it inflicts only

limited damage. In eastern Russia, this mite jumped hosts to *A. mellifera*, followed by near-global spread to *A. mellifera* populations worldwide (Rosenkranz et al. 2010, Martin et al. 2012, Mondet et al. 2014).

Varroa mites are known as effective vectors for several honey bee viruses (Bowen-Walker et al. 1999, Chen et al. 2004, Sumpter and Martin 2004, Berthoud et al. 2010). They are also hypothesized to downregulate honey bee immune genes (Nazzi et al. 2012), which may consequently activate covert virus infections (Yang and Cox-Foster 2005). Viral infections, as a consequence of high *Varroa* mite infestation rates, strongly correlate with the collapse of colonies (Cox-Foster et al. 2007, Highfield et al. 2009, Berthoud et al. 2010, Genersch et al. 2010, Le Conte et al. 2010, Dainat et al. 2012b, Francis et al. 2013). The association between *V. destructor* and Deformed Wing Virus (DWV) in particular is being discussed as one of the main causes for colony losses (de Miranda and Genersch 2010, Schroeder and Martin 2012, Mordecai et al. 2015a). This virus is widely prevalent and has a nearly worldwide distribution

(Ellis and Munn 2005, Gauthier et al. 2007). Even though DWV can be found in *Varroa*-free colonies or bee populations, it rarely leads to overt disease in the absence of *Varroa* mites. Yet, the presence of *Varroa* mites has been shown to dramatically increase the prevalence of DWV (Martin et al. 2012). In addition to being vectored by the mite, DWV is also known to survive and successfully replicate in the mite (Yue and Genersch 2005). Moreover, *Varroa* mites influence the balance of different DWV strains with differing virulence, potentially leading to an increase of more virulent strains (Martin et al. 2012, Mondet et al. 2014, Ryabov et al. 2014, Mordecai et al. 2015b). Investigations of the viral composition of *Varroa* mites and factors that influence virus prevalence and the mite's vector competence will contribute to understanding the dynamics of the *Varroa*-virus system and the potential threat it presents to honey bees.

Recent progress in microbiome studies reveals that host microbial composition has a significant impact on both host susceptibility to pathogen infection, and pathogen performance in infected hosts (Kamada et al. 2013, Dennison et al. 2014, Vogt et al. 2015, reviewed in Bäumler and Sperandio 2016). Not only the complete microbiota but also symbiotic microbes, have been shown to impact host's susceptibility and resistance. Of particular interest are intracellular bacteria of the genus *Wolbachia* (Werren et al. 2008). *Wolbachia* are widely distributed in terrestrial arthropods and filarial nematodes, with an estimated 20–70% of insect species infected (Hilgenboecker et al. 2008, Weinert et al. 2015). Empirical studies show that *Wolbachia* interferes with viruses and other pathogens inside the arthropod host, thereby either impeding or promoting the pathogen's replication and survival (reviewed in Zug and Hammerstein 2015) as well as the host's survival (Wong et al. 2011, Shokal et al. 2016). Anti-pathogenic effects of *Wolbachia* were demonstrated for Dengue virus (Moreira et al. 2009, Bian et al. 2010), West Nile virus (Hussain et al. 2013), and *Plasmodium falciparum* (Moreira et al. 2009), whereas neutral or pro-pathogenic effects of *Wolbachia* were shown for *Brugia pahangi* (Dutton and Sinkins 2005), Japanese encephalitis virus (Tsai et al. 2006), Drosophila C virus (Osborne et al. 2009) and *Plasmodium gallinaceum* (Baton et al. 2013).

Although *Wolbachia* has been previously detected in *V. destructor* (Pattabhiramaiah et al. 2010), information about possible interactions of *Wolbachia* with the mite's virome is lacking. Here, taking a correlative approach, we compare infection frequencies of *Wolbachia* and DWV in *V. destructor* to investigate whether the presence of *Wolbachia* correlates with virus prevalence in the mites. We hypothesize that an anti-pathogenic effect of *Wolbachia* will result in lower virus frequencies among the *Wolbachia*-infected mites compared to *Wolbachia*-free mites, and a pro-pathogenic effect will result in the opposite pattern.

Materials and Methods

Mite Collection

Apis mellifera samples were collected in October 2011 from 18 hives in 9 different apiaries across Hesse (Germany) (2 colonies per apiary). From each hive, bees were shaken from a comb onto a plastic sheet, immediately transferred to a labeled vial, and frozen at -20°C until analysis (Genersch et al. 2010). To collect the mites, individual bees of each sample were visually inspected and mites were removed manually with forceps.

DNA/RNA Extraction

Both DNA for *Wolbachia* detection and RNA for DWV detection were extracted from 10 individual mites per hive (180 total samples)

according to the NucleoSpin TriPrep protocol (Macherey & Nagel, Düren, Germany).

PCR for *Wolbachia* Detection

Wolbachia infection rate is commonly measured by using primers for 16S rDNA, or primers for the outer surface-protein coding gene *wsp* (Marcon et al. 2011, Beckmann and Fallon 2012, Zha et al. 2014). Specifically, we used the *wsp*81f and *wsp*691r (Zhou et al. 1998) primers and the 16S rDNA76f and 16S rDNA1012r (O'Neill et al. 1992) primers (Supp Table 1 [online only]). PCR products were analyzed on an agarose gel. Approximately 10% positive amplicons of both primer pairs were sent for sequencing to confirm identity (Macrogen, Amsterdam, Netherlands) and sequences were deposited in GenBank (Supp Table 2 [online only]).

One-step RT-PCR for DWV Detection

DWV infection was detected with RT-PCR according to the protocol of OneStep-RT-PCR Kit and as previously described in Genersch (2005), using the primer pair F7, B11 (Supp Table 1 [online only]) for DWV detection. Around 10% positive amplicons were sent for sequencing to confirm identity and sequences were deposited in GenBank (Supp Table 2 [online only]). Only a short RNA region was used for DWV detection, so that even degraded DNA caused by long-term storage at -20°C would provide a suitable template (Dainat et al. 2011).

Statistics

All analyses were performed using R 3.1.1. We performed the analysis with the infection frequency of each of the 18 hives, testing 10 individual mites per hive. To determine the relationship between *Wolbachia* prevalence and virus presence in *Varroa* mites, we used a completely balanced experimental design, i.e., equal sample numbers. In a correlative approach, we used the 16S rDNA, *wsp* and an additive combination of both primers, where there were 16 degrees of freedom left.

Results

Using the *wsp* primer, we detected *Wolbachia* in only 26% of *V. destructor*. Less than 70% of mites from one hive were found infected, and 44.4% of hives were *Wolbachia* free (Fig. 1A). In contrast, when using the 16S rDNA primer, 64% of *V. destructor* were positive for *Wolbachia* and all hives were found to be infected (Fig. 1B). Overall, *Wolbachia* prevalence in our samples varied from 30% to 70% in the majority of hives. Notably, not all mites with a positive signal for *wsp* were also positive with the 16S rDNA primer pair. For example, hive 5 showed higher infection frequencies with *wsp* than with 16S rDNA. DWV presence differed substantially between mites from different hives (Fig. 1C). We found a total DWV infection frequency of 61%. Only 5 out of 18 hives had a 100% DWV infection, while in two hives no DWV was detected. Sequencing of positive samples did not reveal false positive *Wolbachia* signals.

To test our hypothesis of the anti- or pro-pathogenic properties of *Wolbachia*, we ran a multivariate correlational analysis between the *Wolbachia* and DWV infection frequencies based on the two *Wolbachia* primers, *wsp* and 16S rDNA. The analysis suggests that *Wolbachia* has a pro-pathogenic function in *Varroa*, indicated by the positive linear correlation between *Wolbachia* prevalence and DWV presence, when *Wolbachia* infection was determined using the *wsp* primer ($t=3.774$, $P=0.002$, Fig. 2A). When *Wolbachia*

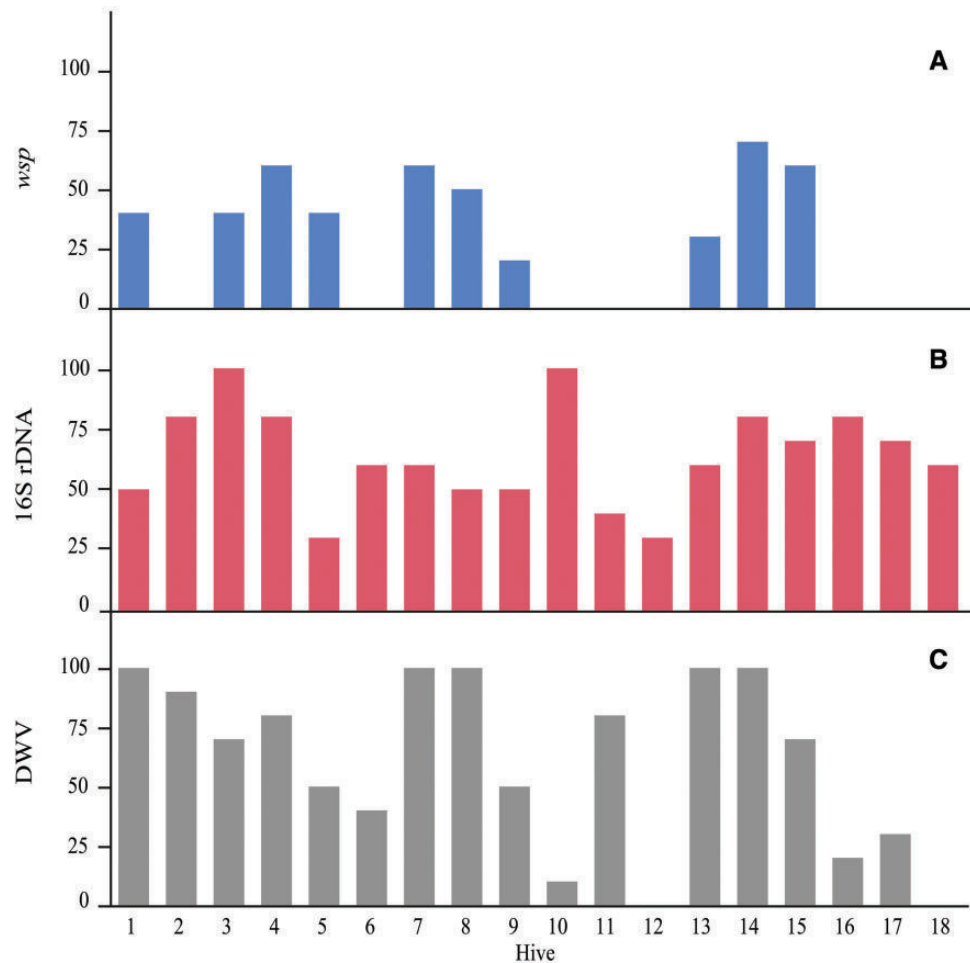


Fig. 1. Infection frequencies of *Wolbachia* (A) using *wsp* primer (B) using 16S rDNA primer and Deformed Wing Virus (C) using DWV primer in *Varroa* mites collected from 18 different hives from across Hesse, Germany in 2011. DNA and RNA from 10 mites from each hive were sampled, identical mites were used with all three primers.

infection was determined using the 16S rDNA primer there was no significant correlation ($t=0.050$, $P=0.961$, Fig. 2B). The additive combination of both primers result in no significant correlation ($t=0.127$, $P=0.901$, Fig. 2C).

Discussion

Wolbachia infections have been recently reported in *Varroa* (Pattabhiramaiah et al. 2010), a vector of DWV (de Miranda and Genersch 2010). To explore the potential of *Wolbachia* bacteria mediating virus transfer, we investigated the *Wolbachia* frequency in *V. destructor*. Our results gave a first indication of *Wolbachia* having an effect on the prevalence of DWV in *Varroa*. The results were remarkably different depending on whether *wsp* or 16S rDNA primers were used. Most notably, mites tested for *Wolbachia* infection using the *wsp* primer resulted in far lower frequencies of infection than those tested with the 16S rDNA primer. This is in line with previous studies showing that *wsp* produces false negatives in certain *Wolbachia*-host systems, particularly when *Wolbachia* titers are low (Schneider et al. 2014). Therefore, the lower percentage of *Varroa* mites that tested positive for *Wolbachia* using the *wsp* primer was not unexpected. However, surprisingly, >20% of the *wsp* positive mites (10 out of 47) were negative for 16S rDNA. A possible

explanation for this finding is that *Varroa* harbors more than one *Wolbachia* strains and that the different strains are detected differentially well by the two primers (de Oliveira et al. 2015). Alternatively, *wsp* may have detected, at least in some samples, a closely related species from the order of Rickettsiales (Simoes et al. 2011). Whatever the reason for the difference between the primers, the results suggest that *Wolbachia* frequencies in our sampling of *V. destructor* are at intermediate levels.

Meta-analysis studies of terrestrial arthropods show that *Wolbachia* infection frequencies are usually either high (>90%) or low (<20%) (Hilgenboecker et al. 2008, Weinert et al. 2015). High *Wolbachia* infected arthropods include *Culex pipiens* (Rasgon and Scott 2003), *Aedes albopictus* (Kitrayapong et al. 2002, Joanne et al. 2015), *Drosophila simulans* (Kriesner et al. 2013), as well as the *Nasonia* species complex (Bordenstein et al. 2001). These examples of high infection frequencies are explained by the joint effects of high maternal transmission rates (95–100%) and *Wolbachia*-induced cytoplasmic incompatibility (Engelstädter and Telschow 2009). Systems with low *Wolbachia* frequencies are less well understood. Low infection rates can be caused by low levels of maternal inheritance (80–90%) and by *Wolbachia* strains that cause male-killing of the insect, as reported in *Drosophila innubila* (Dyer and Jaenike 2004, Unckless and Jaenike 2012). Paternal and horizontal transmission of *Wolbachia* is considered to be negligible in all

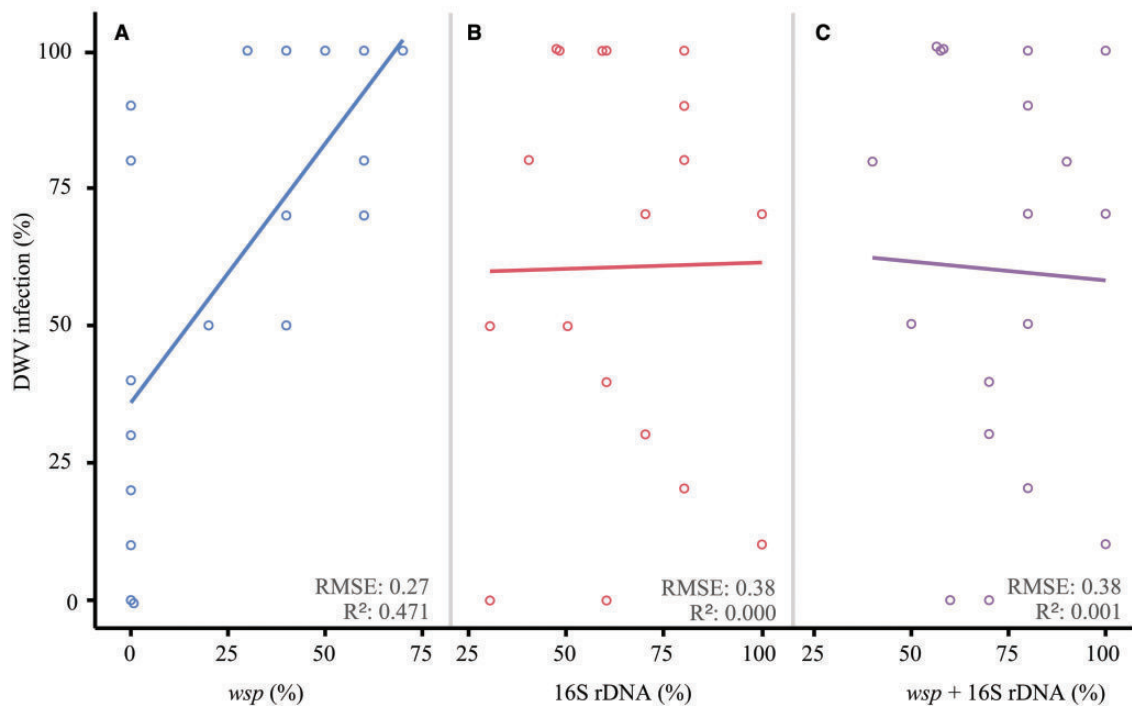


Fig. 2. Relationship between *Wolbachia* prevalence and Deformed Wing Virus (DWV) load in *Varroa* mites. When using the *wsp* primer (A) a positive linear correlation between *Wolbachia* prevalence and DWV load can be detected, in accordance with our hypothesis on pro-pathogenic function of *Wolbachia* infection in *Varroa*. No such relation can be detected upon using the 16S rDNA primer (B) and the additive combination of *wsp* with 16S rDNA primer (C). R^2 and RSME (root-mean-square error) given as estimates for goodness of fit. For better visual presentation overlapping points were jittered.

mentioned species (Hoffmann and Turelli 1988, Schuler et al. 2016). Our observed intermediate *Wolbachia* frequencies in *V. destructor* differ from this general pattern and resemble the frequencies of the two-spotted spider mite *Tetranychus urticae*. This plant herbivore has been extensively studied for *Wolbachia* infection and showed a remarkable temporal and local variation in infection frequencies that ranged between 2.5% and 77.5%, with a median of ~30% (Chen et al. 2009, Yu et al. 2011, Su et al. 2012). Although the factors that drive *Wolbachia* infection dynamics in *T. urticae* are not well understood, this case suggests that *Wolbachia* frequencies can fluctuate around intermediate levels without spreading to fixation or going to extinction. This may also be the case in *V. destructor*, especially when considering the relatively young age of this system. Currently, the system is most likely not evolutionary stable, and instead, strong coevolutionary dynamics are dominating.

In this study, we give a first indication of whether *Wolbachia* infections in *V. destructor* correlates in a pro-pathogenic, neutral, or anti-pathogenic manner with DWV. Our analysis revealed a significant positive correlation between *Wolbachia* infection measured by the *wsp* primer and DWV (Fig. 2). The results based on 16S rDNA and the additive combination of both primers, however, revealed no significant correlation, suggesting that the presence of *Wolbachia* is not correlated to DWV infection (Fig. 2). These results are puzzling at a first sight. A possible explanation is that the *Wolbachia*-infected mites differ with respect to *Wolbachia* titer, and possibly also with respect to the number of present *Wolbachia* strains. The positive correlation between *wsp* and DWV may then be the result of an increased susceptibility to the virus in mites with high *Wolbachia* titer and/or the presence of certain *Wolbachia* strains. However, a more in depth quantitative analysis is needed to answer whether high *Wolbachia* titers and/or certain *Wolbachia* strains really have a pro-pathogenic effect on DWV. Furthermore, the results strongly

suggest careful choice of *Wolbachia*-primers in future studies, especially in systems with presumably low titers.

With our approach, we cannot rule out whether the *Wolbachia* found in mites results from a true infection of the mite or rather from ingested honey bee hemolymph, which was infected with *Wolbachia*. For example, in *Metaseiulus occidentalis* mites, mite starvation reduced and eliminated *Wolbachia* detection (Wu and Hoy 2012). Therefore, the question remains whether *Wolbachia* is a true endosymbiont of *V. destructor*. Future studies should consider starving mites or collecting the respective hosting bee to add to our understanding. Nevertheless, in this study we give a first indication of whether *Wolbachia* infections in *V. destructor* correlates in a pro-pathogenic, neutral, or anti-pathogenic with DWV.

In conclusion, we found strong evidence for intermediate *Wolbachia* frequencies in *V. destructor*, but based on the presented data, we can neither conclude nor disprove that *Wolbachia* affects DWV. We suggest that additional quantitative information on *Wolbachia* and the internal virus titers of corresponding mites will contribute to a better understanding of the role of *Wolbachia* in the composition of the *V. destructor* virome. Furthermore, future studies should consider artificial infection experiments in mite backgrounds with and without *Wolbachia*, as well as differing *Wolbachia* titers and DWV concentrations. These data may reveal the answer to the important question: Do *Wolbachia* infections in *Varroa* mites, and their temporal and spatial variation, play a role the epidemiology of virus infections in bees and possibly influence colony losses?

Supplementary Data

Supplementary data are available at *Journal of Insect Science* online.

Acknowledgments

We gratefully thank H. Strasser, E. Leider, and U. Hubbe for sample collection. This project was funded by the Volkswagen Foundation's Initiative on Evolutionary Biology with grants to G.J. and A.T. S.D., T.G., and G.J. are funded within the LOEWE Center for Insect Biotechnology and Bioresources (ZIB), granted by the German state of Hessen's excellence initiative. G.J. as well as J.F.S. and A.T. were supported by the German Science Foundation (SPP 1399, JO 962/1-1 and TE 976/2-1).

References Cited

- Alaux, C., J.-L. Brunet, C. Dussaubat, F. Mondet, S. Tchamitchan, and M. Cousin. 2010. Interactions between *Nosema* microspores and a neonicotinoid weaken honeybees (*Apis mellifera*). *Environ. Microbiol.* 12: 774–782.
- Anderson, D. L., and J. W. Trueman. 2000. *Varroa jacobsoni* (Acari: Varroidae) is more than one species. *Exp. Appl. Acarol.* 24: 165–189.
- Bascompte, J., P. Jordano, and J. M. Olesen. 2006. Asymmetric coevolutionary networks facilitate biodiversity maintenance. *Science* 312: 431–433.
- Baton, L. A., E. C. Pacidônio, D. Gonçalves, and L. A. Moreira. 2013. wFlu: characterization and evaluation of a native *Wolbachia* from the mosquito *Aedes fluviatilis* as a potential vector control agent. *PLoS One* 8: e59619.
- Bäumler, A. J., and V. Sperandio. 2016. Interactions between the microbiota and pathogenic bacteria in the gut. *Nature* 535: 85–93.
- Beckmann, J. F., and A. M. Fallon. 2012. Decapitation improves detection of *Wolbachia pipiensis* (Rickettsiales: Anaplasmataceae) in *Culex pipiens* (Diptera: Culicidae) mosquitoes by the polymerase chain reaction. *J. Med. Entomol.* 49: 1103–1108.
- Berthoud, H., A. Imdorf, M. Haueter, S. Radloff, and P. Neumann. 2010. Virus infections and winter losses of honey bee colonies (*Apis mellifera*). *J. Apicult. Res.* 49: 60–65.
- Bian, G., Y. Xu, P. Lu, Y. Xie, and Z. Xi. 2010. The endosymbiotic bacterium *Wolbachia* induces resistance to dengue virus in *Aedes aegypti*. *PLoS Pathog.* 6: e1000833.
- Blacquièrre, T., G. Smagghe, C. A. M. van Gestel, and V. Mommaerts. 2012. Neonicotinoids in bees: a review on concentrations, side-effects and risk assessment. *Ecotoxicology* 21: 973–992.
- Bordenstein, S. R., P. O'Hara, and J. H. Werren. 2001. *Wolbachia*-induced incompatibility precedes other hybrid incompatibilities in *Nasonia*. *Nature* 409: 707–710.
- Bowen-Walker, P. L., J. Martin, and A. Gunn. 1999. The transmission of deformed wing virus between honeybees (*Apis mellifera* L.) by the ectoparasitic mite *Varroa jacobsoni* Oud. *J. Invertebr. Pathol.* 73: 101–106.
- Brodschneider, R., and K. Crailsheim. 2010. Nutrition and health in honey bees. *Apidologie* 41: 278–294.
- Chen, X.-L., R. Xie, G. Q. Li, and X. Y. Hong. 2009. Simultaneous detection of endosymbionts *Wolbachia* and *Cardinium* in spider mites (Acari: Tetranychidae) by multiplex-PCR. *Int. J. Acarol.* 35: 397–403.
- Cox-Foster, D. L., Conlan, E. C. Holmes, G. Palacios, J. D. Evans, and N. A. Moran. 2007. A metagenomic survey of microbes in honey bee colony collapse disorder. *Science* 318: 283–287.
- Dainat, B., J. D. Evans, Y. P. Chen, and P. Neumann. 2011. Sampling and RNA quality for diagnosis of honey bee viruses using quantitative PCR. *J. Virol. Methods* 174: 150–152.
- Dainat, B., J. D. Evans, Y. P. Chen, L. Gauthier, and P. Neumann. 2012a. Dead or alive: deformed wing virus and *Varroa destructor* reduce the life span of winter honeybees. *Appl. Environ. Microbiol.* 78: 981–987.
- Dainat, B., J. D. Evans, Y. P. Chen, L. Gauthier, and P. Neumann. 2012b. Predictive markers of honey bee colony collapse. *PLoS One* 7: e32151.
- de Miranda, J. R., and E. Genersch. 2010. Deformed wing virus. *J. Invert. Pathol.* 103(Suppl): S48–S61.
- de Oliveira, C. D., S. Gonçalves, L. A. Baton, P. H. F. Shimabukuro, F. D. Carvalho, and L. A. Moreira. 2015. Broader prevalence of *Wolbachia* in insects including potential human disease vectors. *Bull. Entomol. Res.* 105: 305–315.
- Dennison, N. J., N. Jupatanakul, and G. Dimopoulos. 2014. The mosquito microbiota influences vector competence for human pathogens. *Curr. Opin. Insect Sci.* 3: 6–13.
- Di Pasquale, G., M. Salignon, Y. Le Conte, L. P. Belzunces, A. Decourtye, and A. Kretzschmar. 2013. Influence of pollen nutrition on honey bee health: do pollen quality and diversity matter?. *PLoS One.* 8: e72016.
- Dutton, T. J., and S. P. Sinkins. 2005. Filarial susceptibility and effects of *Wolbachia* in *Aedes pseudoscutellaris* mosquitoes. *Med. Vet. Entomol.* 19: 60–65.
- Dyer, K. A., and J. Jaenike. 2004. Evolutionarily stable infection by a male-killing endosymbiont in *Drosophila innubila*. *Genetics* 168: 1443–1455.
- EFSA 2008. Bee mortality and bee surveillance in Europe. *Efsa J.* 154: 1–28.
- Ellis, J. D., and P. A. Munn. 2005. The worldwide health status of honey bees. *Bee World* 86: 88–101.
- Engelstädter, J., and A. Telschow. 2009. Cytoplasmic incompatibility and host population structure. *Heredity* 103: 196–207.
- Fontaine, C., I. Dajoz, J. Meriguet, and M. Loreau. 2005. Functional diversity of plant–pollinator interaction webs enhances the persistence of plant communities. *PLoS Biol.* 4: e1.
- Francis, R. M., L. Nielsen, and P. Kryger. 2013. *Varroa*-virus interaction in collapsing honey bee colonies. *PLoS One* 8: e57540.
- Gauthier, L., Tentcheva, D. M. Tournaire, B. Dainat, F. Cousserans, Amd, and M. E. Colin. 2007. Viral load estimation in asymptomatic honey bee colonies using the quantitative RT-PCR technique. *Apidologie* 38: 426–435.
- Genersch, E. 2005. Development of a rapid and sensitive RT-PCR method for the detection of deformed wing virus, a pathogen of the honeybee (*Apis mellifera*). *Vet. J.* 169: 121–123.
- Genersch, E., W. von der Ohe, H. Kaatz, A. Schroeder, C. Otten, and R. Büchler. 2010. The German bee monitoring project: a long term study to understand periodically high winter losses of honey bee colonies. *Apidologie* 41: 332–352.
- Goulson, D. 2013. REVIEW: An overview of the environmental risks posed by neonicotinoid insecticides. *J. Appl. Ecol.* 50: 977–987.
- Goulson, D., E. Nicholls, C. Botías, and E. L. Rotheray. 2015. Bee declines driven by combined stress from parasites, pesticides, and lack of flowers. *Science* 347: 1255957.
- Highfield, A. C. El Nagar, L. C. M. Mackinder, L. M. L. J. Noël, M. J. Hall, and S. J. Martin. 2009. Deformed wing virus implicated in overwintering honeybee colony losses. *Appl. Environ. Microbiol.* 75: 7212–7220.
- Hilgenboecker, K. P., Hammerstein, A. Schlattmann, A. Telschow, and J. H. Werren. 2008. How many species are infected with *Wolbachia*? – a statistical analysis of current data: *Wolbachia* infection rates. *FEMS Microbiol. Lett.* 281: 215–220.
- Hoffmann, A. A., and M. Turelli. 1988. Unidirectional incompatibility in *Drosophila Simulans*: inheritance, geographic variation and fitness effects. *Genetics* 119: 435–444.
- Hussain, M., G. Lu, S. Torres, J. H. Edmonds, B. H. Kay, and A. A. Khromykh. 2013. Effect of *Wolbachia* on replication of West Nile virus in a mosquito cell line and adult mosquitoes. *J. Virol.* 87: 851–858.
- Joanne, S., I. Vythilingam, N. Yugavathy, C. S. Leong, M. L. Wong, and S. AbuBakar. 2015. Distribution and dynamics of *Wolbachia* infection in Malaysian *Aedes albopictus*. *Acta Trop.* 148: 38–45.
- Kamada, N., G. Y. Chen, N. Inohara, and G. Núñez. 2013. Control of pathogens and pathobionts by the gut microbiota. *Nat. Immunol.* 14: 685–690.
- Kitrayapong, P., V. Baimai, and S. L. O'Neill. 2002. Field prevalence of *Wolbachia* in the mosquito vector *Aedes albopictus*. *Am. J. Trop. Med. Hyg.* 66: 108–111.
- Klein, A.-M., E. Vaissière, J. H. Cane, I. Steffan-Dewenter, S. A. Cunningham, and C. Kremen. 2007. Importance of pollinators in changing landscapes for world crops. *Proc. R. Soc. Lond B Biol. Sci.* 274: 303–313.
- Kriesner, P., A. Hoffmann, S. F. Lee, M. Turelli, and A. R. Weeks. 2013. Rapid sequential spread of two *Wolbachia* variants in *Drosophila simulans*. *PLoS Pathog.* 9: e1003607.
- Le Conte, Y., M. Ellis, and W. Ritter. 2010. *Varroa* mites and honey bee health: can *Varroa* explain part of the colony losses?. *Apidologie* 41: 353–363.
- Marcon, H. S., E. Coscrato, D. Selivon, A. L. P. Perondini, and C. L. Marino. 2011. Variations in the sensitivity of different primers for detecting *Wolbachia* in *Anastrepha* (diptera: tephritidae). *Braz. J. Microbiol.* 42: 778–785.

- Martin, S. J., C. Highfield, L. Brettell, E. M. Villalobos, G. E. Budge, and M. Powell. 2012. Global honey bee viral landscape altered by a parasitic mite. *Science* 336: 1304–1306.
- Mondet, F., J. R. de Miranda, A. Kretzschmar, Y. Le Conte, and A. R. Mercer. 2014. On the front line: quantitative virus dynamics in honeybee (*Apis mellifera* L.) colonies along a new expansion front of the parasite *Varroa destructor*. *PLoS Pathog.* 10: e1004323.
- Moreira, L. A., Iturbe-Ormaetxe, J. A. Jeffery, G. Lu, A. T. Pyke, and L. M. Hedges. 2009. A *Wolbachia* symbiont in *Aedes aegypti* limits infection with dengue, chikungunya, and *Plasmodium*. *Cell* 139: 1268–1278.
- Nazzi, F., S. P. Brown, D. Annoscia, F. Del Piccolo, G. Di Prisco, and P. Varricchio. 2012. Synergistic parasite-pathogen interactions mediated by host immunity can drive the collapse of honeybee colonies. *PLoS Pathog.* 8: e1002735.
- O'Neill, S. L., Giordano, A. M. Colbert, T. L. Karr, and H. M. Robertson. 1992. 16S rRNA phylogenetic analysis of the bacterial endosymbionts associated with cytoplasmic incompatibility in insects. *Proc. Natl. Acad. Sci.* 89: 2699–2702.
- Pattabhiramaiah, M., D. Brückner, and M. S. Reddy. 2010. Horizontal transmission of *Wolbachia* in the honeybee subspecies *Apis mellifera carnica* and its ectoparasite *Varroa destructor*. *Int. J. Environ. Sci.* 2: 526–535.
- Potts, S. G., C. Biesmeijer, C. Kremen, P. Neumann, O. Schweiger, and W. E. Kunin. 2010a. Global pollinator declines: trends, impacts and drivers. *Trends Ecol. Evol.* 25: 345–353.
- Potts, S. G., P. M. Roberts, R. Dean, G. Marris, M. A. Brown, and R. Jones. 2010b. Declines of managed honey bees and beekeepers in Europe. *J. Apicul. Res.* 49: 15–22.
- Rasgon, J. L., and T. W. Scott. 2003. *Wolbachia* and cytoplasmic incompatibility in the California *Culex pipiens* mosquito species complex: parameter estimates and infection dynamics in natural populations. *Genetics* 165: 2029–2038.
- Rosenkranz, P., P. Aumeier, and B. Ziegelmann. 2010. Biology and control of *Varroa destructor*. *J. Invert. Pathol.* 103: S96–S119.
- Ryabov, E. V., R. Wood, J. M. Fannon, J. D. Moore, J. C. Bull, and D. Chandler. 2014. A virulent strain of Deformed Wing Virus (DWV) of honeybees (*Apis mellifera*) prevails after *Varroa destructor*-mediated, or in vitro, transmission. *PLoS Pathog.* 10: e1004230.
- Sandrock, C., M. Tanadini, L. G. Tanadini, A. Fauser-Mislin, S. G. Potts, and P. Neumann. 2014. Impact of chronic neonicotinoid exposure on honeybee colony performance and queen superseding. *PLoS One* 9: e103592.
- Schneider, D. I., Klasson, A. E. Lind, and W. J. Miller. 2014. More than fishing in the dark: PCR of a dispersed sequence produces simple but ultrasensitive *Wolbachia* detection. *BMC Microbiol.* 14: 121.
- Schroeder, D. C., and S. J. Martin. 2012. Deformed wing virus: The main suspect in unexplained honeybee deaths worldwide. *Virulence* 3: 589–591.
- Simoes, P. M., Mialdea, D. Reiss, M. F. Sagot, and S. Charlat. 2011. *Wolbachia* detection: an assessment of standard PCR Protocols. *Mol. Ecol. Resour.* 11: 567–572.
- Spleen, A. M., J. Lengerich, K. Rennich, D. Caron, R. Rose, and J. S. Pettis. 2013. A national survey of managed honey bee 2011–12 winter colony losses in the United States: results from the Bee Informed Partnership. *J. Apicul. Res.* 52: 44–53.
- Steinhauer, N. A., Rennich, M. E. Wilson, D. M. Caron, E. J. Lengerich, and J. S. Pettis. 2014. A national survey of managed honey bee 2012–2013 annual colony losses in the USA: results from the Bee Informed Partnership. *J. Apicul. Res.* 53: 1–18.
- Sumpter, D. J. T., and S. J. Martin. 2004. The dynamics of virus epidemics in *Varroa*-infested honey bee colonies. *J. Anim. Ecol.* 73: 51–63.
- Tsai, K.-H., G. Huang, W. J. Wu, C. K. Chuang, C. C. Lin, and W. J. Chen. 2006. Parallel infection of Japanese encephalitis virus and *Wolbachia* within cells of mosquito salivary glands. *J. Med. Entomol.* 43: 752–756.
- Unckless, R. L., and J. Jaenike. 2012. Maintenance of a male-killing *Wolbachia* in *Drosophila innubila* by male-killing dependent and male-killing independent mechanisms. *Evology* 66: 678–689.
- van der Zee, R., R. Brodschneider, V. Brusbardis, J. D. Charrière, R. Chlebo, and M. F. Coffey. 2014. Results of international standardised beekeeper surveys of colony losses for winter 2012–2013: analysis of winter loss rates and mixed effects modelling of risk factors for winter loss. *J. Apicul. Res.* 53: 19–34.
- van der Zee, R., L. Pisa, S. Andonov, R. Brodschneider, J. D. Charrière, and R. Chlebo. 2012. Managed honey bee colony losses in Canada, China, Europe, Israel and Turkey, for the winters of 2008-9 and 2009-10. *J. Apicul. Res.* 51: 100–114.
- van Engelsdorp, D., and M. D. Meixner. 2010. A historical review of managed honey bee populations in Europe and the United States and the factors that may affect them. *J. Invert. Pathol.* 103(Suppl): S80–S95.
- van Engelsdorp, D., J. D. Evans, C. Saegerman, C. Mullin, E. Haubruge, and B. K. Nguyen. 2009. Colony collapse disorder: a descriptive study. *PLoS One.* 4: e6481.
- Vogt, S. L., Peña-Díaz, and B. B. Finlay. 2015. Chemical communication in the gut: Effects of microbiota-generated metabolites on gastrointestinal bacterial pathogens. *Anaerobe* 34: 106–115.
- Weinert, L. A., V. Araujo-Jnr, M. Z. Ahmed, and J. J. Welch. 2015. The incidence of bacterial endosymbionts in terrestrial arthropods. *Proc. R. Soc. B: Biol. Sci.* 282: 20150249–20150249.
- Werren, J. H., Baldo, and M. E. Clark. 2008. *Wolbachia*: master manipulators of invertebrate biology. *Nat. Rev. Microbiol.* 6: 741–751.
- Wu, K., and Hoy M. A. 2012. Extended starvation reduced and eliminated *Wolbachia*, but not *Cardinium*, from *Metaseiulus occidentalis* females (Acari: Phytoseiidae): A need to reassess *Wolbachia*'s status in this predatory mite? *Journal of Invertebrate Pathology.* 109, 20–26.
- Yang, X., and D. L. Cox-Foster. 2005. Impact of an ectoparasite on the immunity and pathology of an invertebrate: evidence for host immunosuppression and viral amplification. *Proc. Natl. Acad. Sci. USA* 102: 7470–7475.
- Yu, M.-Z., J. Zhang, X. F. Xue, and X. Y. Hong. 2011. Effects of *Wolbachia* on mtDNA variation and evolution in natural populations of *Tetranychus urticae* Koch. *Insect Mol. Biol.* 20: 311–321.
- Yue, C., E. Genersch. 2005. RT-PCR analysis of Deformed wing virus in honeybees (*Apis mellifera*) and mites (*Varroa destructor*). *J. Gen. Virol.* 86: 3419–3424.
- Zha, X., W. Zhang, C. Zhou, L. Zhang, Z. Xiang, and Q. Xia. 2014. Detection and characterization of *Wolbachia* infection in silkworm. *Genet. Mol. Biol.* 37: 573–580.
- Zhou, W., F. Rousset, and S. O'Neill. 1998. Phylogeny and PCR-based classification of *Wolbachia* strains using *wsp* gene sequences. *Proc. R. Soc. Lond. B Biol. Sci.* 265: 509–515.
- Zug, R., and P. Hammerstein. 2015. Bad guys turned nice? A critical assessment of *Wolbachia* mutualisms in arthropod hosts: *Wolbachia* mutualisms in arthropods. *Biol. Rev.* 90: 89–111.

Honeybee colonies compensate for pesticide-induced brood mortality at the cost of reproductive success

Matthias Schott^{1,2}, Maximilian Sandmann¹, James Cresswell³, Matthias A. Becher⁴, Gerrit Eichner⁵, Dominique Tobias Brandt⁶, Rayko Halitschke⁷, Stephanie Krueger⁸, Gertrud Morlock⁸, Rolf-Alexander Düring⁹, Andreas Vilcinskas², Marina Doris Meixner¹, Ralph Bächler¹, Anneli Brandt^{1*}

¹LLH Bee Institute, Erlenstr. 9, 35274 Kirchhain, Germany; ²Institute of Insect biotechnology, Justus-Liebig-University Giessen, Giessen, Germany; ³Biosciences, University of Exeter, Exeter, EX4 4PS, UK; ⁴Environment & Sustainability Institute, Biosciences, University of Exeter, Penryn Campus, Penryn, Cornwall TR10 9FE, UK; ⁵Mathematical Institute, Justus-Liebig University of Giessen, Giessen, Germany; ⁶Institute of Pharmacology, Biochemical-Pharmacological Centre (BPC), University of Marburg, Karl-von-Frisch-Str. 1, 35032 Marburg, Germany; ⁷Department of Molecular Ecology, Max Planck Institute for Chemical Ecology, Hans Knöll Str. 8, 07745 Jena, Germany; ⁸Chair of Food Science, Institute of Nutritional Science, Justus Liebig University Giessen, Heinrich-Buff-Ring 26-32, 35392 Giessen; ⁹Institute of Soil Science and Soil Conservation, Justus-Liebig-University of Giessen, Heinrich-Buff-Ring 58, 35392 Giessen, Germany

*Corresponding author

Anneli Brandt

Bee Institute Kirchhain

Erlenstr. 9,

35274 Kirchhain, Germany

E-mail: anneli.brandt@llh.hessen.de

Tel.: +49 6422 940632, Fax: +49 6422 940633

Abstract

Sublethal doses of pesticides affect individual honeybees, but colony-level effects are less well understood and it is unclear how the two levels integrate. We studied the effect of the neonicotinoid pesticide clothianidin at field realistic concentrations on small colonies. We found that exposure to clothianidin affected royal jelly production of individual workers and created a strong dose-dependent increase in mortality of individual larvae, but strikingly the population size of capped brood remained stable. Thus, hives exhibited short-term resilience. Using a demographic matrix model, we found that the basis of resilience in dosed colonies was a substantive increase in brood initiation rate to compensate for increased brood mortality. However, computer simulation of full size colonies revealed that the increase in brood initiation led to severe reductions in colony reproduction (swarming) and long-term survival. This experiment reveals social regulatory mechanisms on colony-level that enable honeybees to partly compensate for effects on individual level.

Key words: *Apis mellifera*, neonicotinoid, nurse bee, hypopharyngeal gland, brood development

Introduction

Honeybees provide vital pollination services to crops and wild plants and thus play a key role in global food security and the maintenance of biodiversity^{1,2}. However, the number of managed honeybees has declined over the last few decades in North America³⁻⁵ and Europe^{5,6}. This substantial environmental impact on honeybee colonies is thought to be driven mainly by pathogens and parasites⁷, but the quality and diversity of the pollen diet⁸⁻¹⁰ as well as exposure to pesticides^{5,11} may also affect bee health and survival. In particular, the widespread use of neonicotinoids is considered a major threat to honeybee health^{5,12-17}. Neonicotinoid insecticides are among the most important crop protection chemicals and they are widely used in seed dressings and spray applications^{13,14,18}. Neonicotinoids are neurotoxins that act as nicotinic acetylcholine receptor agonists to disrupt neuronal cholinergic signal transduction, leading to abnormal behavior in target pests, or immobility and death at higher doses^{13,19,20}. Non-target insects such as bees also come into contact with these systemic insecticides via pollen, nectar or guttation droplets. Insecticide residues are carried back to the colony by forager bees and remain stored in bee bread or honey until they are fed to larvae, workers, drones, or the queen^{7,21,22}.

Honeybees are highly eusocial insects, with labor division and intensive brood care, where adult members of a colony care cooperatively for the young²³. As nurse bees, young workers produce brood food (royal jelly) in the hypopharyngeal gland (HPG). The development of this gland begins soon after hatching, and the lobes of the gland (acini) reach their maximum size and weight when the workers are 8–12 days old^{24,25}. Several chemical compounds reduce the size of the HPG in nurse bees: neonicotinoid insecticides, the varroacide coumaphos, the insect growth regulator fenoxycarb, and the fungicide captan²⁶⁻²⁹. The effect of neonicotinoids on brood mortality is a matter of discussion. Laboratory survival tests show that artificially-reared larvae can consume neonicotinoids in quantities larger than would ever be encountered in the field without direct lethal effects³⁰. However, a reduced number of brood cells has been observed in some field studies^{11,31} which may indicate that neonicotinoids affect brood mortality indirectly, for example due to insufficient brood care by nurse bees affected by the pesticides.

Numerous studies have demonstrated that neonicotinoids affect the behavioral or physiological traits of individual honeybees^{21,32-35}. However, the assessment of the impact on colony growth and survival has been divergent, ranging from negative impact³⁶⁻³⁹ to no impact³⁹⁻⁴³, sometimes even in the same study³⁸. We therefore investigated this phenomenon using small nucleus colonies rather than full-sized standard colonies, thus reducing the number of individuals substantially. This allowed us to study the sublethal effects of the neonicotinoid clothianidin at the physiological level in individual larvae and nurse bees and also to determine its impact on brood development of an entire colony.

Using a demographic modeling approach, we tested for compensatory mechanisms at the colony level and extrapolated the results from small nucleus colonies to full-sized colonies using the agent-based honeybee model BEEHAVE⁴⁴.

Results

The experimental scheme, climate recordings, clothianidin levels in the spiked feeding solutions, clothianidin residues in worker bees, protein content and antimicrobial activity of royal jelly and the statistical report are presented in the supplementary data (**Figs S1–S4**).

Hypopharyngeal gland size

After spending 12 days in the experimental colonies, age-defined workers of the control hives had significantly larger acini than those of colonies exposed to clothianidin (**Fig. 1A–C**; Mixed-effects ANOVA $P = 0.01199$, *post hoc* Dunnett contrasts: control vs. 1 $\mu\text{g/L}$: $P < 0.001$; control vs. 10 $\mu\text{g/L}$: $P = 0.03447$; control vs. 100 $\mu\text{g/L}$ $P = 0.00269$). The mean diameters of the acini were 171.22 μm (SEM = 2.24, $n = 31$) for the controls, 129.66 μm (SEM = 8.60, $n = 22$) in the 1 $\mu\text{g/L}$ group, 147.92 μm (SEM = 5.79, $n = 22$) in the 10 $\mu\text{g/L}$ group, and 131.06 μm (SEM = 6.39, $n = 23$) in the 100 $\mu\text{g/L}$ group.

In addition, we measured the acinus diameter of randomly chosen worker bees of undefined age during week 7. The mean diameters of the acini were 144.36 μm (SEM = 4.43, $n = 28$) for the controls, 133.59 μm (SEM = 7.61, $n = 22$) in the 1 $\mu\text{g/L}$ group, 138.04 μm (SEM = 5.02, $n = 22$) in the 10 $\mu\text{g/L}$ group, and 109.39 μm (SEM = 4.83, $n = 29$) in the 100 $\mu\text{g/L}$ group. Workers in the control hives had significantly larger acini than those exposed to 100 $\mu\text{g/L}$ clothianidin (mixed-effects ANOVA $P = 0.01379$; *post hoc* Dunnett contrasts: control vs. 100 $\mu\text{g/L}$: $P = 0.000699$).

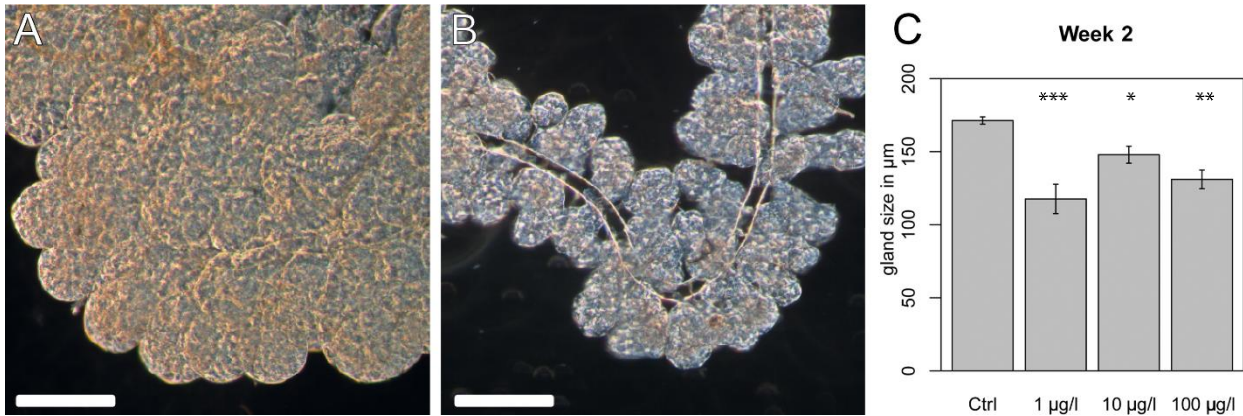


Fig 1. Hypopharyngeal gland size in age-defined worker bees. Age-defined worker bees, which were placed in the colonies and recovered in week 2 (12 days after hatching), were analyzed for the acini size of the HPG. (A) HPG of a control worker bee. (B) HPG of a worker bee from a colony exposed to 100 µg/L clothianidin (bar = 100 µm). (C) Clothianidin exposure reduced the acinus diameter of HPGs. Control (Ctrl) individuals had larger acini than workers exposed to clothianidin (control, n = 31; 1 µg/L, n = 22; 10 µg/L, n = 22; 100 µg/L, n = 23). Mixed-effects ANOVA, $P = 0.0120$; *post hoc* Dunnett contrasts, control vs. 1 µg/L, $P < 0.001$; control vs. 10 µg/L, $P = 0.0345$; control vs. 100 µg/L, $P = 0.0027$). Raw data and technical details of the analysis are presented in the supplementary statistical report, section 2.1.

HPTLC analysis of royal jelly and larvae

The lipid composition of royal jelly during weeks 3 and 7 was analyzed using non-targeted High-performance thin-layer chromatography (HPTLC). Quantitative differences in the lipid composition were observed in the 10 and 100 µg/L clothianidin treatment groups compared to the control colonies in week 3. Both, a clear reduction of lipids (**Fig 2A**) and in the antimicrobial activity against the luminescent *A. fischeri* bacteria (**SFig 23**)⁴⁵ were observed. The blank Sugi strips as well as the part of the Sugi test strip that had not contacted the sample showed no lipid signals. The results of the combined, orthogonal physicochemical analysis and activity-based detection of HPTLC-separated compounds suggest a decline in antimicrobial activity corresponding to the decline in the amount of lipids in the royal jelly. The lipid profiles of larvae also showed clear differences between the different treatment groups during week 3 (**Fig. 2B, C**). The profiling of larval liposoluble components showed a similar decline in the concentration of several compounds in colonies treated with 10 and 100 µg/L clothianidin compared to untreated control larvae.

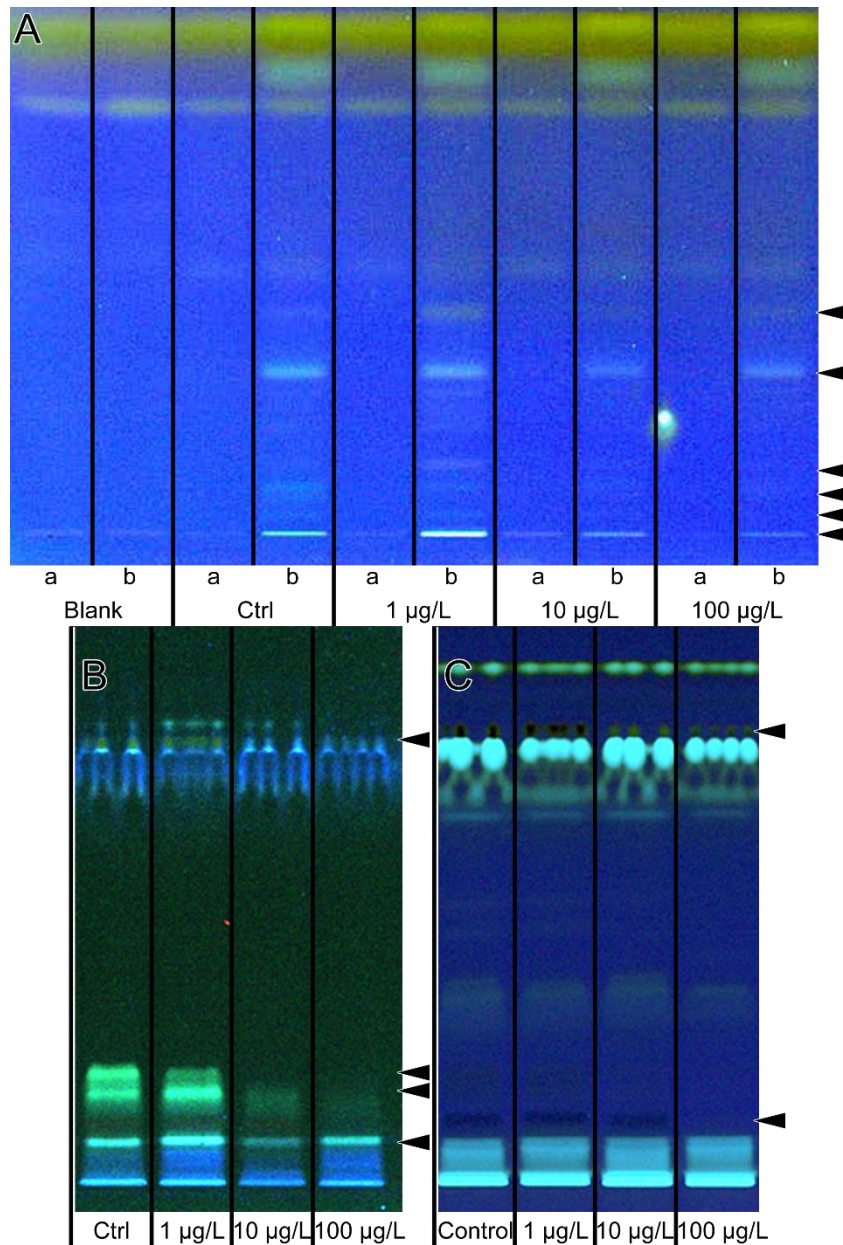


Fig 2. Lipid profiles of royal jelly samples (A) and larvae (B, C) from week 3. Samples of royal jelly were taken using absorptive filter strips (Sugi strips), extracted with *n*-hexane and separated by HPTLC. Each Sugi strip was halved: one half without the sample (track a) and the other with absorbed sample (track b). A fresh Sugi strip from the same batch as the strips used in the experiment cut in two equal halves served as the blank. The lanes are labeled to show the dose of clothianidin treatments (Ctrl = no clothianidin). The analysis of larvae is shown before (B) and after derivatisation (C). For royal jelly, the declining quantity of substances was observed for the lipid profiling (UV 366 nm after derivatization). The latter also was evident for the larvae.

Brood survival

To assess whether clothianidin exposure affected brood survival, we traced the development of individual, newly-hatched larvae. At the beginning of the experiment (brood survival phase A, weeks 1–4) as shown in **Fig. 3A**, an average of 78% of the tracked larvae in control colonies developed normally to capped brood and the cells were empty within the expected time frame (SD 8.2%, for a total of 230 larvae in week 1 in $n = 4$ hives), which was considered as survival of the larvae. In contrast, an average of only 54% of the larvae in the 1 $\mu\text{g/L}$ treatment group survived (SD 11%, for a total of 244 larvae in week 1 in $n = 4$ hives). In colonies exposed to 10 $\mu\text{g/L}$ clothianidin, only 46% of the larvae survived (SD 24%, for a total of 248 larvae in week 1 in $n = 4$ hives) of the monitored larvae survived. In the 100 $\mu\text{g/L}$ treatment group, only 52% of the larvae survived (SD 23%, for a total of 303 larvae in week 1 in $n = 5$ hives). Clothianidin exposure significantly affected the brood survival time (exposure-by-time interaction in mixed-effects ANOVA, $P = 0.02929$; one-sided tests for *post hoc* Dunnett contrasts in weeks 2 and 3). In week 2, none of the clothianidin treatments reduced brood survival significantly, but in week 3 each clothianidin treatment had a significant effect (control vs. 1 $\mu\text{g/L}$, $P = 0.0414$; control vs. 10 $\mu\text{g/L}$, $P = 0.0241$; control vs. 100 $\mu\text{g/L}$, $P = 0.0418$).

In brood survival phase B (weeks 4–7) as shown in **Fig. 3B**, the average brood survival was 82.9% (SD = 10.2%, for a total of 260 larvae in week 4 in $n = 4$ hives) in the control group, 34.6% (SD = 11.1%, for a total of 280 larvae in week 4 in $n = 4$ hives) in the 1 $\mu\text{g/L}$ treatment group, and 40.3% (SD = 23.5%, for a total of 218 larvae in week 4 in $n = 4$ hives) in the 10 $\mu\text{g/L}$ treatment group. In all colonies exposed to 100 $\mu\text{g/L}$ clothianidin, fewer than 50 larvae were present by week 4 (11–34 larvae per colony, with an average number of larvae of 19.25). The average brood survival was 6.7% (SD = 13.3%, for a total of 77 larvae in week 4 in $n = 4$ hives) in the 100 $\mu\text{g/L}$ group. Clothianidin exposure significantly affected brood survival over time (exposure-by-time interaction in mixed-effects ANOVA, $P = 0.03776$; one-sided tests for *post hoc* Dunnett contrasts in weeks 5 and 6 in each clothianidin treatment group revealed a significantly lower brood survival compared to the control group $P < 0.0001$ in all tests). For the detailed analysis, see the supplementary statistical report.

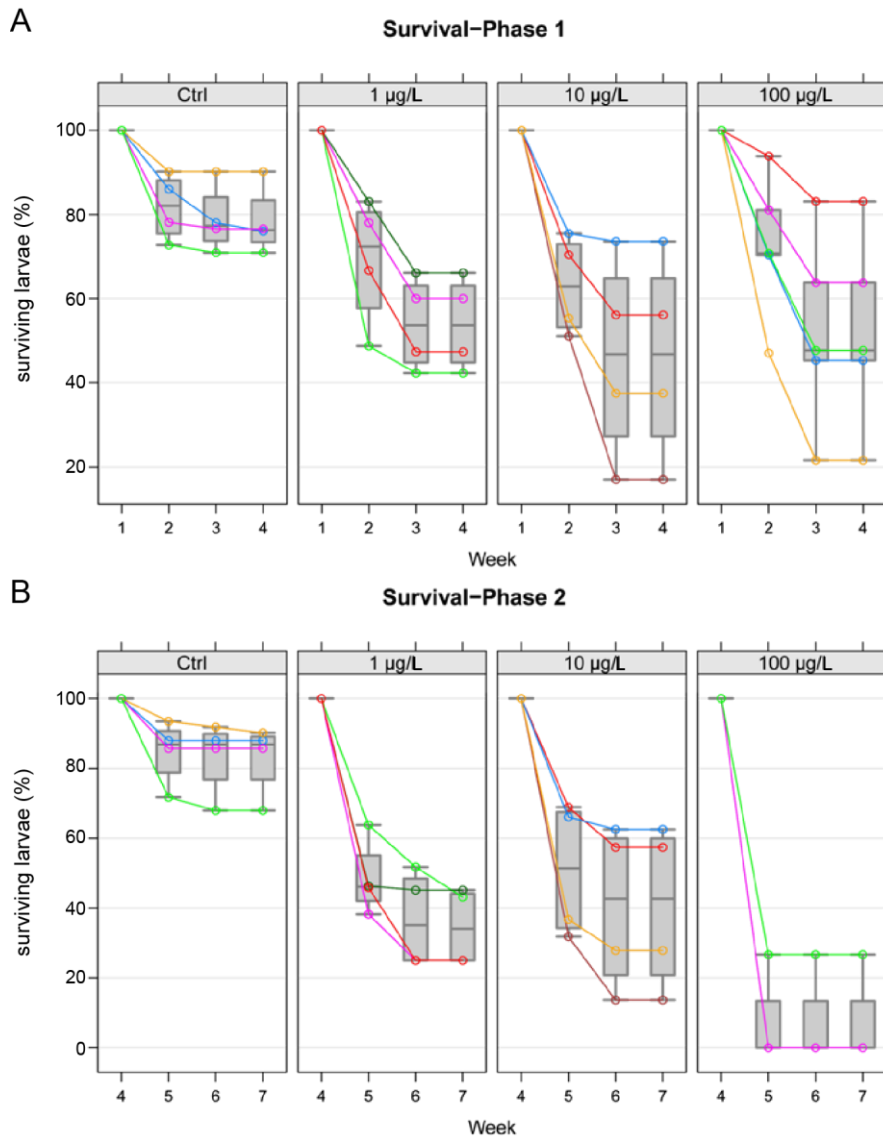


Fig 3. Survival of individually tracked larvae. Individually marked brood cells were tracked from the first larval stage (day 4–5 after egg laying) to emergence. (A) The percentage of brood surviving from week 1 to week 4 (survival phase A). Colonies exposed to clothianidin showed a reduced brood survival. Clothianidin exposure significantly affects brood survival (exposure-by-time interaction in mixed-effects ANOVA, $p = 0.0293$). One-sided tests for *post hoc* Dunnett contrasts yielded no significant P -values in week 2, but in week 3 all clothianidin treatments showed significant differences (control vs. 1 µg/L, $P = 0.0414$; control vs. 10 µg/L, $P = 0.0241$; control vs. 100 µg/L, $P = 0.0418$). (B) The percentage of brood surviving from week 4 to week 7 (survival phase B). Clothianidin exposure reduced the number of surviving brood (exposure-by-time interaction in mixed effects ANOVA, $P = 0.03776$). One-sided tests for *post hoc* Dunnett contrasts in weeks 5 and 6: each clothianidin treatment has a significantly lower brood survival than the control group ($P < 0.0001$ in all cases). Technical details of the analysis are provided in the supplementary statistical report, section 2.3.

Brood quantification

To achieve the total quantification of brood cells of a colony, all cells containing eggs, larvae, and pupae were counted at all sampling time points for each colony (**Fig. 4**). Detailed results and analysis are provided in the supplementary statistical report. The temporal profiles for the mean numbers of eggs differed significantly between the treatment groups (main effect of quadratic time and its interaction with treatment in a linear mixed-effects model, $P \ll 0.0001$). When comparing the parabolic temporal profiles of eggs in the treatment vs. control groups we observed significant differences in both the (local) slope during week 3 and the (global) curvature of the temporal trend in mean egg numbers ($P < 0.03$ in all tests except 100 $\mu\text{g/L}$ group vs. control, which showed no difference in curvature).

Likewise, the temporal profiles of the mean number of larvae differed significantly between the treatment groups (main effect of quadratic time and its interaction with treatment in a linear fixed-effects model, given that the random hive effect was non-significant, $P < 0.0001$). However, when comparing the parabolic temporal profiles of larvae in the treatment groups with the control, we found that only the profile of the 100 $\mu\text{g/L}$ treatment group differed significantly from the control in terms of the (local) slope during week 3 and the (global) curvature ($P < 0.014$ in both cases).

The temporal profiles of the mean numbers of capped brood cells also differed significantly between the treatment groups (main effect of quadratic time and its interaction with treatment in a linear fixed-effects model, given that the random hive effect was non-significant, $P = 0.00035$). And as for the larvae, comparing the parabolic profiles of capped brood cells in the treatment groups with the control, we found that only the profile of the 100 $\mu\text{g/L}$ group differed significantly from the control in terms of the (local) slope during week 3 and the (global) curvature ($P < 0.01$ in both cases).

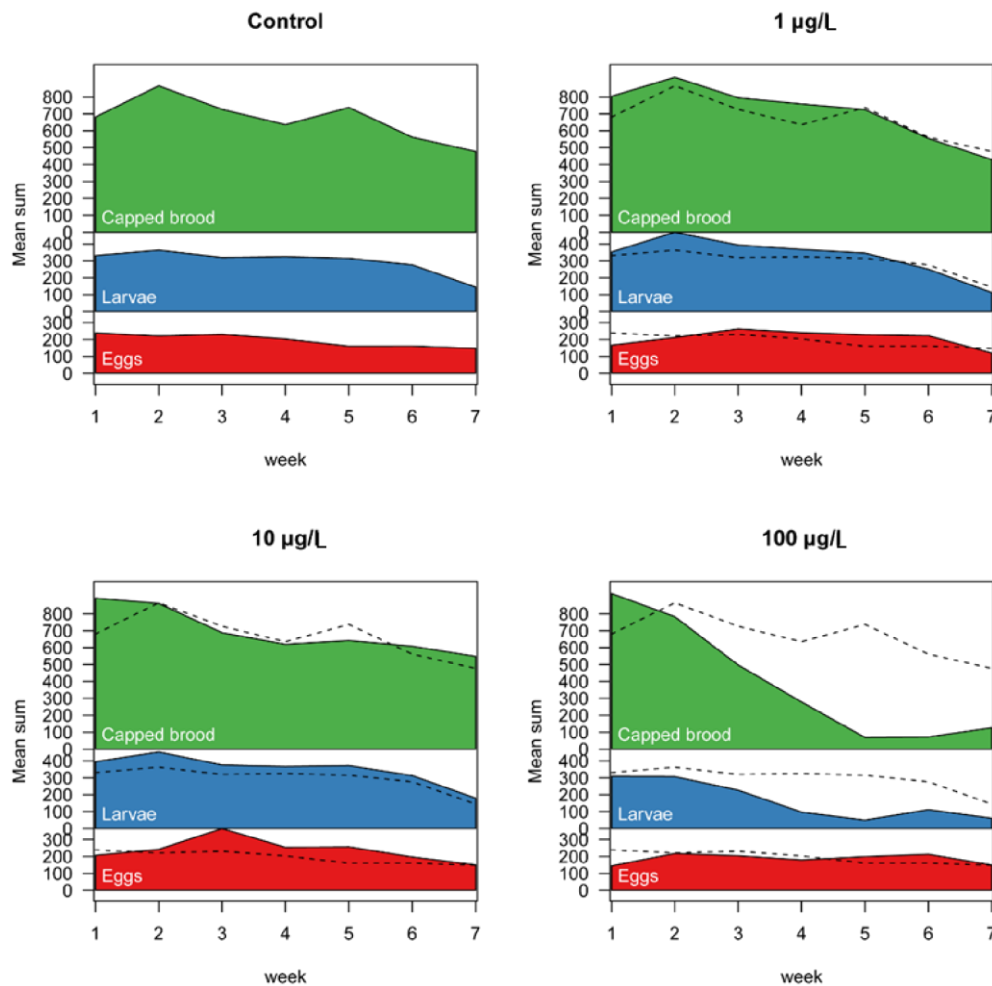


Fig 4. Brood quantification. Every week, the mean number of eggs (red), larvae (blue), and pupae (green) was determined for every colony over a period of 7 weeks. The black dashed line depicts the mean values of the control. In colonies exposed to lower or medium concentrations of clothianidin, the mean number of eggs, larvae or capped brood were similar or tended to exceed the numbers of the control group. The trends for the eggs, larvae, and capped brood cells all differed significantly between the treatment groups (main effects of quadratic time and their interaction with treatment in linear mixed-effects models, $P < 0.001$ in all cases). Pairwise comparisons showed that the temporal profiles of eggs differed significantly from the control for all clothianidin doses ($P < 0.03$ in all cases), and that for larvae and capped brood cells only the 100 µg/L group differed significantly from the control. Weeks 6 and 7 were already in September, thus a seasonally related drop in brood nest size was observed at the end of the experiment. Raw data and technical details of the analysis are provided in the supplementary statistical report, section 2.2.

Demographic compensation

The demographic model was used to estimate the number of new larvae that must hatch each week in order to maintain a stable number of larvae given the survivorship schedule of larvae week by week. In order to maintain a stable larval population, the colonies dosed with 1 µg/L clothianidin needed to hatch 1.57-fold more larvae per week than untreated controls, and this increased to 1.75-fold and 1.91-fold in the colonies dosed with 10 and 100 µg/L clothianidin, respectively (**Table 1**).

Table 1 Modeling of demographic compensation

Clothianidin	L_t observed	h
Control	300	56
1 µg/L	300	88
10 µg/L	300	98
100 µg/L	300	107

In order to maintain a stable larval population (L_t observed), colonies exposed to clothianidin would need to hatch more larvae per week than controls (h denotes the number of eggs that hatch into larvae each week).

In the control colonies, a relatively stable ratio between the brood stages was maintained throughout the experiment. The median ratio of the number of larvae to the number of eggs was 1.57, but this declined to 1.48, 1.38 and 0.60 in the colonies dosed with 1, 10 and 100 µg/L clothianidin, respectively (**Fig. 5A**). The colonies exposed to clothianidin had to produce more eggs to maintain a stable number of larvae. The larvae-to-eggs ratio temporal profile differed significantly between the treatment groups (treatment-by-time interaction in a linear mixed-effects model, $P = 0.0076$). Pairwise comparisons of the treatment groups with the control revealed significant differences in the temporal profiles for the 1 and 100 µg/L treatment groups ($P < 0.016$ in both cases). The analysis was carried out by omitting an extreme outlier in week 2 in one hive of the 10 µg/L group.

The average ratio of the number of capped brood cells to the number of larvae (from the previous week, for weeks 2–7) was 2.03 (median) but was consistently slightly lower in the colonies exposed

to clothianidin at doses of 1 $\mu\text{g/L}$ (median = 1.92) or 10 $\mu\text{g/L}$ (mean = 1.71) throughout the experiment (**Fig. 5B**). In the 100 $\mu\text{g/L}$ treatment group, the median ratio was 1.28, but the profile was biphasic, with a median ratio of 1.58 up to the end of week 4, falling sharply to 0.17 in week 5. Nevertheless, there was no significant difference in the temporal profiles of the capped brood-to-larvae ratio between the treatment groups. Detailed results and analysis are provided in the supplementary statistical report.

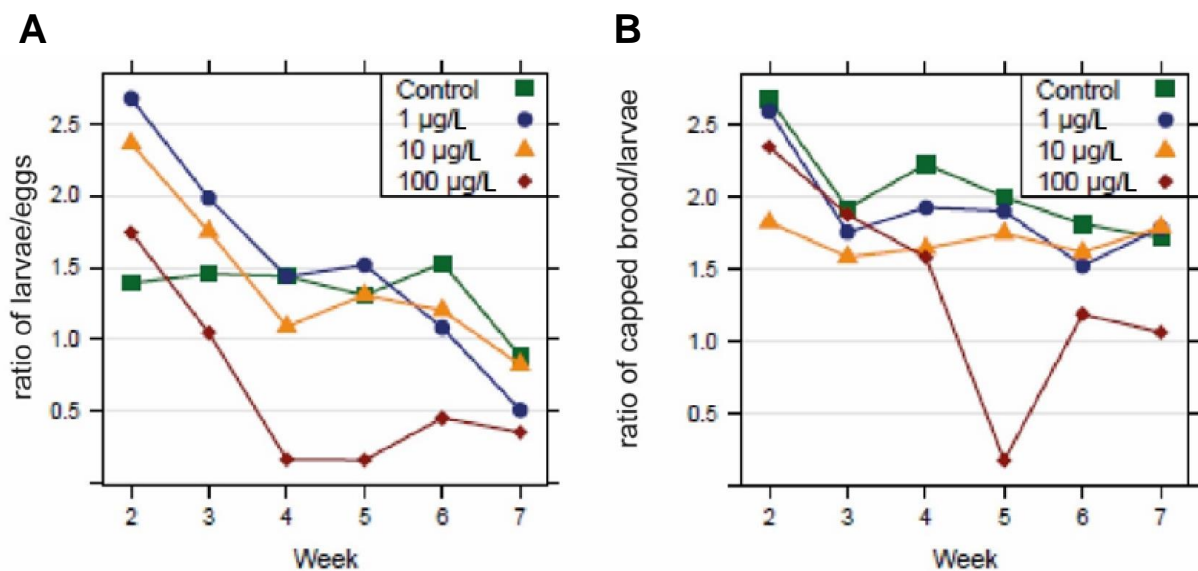


Fig 5. Ratio between developmental stages. (A) The ratio of the number of larvae/eggs. The eggs in week 2 become the larvae of week 3, so the number of larvae is shifted by 1 week. The ratio of controls is stable throughout the experiment (mean = 1.5) until week 7, where a seasonally related drop in brood activity was observed. (B) The ratio of capped brood/larvae (number of capped brood shifted by 1 week) was stable in the controls (mean = 2.06), and the 1 $\mu\text{g/L}$ (mean = 1.92) and 10 $\mu\text{g/L}$ (mean = 1.7) groups, but dropped in the 100 $\mu\text{g/L}$ treatment group in weeks 4 and 6 (mean = 1.44).

BEEHAVE simulations

To estimate the impact of our findings on colony development in standard-sized hives we applied two BEEHAVE simulations. To mimic the situation of the experimental nucleus colonies in BEEHAVE (**simulation A**), we tested a wide range of values for *ProteinNursesModifier_Exposed*, which represents the protein content of jelly fed to the larvae. The best fits are shown in **Table 2** based on a comparison of modeled and experimental brood survival. The output of these simulations was the average brood survival when comparing brood cohort sizes at ages of 19 vs. 3 days. The modeled brood survival was then compared to the results of the experimental brood survival to determine the values for *ProteinNursesModifier_Exposed* that represent the tested concentrations of clothianidin.

To estimate the potential impact of clothianidin exposure on standard-sized colonies (**simulation B**), we ran BEEHAVE under default settings but reduced the protein content of the jelly (*ProteinFactorNurses*). The degree to which the protein was depleted during exposure was defined by *ProteinNursesModifier_Exposed*, with values set according to the results of the previous set of simulations (**Table 2**). Swarming was either prevented or allowed (following the colony remaining in the hive). Colony sizes at the end of the year decreased with increasing concentrations of clothianidin, particularly when swarming was prevented (**Fig. 6**). No swarms at all formed at the highest clothianidin concentration. For the lower clothianidin concentrations, each colony released a single swarm during the first year, whereas the control colonies produced on average 1.2 (± 0.41) swarms in the first year.

At the end of the first year, one of the control colonies died after producing two swarms, but all other colonies survived ($n = 30$). When we extended the simulations over 3 years, two colonies in the 100 $\mu\text{g/L}$ treatment group died after the second year and another nine died at the end of the third year (regardless of whether or not swarming was allowed, as these colonies did not swarm at all). No other colonies died after years 2 or 3. The mean colony sizes after 3 years (without swarming) were 11,335.3 worker bees (control, SD = 1,209.9), 9,951.4 (1 $\mu\text{g/L}$, SD = 943.5), 9,225.6 (10 $\mu\text{g/L}$, SD = 1,116.6), and 3,097.1 (100 $\mu\text{g/L}$, SD = 2,427.8).

Table 2 Simulation of mating nucleus colonies in BEEHAVE

Clothianidin	Brood survival experiments	Brood survival model	<i>ProteinNursesModifier_Exposed</i>
control	0.8	0.92 \pm 0.14	1
1 $\mu\text{g/L}$	0.4	0.38 \pm 0.16	0.82
10 $\mu\text{g/L}$	0.2	0.20 \pm 0.12	0.77
100 $\mu\text{g/L}$	0.0	0.02 \pm 0.03	0

Modification of the factor *ProteinNursesModifier_Exposed* in BEEHAVE simulations resulted in brood survival rates similar to experimental data obtained in field experiments. The factor *ProteinNursesModifier_Exposed* reduces the protein content of the jelly fed to the larvae (*ProteinFactorNurses*) in the model. A wide range of values for *ProteinNursesModifier_Exposed* was

tested, and the best fits are shown based on a comparison of modeled and experimental brood survival.

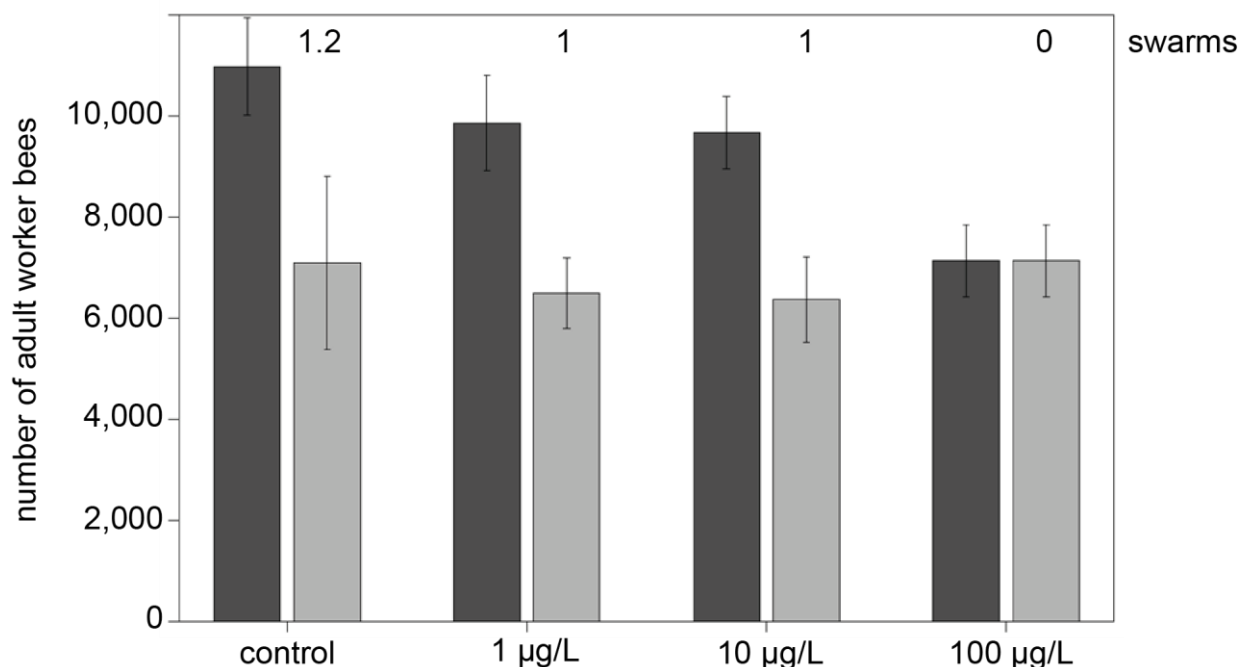


Fig. 6. Colony sizes decline with increasing concentrations of clothianidin in simulated full-sized colonies. To estimate the potential impact of clothianidin exposure on standard-sized colonies, a BEEHAVE simulation was conducted under default settings but with less protein in the jelly (*ProteinFactorNurses*) as defined by *ProteinNursesModifier_Exposed*, with values set according to the results of the previous set of simulations (**Table 2**⁴⁶). Colony sizes (mean number of worker bees) at the end of the year decreased with increasing concentrations of clothianidin, particularly when swarming was prevented (dark grey). When swarming was allowed (light grey), the control group produced 1.2 swarms in the first year. For the 1 and 10 µg/L treatment groups, each colony released a single swarm during the first year. No swarms at all were produced in the 100 µg/L group.

DISCUSSION

Brood care is fundamental to the maintenance of a honeybee colony and lies at the heart of its social interactions^{25,46}. We dissected the brood care activity of a colony by measuring the HPG size of individual nurse bees, by chemical analysis of royal jelly and larval composition, by tracking the survival of individual larvae, and by monitoring the overall brood production of the colony precisely. By this means, we established small nucleus colonies as convenient pesticide testing systems, allowing us to investigate the key aspects of social interactions and the manner in which colonies compensate for external stressors. The experimental setup covered a range of field-realistic exposure levels to the neonicotinoid clothianidin, which reaches mean levels of 9.4 µg/kg (maximum 41.2 µg/kg, mean prevalence 11%) in pollen and 1.9 µg/kg (maximum 10.1 µg/kg, mean prevalence 17%) in honey⁴⁷. In the field, a colony is likely to be exposed to such concentrations for a shorter time than our chronic exposure scenario, where colonies received clothianidin over a period of 7 weeks.

Our HPG measurements revealed that age-defined workers in all colonies exposed to clothianidin had significantly smaller acini than untreated controls. Smaller HPGs could lead to malnutrition, because young larvae and the queen feed exclusively on royal jelly and older larvae receive royal jelly in a suspension with honey²⁵. Neonicotinoids are known to reduce the size of the HPG in individual nurse bees²⁸⁻³⁰ and also to reduce the levels of acetylcholine in their royal jelly³⁰. We also found that the lipid composition of the royal jelly and larvae changed when colonies were exposed to clothianidin. Accordingly, the expression of larval genes involved in lipid and carbohydrate metabolism, and the lipid composition of larvae, was also shown to change when honeybee colonies were exposed to field-realistic concentrations of imidacloprid⁴⁸. We found that neither the composition nor concentration of protein in royal jelly was affected by clothianidin. However, the method we used is only sensitive enough to detect substantial changes in protein composition, and more sensitive methods such as mass spectrometry would be required to measure subtle alterations. Only the highest concentration of clothianidin we tested (100 µg/L) caused a general decrease in protein levels, although there was no significant difference in the quantity of total extracted protein. This may indicate that high concentrations of clothianidin stimulate the activity of proteases in royal jelly. Even though the protein concentration in royal jelly appeared to be unaffected by clothianidin exposure, there may be an impact on the overall amount of brood food produced by individual nurse bees, and this should be examined in future experiments.

Royal jelly is not only fed to larvae and queens but also to drones⁴⁹, young workers and even foragers⁵⁰. The capacity for pollen digestion enables nurse bees to exploit pollen nutrients efficiently and distribute the protein-rich food to other members of the colony, which take on more specialized

tasks such as reproduction and foraging⁵⁰. As well as the observed negative impact on brood survival a deficiency of nurse bees could indirectly affect adult workers and drones by reducing the amount of high-quality royal jelly available as food⁵¹. Given the key role of nurse bees in the provision of nutrition not only to the brood and queen but also all other members of the hive, there is an urgent need to study how pesticides affect their eusocial interactions.

Workers can regulate the egg-laying rate of a queen by controlling the quantity and quality of the food provided to the queen by nurse bees⁵². The undernourishment of a queen can inhibit egg laying and thus reduce the growth and survival of a colony. However, we found that the number of eggs in the colony differed little between the treatment groups, although there was a trend for higher egg numbers in colonies exposed to clothianidin. Given the 7-day intervals between assessments and the 3-day developmental period of an egg, we cannot be sure that the egg-laying rate of the queen was not affected.

The effect of neonicotinoids on brood mortality is controversial. Laboratory survival tests show that artificially reared larvae can consume large quantities of neonicotinoids (more than they would encounter under realistic field conditions) without direct lethal effects³⁰. However, a reduction of the number of brood cell has been observed in some field studies^{11,29,31} which suggests that neonicotinoids may have an indirect impact on brood mortality, for example by preventing exposed nurse bees from completing their nurturing tasks effectively.

In the experimental colonies, we observed an absolute reduction in the number of brood cells only in the group exposed to highest clothianidin concentration (100 µg/L). The effect was first observed after 3 weeks of exposure. In the second phase of the experiment, the number of larvae or capped brood cells declined even further. By week 4, no larvae at all were observed in 60% of the colonies, and in the remainder only very young larvae were present (developmental stage 4–5 after egg laying). The stronger effect on brood cell numbers from week 3 onwards may reflect the dilution of the active ingredient in the first few weeks of the experiment, given the relatively large initial food stores and the freedom of the bees to forage. Furthermore, the active nurse bees in the second phase of the experiment were exposed to clothianidin during their entire development and adult life, potentially having a substantial impact on their behavior. In the European Union, a honeybee brood test is required for the risk assessment of pesticides according to OECD guideline 75. Like our brood survival assessment, this test tracks the individual fate of a brood cell and determines the brood survival rate⁵¹. However, only one brood cycle is mandatory for the OECD test, whereas our data show that negative effects can be more severe in the second brood cycle.

In the small nucleus colonies, brood survival was reduced even by field-realistic concentrations of clothianidin (1 or 10 µg/L), particularly in the second phase of the experiment, where the survival of

individually tracked larvae was 40% or lower. Concurrently, the absolute numbers of larvae and pupae in the exposed colonies were close to normal levels, and in some weeks even higher than in the untreated controls. This clearly shows that the colonies compensated for the increase in mortality by producing more brood. Indeed, the colonies in the 1 µg/L treatment group needed to produce 1.57-fold more larvae than the control group to maintain a stable population, and this demand increased at higher concentrations of clothianidin. The contrast between the low survival rate of the larvae and pupae yet the near normal absolute brood numbers under field-realistic exposure conditions provides evidence of a remarkable additional brood-rearing effort in the colonies exposed to the pesticide, allowing them to compensate for the negative effects of clothianidin on brood survival.

The overall costs for the colony of this compensatory brood activity are difficult to assess. First, we should consider the number of eggs produced by the queen. Only fertilized eggs develop into worker bees, so colony growth and survival depends on the ability of the queen to produce fertilized eggs. The lifetime performance of a queen is limited by the number of sperm she receives on her nuptial flights and stores in her spermatheca. In our experimental setting, a queen will never reach the limits of her egg-laying capacity, but in a full-sized colony a queen might approach her reproductive limits earlier than normal and would need to be replaced by the colony or the beekeeper. Premature queen supersedure and shorter queen lifespans are important drivers of honeybee colony mortality^{7,11,37,38,53,54}. The accelerated egg-laying we observed to compensate for increased brood mortality might contribute to that problem. Second, to estimate the energetic costs of losing and replacing brood for the colony, we must consider that most of the larvae and pupae that eventually die are consumed by the workers, thus the nutrients are recycled and not completely lost to the colony. Third, it is difficult to judge the effect of the reduced brood-rearing capacity on the life traits of individual worker bees. This phenomenon can extend the lifespan of workers⁵⁵, but more workers may get involved in brood-rearing tasks to compensate for the more limited capacity of nurse bees to produce royal jelly. We do not know how the disruption of this complex interaction affects overall colony fitness. As eusocial insects, honeybees depend on task specialization, which is precisely adjusted to the needs of the colony. The increase in brood mortality and the inability of nurse bees to produce sufficient royal jelly could easily interfere with this delicate balance with a serious impact on colony fitness.

Because our experiments involved nucleus colonies, it is unclear to what extent the observed effects of clothianidin exposure can be extrapolated to full-sized colonies. We estimated the impact on colony development in standard hives using the honeybee model BEEHAVE^{44,56}, which simulates colony dynamics and agent-based foraging in realistic landscapes. The model was assessed by the European Food Safety Authority (EFSA), which concluded it would be a good starting point to model the impact of pesticides and other stressors on honeybee colonies^{57,58}. Although BEEHAVE does not

explicitly incorporate pesticides, it can be used to address their effects on the behavior and mortality of bees indirectly^{59,60}. Accordingly, exposure in our simulations was not dependent on the foraging activities of the bees but was imposed by impairing the ability of in-hive bees to feed larvae due to the production of lower amounts of high-quality royal jelly. We observed strong effects on swarming and colony survival when we simulated clothianidin concentrations of 100 µg/L. Lower concentrations of clothianidin, closer to field-realistic doses, had little impact on overwintering colony sizes and no effect on colony survival, agreeing with previous findings reported by Cutler and colleagues⁶¹. Although such colonies might appear strong and healthy, we found that clothianidin had a strong negative effect on the number of swarms produced, particularly at high doses. This effect was not considered by Cutler and colleagues⁶¹ but was reported by Sandrock and coworkers for clothianidin and thiamethoxam¹¹. Less frequent swarming would lower the resilience of bee populations in response to other stressors and make them more vulnerable to colony losses due to factors such as climate, weather, diseases or forage gaps.

The sublethal effects of neonicotinoid exposure on individual honey bees have been confirmed, but the impact on the performance and survival of colonies remains controversial³⁸. Nevertheless, colony-level performance is of primary interest in managed honeybees because lower performance and higher rates of colony loss directly affect beekeepers and pollination services. The inability to substantiate the sublethal effects of pesticides and reliably detect them in field trials^{40,41} may reflect two major problems, which are discussed in turn below.

First, higher-tier field trials for the risk assessment of pesticides often lack statistical power as a result of the relatively low sampling size (colony number). Only well-resourced enterprises such as the agrochemical industry have the means to commission large-scale higher-tier field experiments. The outcome of these experiments is in most cases confidential and the data are not available for scientific or public evaluation. However, with our small nucleus colony approach, it is easy to scale up the number of colonies to achieve sufficient statistical power and to perform field trials at a fraction of the cost of semi-field/field trials with full-sized colonies, thus allowing independent research without industry funding.

Second, the ability of colonies to compensate for the impact of pesticides adds a layer of complexity to investigations looking for the sublethal effects of pesticides. A colony is a functionally organized cooperative group in which the tasks and activity levels of each individual are flexible and rapidly adjusted according to the group's needs⁶². The large number of interacting individuals allows the colony to adaptively reallocate work and resources to compensate for potential negative effects on individuals. This plasticity enables the colony to react adaptively to environmental stressors, masking the effects on individuals. Indeed, the ability of a honeybee colony to withstand or recover quickly from disturbances is known as resilience, which is an intrinsic property of many complex systems.

However, events leading to loss of resilience in complex systems are rarely predictable and are often irreversible⁶³. In honeybee colonies, this point arrives when the compensatory capacity of the colony reaches its limits, triggering the sudden breakdown of a seemingly healthy colony, especially when multiple stressors act together.

As a super-organism, a honeybee colony can compensate for many stressors due to the presence of many individuals and the complex social interactions among them⁵⁵. With our small nucleus colony approach, we reduced the number of bees but maintained the social coherence of the colony⁶⁴, allowing us to investigate the compensatory capacity of the colony in detail. This sensitive model system allows the assessment of single or multiple stressors on the compensatory capacity of the colony, and will help to close the knowledge gap between laboratory cage experiments and field trials with full-sized colonies. This will facilitate not only scientific investigations, but also the regulatory testing for new pesticides.

Methods

Clothianidin exposure in field experiments

The experimental bee yard was situated in a suburban area in Kirchhain (Germany) with sufficient natural pollen sources in late summer. The field experiment took place with 20 *Apis mellifera carnica* colonies in Kirchhainer mating nuclei (25.5 x 19.8 x 17 cm), established with freely mated sister queens and 180 g of bees each. Two weeks before the clothianidin treatment was initiated, the colonies containing freshly mated queens were allowed to establish and build up a brood nest. Two days before clothianidin exposure (sampling day 0, S0; **Suppl. Fig. 1**), the colony strength was assessed and the treatment groups were randomly assigned to the hives such that differences between treatment groups were minimized with respect to the strength of their colonies. Every week, from July 30 to September 10, each colony received 400 mL of Apiinvert (Südzucker AG, Mannheim, Germany) sugar syrup (39% w/v fructose, 31% w/v saccharose and 30% w/v glucose) spiked with clothianidin (1, 10 or 100 µg/L). Control colonies received sugar syrup containing the same concentration of the solvent (water) as the clothianidin-treated groups. The syrup was fed in zip-lock bags placed inside the food chamber containing a climbing aid. After 1 week, the leftovers were removed and weighed to record food consumption. For all four experimental groups, the analyzed clothianidin levels were close to the target concentrations (Suppl. Table 1). Environmental data were recorded during the study period using a USB data logger (EL-USB-2, Lascar Electronics Ltd., temperature accuracy ± 0.5 °C, relative humidity accuracy ± 3%) located under the colonies.

Sampling

During weeks 3 and 7, random samples of worker bees, larvae and royal jelly were taken from each colony. In detail, 20 randomly chosen worker bees located on a brood comb and five larvae (larval stage: day 7 or 8 after egg laying) were immediately frozen for chemical analysis. To collect royal jelly, extra thick blotting paper (Protean, Xi size; Bio-Rad, Hercules, CA, USA) was cut into strips, cleaned in pure ethanol and acetone (Carl Roth, Karlsruhe, Germany) and dried in a heating cabinet at 80 °C. Each strip was inserted into five brood cells containing a small larva (developmental day 4–5) to suck up the royal jelly and the strips were immediately frozen. To document brood development, each side of each comb was photographed within an empty hive box transformed into a photo box containing a digital camera (Canon PowerShot A1000 IS, Tokyo, Japan) and a ring-flash (Aputure Amaran AHL-C60 LED, Shenzhen, China). Sampling took place every week. The colonies were sampled starting with the control and then from the lowest to highest concentration of clothianidin to minimize the risk of carryover.

HPG size measurements

To obtain worker bees of a defined age, single frames of late-stage capped brood (Binder, Tuttlingen, Germany) were brought to the laboratory and incubated in the dark at 32 °C, with humidity provided by open water jars. The frames with worker brood were collected from two full-sized colonies, which were regularly inspected for symptoms of disease and tested for Chronic bee paralysis virus, Deformed wing virus, Acute bee paralysis virus, and Sac brood virus⁶⁵. Newly-emerged bees (≤ 24 h) were collected, color marked, and transferred to the experimental colonies on June 25. During the second week of exposure, the marked bees were removed from the colonies after 12 days in the hive and immobilized on ice. The HPGs were dissected in ice-cold phosphate-buffered saline (PBS, pH 7.4). The specimens were fixed in formaldehyde (4% in PBS, Carl Roth), rinsed three times in PBS, and mounted in Aquapolymount (Polysciences, Eppelheim, Germany). Three pictures of each gland (only one gland per bee) were photographed at 400x magnification using a phase contrast/fluorescence microscope (Leica DMIL, Leica camera DFC 420C) and LAS v4.4 image-capturing software (Leica Microsystems, Wetzlar, Germany). To measure the size of each gland, the diameters of 30 acini per bee were measured using ImagJ v1.49o (<http://rsb.info.nih.gov/ij/index.html>).

High-performance thin-layer chromatography

HPTLC was chosen as sensitive analytical method in order to detect qualitative and semi-quantitative differences in the composition of brood food and larvae of dosed hives. Individual larvae differing in their weights (200-500 mg/larva) were solely macerated and extracted in 1 mL *n*-hexane (>99% pure, Rotisolv, Carl Roth) in an ultrasonic bath for 1 min and then vortexed for 1 min. For the analysis of royal jelly, adsorptive filter strips (Sugi strips, Kettenbach, Eschenburg, Germany) were cut in half and

one part was dipped in brood combs until maximal absorption of the material, whereas the other strip was used as background control strip, and both strips were extracted as above. The supernatants of larvae and royal jelly were transferred to a fresh vial 1000 μ L isopropylacetate/methanol (3/2, v/v). After maceration for 1 min, the mix was vortexed for 1 min and the supernatant was transferred to another vial. Between extractions, the samples were cooled on ice and stored at -20°C .

The isopropylacetate/methanol extracts (20 μ L/band for royal jelly and 7 μ L/band for larvae) were sprayed onto the silica gel 60 F₂₅₄ HPTLC plate (Merck, Darmstadt, Germany) using an Automatic TLC Sampler 4. The plate of royal jelly was developed with a mobile phase consisting of chloroform/methanol/water/ammonia (30/17/2/1, v/v/v/v, all Carl Roth⁶⁶ and the plate of larvae with an 8-step gradient development based on methanol, chloroform, toluene and n-hexane^{66,67}. After drying in a stream of cold air for 2 min, the plate images were documented at UV 366 nm using the TLC Visualizer. For derivatisation, the chromatogram was dipped into the primuline solution (100 mg primuline in 200 mL acetone/water, 4/1 v/v, Sigma-Aldrich, Steinheim, Germany) at an immersion speed of 2.5 cm/s and an immersion time of 1 s, dried and derivatised as before. The data were processed using winCATS version 1.4.2.8121 (all instrumentation from CAMAG).

The bacterium *Aliivibrio fischeri* (NRRL-B11177, strain 7151), obtained from the German Collection of Microorganisms and Cell Cultures (DSMZ, Leibniz Institute, Berlin, Germany), was used to assess a non-targeted, broad range of effective substances within the royal jelly. HPTLC plates were developed as described above, neutralized and immersed in a bacterial suspension, prepared according to DIN EN ISO 11348-1⁸⁴⁵ at an immersion speed of 3 cm/s and an immersion time of 2 s. The bioluminescence of the wet bioautogram was recorded in an interval of 3 min over 30 min using the BioLuminizer (CAMAG).

Brood assessment

The free extension of the open source program ImagJ, Fiji (<http://fiji.sc/Fiji>) was used to count all cells with eggs, larvae, or sealed brood, for every colony on every sampling day. The photos of a single comb from different sampling days were aligned in the program and all brood cells were counted. Because the colonies had no wax foundations, some cells on the edges of these naturally-built combs were at an unfavorable angle. Therefore, most but presumably not all cells with brood were visible in the photos. This uncertainty was similar in all hives. To estimate the brood survival, we first tracked the development of individual eggs, but found a high mortality rate even in control colonies. Therefore, we tracked the development of individual larvae (day 4–5 after egg laying) over 4 weeks (= sampling weeks). Brood survival was estimated for two periods during the experiment (weeks 1–4 and 3–7).

Modeling of demographic compensation

The aim of the model was to estimate the number of new larvae that must hatch each week in order to maintain a stable number of larvae up to 7 weeks of age given the survivorship schedule of larvae week by week. Let h denote the number of eggs that hatch into larvae each week, and let the probability that any individual larva dies in each successive week be m_i , where i takes values in the set $\{1, 2, \dots, 7\}$ to indicate each of seven successive weeks, after which we assume that surviving larvae pupate. We used a demographic matrix model⁶⁸ to describe the state of the population of larvae each week as follows. Let l_x denote the number of larvae in the colony that are aged x weeks post-hatching and let m_x denote their *per capita* weekly mortality rate. The population of larvae is distributed into seven age classes and we also assign a class to queens, which give rise to larvae by producing eggs. Using the Lefcovitch matrix approach, the larval population of a colony can thus be viewed as a state vector n_t whose week-by-week change is the product of a matrix A and the population state vector n_t , as shown in Equation (1):

$$An_t = \begin{bmatrix} \mathbf{0} & \mathbf{0} & \mathbf{0} & \dots & \mathbf{0} & h \\ (1 - m_1) & \mathbf{0} & \mathbf{0} & \dots & \mathbf{0} & \mathbf{0} \\ \mathbf{0} & (1 - m_2) & \mathbf{0} & \dots & \mathbf{0} & \mathbf{0} \\ \vdots & \vdots & \vdots & \ddots & \vdots & \vdots \\ \mathbf{0} & \mathbf{0} & \mathbf{0} & \dots & (1 - m_7) & \mathbf{0} \\ \mathbf{0} & \mathbf{0} & \mathbf{0} & \dots & \mathbf{0} & 1 \end{bmatrix} \begin{bmatrix} l_1 \\ l_2 \\ l_3 \\ \vdots \\ l_7 \\ Q \end{bmatrix} \quad (1)$$

The lowermost element of n_t is the number of queens (Q) which is here set to $Q = 1$ for all models, and the total number of larvae in the colony at any time is $L_t = \sum_x l_x$. Given the observed mortality schedule (m_x), we used the model to solve for the value of h that produces a stable value for L_t , as shown in Equation (2):

$$An_t = n_t \quad (2)$$

We determined the mortality schedule by observing the survivorship of a larval cohort. For example, if a cohort of S_t larvae was originally marked at time t and, of these, S_{t+1} survived until the following week, the *per capita* weekly mortality rate would be estimated as shown in Equation (3):

$$m_t = 1 - \frac{S_{t+1}}{S_t} \quad (3)$$

BEEHAVE simulations

To predict the impact of clothianidin on colony development in standard hives we used BEEHAVE, a honeybee model that simulates colony dynamics and agent-based foraging in realistic landscapes (Becher et al. 2014, Becher et al. 2016; <http://beehave-model.net/>). Although BEEHAVE does not explicitly allow the incorporation of pesticides, the effect of pesticides on behavior and mortality can

nevertheless be addressed (Rumkee et al. 2016, Thorbek et al. 2016). BEEHAVE simulates the development of a single honeybee colony, starting with 10,000 foragers on January 1. Colony dynamics are based on a daily egg laying rate, with the developmental stages eggs, larvae, pupae, and adults (in drones) or in-hive workers and foragers (in workers). The brood needs to be tended by in-hive bees, and the larvae additionally need to be fed with nectar and pollen. Foragers can scout for new food sources or collect nectar and pollen from sources already known. Successful foragers can recruit nestmates to the food source. Mortality rates depend on the developmental stage and the time spent on foraging. The colony dies if it either runs out of honey or if the colony size falls below 4,000 bees at the end of the year. Swarming may take place when the brood nest grows to more than 17,000 bees before July 18. Under default conditions, two food sources are present at distances of 500 or 1,500 m. Daily foraging conditions are based on weather data from Rothamsted, UK.

We ran two sets of simulations: **(A)** We first set up BEEHAVE to mimic our experimental nucleus colonies. We then determined how the protein content of the jelly produced by nurses (*ProteinFactorNurses*) had to be modified to replicate the larval mortality we observed in our empirical data. **(B)** We then set up BEEHAVE under default conditions but modified *ProteinFactorNurses* according to the results from the previous simulations to assess the impact of clothianidin exposure under more realistic conditions.

To mimic the experimental nucleus colonies (simulation A), the maximum honey store (*MAX_HONEY_STORE_kg*) was reduced to 0.77 kg and the maximum size of the brood nest (*MAX_BROODCELLS*) was reduced to 250. Furthermore, *HoneyIdeal* was set to 'true', so that even though the honey store was small it was filled every day, reflecting the feeding of the experimental bees. In contrast, *PollenIdeal* was set to 'false', because the experimental colonies still had to forage for pollen. On day 209 (July 28), we set the number of pupae to 100 and the number of workers to 650, similar to the experimental colony sizes. During the exposure to clothianidin between days 211 (July 30) and 253 (September 10), the protein content of the jelly fed to the larvae (*ProteinFactorNurses*) was modified by the new variable *ProteinNursesModifier_Exposed*. We tested for *ProteinNursesModifier_Exposed* values from 0.6 to 1 in steps of 0.01. The main output of the simulation was the survival of the brood, calculated from the brood cohort sizes aged 19 days divided by the sizes of these cohorts when they were 3 days old. We calculated the mean brood survival over 30 replicates, using the last 10 cohorts only (i.e. those reaching the age of 19 days between September 1 and 10). Those parameter values for *ProteinNursesModifier_Exposed* resulting in brood survival most similar to the experimental brood survival were then chosen to represent the clothianidin concentrations of 100, 10 and 1 µg/L.

To assess the impact of clothianidin on standard colonies under more realistic conditions (simulation B), we ran BEEHAVE under default settings but reduced the protein content of the jelly

(*ProteinFactorNurses*) during times of exposure. We assumed that colonies would be exposed when rapeseed plants are flowering, defined in the model as the period between days 95 (April 5) and 130 (May 10). *ProteinNursesModifier_Exposed* values representing the tested concentrations of clothianidin were derived from the previous set of simulations, and for the control we set *ProteinNursesModifier_Exposed* to 1 (i.e. no effect of clothianidin). Swarming was either prevented or allowed, in which case the simulation followed the colony remaining in the hive.

Statistical methods

Statistical analysis was carried out using *R* v3.4.2, (R-Core Team 2017), including the add-on packages *lme4* (Bates et al., 2015) for linear mixed-effects models, *pbkrtest* (Halekoh et al., 2014) for testing fixed effects in mixed-effects models, *parallel* (R-Core Team 2017) to increase computational power, *RLRsim* (Scheipl et al. 2008) for testing random effects in mixed-effects model, *multcomp* (Hothorn et al. 2008) for multiple comparisons, and *lattice* (Sarkar 2008) for various graphical displays. We used linear mixed-effects models for one- and two-factorial analysis of variance (ANOVA) or regressions as indicated and where necessary. In those models, the hives/colonies were modeled as random effects to reflect the (longitudinal) grouping structure in the data. For the analysis of larval survival, we used a logarithmic transformation of the proportion of surviving larvae. When testing fixed effects in mixed-effects models, we used the Kenward-Roger method (and double-checked the results by comparing them with parametric bootstrap values). Where sufficient, we simplified the analysis using linear (fixed-effects) models. Model diagnostics were performed for all fitted models using qualitative tools such as normal q-q-plots for residuals and plots of residuals vs. fitted values to assess the validity of model assumptions like homoscedastic normality. Dunnett's test (or customized contrasts as appropriate) was used for multiple comparisons in *post hoc* analysis, and *P* values were appropriately adjusted for multiple testing within well-defined test families using the single-step or Westfall's method. Model and analysis details, model diagnostic graphs, and further information are available in the supplemental statistical report.

Acknowledgments

We thank W. Strasser for preparing the queens and colonies, M. Gabel for assistance in sample collection, and S. Backhaus, G. Waldschmidt and E. Leider for help with dissecting the specimens and G. Bischoff for the quantification of clothianidin. This work was supported by the European Union and the Hessen State "Förderung von Maßnahmen zur Verbesserung und Erzeugung und Vermarktung von Honig in Hessen" and the Hessen State Ministry of Higher Education, Research and the Arts (HMWK) via the collaborative research projects granted under the LOEWE Centers for "Insect Biotechnology and Bioresources". We thank Richard M. Twyman for editing of the manuscript.

Author contributions

AB, MS and MSa designed the methods and experiments, AB and MSa carried out the field experiments and took samples. AB and MSa quantified the brood cells and larval mortality. JC and MS analyzed the demographic brood compensation. MB conducted the BEEHAVE analysis. ST and GM were responsible for the HPTLC analysis. DB analyzed royal jelly proteins. MS and GE conducted the statistical analysis. AB wrote the paper with support from JC, MB, MDM, R-AD, AV, GM, and RB.

Conflict of interest:

The authors have no financial and personal relationships that might bias or be seen to bias their work.

References

- 1 Bascompte Jordi, P. J., Jens M. Olesen. Asymmetric Coevolutionary Networks Facilitate Biodiversity Maintenance. *Science* 312, 431-443, doi:10.1126/science.1123412 (2006).
- 2 Klein, A.-M., Vaissière, B. E., Cane, J. H., Steffan-Dewenter, I., Cunningham, S. A., Kremen, C. . Importance of pollinators in changing landscapes for world crops, (2007).
- 3 Council, N. R. Status of Pollinators in North America. (The National Academies Press, 2007).
- 4 vanEngelsdorp, D., Hayes, J., Jr., Underwood, R. M. & Pettis, J. A Survey of Honey Bee Colony Losses in the U.S., Fall 2007 to Spring 2008. *PloS one* 3, e4071, doi:10.1371/journal.pone.0004071 (2009).
- 5 Goulson, D., Nicholls, E., Botias, C. & Rotheray, E. L. Bee declines driven by combined stress from parasites, pesticides, and lack of flowers. *Science* 347, 1255957, doi:10.1126/science.1255957 (2015).
- 6 Potts, S. G. et al. Declines of managed honey bees and beekeepers in Europe. *Journal of Apicultural Research* 49, 15-22, doi:10.3896/ibra.1.49.1.02 (2010).
- 7 Genersch, E. et al. The German bee monitoring project: a long term study to understand periodically high winter losses of honey bee colonies*. *Apidologie* 41, 332-352 (2010).
- 8 Brodschneider, R. & Crailsheim, K. Nutrition and health in honey bees. *Apidologie* 41, 278-294, doi:10.1051/apido/2010012 (2010).
- 9 Frias, B., Barbosa, C. & Lourenço, A. Pollen nutrition in honey bees (*Apis mellifera*): impact on adult health. *Apidologie*, 1-11, doi:10.1007/s13592-015-0373-y (2015).
- 10 Di Pasquale, G. et al. Variations in the Availability of Pollen Resources Affect Honey Bee Health. *PloS one* 11, e0162818, doi:10.1371/journal.pone.0162818 (2016).

- 11 Sandrock, C. et al. Impact of chronic neonicotinoid exposure on honeybee colony performance and queen supersedure. *PloS one* 9, e103592, doi:10.1371/journal.pone.0103592 (2014).
- 12 Desneux, N., Decourtye, A. & Delpuech, J. M. The sublethal effects of pesticides on beneficial arthropods. *Annual review of entomology* 52, 81-106, doi:10.1146/annurev.ento.52.110405.091440 (2007).
- 13 Elbert, A., Haas, M., Springer, B., Thielert, W. & Nauen, R. Applied aspects of neonicotinoid uses in crop protection. *Pest management science* 64, 1099-1105, doi:10.1002/ps.1616 (2008).
- 14 Jeschke, P., Nauen, R., Schindler, M. & Elbert, A. Overview of the status and global strategy for neonicotinoids. *Journal of agricultural and food chemistry* 59, 2897-2908, doi:10.1021/jf101303g (2011).
- 15 Vanbergen, A. J. & Initiative, t. I. P. Threats to an ecosystem service: pressures on pollinators. *Frontiers in Ecology and the Environment* 11, 251-259, doi:10.1890/120126 (2013).
- 16 van der Sluijs, J. P. et al. Neonicotinoids, bee disorders and the sustainability of pollinator services. *Current Opinion in Environmental Sustainability* 5, 293-305, doi:http://dx.doi.org/10.1016/j.cosust.2013.05.007 (2013).
- 17 Pisa, L. W. et al. Effects of neonicotinoids and fipronil on non-target invertebrates. *Environmental science and pollution research international* 22, 68-102, doi:10.1007/s11356-014-3471-x (2015).
- 18 Simon-Delso, N. et al. Systemic insecticides (neonicotinoids and fipronil): trends, uses, mode of action and metabolites. *Environmental science and pollution research international* 22, 5-34, doi:10.1007/s11356-014-3470-y (2015).
- 19 Matsuda, K. et al. Neonicotinoids: insecticides acting on insect nicotinic acetylcholine receptors. *Trends in pharmacological sciences* 22, 573-580 (2001).
- 20 Tomizawa, M. & Casida, J. E. Unique neonicotinoid binding conformations conferring selective receptor interactions. *Journal of agricultural and food chemistry* 59, 2825-2828, doi:10.1021/jf1019455 (2011).
- 21 Blacquiere, T., Smagghe, G., van Gestel, C. A. & Mommaerts, V. Neonicotinoids in bees: a review on concentrations, side-effects and risk assessment. *Ecotoxicology* 21, 973-992, doi:10.1007/s10646-012-0863-x (2012).
- 22 Mitchell, E. A. D. et al. A worldwide survey of neonicotinoids in honey. *Science* 358, 109-111, doi:10.1126/science.aan3684 (2017).
- 23 Wilson, E. O. & Hölldobler, B. Eusociality: Origin and consequences. *Proceedings of the National Academy of Sciences of the United States of America* 102, 13367-13371, doi:10.1073/pnas.0505858102 (2005).
- 24 Knecht, D. & Kaatz, H., H. Patterns of larval food production by hypopharyngeal glands in adult worker honey bees. *Apidologie* 21, 457-468 (1990).

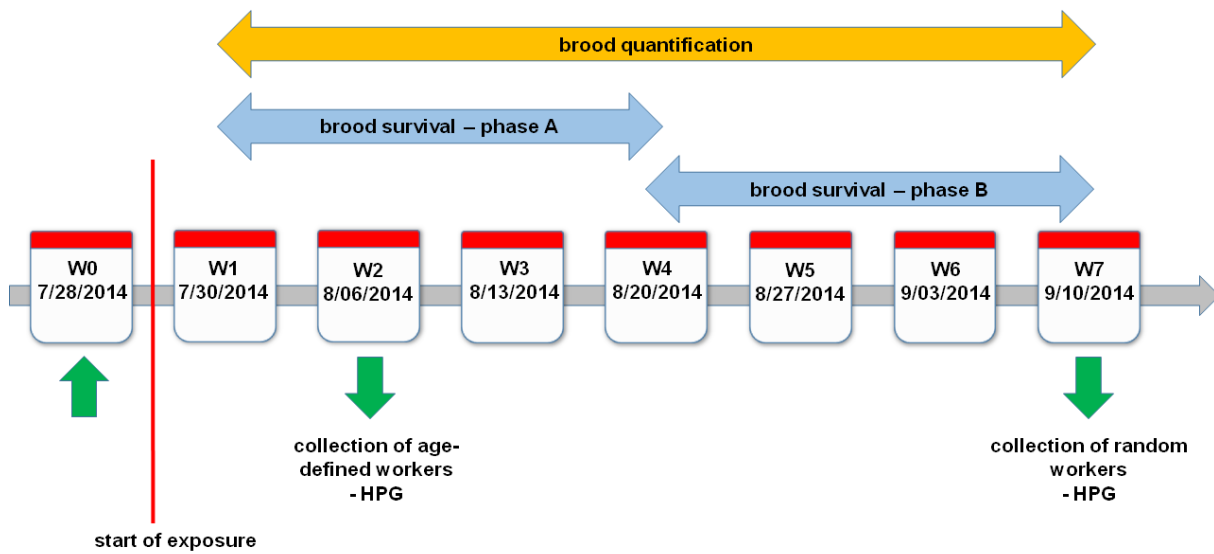
- 25 Crailsheim, K. & Hrasnigg, N. Adaptation of hypopharyngeal gland development to the brood status of honeybee (*Apis mellifera* L.) colonies. *Journal of insect physiology* 44, 929-939 (1998).
- 26 Škerl, M. I. S. & Gregorc, A. Heat shock proteins and cell death in situ localisation in hypopharyngeal glands of honeybee (*Apis mellifera carnica*) workers after imidacloprid or coumaphos treatment. *Apidologie* 41, 73-86, doi:10.1051/apido/2009051 (2010).
- 27 Hatjina, F. et al. Sublethal doses of imidacloprid decreased size of hypopharyngeal glands and respiratory rhythm of honeybees in vivo. *Apidologie* 44, 467-480, doi:10.1007/s13592-013-0199-4 (2013).
- 28 Heylen, K., Gobin, B., Arckens, L., Huybrechts, R. & Billen, J. The effects of four crop protection products on the morphology and ultrastructure of the hypopharyngeal gland of the European honeybee, *Apis mellifera*. *Apidologie* 42, 103-116, doi:10.1051/apido/2010043 (2011).
- 29 De Smet, L. et al. Stress indicator gene expression profiles, colony dynamics and tissue development of honey bees exposed to sub-lethal doses of imidacloprid in laboratory and field experiments. *PLoS one* 12, e0171529, doi:10.1371/journal.pone.0171529 (2017).
- 30 Wessler, I. et al. Honeybees Produce Millimolar Concentrations of Non-Neuronal Acetylcholine for Breeding: Possible Adverse Effects of Neonicotinoids. *PLoS one* 11, e0156886, doi:10.1371/journal.pone.0156886 (2016).
- 31 Wu-Smart, J. & Spivak, M. Sub-lethal effects of dietary neonicotinoid insecticide exposure on honey bee queen fecundity and colony development. *PLoS one* 6, 32108, doi:10.1038/srep32108 <https://www.nature.com/articles/srep32108#supplementary-information> (2016).
- 32 Di Prisco, G. et al. Neonicotinoid clothianidin adversely affects insect immunity and promotes replication of a viral pathogen in honey bees. *Proceedings of the National Academy of Sciences of the United States of America* 110, 18466-18471, doi:10.1073/pnas.1314923110 (2013).
- 33 Fischer, J. et al. Neonicotinoids interfere with specific components of navigation in honeybees. *PLoS one* 9, e91364, doi:10.1371/journal.pone.0091364 (2014).
- 34 Baines, D., Wilton, E., Pawluk, A., de Gorter, M. & Chomistek, N. Neonicotinoids act like endocrine disrupting chemicals in newly-emerged bees and winter bees. *Scientific reports* 7, 10979, doi:10.1038/s41598-017-10489-6 (2017).
- 35 Brandt, A. et al. Immunosuppression in Honeybee Queens by the Neonicotinoids Thiacloprid and Clothianidin. *Scientific reports* 7, 4673, doi:10.1038/s41598-017-04734-1 (2017).
- 36 Budge, G. E. et al. Evidence for pollinator cost and farming benefits of neonicotinoid seed coatings on oilseed rape. *Scientific reports* 5, 12574, doi:10.1038/srep12574 (2015).
- 37 Tsvetkov, N. et al. Chronic exposure to neonicotinoids reduces honey bee health near corn crops. *Science* 356, 1395-1397, doi:10.1126/science.aam7470 (2017).

- 38 Woodcock, B. A. et al. Country-specific effects of neonicotinoid pesticides on honey bees and wild bees. *Science* 356, 1393-1395, doi:10.1126/science.aaa1190 (2017).
- 39 Osterman, J. et al. Clothianidin seed-treatment has no detectable negative impact on honeybee colonies and their pathogens. *Nature communications* 10, 692, doi:10.1038/s41467-019-08523-4 (2019).
- 40 Cutler, G. C., Scott-Dupree, C. D., Sultan, M., McFarlane, A. D. & Brewer, L. A large-scale field study examining effects of exposure to clothianidin seed-treated canola on honey bee colony health, development, and overwintering success. *PeerJ* 2, e652, doi:10.7717/peerj.652 (2014).
- 41 Rundlof, M. et al. Seed coating with a neonicotinoid insecticide negatively affects wild bees. *Nature* 521, 77-80, doi:10.1038/nature14420 (2015).
- 42 Rolke, D., Fuchs, S., Grünwald, B., Gao, Z. & Blenau, W. Large-scale monitoring of effects of clothianidin-dressed oilseed rape seeds on pollinating insects in Northern Germany: effects on honey bees (*Apis mellifera*). *Ecotoxicology* 25, 1648-1665, doi:10.1007/s10646-016-1725-8 (2016).
- 43 Odemer, R., Nilles, L., Linder, N. & Rosenkranz, P. Sublethal effects of clothianidin and *Nosema* spp. on the longevity and foraging activity of free flying honey bees. *Ecotoxicology* 27, 527-538, doi:10.1007/s10646-018-1925-5 (2018).
- 44 Becher, M. A. et al. BEEHAVE: a systems model of honeybee colony dynamics and foraging to explore multifactorial causes of colony failure. *Journal of Applied Ecology* 51, 470-482, doi:10.1111/1365-2664.12222 (2014).
- 45 EN, D. in ISO 11348-1 Vol. Section 5 (2007).
- 46 Michener, C. D. *The Social Behavior of the Bees: A Comparative Study*. (Harvard University Press, 1974).
- 47 Sanchez-Bayo, F. & Goka, K. Pesticide Residues and Bees – A Risk Assessment. *PLoS one* 9, e94482, doi:10.1371/journal.pone.0094482 (2014).
- 48 Derecka, K. et al. Transient exposure to low levels of insecticide affects metabolic networks of honeybee larvae. *PLoS one* 8, e68191, doi:10.1371/journal.pone.0068191 (2013).
- 49 Hrassnigg, N. & Crailsheim, K. Differences in drone and worker physiology in honeybees (*Apis mellifera*). *Apidologie* 36, 255-277 (2005).
- 50 Crailsheim, K. The protein balance of the honey bee worker. *Apidologie* 21, 417-429 (1990).
- 51 Oomen, P. A., De Ruijter, A. & van der Steen, J. Method for honeybee brood feeding tests with insect growth-regulating insecticides. *EPPO Bulletin* 22, 613-616, doi:10.1111/j.1365-2338.1992.tb00546.x (1992).
- 52 Winston, M. L. *The Biology of the Honey Bee*. (Harvard University Press, 1987).
- 53 Williams, G. R. et al. Neonicotinoid pesticides severely affect honey bee queens. *Scientific reports* 5, 14621, doi:10.1038/srep14621 (2015).

- 54 Pettis, J. S., Rice, N., Joselow, K., vanEngelsdorp, D. & Chaimanee, V. Colony Failure Linked to Low Sperm Viability in Honey Bee (*Apis mellifera*) Queens and an Exploration of Potential Causative Factors. *PloS one* 11, e0147220, doi:10.1371/journal.pone.0147220 (2016).
- 55 Amdam, G. V., Rueppell, O., Fondrk, M. K., Page, R. E. & Nelson, C. M. The nurse's load: early-life exposure to brood-rearing affects behavior and lifespan in honey bees (*Apis mellifera*). *Experimental gerontology* 44, 467-471, doi:10.1016/j.exger.2009.02.013 (2009).
- 56 Becher, M. A. et al. BEESCOUT: A model of bee scouting behaviour and a software tool for characterizing nectar/pollen landscapes for BEEHAVE. *Ecological modelling* 340, 126-133, doi:10.1016/j.ecolmodel.2016.09.013 (2016).
- 57 Aagaard, A. et al. Statement on the suitability of the BEEHAVE model for its potential use in a regulatory context and for the risk assessment of multiple stressors in honeybees at the landscape level. doi: <https://doi.org/10.2903/j.efsa.2015.4125> (2015).
- 58 Rortais, A. et al. Risk assessment of pesticides and other stressors in bees: Principles, data gaps and perspectives from the European Food Safety Authority. *Science of The Total Environment* 587-588, 524-537, doi:<https://doi.org/10.1016/j.scitotenv.2016.09.127> (2017).
- 59 Rumke, J. C. O., Becher, M. A., Thorbek, P., Kennedy, P. J. & Osborne, J. L. Predicting Honeybee Colony Failure: Using the BEEHAVE Model to Simulate Colony Responses to Pesticides. *Environmental science & technology* 49, 12879-12887, doi:10.1021/acs.est.5b03593 (2015).
- 60 Thorbek, P., Campbell, P. J., Sweeney, P. J. & Thompson, H. M. Using BEEHAVE to explore pesticide protection goals for European honeybee (*Apis mellifera* L.) worker losses at different forage qualities. *Environmental Toxicology and Chemistry* 36, 254-264, doi:10.1002/etc.3504 (2017).
- 61 Christopher Cutler, G. & Scott-Dupree, C. D. A field study examining the effects of exposure to neonicotinoid seed-treated corn on commercial bumble bee colonies. *Ecotoxicology* 23, 1755-1763, doi:10.1007/s10646-014-1340-5 (2014).
- 62 Seeley, T. *The wisdom of the hive.* (Harvard University Press, 1995).
- 63 Gao, J., Barzel, B. & Barabási, A.-L. Universal resilience patterns in complex networks. *Nature* 530, 307-312, doi:10.1038/nature16948 <http://www.nature.com/nature/journal/v530/n7590/abs/nature16948.html#supplementary-information> (2016).
- 64 Bromenshenk, J., Gudatis, J., Carlson, S., Thomas, J. & Simmons, M. Population dynamics of honey bee nucleus colonies exposed to industrial pollutants. *Apidologie*, 2, 359 - 369 (1991).
- 65 Brandt, A., Gorenflo, A., Siede, R., Meixner, M., Büchler, R. The Neonicotinoids Thiacloprid, Imidacloprid and Clothianidin affect the immunocompetence of Honey Bees (*Apis mellifera* L.) *Journal of insect physiology* 86, 40-47 (2016).
- 66 Handloser, D., Widmer, V. & Reich, E. Separation of Phospholipids by HPTLC – An Investigation of Important Parameters. *Journal of Liquid Chromatography & Related Technologies* 31, 1857-1870, doi:10.1080/10826070802188940 (2008).

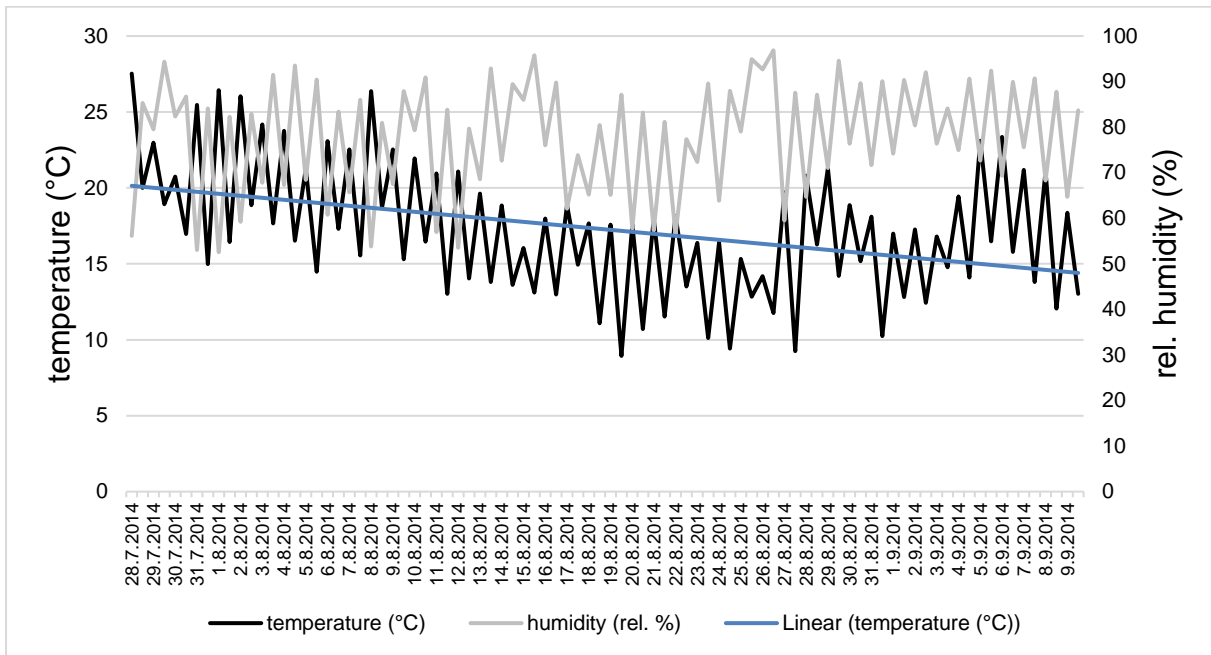
- 67 Kabrodt, K. & Schellenberg, I. Optimization of an AMD2 method for determination of starum corneum lipids. CAMAG Bibliography Service 105, 10-12 (2010).
- 68 Caswell, H. Matrix Population Models: construction, analysis, and interpretation. 2. Edition edn, (Sinauer Associates, Inc. Publishers Sunderland, Massachusetts, 2001).

Supplemental information

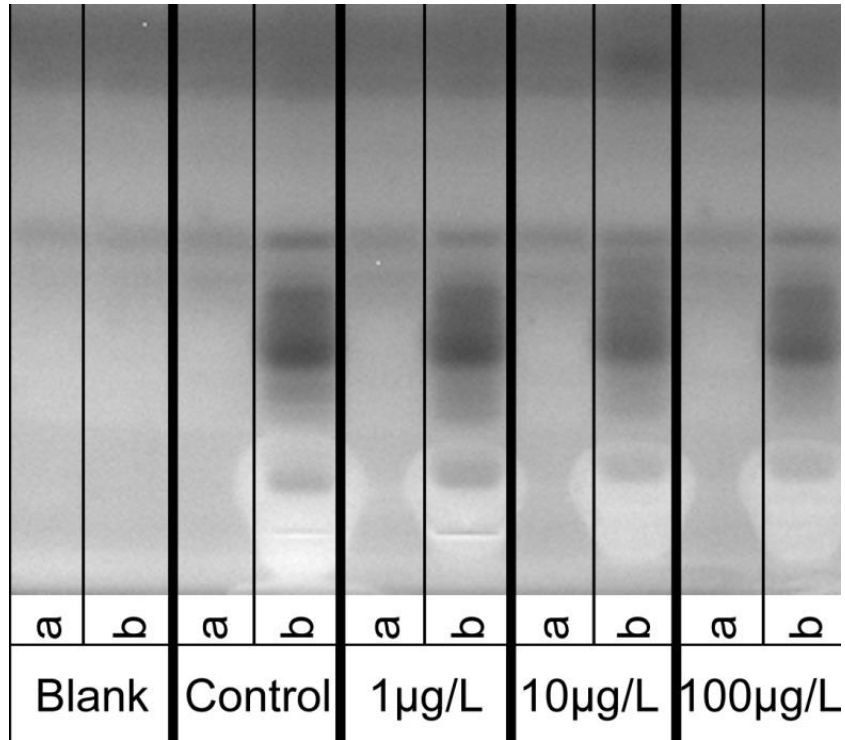


SFig 1. Sampling scheme. Each week (W1–7), all combs were photographed and samples of worker bees, larvae, and royal jelly were taken. To determine the size of the hypopharyngeal gland, 15 newly-hatched and marked worker bees were introduced into each colony during week 1 and recovered in week 2 (age-defined marked bees, green arrows). In week 7, randomly chosen worker bees of undefined age were taken from brood combs for the same reason (random bees). The total number of eggs, larvae and pupae were recorded for every week and colony (brood quantification). To determine the survival rate of individually tracked larvae, at least 50 individual cells per colony were followed over 4 weeks in the first half of the experiment (first brood cycle, brood survival phase A) and in the second half of the experiment (second brood cycle, brood survival phase B).

Climate recordings

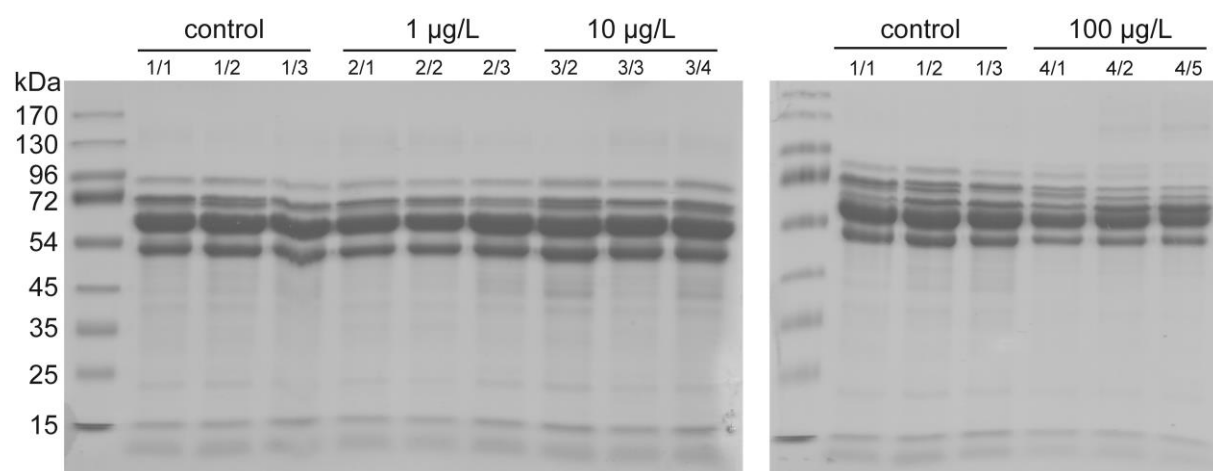


SFig 2. Climate data. Throughout the study period (July 28 to September 10, 2014), the temperature (°C) and relative humidity (%) were recorded twice daily (8:05 a.m. and 8:05 p.m.). A data logger recorded the temperature and relative humidity within the colonies over the study period. The daily temperature varied between 14.2 and 27.5 °C (8:00–20:00 h) and between 8.9 and 20 °C overnight (20:00–8:00 h). The relative humidity was 52.6–92.6% during the day and 73.8–96.9% overnight. The 20 colonies were all placed within an area of ~20 m². The control and treatment groups were randomly distributed within these colonies and were thus exposed to very similar environmental conditions.



SFig 3: HPTLC plate from Fig 2 showing the *A. fisherii* antimicrobial activity test. Each Sugi strip was cut halved to provide one part without the sample (a) and another with the sample (b). The blank is a fresh Sugi strip from the same batch as the strips used in the experiment, cut into equal halves. The other lanes show the clothianidin doses (Control = no clothianidin).

Protein analysis of royal jelly



SFig 4. Protein composition of royal jelly. The concentration and composition of major proteins in royal jelly was unaffected by clothianidin exposure. Royal jelly samples from week 4 (15 µg of protein per lane) were analyzed by SDS-PAGE in 12% polyacrylamide gels followed by staining with Coomassie Brilliant Blue. A visible decrease in protein levels was observed only in the 100 µg/L treatment group, although there were no significant differences in the quantity of total extracted proteins. Blotting strips were dipped in brood combs. Royal jelly was extracted by incubation in 100 µl RIPA high salt buffer (50 mM Tris HCl pH 7.6, 500 mM NaCl, 10 mM MgCl₂, 2 mM EDTA, 1% Triton X-100, 0.25% sodium deoxycholate, 0.1% SDS and Roche EDTA-free Protease cocktail mix) for 30 min at 4 °C. The protein concentration was determined using the DC Protein assay kit (Bio-Rad).

Clothianidin uptake

Suppl. Table 1. The clothianidin concentrations in spiked sugar syrup were close to the target concentrations, residues were detected in worker bees.

treatment group	clothianidin ($\mu\text{g/L}$) in sugar syrup (mean \pm SEM)	Clothianidin in workers (ng/bee) (mean)
control	0.0 \pm 0.00	0.00
1 $\mu\text{g/L}$	1.2 \pm 0.11	0.05
10 $\mu\text{g/L}$	10.1 \pm 0.29	0.20
100 $\mu\text{g/L}$	99.8 \pm 0.70	2.63

We analyzed the sugar syrup used to feed the experimental colonies to assess its exact clothianidin content. For all four experimental groups, the final spiked pesticide levels were close to the target concentrations (**Suppl. Table 1**). The consumption of the spiked syrup was recorded every week to estimate the total clothianidin uptake over the study period. The provided amount of 400 mL (= 540 g) syrup each week per colony was completely consumed each week with the exception of week 6 in the highest concentration treatment. All five colonies in the 100 $\mu\text{g/L}$ clothianidin treatment group were visibly weakened and did not consume all the sugar syrup, which was provided during week 6 (residual syrup: 76.7, 114.5, 142.2 and 18.0 g, respectively). To determine the clothianidin levels in bees exposed to the different pesticide levels, 10 randomly chosen worker bees from each hive were analyzed on week 7 (**Suppl. Table 1**). Clothianidin was detected in the bee sample from only one colony of the control group (colony I, 0.004 ng/bee).

Analytical Method

LC/MS/MS was used for the identification and quantification of the substances in the samples. The system used was a Prominence UFLC XR HPLC (SHIMADZU) coupled to a triple quadrupole mass spectrometer 4000 Q TRAP® (AB SCIEX) equipped with an electro spray ionization (ESI) source. Clothianidin and its metabolites clothianidin-metabolite TZMU and clothianidin-metabolite TZNG were identified by their retention time and three MRM transitions. The residues in the samples were quantified with reference standards in matrix (concentrations: 0.1, 0.5, 1, 5, 10, 25, 50 and 100

pg/ μ L). The quantification was carried out by the internal standard method. The values shown for the samples are averages of measurements out of duplicate injections of the sample extracts. The limit of detection (LOD) was determined as the lowest concentration tested in which the peak signal of the main MRM, which was used for quantification, was three times higher than the background noise of the chromatogram. The LOD was 0,5 pg/ μ L for clothianidin, 1 pg/ μ L for clothianidin-metabolite TZMU and 5 pg/ μ L for clothianidin-metabolite TZNG.

Sex-dependent immunosuppression response to the neonicotinoid insecticide thiacloprid in the red mason bee *Osmia bicornis* L.

Annely Brandt^{1*}, Birgitta Hohnheiser¹, Fabio Sgolastra², Jordi Bosch³, Marina Doris Meixner¹,
Ralph B uchler¹

¹LLH Bee Institute, Erlenstr. 9, 35274 Kirchhain, Germany;

²Dipartimento di Scienze e Tecnologie Agro-Alimentari, Universit  di Bologna, Bologna, Italy;

³CREAF, Bellaterra 08193, Spain

*Corresponding author

Email: annely.brandt@llh.hessen.de

LLH-Bee Institute Kirchhain

Erlenstr. 9

D-35274 Kirchhain

Tel.: +49 6422 940632

Fax: +49 6422 940633

Solitary bees are frequently exposed to pesticides, which are considered as one of the stress factors that may lead to population declines. A strong immune defence is vital for the fitness of bees, however, the immune system can be weakened by environmental factors that may render bees more vulnerable to parasites and pathogens.

Here we demonstrate for the first time that field-realistic concentrations of the commonly used neonicotinoid pesticide thiacloprid can severely affect the immunocompetence of *Osmia bicornis*. In detail, males exposed to thiacloprid solutions of 200 and 555 µg/kg showed a reduction in hemocyte density. Moreover, functional aspects of the immune defence - the antimicrobial activity of the hemolymph - were impaired in males. In females, however, only a concentration of 555 µg/kg elicited similar immunosuppressive effects. Although males are smaller than females, they consumed more food solution. This led to a 2.77 times higher exposure in males, probably explaining the different concentration thresholds observed between the sexes. In contrast to honeybees, dietary exposure to thiacloprid did not affect melanisation or wound healing in *O. bicornis*.

Our results demonstrate that neonicotinoid insecticides can negatively affect the immunocompetence of *O. bicornis*, possibly leading to an impaired disease resistance capacity.

Key words: *solitary bee, pesticide, immune system, hemocyte, antimicrobial activity*

Introduction

Bees (Anthophila) are important pollinators of wild plants and cultivated plants, and therefore are essential for ecosystem function and agricultural production^{1,2}. Over the past decades, serious declines in bee abundance and diversity have been reported in Europe and Northern America³⁻⁵. Multiple factors, such as habitat degradation, poor nutrition, parasites, pathogens, and pesticides, acting alone or in combination have contributed to these declines. Among pesticides, the use of neonicotinoid insecticides has been highlighted as important factors underlying bee losses⁶⁻⁹.

Neonicotinoids act as agonists of the nicotinic acetylcholine receptor, thus disrupting the neuronal cholinergic signal transduction, which results in abnormal behaviour, immobility and death of target pest insects. Beneficial insects such as bees can be exposed through ingestion of contaminated pollen and nectar of treated plants¹⁰⁻¹².

Harmful sublethal effects of orally ingested neonicotinoids on honeybees (*Apis mellifera* L.¹³, bumblebees (*Bombus* spp.¹⁴, and solitary bees^{9,15-18} have been reported in numerous laboratory and field trials, raising concerns over their widespread use and the potential threat to valuable pollination services for crops and wild plants³. So far, the majority of studies have focused on three neonicotinoid insecticides commonly used as seed dressings: imidacloprid, thiamethoxam and clothianidin. These insecticides are now considered to pose a serious risk to bees, and their use in the European Union has been restricted since 2013¹⁹. However, other neonicotinoids, such as thiacloprid and acetamiprid, are classified as not dangerous for bees, and in some regions or countries are frequently applied to flowering crops when bees are actively foraging²⁰. Their potential effects on bees have been largely overlooked, even though thiacloprid and acetamiprid were shown to cause sublethal impairments to bees under agronomically realistic conditions^{13,21-23}.

Sublethal exposure to agricultural pesticides has long been acknowledged to have ecologically relevant effects on bees^{13,20,24}. However, potential effects on immune function and disease resistance have only recently been recognized^{25,26}. Compromised immunity caused by

exposure to neonicotinoids has been demonstrated in honeybees^{22,23,27} and bumblebees²⁵, but information on solitary bees is largely missing. Honeybee exposure to neonicotinoids has been associated with negatively modulated immune signalling and increased virus replication²⁷, with reduced hemocyte numbers, wound healing, and cellular responses to bacterial infection^{22,23,28}, and with reduced activity of an enzyme involved in social immune food sterilisation²⁹. In bumblebees, exposure to high doses of imidacloprid reduced constitutive levels of phenoloxidase²⁵. Investigating the immune response of other bee taxa is important for three reasons. First, several studies have shown that different bee species may have different sensitivities to pesticides^{15,30-35}. Second, different bee species may lead differences in routes and levels of pesticide exposure^{36,37}. Third, social bees are considered less vulnerable to pesticides, because effects at the individual level can be buffered by the colony (colony resilience³⁸). These inter-specific differences have underscored the need to include several bee species in pesticide risk assessment schemes^{15,16,38,39}.

Two *Osmia* species, *Osmia cornuta* and *O. bicornis* have been proposed as model species by the EFSA Guidance Document on the risk assessment of plant protection products on solitary bees⁴⁰. Most bee risk assessment schemes and ecotoxicological studies focus on females⁴⁰. However, assessing the effects of pesticides on males is important for two reasons. First, in the vast majority of bee species, including all solitary species, males are also exposed to pesticides via nectar ingestion. Second, sex-specific differences in humoral immune parameters have been described for two solitary bee species^{41,42}. For these reasons, we decided to investigate potential response differences between the sexes.

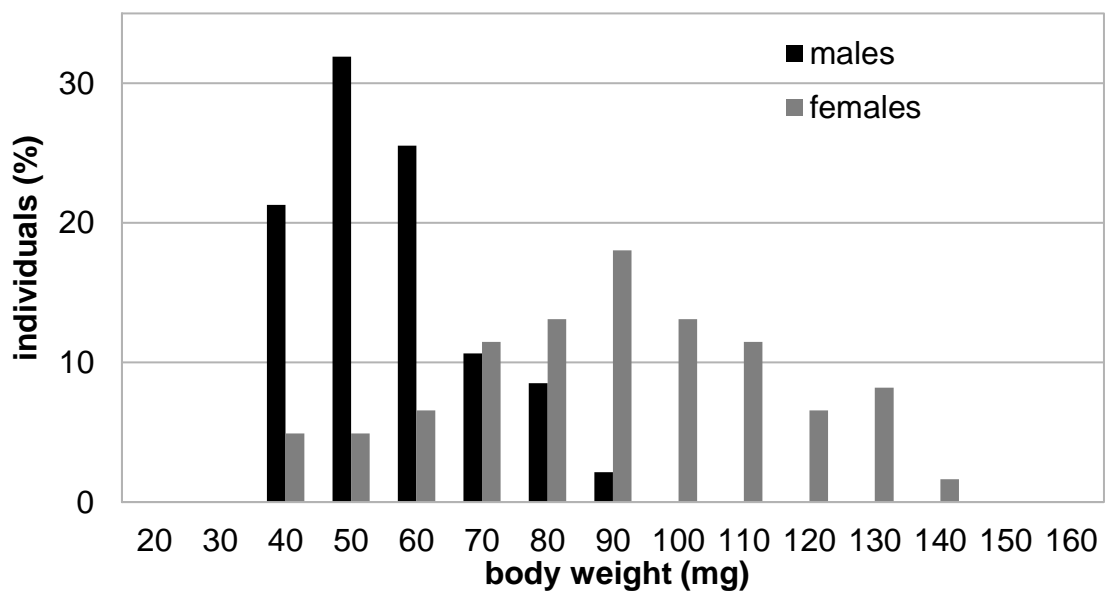
In this study, we investigate potential differences between the sexes in the immune response of a solitary bee, the red mason bee, *Osmia bicornis* L. (syn. *Osmia rufa* L.) to oral ingestion of thiacloprid. The objectives of our study are: (1) To describe functional parameters (hemocyte density, antimicrobial activity of the hemolymph, and melanisation response) of the immune system; (2) To examine, whether these parameters are affected by orally ingested sublethal concentrations of thiacloprid; (3) To compare the responses of males and females.

Results

Food consumption

Bees of both sexes consumed low amounts of sugar solution the first two days of exposure, but uptake increased on day three. Although females are heavier than males (Suppl. Fig 1), they consumed less feeding solution (Table 2). Hence, the total thiacloprid dosage of males in treatment 200 was 2.77 times higher than that of females. Based on these results, additional experiments with adjusted concentrations of 555 $\mu\text{g}/\text{kg}$ thiacloprid were performed to reach a similar dosage per mg body weight in females as in males of the treatment 200 group.

Pollen consumption was observed in both males and females. However, it was difficult to quantify because bees spread crumbles of the pollen patty all over the cage.



Suppl. Fig. 1 Body weight of individual bees. The weight of individual males (n = 269) and females (n = 327) were measured after the immune tests.

Total hemocyte counts

In males, a reduction in the total number of hemocytes was observed in the treatment groups 200 and 555 (Fig. 1a, KWT, $p = 0.001$; MWU, control₂₀₁₆ vs. treatment 200, $p = 0.001$; Fig. 1b, KWT, $p < 0.000$; MWU, control₂₀₁₈ vs. treatment 555, $p < 0.000$). However, in females exposure to 100 or 200 $\mu\text{g}/\text{kg}$ thiacloprid did not significantly reduce the total hemocyte counts (Fig. 1c, KWT, $p = 0.187$). Only when we exposed females to 555 $\mu\text{g}/\text{kg}$ (comparable to the dosage/mg body weight ingested by males in treatment 200), we observed a significantly reduced number of hemocytes (Fig. 1d, KWT, $p < 0.000$; MWU control₂₀₁₈ vs. treatment 555, $p < 0.000$). Unexpectedly, the total number of hemocytes differed between the years (control₂₀₁₆ vs. control₂₀₁₈: females, MWU, $p < 0.000$; males, MWU, $p = 0.004$).

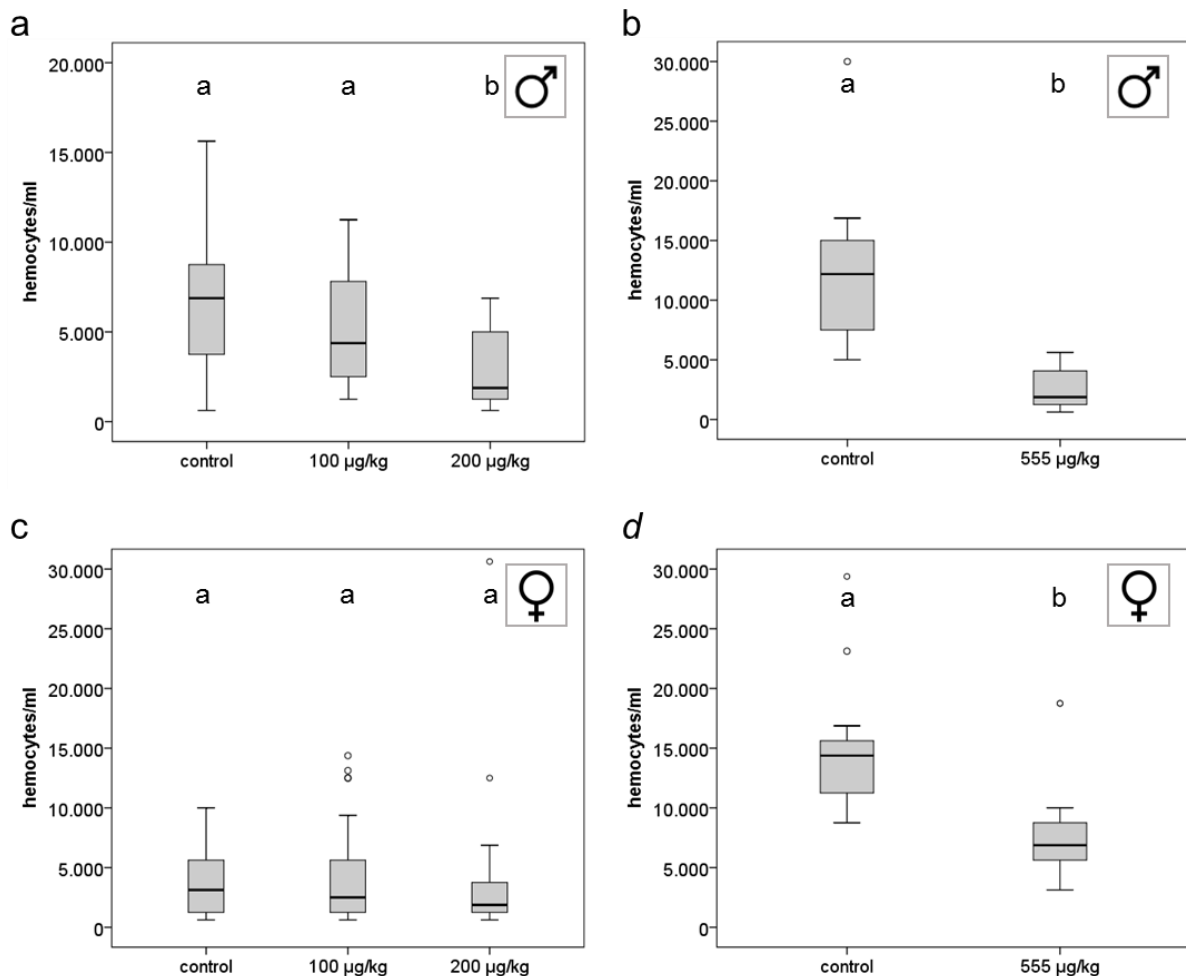


Fig. 1 Hemocyte counts in males and females in relation to thiacloprid concentration of feeding solution (a, b) Males exposed to thiacloprid showed a significantly reduced total number of hemocytes **(c)** Hemocyte density of females exposed to 100 or 200 µg/kg thiacloprid showed no differences from control. **(d)** Exposure to 555 µg/kg resulted in reduced hemocyte density in females.

Antimicrobial activity of the hemolymph

The size of the inhibition zones was significantly reduced in males exposed to 200 or 555 $\mu\text{g}/\text{kg}$ thiacloprid (Fig. 2b; KWT, $p = 0.002$; MWU control_{2016} vs. treatment 200, $p = 0.0008$; control_{2018} vs. treatment 555, $p < 0.000$). The antimicrobial activity was not significantly reduced in females exposed to 100 or 200 $\mu\text{g}/\text{kg}$ thiacloprid (Fig. 2c; KWT, $p = 0.454$). Only females exposed to 555 $\mu\text{g}/\text{kg}$ thiacloprid showed significantly reduced inhibition zones (Fig. 2d, MWU, control_{2018} vs. treatment 555, $p < 0.000$).

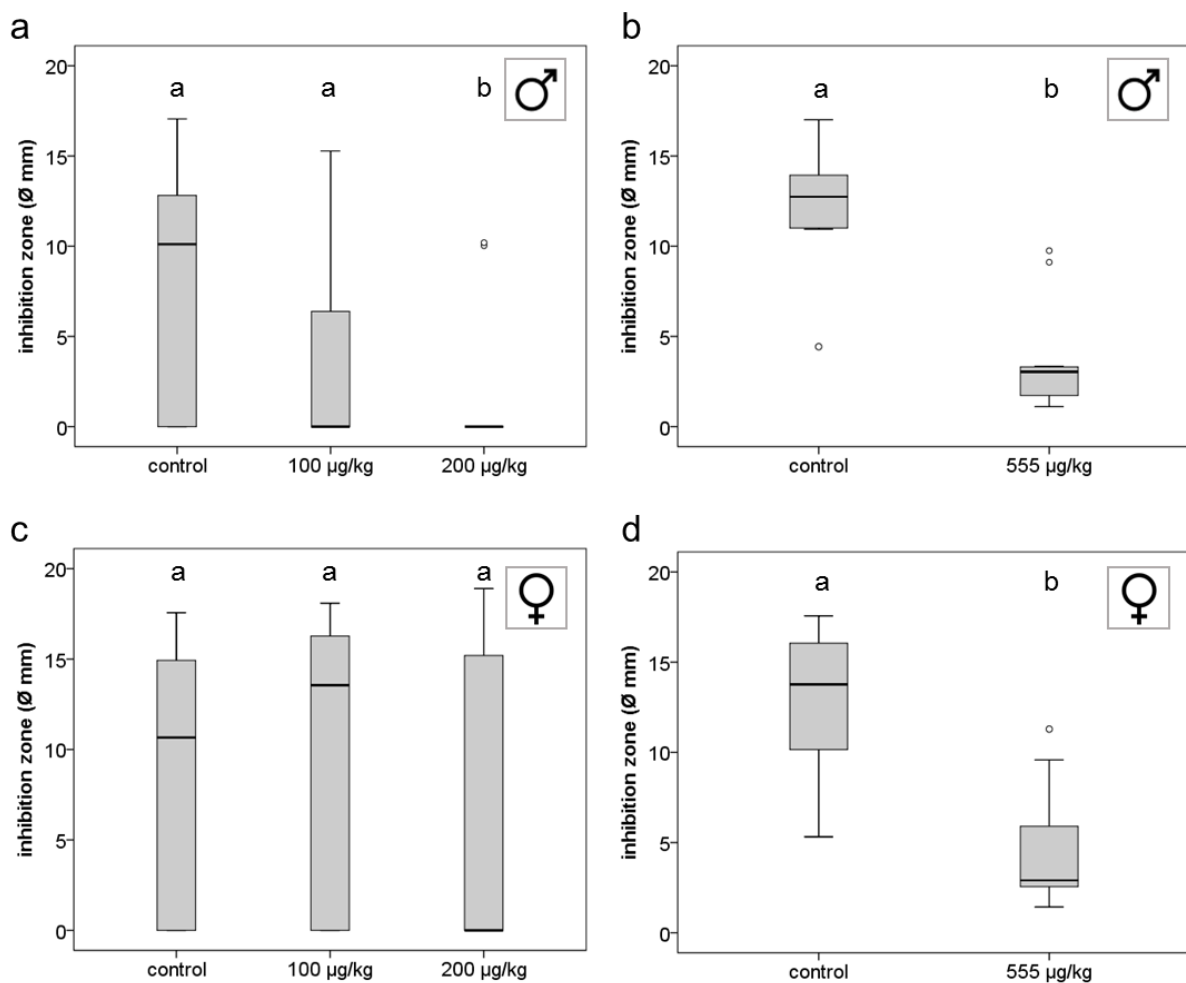


Fig. 2 Antimicrobial activity of hemolymph of males and females in relation to thiacloprid concentration of feeding solution. (a, b) the diameters of inhibition zones were significantly reduced in males exposed to thiacloprid (c) females exposed to lower concentrations of thiacloprid showed no effect on antimicrobial activity (d) the inhibition zone

diameters of females exposed to the highest concentration (555 $\mu\text{g}/\text{kg}$) were significantly reduced.

Encapsulation response

The encapsulation response to thiacloprid exposure was not significantly reduced in males (Fig. 3a; KWT, $p = 0.295$) or females (Fig. 3b; KWT, $p = 0.303$).

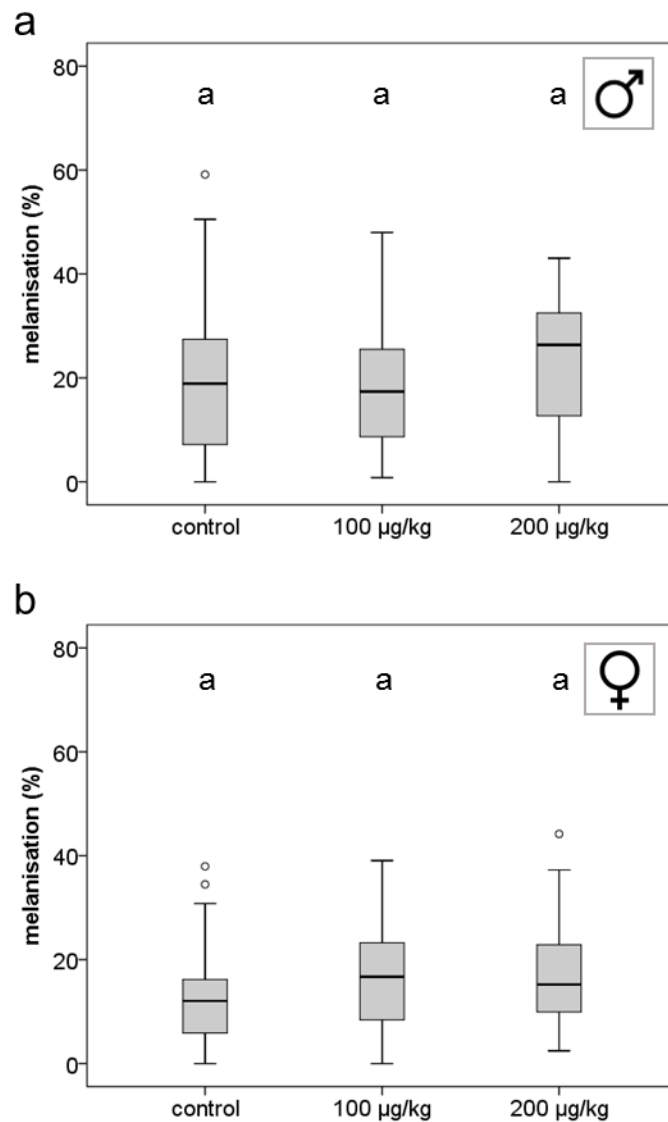


Fig. 3 Exposure to thiacloprid had no effect on the melanisation response. The three day-exposure of young females (a), and males (b) had no effect on the melanisation of an implanted nylon filament compared to control.

Discussion

We provide the first demonstration that the commonly used neonicotinoid insecticide thiacloprid impairs the immune defence of the solitary bee *Osmia bicornis*. The number of hemocytes as well as the antimicrobial activity of the hemolymph were negatively affected by sublethal, environmentally relevant concentrations of thiacloprid. Although males are smaller than females, they consumed significantly more food than females. This led to a higher exposure in males even at field-realistic concentrations of thiacloprid, probably explaining the different concentration thresholds observed between the sexes. In contrast to honeybees, dietary exposure to thiacloprid did not affect the melanisation or wound healing response in *O. bicornis*.

Thiacloprid is generally regarded as non-harmful to bees based on its relatively low acute toxicity to honeybees (oral acute $LD_{50_{48h}} = 17.32 \mu\text{g}/\text{honeybee}^{43}$). The thiacloprid concentrations we used fall within the range of concentrations found in field situations. In pollen collected by honeybees, mean thiacloprid residues were $75.1 \mu\text{g}/\text{kg}$ (max.: $1002 \mu\text{g}/\text{kg}$, mean prevalence of 17.7%) and $6.5 \mu\text{g}/\text{kg}$ in honey (max.: $208 \mu\text{g}/\text{kg}$, 64% prevalence⁴⁴). In the German bee monitoring project, the highest concentration of thiacloprid in beebread samples was $498 \mu\text{g}/\text{kg}^{45}$.

In general, hemocytes are the key components of the cellular immune defence of insects. They are responsible for phagocytosis or encapsulation of pathogens as well as for wound closure^{46,47}. On average, female *O. bicornis* had lower total hemocyte counts than males. Interestingly, only the highest concentration of $555 \mu\text{g}/\text{kg}$ thiacloprid reduced the hemocyte density in females. In contrast, we found a reduction of hemocyte number in males dosed as low as with $200 \mu\text{g}/\text{kg}$, indicating a disturbance of the immune system after exposure to concentrations frequently found under field conditions⁴⁵. This reduction of hemocytes in neonicotinoid-exposed *O. bicornis* could limit the capacity of the red mason bees to mount a rapid immune response⁴⁸.

One essential functional aspect of the bee's immune system is the induced immunity as measured by humoral antimicrobial activity of the hemolymph. The humoral immune response is mediated by antimicrobial peptides that are produced by hemocytes and fat body cells. These are biologically active molecules with antibacterial, antifungal, or antiviral properties^{47,49}. Together with the reduction of hemocyte density, the reduced antimicrobial activity in thiacloprid-exposed males (200 and 555 µg/kg) and females (555 µg/kg) could likely impair the immune strength of *O. bicornis* and increase their susceptibility towards pathogens.

In insects, hemocytes actively encapsulate infected cells or intruding pathogens and migrate to wounds in order to close them. Concurrently, hemocytes produce prophenoloxidase, the precursor of the enzyme phenoloxidase, which catalyses the melanisation reaction⁴⁷. In both female and male *O. bicornis*, a melanisation reaction of an implanted nylon fibre was observed. However, contrary to findings in *A. mellifera* workers²³ and queens²², where thiacloprid significantly reduced the melanisation response, no reduction was observed in *O. bicornis*. This finding may reflect differences in the pathogen and parasite pressure of these two species. In contrast to *O. bicornis*, honeybees have co-evolved with hemolymph sucking parasites (*Acarapis woodi*, *Tropilaelaps* spp., and recently *Varroa destructor*) which might explain this divergence between *O. bicornis* and *A. mellifera*. Our results emphasises the need to test different species and not to generalize the findings of honeybee studies to other bee species.

Neonicotinoids have been shown to affect the immunocompetence of honeybees. Like in *O. bicornis*, thiacloprid has been shown to reduce the hemocyte density, especially the proportion of active, differentiated immune cells in honeybees as well as the antimicrobial activity of the hemolymph^{22,23}. Neonicotinoids negatively modulate NF-κB immune signalling and promote the replication of deformed wing virus²⁷. Moreover, thiacloprid increases the mortality of *Nosema ceranae* infected honeybees⁵⁰. Whether neonicotinoids affect the disease susceptibility of *O. bicornis* remains to be elucidated.

The observed differences in immunocompetence between male and female *O. bicornis* are likely related to the differences in food uptake, resulting in unequal exposure levels. Indeed,

we observed huge differences in absolute food uptake between females and males across all four treatments. For example, males of the 200 treatment consumed 0.5 ng thiacloprid per mg body weight, whereas females consumed only 0.18 ng/mg. After including an additional higher concentration of 555 µg/kg, to account for these differences, reduction of immunocompetence was also observed in females.

The higher food consumption of males can be explained by behavioural differences between the sexes in the post-emergence phase. On average, males emerge 2-4 days before females. They actively patrol nesting sites and try to mate with emerging females, most of which are mated right upon emergence. Once mated, newly emerged females typically hide in crevices and undergo a 2-5-day pre-nesting period, during which they complete ovary maturation⁵¹. We observed similar behavioural patterns in our experimental flight cages where males were flying and walking extensively, whereas females were mostly hiding in the artificial nesting tubes.

Interestingly, sex-specific differences in immune parameters of *O. bicornis*⁴¹ and *Megachile rotundata*⁴² were previously reported, indicating lower concentrations and activity levels of phenoloxidase and alkaline phosphatase, and of enzymatic and non-enzymatic antioxidant and proteolytic systems in males. Based on our experimental data, we cannot determine whether physiological or behavioural differences or both caused the divergent immunosuppressive effects between the sexes.

The current risk assessment scheme for the approval and authorization of pesticides focuses on *A. mellifera*, implicating that data obtained with honey bees can be extrapolated to other bee species without considering inter-specific differences¹⁵. *A. mellifera* is generally considered as extremely sensitive to pesticides and a good indicator species for environmental pollution. However, the extrapolation of a risk assessment to other bees may not be appropriate. The response to pesticides and the differences in the level of exposure may vary significantly between bee taxa^{35,40}. Indeed, our results indicate clear differences between red mason bees and honeybees and emphasize the need for comparative studies and independent pesticide risk assessment procedures for non-*Apis* bees.

Currently, only the food intake of adult females is considered as relevant; while food intake of adult male is regarded “not relevant” or unknown^{40,52}. However, our results show clear sex-specific differences in food uptake and exposure level and – most likely as a consequence - an elevated response of males towards field realistic thiacloprid concentrations. Therefore, male bees should be included in future risk assessment schemes for approval and authorization of pesticides.

The interaction of pathogens and pesticides is of grave concern in relation to pollinator health. Multiple stressors on bee health act not in isolation, but rather interact, with possible synergistic effects on bees and bee populations^{5,53}. Our findings highlight the importance of including non-*Apis* species and both sexes in eco-toxicological studies and risk assessment procedures²⁴.

Methods

***Osmia bicornis* population management**

Osmia bicornis cocoons reared at the arboretum of the Botanical Garden of the University of Rostock (Germany) were obtained from Johann-Christoph Kornmilch (bienenhotel.de, Rostock, Germany). The cocoons were shipped in January and stored in the dark at 4° - 7°C. To induce adult emergence, cocoons were placed in cages (30 x 30 x 30 cm, Aerarium, bioform, Nürnberg, Germany) under natural light at room temperature (1st of March - 4th of May 2016 and 2018; average temperature 22.6°C, min 20.0°C, max. 24.2°C; relative humidity 62%, min. 58.8%, max. 72%, datalogger EL-USB-2, Lascar electronics, Whiteparish). We separated female and male cocoons based on size, and kept them in separate cages for the whole study. Approximately 24 hours after emergence, we transferred the bees to new cages in groups of 5 to 10 individuals, where the exposure to thiacloprid took place. We conducted three independent replicates (cages) per treatment and sex for each immune assay.

Test solutions

A stock solution of 2 mg/ml thiacloprid (Sigma Aldrich, St. Louis, USA; purity 99.9%) in acetone was prepared in a glass flask and stored in the dark at 15°C until use. The stock solution was

added to a 50% feeding solution of invert sugar (Ambrosia, Germany) in distilled water (w/v) to reach three test concentrations: 100, 200, and 555 µg/kg (henceforward referred to as treatment 100, 200 and 555). The final concentration of acetone in the test solutions was adjusted to 0.0086% (v:v) in all treatments.

A pollen patty was prepared from pollen collected by honey bees at the Bee Institute Kirchhain or obtained from Imkereibedarf Bährle (Aschaffenburg, Germany). The pollen was stored at -20°C for 8 - 10 months and then pulverized in a coffee grinder. The resulting pollen powder was mixed with the thiacloprid-spiked feeding solution to obtain the same concentrations as the feeding solution (100, 200, 555 µg of thiacloprid per kg of pollen patty).

Neonicotinoid exposure

Test cages were placed close to each other (~2 cm), so bees of both sexes could see, hear and smell each other. Fragments of egg carton and 5 cm segments of black plastic drinking straws were placed in each flight cage as hiding sites. Cages were kept at room temperature under natural light conditions.

Caps of 1.5 ml microcentrifuge tubes (Eppendorf, Hamburg, Germany) were cut off and used as containers for the feeding solution (two caps per cage) and pollen paste (two caps per cage). The bottoms of the caps were coloured red or blue and placed on a green piece of cardboard to attract the bees. Both females and males found the food sources immediately, and feeding was observed frequently.

Each cage was assigned to one of four thiacloprid treatments and exposed for three days. Feeding caps were weighed and renewed every day. For each treatment group and sex, three cages were set up on independent dates (Table 1). In 2016, we tested the 0, 100 and 200 µg/kg treatments. Then, based on the discrepancies observed between the dosage per bodyweight in males and females, additional experiments with 0 and 555 treatments were conducted (three groups for each treatment and sex on independent dates in 2018) to obtain data on a dosage taken up by females equivalent to the 200 treatment in males (Table 1).

Hemolymph extraction and total hemocyte counts

Bees were anesthetized on ice, and hemolymph was extracted by inserting a microinjection needle (Hartenstein, Würzburg, Germany) into the proximal abdomen between the 3rd and 4th tergum. Hemolymph (1 µl) was transferred to PCR-tubes (Biozym, Hessisch Oldendorf, Germany) containing 1 µl of DAPI-staining solution (4',6-diamidino-2-phenylindole; 1:100 dilution, lifetechnologies, Carlsbad, California, USA) and 3 µl PBS (pH 7.4; Sigma Aldrich, St. Louis, USA). Hemocytes were counted in a counting chamber (Bürker, Carl Roth, Karlsruhe, Germany) under a phase contrast/fluorescent microscope (Leica DMIL, Leica camera DFC 420C).

Encapsulation response

A 2.5 mm nylon filaments were partly inserted into the abdomen of anesthetized bees as previously described for honeybees^{22,23}. After implantation, females were transferred to 1.5 ml microcentrifuge tubes and males to PCR-tubes with holes poked through the cap and sidewalls. After four hours at room temperature, the nylon filament was extracted, fixed in formaldehyde solution for at least 1 hour, rinsed three times in PBS, and subsequently mounted in glycerol (85%, Carl Roth). For each explant, three pictures were taken at different focal depths. The mean grey value per filament was calculated using image analysis software and taken as a measure of melanisation⁵⁴. The mean grey value of a non-implanted filament was subtracted from the mean grey value of the implanted filaments²².

Antimicrobial response

On day two of the exposure phase, the immune system was challenged by the injection of 1 µl of heat-inactivated *Escherichia coli* (OD 0.5). Hemolymph was collected and stored at - 20°C. Bacterial test plates (ø 9 cm) were prepared by adding 0.8 ml of live *Micrococcus luteus* bacteria suspension (OD 0.5) to 150 ml of sterile broth medium (48°C, 1.5 g Agar No. 1, Oxoid; 3.75 g nutrient broth, Applichem). For each test plate, five holes (ø 3.33 mm) were punched into the agar with a 1 ml pipette tip, and 1 µl of hemolymph solution was added to each hole. Plates were incubated at 38°C overnight, and the diameter of inhibition zones was measured with a digital calliper.

Statistical methods

All statistical tests were run with SPSS for Windows (v. 20). Total hemocyte counts, melanisation/mean grey values, and mean diameters of inhibition zones were not normally distributed. Thus non-parametric statistics were applied. Each immunocompetence measure was compared across treatments using Kruskal–Wallis tests (KWT) followed by post-hoc pairwise comparisons with Mann–Whitney U tests (MWU) and Bonferroni corrections (when more than two groups were compared).

Ethics

Ethical approval and the licences were obtained from the Hessian Regional Council of Giessen (RPGI), Germany.

Availability of relevant data and materials

The datasets supporting this article have been uploaded as part of the supplementary material.

Conflict of interest:

The authors have no competing interests.

Author contributions

AB and BH designed the study and performed the experiments. AB and BH analysed the data and AB, FS, JB wrote the manuscript. All authors edited and approved the manuscript.

Acknowledgments

We gratefully thank S. Backhaus for technical support.

Funding

This research was supported by the EU and Land Hessen „Förderung von Maßnahmen zur Verbesserung der Erzeugung und Vermarktung von Honig in Hessen“.

References

- 1 Klein, A.-M., Vaissière, B. E., Cane, J. H., Steffan-Dewenter, I., Cunningham, S. A., Kremen, C. . Importance of pollinators in changing landscapes for world crops. *Proceedings of the Royal Society of London B: Biological Sciences* **274**, 303–313, doi:doi:10.1098/rspb.2006.3721 (2007).
- 2 Garibaldi, L. A. *et al.* Wild pollinators enhance fruit set of crops regardless of honey bee abundance. *Science* **339**, 1608-1611, doi:10.1126/science.1230200 (2013).
- 3 Potts, S. G. *et al.* Global pollinator declines: trends, impacts and drivers. *Trends in ecology & evolution* **25**, 345-353, doi:10.1016/j.tree.2010.01.007 (2010).
- 4 vanEngelsdorp, D. & Meixner, M. D. A historical review of managed honey bee populations in Europe and the United States and the factors that may affect them. *Journal of invertebrate pathology* **103**, S80-S95, doi:https://doi.org/10.1016/j.jip.2009.06.011 (2010).
- 5 Goulson, D., Nicholls, E., Botias, C. & Rotheray, E. L. Bee declines driven by combined stress from parasites, pesticides, and lack of flowers. *Science* **347**, 1255957, doi:10.1126/science.1255957 (2015).
- 6 Whitehorn, P. R., Tinsley, M. C., Brown, M. J., Darvill, B. & Goulson, D. Genetic diversity, parasite prevalence and immunity in wild bumblebees. *Proceedings. Biological sciences / The Royal Society* **278**, 1195-1202, doi:10.1098/rspb.2010.1550 (2011).
- 7 Goulson, D. REVIEW: An overview of the environmental risks posed by neonicotinoid insecticides. *Journal of Applied Ecology* **50**, 977-987, doi:10.1111/1365-2664.12111 (2013).
- 8 van der Sluijs, J. P. *et al.* Conclusions of the Worldwide Integrated Assessment on the risks of neonicotinoids and fipronil to biodiversity and ecosystem functioning. *Environmental science and pollution research international* **22**, 148-154, doi:10.1007/s11356-014-3229-5 (2015).
- 9 Woodcock, B. A. *et al.* Impacts of neonicotinoid use on long-term population changes in wild bees in England. *Nature communications* **7**, 12459, doi:10.1038/ncomms12459 (2016).
- 10 Sanchez-Bayo, F. *et al.* Are bee diseases linked to pesticides? - A brief review. *Environment international* **89-90**, 7-11, doi:10.1016/j.envint.2016.01.009 (2016).
- 11 Desneux, N., Decourtye, A. & Delpuech, J. M. The sublethal effects of pesticides on beneficial arthropods. *Annual review of entomology* **52**, 81-106, doi:10.1146/annurev.ento.52.110405.091440 (2007).
- 12 David, A. *et al.* Widespread contamination of wildflower and bee-collected pollen with complex mixtures of neonicotinoids and fungicides commonly applied to crops. *Environment international* **88**, 169-178, doi:10.1016/j.envint.2015.12.011 (2016).
- 13 Blacquiere, T., Smagghe, G., van Gestel, C. A. & Mommaerts, V. Neonicotinoids in bees: a review on concentrations, side-effects and risk assessment. *Ecotoxicology* **21**, 973-992, doi:10.1007/s10646-012-0863-x (2012).

- 14 Whitehorn, P. R., O'Connor, S., Wackers, F. L. & Goulson, D. Neonicotinoid pesticide reduces bumble bee colony growth and queen production. *Science* **336**, 351-352, doi:10.1126/science.1215025 (2012).
- 15 Arena, M. & Sgolastra, F. A meta-analysis comparing the sensitivity of bees to pesticides. *Ecotoxicology* **23**, 324-334, doi:10.1007/s10646-014-1190-1 (2014).
- 16 Woodcock, B. A. *et al.* Country-specific effects of neonicotinoid pesticides on honey bees and wild bees. *Science* **356**, 1393-1395, doi:10.1126/science.aaa1190 (2017).
- 17 Jin, N., Klein, S., Leimig, F., Bischoff, G. & Menzel, R. The neonicotinoid clothianidin interferes with navigation of the solitary bee *Osmia cornuta* in a laboratory test. *The Journal of experimental biology* **218**, 2821-2825, doi:10.1242/jeb.123612 (2015).
- 18 Sgolastra, F. *et al.* Combined exposure to sublethal concentrations of an insecticide and a fungicide affect feeding, ovary development and longevity in a solitary bee. *Proceedings of the Royal Society B: Biological Sciences* **285**, 20180887, doi:doi:10.1098/rspb.2018.0887 (2018).
- 19 European Commission. Commission implementing Regulation (EU) No 485/2013 of 24 May 2013 amending Implementing Regulation (EU) No 540/2011, as regards the condition of approval of the active substances clothianidin, thiamethoxam and imidacloprid, and prohibiting the use and sale of seeds treated with plant protection products containing those active substances. . *Official Journal of the European Union, L139/12 25.5.2013*. (2013).
- 20 Klatt, B. K., Rundlöf, M. & Smith, H. G. Maintaining the Restriction on Neonicotinoids in the European Union – Benefits and Risks to Bees and Pollination Services. *Frontiers in Ecology and Evolution* **4**, doi:10.3389/fevo.2016.00004 (2016).
- 21 Godfray, H. C. *et al.* A restatement of the natural science evidence base concerning neonicotinoid insecticides and insect pollinators. *Proceedings. Biological sciences / The Royal Society* **281**, doi:10.1098/rspb.2014.0558 (2014).
- 22 Brandt, A. *et al.* Immunosuppression in Honeybee Queens by the Neonicotinoids Thiacloprid and Clothianidin. *Scientific reports* **7**, 4673, doi:10.1038/s41598-017-04734-1 (2017).
- 23 Brandt, A., Gorenflo, A., Siede, R., Meixner, M., Büchler, R. The Neonicotinoids Thiacloprid, Imidacloprid and Clothianidin affect the immunocompetence of Honey Bees (*Apis mellifera* L.) *Journal of insect physiology* **86**, 40-47 (2016).
- 24 Cabrera, A. R. *et al.* Initial recommendations for higher-tier risk assessment protocols for bumble bees, *Bombus* spp. (Hymenoptera: Apidae). *Integrated environmental assessment and management* **12**, 222-229, doi:10.1002/ieam.1675 (2016).
- 25 Czerwinski, M. A. & Sadd, B. M. Detrimental interactions of neonicotinoid pesticide exposure and bumblebee immunity. *Journal of Experimental Zoology Part A: Ecological and Integrative Physiology* **327**, 273-283, doi:10.1002/jez.2087 (2017).
- 26 Sánchez-Bayo, F. & Desneux, N. Neonicotinoids and the prevalence of parasites and disease in bees. *Bee World* **92**, 34-40, doi:10.1080/0005772x.2015.1118962 (2015).
- 27 Di Prisco, G. *et al.* Neonicotinoid clothianidin adversely affects insect immunity and promotes replication of a viral pathogen in honey bees. *Proceedings of the National*

- Academy of Sciences of the United States of America* **110**, 18466-18471, doi:10.1073/pnas.1314923110 (2013).
- 28 López, J. H. *et al.* Sublethal pesticide doses negatively affect survival and the cellular responses in American foulbrood-infected honeybee larvae. *Scientific reports* **7**, 40853, doi:10.1038/srep40853 (2017).
- 29 Alaux, C. *et al.* Interactions between *Nosema* microspores and a neonicotinoid weaken honeybees (*Apis mellifera*). *Environmental microbiology* **12**, 774-782, doi:10.1111/j.1462-2920.2009.02123.x (2010).
- 30 Ladurner, E., Bosch, J., Kemp, W. & Maini, S. *Assessing delayed and acute toxicity of five formulated fungicides to Osmia lignaria Say and Apis mellifera*. Vol. 36 (2005).
- 31 Scott-Dupree, C. D., Conroy, L. & Harris, C. R. Impact of currently used or potentially useful insecticides for canola agroecosystems on *Bombus impatiens* (Hymenoptera: Apidae), *Megachile rotundata* (Hymenoptera: Megachilidae), and *Osmia lignaria* (Hymenoptera: Megachilidae). *Journal of economic entomology* **102**, 177-182 (2009).
- 32 Biddinger, D. J. *et al.* Comparative Toxicities and Synergism of Apple Orchard Pesticides to *Apis mellifera* (L.) and *Osmia cornifrons* (Radoszkowski). *PLoS one* **8**, e72587, doi:10.1371/journal.pone.0072587 (2013).
- 33 Heard, M. S. *et al.* Comparative toxicity of pesticides and environmental contaminants in bees: Are honey bees a useful proxy for wild bee species? *The Science of the total environment* **578**, 357-365, doi:10.1016/j.scitotenv.2016.10.180 (2017).
- 34 Uhl, P. *et al.* Interspecific sensitivity of bees towards dimethoate and implications for environmental risk assessment. *Scientific reports* **6**, 34439, doi:10.1038/srep34439 (2016).
- 35 Sgolastra, F. *et al.* Synergistic mortality between a neonicotinoid insecticide and an ergosterol-biosynthesis-inhibiting fungicide in three bee species. *Pest management science* **73**, 1236-1243, doi:10.1002/ps.4449 (2017).
- 36 Gradish, A. E. *et al.* Comparison of Pesticide Exposure in Honey Bees (Hymenoptera: Apidae) and Bumble Bees (Hymenoptera: Apidae): Implications for Risk Assessments. *Environ Entomol* **48**, 12-21, doi:10.1093/ee/nvy168 (2019).
- 37 Cham, K. O. *et al.* Pesticide Exposure Assessment Paradigm for Stingless Bees. *Environ Entomol* **48**, 36-48, doi:10.1093/ee/nvy137 (2018).
- 38 Rundlof, M. *et al.* Seed coating with a neonicotinoid insecticide negatively affects wild bees. *Nature* **521**, 77-80, doi:10.1038/nature14420 (2015).
- 39 Sgolastra, F. *et al.* Pesticide Exposure Assessment Paradigm for Solitary Bees. *Environ Entomol* **48**, 22-35, doi:10.1093/ee/nvy105 (2018).
- 40 EFSA. Scientific opinion on the science behind the development of a risk assessment of plant protection products on bees (*Apis mellifera*, *Bombus* spp. and solitary bees). *EFSA J* **10**, 2668 (2012).
- 41 Strachecka, A. *et al.* Insights into the biochemical defence and methylation of the solitary bee *Osmia rufa* L: A foundation for examining eusociality development. *PLoS one* **12**, e0176539, doi:10.1371/journal.pone.0176539 (2017).

- 42 Frohlich, D. R., Burris, T. E. & Brindley, W. A. Characterization of glutathione S-transferases in a solitary bee, *Megachile rotundata* (Fab.) (hymenoptera: megachilidae) and inhibition by chalcones, flavone, quercetin and tridiphanediol. *Comparative Biochemistry and Physiology Part B: Comparative Biochemistry* **94**, 661-665, doi:[https://doi.org/10.1016/0305-0491\(89\)90146-6](https://doi.org/10.1016/0305-0491(89)90146-6) (1989).
- 43 Hertfordshire, U. o. The Pesticide Properties DataBase (PPDB) developed by the Agriculture & Environment Research Unit (AERU). *University of Hertfordshire, 2006-2013* (2013).
- 44 Sanchez-Bayo, F. & Goka, K. Pesticide Residues and Bees – A Risk Assessment. *PLoS one* **9**, e94482, doi:10.1371/journal.pone.0094482 (2014).
- 45 Rosenkranz, P. *et al.* DeBiMo-Zwischenbericht. *Deutsches Bienenmonitoring* (2017).
- 46 Negri, P. *et al.* Cellular immunity in *Apis mellifera*: studying hemocytes brings light about bees skills to confront threats. *Apidologie*, 1-10 (2015).
- 47 Evans, J. D. *et al.* Immune pathways and defence mechanisms in honey bees *Apis mellifera*. *Insect molecular biology* **15**, 645-656, doi:10.1111/j.1365-2583.2006.00682.x (2006).
- 48 Wilson-Rich, N., Dres, S. T. & Starks, P. T. The ontogeny of immunity: development of innate immune strength in the honey bee (*Apis mellifera*). *Journal of insect physiology* **54**, 1392-1399 (2008).
- 49 Tonk, M., Vilcinskas, A. & Rahnamaeian, M. Insect antimicrobial peptides: potential tools for the prevention of skin cancer. *Applied microbiology and biotechnology* **100**, 7397-7405, doi:10.1007/s00253-016-7718-y (2016).
- 50 Retschnig, G., Neumann, P. & Williams, G. R. Thiacloprid-Nosema ceranae interactions in honey bees: host survivorship but not parasite reproduction is dependent on pesticide dose. *Journal of invertebrate pathology* **118**, 18-19, doi:10.1016/j.jip.2014.02.008 (2014).
- 51 Bosch, J., Sgolastra, F. & Kemp, W. P. in *Bee Pollination in Agricultural Ecosystems* (eds Rosalind R. James & Theresa L. Pitts-Singer) Ch. 6, 83 - 104 (Oxford University Press, 2008).
- 52 Authority, E. F. S. Scientific opinion on the science behind the development of a risk assessment of plant protection products on bees (*Apis mellifera*, *Bombus* spp. and solitary bees). *EFSA J* **10**, 2668 (2012).
- 53 Vanbergen, A. J. & Initiative, t. I. P. Threats to an ecosystem service: pressures on pollinators. *Frontiers in Ecology and the Environment* **11**, 251-259, doi:10.1890/120126 (2013).
- 54 Rasband, W. S. ImageJ. *U. S. National Institutes of Health, Bethesda, Maryland, USA*, doi:<http://imagej.nih.gov/ij/>, 1997-2016.

Tables

Table 1 Results of immune test and number of individuals per treatment group and sex

For each experiment, at least three independent test runs were conducted. The total number of males and females (*n*) involved in each experiment is given.

Immune parameter mean \pm s.e.m, <i>n</i> = number of individuals	Experiments in 2016			Experiments in 2018	
	<i>Control</i>	<i>100 μg/kg</i>	<i>200 μg/kg</i>	<i>Control</i>	<i>555 μg/kg</i>
Males					
Total hemocyte count (cells/ml)	6815.48 \pm 782.81	5135.87 \pm 596.54	2946.43 \pm 437.70	12109.38 \pm 1496.53	2708.33 \pm 699.29
<i>n</i>	21	23	21	16	15
Inhibition zone (mm)	7.02 \pm 2.88	3.59 \pm 1.04	0.92 \pm 1.39	12.42 \pm 3.10	3.33 \pm 0.86
<i>n</i>	26	19	22	16	15
Encapsulation (% grey value)	20.26 \pm 3.42	18.66 \pm 2.46	24.39 \pm 2.94	-	-
<i>n</i>	22	26	27		
Females					
Total hemocyte count (cells/ml)	3574.22 \pm 457.41	4264.71 \pm 691.95	3382.35 \pm 916.22	14791.67 \pm 1121.91	8198.53 \pm 1010.70
<i>n</i>	32	34	34	18	17
Inhibition zone (mm)	8.12 \pm 1.23	9.48 \pm 1.56	6.81 \pm 1.39	13.6 \pm 3.62	4.33 \pm 1.08
<i>n</i>	30	25	33	13	16
Encapsulation (% grey value)	13.44 \pm 1.86	16.44 \pm 1.98	17.37 \pm 1.91	-	-
<i>n</i>	22	26	27		
Confocal images (<i>n</i>)	5	-	-	-	-

Table 2 Consumption (mean \pm SE) of sugar solution over three days, thiacloprid uptake per bee and per mg of body weight in males and females. The thiacloprid dosage per body weight of males in treatment 200 is approx. the same as in females in treatment 555 (bold).

Sex	Treatment	Thiacloprid concentration	Sugar solution consumed (mg/bee)	Thiacloprid consumed (μg/bee)	Thiacloprid dosage (ng/mg body weight)
Males	control	0	171.55 \pm 15.32	0.000	0.00
	100	100 μ g/kg	179.80 \pm 23.89	0.018	0.35
	200	200 μ g/kg	130.95 \pm 25.17	0.026	0.50
	555	555 μ g/kg	128.45 \pm 19.17	0.072	1.34
Females	control	0	97.22 \pm 22.3	0.000	0.00
	100	100 μ g/kg	79.06 \pm 18.42	0.008	0.09
	200	200 μ g/kg	80.46 \pm 23.39	0.016	0.18
	555	555 μ g/kg	85.88 \pm 17.55	0.046	0.52